Identification of Biomarkers and Copper Binding Proteins in Tilapia and Zebrafish by Proteomics Approaches

CHEN, Dongshi

A Thesis Submitted in Partial Fulfilment
of the Requirements for the Degree of
Doctor of Philosophy
in
Biochemistry

The Chinese University of Hong Kong
September 2010

Thesis/Assessment Committee

Professor Cheung Wing Tai
(Chairman)

Professor Christopher Cheng Hon Ki
(Committee member)

Professor Chan King Ming
(Thesis supervisor)

Professor Kenneth Leung Mei Yee
(Additional examiner, School of Biological Sciences, The University of Hong Kong)

Professor Christer Hogstrand
(External examiner, King's College London)

Publication and presentations derived from results of this thesis research

Full paper

Chen, D.-S., and Chan, K.M. (2009) Changes in the protein expression profiles of the Hepa-T1 cell line when exposed to Cu^{2+}. Aquatic Toxicology 94: 163-176.

Manuscript Submitted

Chen, D.-S., and Chan, K.M: Identification of hepatic copper-binding proteins from tilapia: analyses of copper-binding proteins by fast performance liquid chromatography and immobilized metal affinity chromatography with proteomic approaches.

Conference Abstracts

Chen, D.-S., and Chan, K.M. (2008) Identification of novel copper binding proteins and biomarkers relating to Cu^{2+} toxicity in *Tilapia* with proteomic approaches. In: Fifth SETAC World Congress, Sydney, Austrália, August 3-7, 2008 (Oral Presentation by Chen, D.S.)

Chan, K.M. and Chen, D.-S. (2009) Proteomic Study of a tilapia cell line Hepa T1 exposed to Cu^{2+}. In: 15th International Symposium on Pollutant Responses in marine Organisms in Bordeaux, France, May 17-20, 2009. (Oral Presentation by Chan, K.M.) (Abstract #61).

Chen, D.-S., Zhang, D., Yu, J. C., and Chan, K.M. (2010) Toxicities and induction of metallothionein and copper transporters of zebrafish larvae exposed to Cu_2O nanoparticle and $CuCl_2$. In: 5th International Conference on Marine Pollution & Ecotoxicology, City University of Hong Kong, June 1-3, 2010 (Oral Presentation by Chen, D.S.).

ABSTRACT

Copper is an essential element in a variety of biological processes, but it can be toxic when present in excessive amounts. The central regulators of cellular copper metabolism include copper-binding proteins, copper transporters, metal membrane active transporters and copper-dependent enzymes. Until now, several copper transporters and copper related proteins have been identified. However, a full profile of pathway in which copper ions cause cellular changes in proteins and lead to toxic effects is less well-known. Hence, there is a need to identify more copper binding proteins to fulfill a complete copper transportation system. The aims of this study are to identify some novel copper binding proteins and proteins related to Cu^{2+} toxicity or detoxification mechanisms in the tilapia (*Oreochromis niloticus*) and the zebrafish (*Danio rerio*) using a proteomic approach, and to reveal the mechanism of copper tolerance and copper sensitivity by comparing the different biochemical responses to copper exposures between the two model species.

Firstly, a cell line derived from the liver of tilapia, Hepa-T1, was used as a model and exposed to two sub-lethal concentrations of waterborne copper for 96 h. The proteins expressed in Hepa T1 were investigated by differential protein profiling using two-dimensional gel electrophoresis (2-DE). It was found that Cu^{2+} (120 μM and 300 μM) caused differential expression of 93 different proteins, 18 of which were further verified by real-time quantitative polymerase chain reaction (PCR) analysis. Following analysis with ingenuity pathway software, several proteins were found to be involved in lipid metabolism, tissue connective development and cell cycle control, thus indicating that copper toxicity affects these cellular functions.

Secondly, the high copper contents in the liver of the tilapia make this fish a suitable model for the study of copper binding proteins. Liver was dissected from tilapia injected with Cu^{2+} and cytosolic fractions were separated by using Superdex 75 column chromatography followed with atomic absorption spectrometry. Fractions containing copper-binding proteins were found in two major peaks, analyzed using differential proteomic approaches, and loaded on a Cu chelating ion-immobilized affinity column (Cu-IMAC). Of the 113 differentially expressed proteins in these two peaks, some well-characterized copper binding proteins were found, including copper transporter ATP7A, cytochrome c oxidase, metallothionein, collagen, catalase, and vitellogenin. These proteins are mainly involved in endocrine disruption, mitochondria dysfunction, ion competition, lipid metabolism, copper transfer, and cytoskeleton disruption. In addition, a more concrete image about copper transportation pathway was hypothesized according to the function of the novel copper binding proteins identified.

Thirdly, zebrafish liver cell line (ZFL) was also used as a model to study the mechanism of copper toxicity. After processing similar experimental procedures of previous Hepa T1 experiment, 72 different proteins were identified to be regulated by Cu^{2+} (100 μM and 200 μM). More than 50 % of these proteins were also found differentially expressed in the tilapia. The results suggested that the toxicity mechanism between zebrafish and tilapia was generally conserved. Although, in ZFL, the regulation of several proteins, related to ROS effect, mitochondrion copper transportation, and stress response, was quite different from that in tilapia.

Fourthly, to further reveal the mechanism of copper tolerance and sensitivity in tilapia and zebrafish, two important copper transporters (ATP7A & B) and metallothionein (MT) were chosen for studying. Until now, a full length of ATP7A and

partial length of ATP7B were obtained in tilapia. Then a real time quantitative PCR was conducted to study the different regulations of these three genes in tilapia and zebrafish. It was found that Cu^{2+} could induce more MT and ATP7A & B in tilapia than zebrafish both *in vivo* and *in vitro*. These results help us to understand that the copper tolerance of tilapia is possibly due to higher expression level of both copper transporters and MT.

Last but not least, I also compared the toxicity and biomarker gene expression in zebrafish exposed to Cu_2O nanoparticle (NP) and $CuCl_2$, respectively. It was found that the toxicity of $CuCl_2$ is much higher than that of Cu_2O NP. Then seven genes, including MT, ATP7A & B, copper transporter 1 (Ctr1), metal regulatory transcription factor 1 (MTF1), glutathione sulfur transferase (GST), Cu/Zn superoxide dismutase (Cu/Zn SOD), were chosen for studying. It was found that both Cu_2O NP and $CuCl_2$ up-regulated the mRNA levels of MT, Cu/Zn SOD, and Ctr1, ATP7A & 7B, but down-regulated the mRNA levels of GST. Interestingly, the inductions of MT, Ctr1, ATP7A & B in the Cu_2O NP exposure groups were much higher than that of $CuCl_2$ exposure groups *in vivo*. Furthermore, as determined by using Ctr1, ATP7A and ATP7B gene expression, the no observable effect levels (NOELs) of $CuCl_2$ and nano-Cu_2O were 11 ppb and 50 ppb, whereas the lowest observable effect levels (LOELs) of $CuCl_2$ and nano-Cu_2O were 43 ppb and 125 ppb.

In conclusion, this study provided a comprehensive profile of gene expression in fish liver cells after the administration of waterborne copper ions. Many copper binding proteins and copper transporters were identified and some are useful biomarkers of effects and exposures to copper contamination. Tilapia as a copper resistant species relative to zebrafihs can have stronger expression of copper transporters and binding proteins than zebrafish.

摘要

铜是各种生物功能的必需元素，但是如果超过一定数量，就会变成有毒的。细胞中的铜代谢主要受一些蛋白调控，包括铜结合蛋白，转运蛋白，金属膜转运蛋白，和铜依赖性酶。到目前为止，一些铜转运蛋白以及相关蛋白已经被鉴定出来。但是，铜如何调控细胞内蛋白表达变化，通过何种途径起毒性作用仍然不是很清楚。这就需要鉴定出更多的铜结合蛋白来完善铜转运系统图谱。本次研究的目的是利用蛋白质组学的方法，在非洲鲫鱼（*Oreochromis niloticus*）和斑马鱼（*Danio rerio*）中鉴定一些新的铜结合蛋白，以及跟铜离子毒性及解毒机理相关的蛋白；并且通过对比两个物种在铜暴露之后的反应差异，揭示铜耐受性和敏感性的机理。

首先，我们利用非洲鲫鱼肝脏细胞（Hepa T1）做为模型，并且将其暴露于两个亚致死浓度的铜离子 96 小时。接着用双向蛋白电泳来检测 Hepa T1 蛋白表达的变化。结果发现 120 mM 和 300 mM 的铜离子可以诱导 93 个蛋白表达变化，其中 18 个用实时定量 PCR 进一步确定。利用 Ingenuity Pathway Analysis （IPA）软件进行分析，发现这些差异表达蛋白主要跟脂肪代谢，组织发育，以及细胞生长周期相关，这意味着铜离子的毒性是通过影响这些功能发挥作用。

其次，非洲鲫鱼肝脏中富集铜离子浓度，因此适用于做为铜结合蛋白研究的模型。从注射铜离子的非洲鲫鱼解剖出肝脏，进一步提取出细胞质蛋白，然后利用 Superdex 75 凝胶柱进行分离，并且用原子吸收光谱检测分离后各组分的金属浓度。实验发现，铜结合蛋白主要集中在两个吸收峰，接着将这两个吸收峰组分进行差异蛋白组分析，以及金属螯合层析分离。在这两个吸收峰中，113 个蛋白有表达差异，

并且鉴定出一些常见的同结合蛋白，包括 transporter ATP7A、cytochrome c oxidase、metallothionein、collagen、catalase、和 vitellogenin.这些蛋白主要跟内分泌阻断，线粒体功能紊乱，离子竞争，脂肪代谢，以及细胞骨架破坏相关。此外，根据新鉴定出的铜结合蛋白的功能，我们做出一个更详细的铜离子装运系统图。

然后，我们利用斑马鱼肝脏细胞系（ZFL）做为模型来研究铜对斑马鱼的毒性机理。利用之前研究 Hepa T1 的方法，我们发现 100 uM 和 200 uM 的铜离子可以诱导 72 个蛋白发生表达差异。其中，50 %的蛋白跟之前的 Hepa T1 差异蛋白匹配，这表明铜离子对斑马鱼和非洲鲫鱼的毒性机理相似。即便如此，在 ZFL 中，一些跟 ROS 作用，线粒体蛋白转运，以及胁迫反应的蛋白调控跟非洲鲫鱼还是相差很大。这些结果可以帮助我们了解到非洲鲫鱼的铜耐受性和斑马鱼的敏感性可能跟这些蛋白的表达调控有关。

再者，为了更好地了解非洲鲫鱼的铜耐受性和斑马鱼的敏感性，我们选择了两个重要的铜转运蛋白(ATP7A & B)和金属硫蛋白（MT）进行研究。到目前为止，我们已经得到非洲鲫鱼 ATP7A 的全长 cDNA，以及 ATP7B 的部分 cDNA。然后利用实时定量 PCR 来研究这三个基因在非洲鲫鱼和斑马鱼中的表达调控。体内和体外实验结果发现，比起斑马鱼，铜离子可以诱导非洲鲫鱼的 MT，ATP7A & B 上调更高。这些结果说明非洲鲫鱼的较高铜耐受性可能跟铜转运蛋白和金属硫蛋白的高表达水平有关。

最后，我们利用 CuO nanoparticle (NP)和 $CuCl_2$比较了可溶性铜跟不可溶性铜对斑马鱼的毒性差异。结果发现 $CuCl_2$的毒性高于 CuO NP。接下来，我们选择了

7 个基因做为研究对象，包括 MT, ATP7A & B, copper transporter 1 (Ctr1), metal regulatory transcription factor 1 (MTF1), glutathione sulfur transferase (GST), Cu/Zn superoxide dismutase (Cu/Zn SOD)。结果表明 Cu_2O NP 和 $CuCl_2$ 可以诱导 MT，Cu/Zn SOD，Ctr1 和 ATP7A & B 在 mRNA 水平上表达上调，但是 GST 表达下调。有趣的是，在体内相对于 $CuCl_2$，Cu_2O NP 可以诱导 MT，Ctr1，ATP7A & B 上调更高。此外，通过综合考虑 Ctr1，ATP7A & B 的表达情况，我们得出了 $CuCl_2$ 和 Cu_2O NP 的 no observable effect levels (NOELs) 分别是 11 ppb 和 50 ppb，然而它们的 lowest observable effect levels (LOELs)分别是 43 ppb 和 125 ppb.

总而言之，本研究为干细胞暴露在铜离子中的蛋白表达作出了较详细的分析。实验也确定了很多铜离子结合蛋白和可作为生物标记用的蛋白。本研究亦比较了非洲鲫鱼和斑马鱼在铜离子中的蛋白质，除了斑马鱼与 ROS 作用，线粒体蛋白转运，以及胁迫反应的蛋白调控有关之外，非洲鲫鱼的较高铜耐受性可能跟铜转运蛋白和金属硫蛋白的高表达水平有关。

Acknowledgements

Fristly, I would like to express my sincere acknowledgement to my supervisor. Professor K.M. Chan for his patience guidance and providing critial comments and suggestion during my research project. In these three years, he has not only provided me with best technical supports but also taught me the way of thinking. Besides, he also gave me many oppurtunities to parcitipate in some international conferences, which could improve my presentation skills and increase my knowledges about others' work. Personally, he is also a good supervisor who really cares about students' feeling and difficulties, which is very important to somebody like me, who has a family

Secondly, I would like to thank my labmates, including Dr. G.H. Wan, Mr. J.Y. Zhu, Mr. Eric Liang, Ms. W.S. Chow, and Mr. Alex Shek, for their help and suggestion when I encounter difficulties in my research work. I am also grateful to all of the administrtive staffs and technicians in Department of Biochemistry, and Ms. Yang in Molecular Biolgogical Programme, for giving me technical supports of MALDI-TOF MS/MS. Moreover, I want to thank Mr. M.L. Chen and Mr. J.Z. Li for their help and suggestions during my research work. Special thanks also go to Professor Jimmy Yu and Ms D. Zhang from Chemistry Department for providing the nano copper particles for testings.

Last but not least, I wish to thank my family, especially my wife, for their supports and consideration.

Table of Contents

List of Figures

List of Tables

List of Abbreviations

2-DE	Two-dimensional gel electrophoresis
AAS	atomic absorbance spectrometry
AD	Alzheimer's Disease
ALDh	aldehyde dehydrogenases
APOA-IV	apolipoprotein A-IV
APP	amyloid precursor protein
ATP7A/B	ATPase, Cu transporting alpha/beta polypeptide
ATOX1	copper transport protein ATOX1
BSA	Bovine serum albumin
CAT	catalase
CCO	copper chaperone for SOD1
COX 1/2/11/17	cytochrome c oxidase 1/2/11/17
CTR	high-affinity copper uptake protein
CYP1A1	cytochrome P450, family 1, subfamily A, polypeptide 1
DMT1	divalent metal transporter 1
DTT	dithiothreitol
FET3	iron transport multi-copper oxidase
FPLC	fast performance liquid chromatography
FTR1	iron transporter 1
GAPDH	glyceraldehyde 3-phosphate dehydrogenase
GH	growth hormone
IEF	isoelectric focusing
IGF1	insulin–like growth factor 1
IGFBP5	IGF-binding protein 5
IMAC	immobilized metal affinity chromatography
IPA	Ingenuity pathway analysis
LC50	median lethal concentration
LDL	low-density lipoprotein
MALDI-TOF MS	Matrix-assisted laser desorption/ionization-time of flight, Mass spectrometer

MT	metallothionein
ND5	NADH dehydrogenase subunit 5
PCR	polymerase chain reaction
PI	propidium iodide
PMSF	phenylmethanesulphonylfluoride
PRL	prolactin
PRLR	prolactin receptor
SCO1	SCO cytochrome oxidase deficient homolog 1
Cu/Zn SOD	Cu/Zn superoxidase dismutase
STAT3	signal transducer and activator of transcription 3
STC	stanniocalcin
TF	transferrin
TFR	transferrin receptor
TPM	tropomyosin
VIM	vimentin
VTG	vitellogenin
Zic	zic family member protein
ZFP	Zinc finger protein

Chapter One

INTRODUCTION

1.1 Environmental health concerns of copper

Copper is a reddish metal occurs naturally in rock, soil, water, sediment, and air. Its average concentration in the earth's crust is about 50 parts per million (ppm) in normal soil. Copper can be easily molded or shaped. Its "reddish-gold" color is most commonly seen in the penny, electrical wiring, and some water pipes. It is also found in many mixtures of metals, called alloys, such as brass and bronze. Many compounds (substances formed by joining two or more chemicals) of copper exist. These include natural occurring minerals as well as man-made chemicals, including nanoparticles. Many copper compounds can be recognized by their blue-green color. When we speak of copper, we will not only be referring to copper metal, but also to compounds of copper that may be in the environment. Copper is extensively mined and processed in worldwide and is primarily used as the metal or alloy in the manufacture of wire, sheet metal, pipe, and other metal products. Copper compounds are most commonly used in agriculture to treat plant diseases, like mildew, or for water. The most commonly used compound of copper is copper sulfate which is blue in colour and a compound used as fungicide and algacide. It is generally believed that copper is an essential element to human health and tight regulatory system is available in our body, thus normally we can handle excessive copper exposures. Since copper is a easily avaiblabe metal and the extensive use of copper pipes to replace plastic or iron pipes, copper uptake in human body has been a concern of environmental health issue.

In 1992, copper was included by the World Health Organization (WHO) in the "List

of Chemicals of Health Significance in Drinking-water", with a provisional guideline value of 2 mg/liter (ppm). WHO estimated that 30 mg of copper was the accepted maximum daily copper load. Considering an average adult body weight of 60 Kg and that a total of 10 % of the copper could be obtained through drinking water (an average adult has an intake of 2 liters per day); a concentration limit of 1.5 mg of copper per liter was suggested. The WHO approximated this to 2 mg/L, as the provisional guideline value (PGV) based on human health effects. This caused the immediate concern of the copper industry, since up to that point, copper had been regulated on the basis of its effects on the color and taste of water, as well as on the possible staining of laundry and sanitary appliances. The report of the International Programme on Chemical Safety (IPCS) made reference to an unpublished study in dogs, which found transitory effects such as necrosis and increased liver fibrosis in animals daily exposed to 5 mg of copper per kg of body weight. Thus, the recommendation was not based on epidemiological or clinical studies in humans, or on animal studies. In addition, no risk analysis or considerations on the duration of exposure were made.

1.2 Copper related diseases

Copper occurs naturally in plants and animals and plays a vital role as a catalytic co-factor for a variety of metalloenzymes including superoxide dismutase (for protection against free radicals), cytochrome c oxidase (mitochondrial electron transport chain), tyrosinase (pigmentation), peptidylglycine alpha-amidating mono-oxygenase (PAM) (neuropeptide and peptide hormone processing) and lysyl oxidase (collagen maturation) (Harris, 2000; Pena et al., 1999; Uauy et al., 1998). At the same time, copper is toxic to both eukaryotic and prokaryotic cells, not least due to its ability to catalyze, via the

so-called Fenton reaction, the generation of aggressive free radicals. Also by binding ectopically to proteins, copper can disturb their structure (Bartsch and Nair, 2004; Koch et al., 1997; Valko et al., 2005). Therefore, every organism has a number of elaborate mechanisms at its disposal to control cellular uptake, distribution, detoxification and elimination of copper (Bertinato and L'Abbe, 2004; Puig and Thiele, 2002a).

Cellular contents of copper are tightly controlled and balanced, otherwise, free copper ions will cause serious impacts and toxic effects. Menkes disease and Wilson disease are well known inherited disorders of copper metabolism in humans (Table 1.1). The essential role of copper in the developing central nervous system is evidenced by Menkes disease, during which impaired copper transport into and within the developing brain results in demyelination and neurodegeneration (Kaler, 1998; Kodama et al., 1999). Brain copper accumulation in Wilson's disease results in dystonia, dysarthria, and other Parkinsonian symptoms, as well as psychiatric symptoms of depression, cognitive deterioration, personality change, psychosis, and schizophrenia (Ferenci, 2004). Although the signs and symptoms of Menkes and Wilson's diseases are distinct, each disorder results from inherited loss-of-function mutations in genes encoding homologous copper-transporting P-type adenosine triphosphatases (Atpases) ATP7A (Menkes) and ATP7B (Wilson's) (Fig 1.1).

Table 1.1 Hereditary disorders of copper metabolism (Modified from Madsen and Gitlin, 2007)

	Wilson's disease	**Menkes disease**
Genetics	Autosomal recessive Loss-of-function mutations ATP7B gene	X-linked Loss-of-function mutations ATP7A gene
Presentation	Late childhood: liver second–third decade, neuropsychiatric	Early infancy
Defect	Biliary copper excretion	Copper transport across the placenta, brain, and gastrointestinal tract
Pathogenesis	Copper accumulation	Copper deficiency
Clinical	Cirrhosis, dystonia, dysarthria Parkinsonian tremor, psychiatric	Hypothermia, hypopigmentation, abnormal hair, tortuous arteries intractable seizures, failure to thrive
Pathology	Basal ganglia copper accumulation	Cerebral and cerebellar degeneration
	Neuronal cell loss	Purkinje cell axonal swelling Abnormal arborization

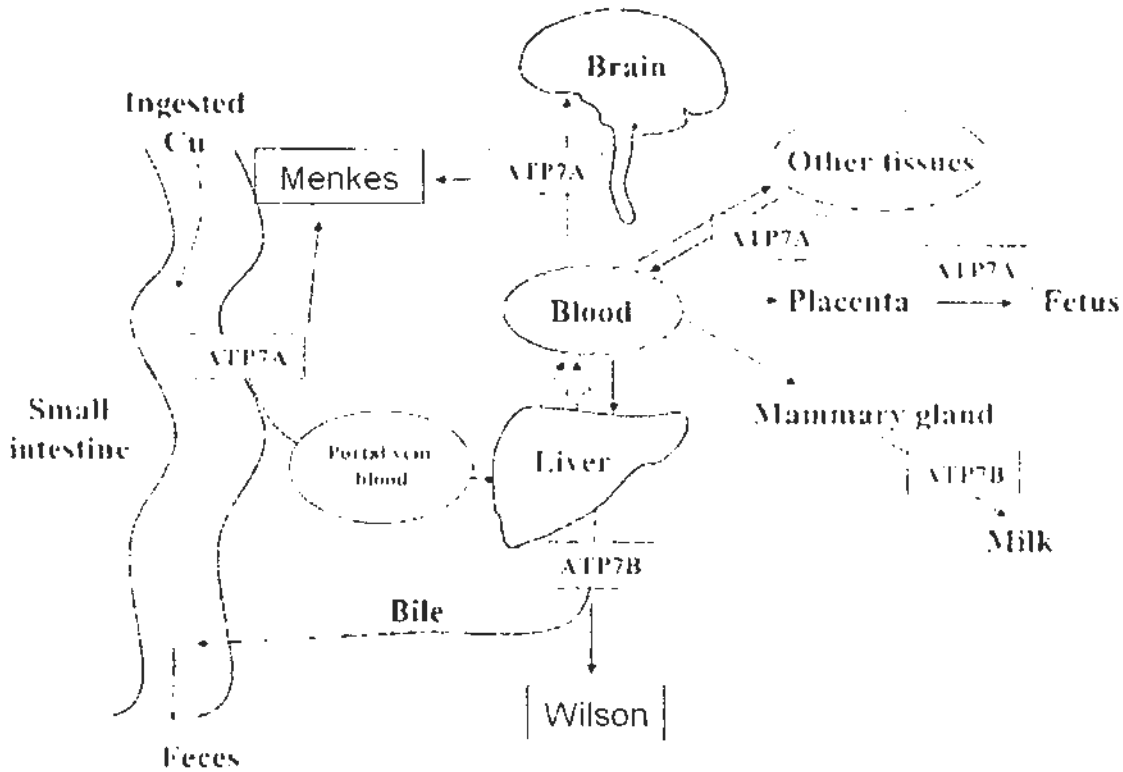

Fig. 1.1. Homeostatic regulation of copper in mammals (redrawn from Mercer and Llanos, 2003). The directions of copper flow are shown by the arrows and the steps involving the Cu ATPases, ATP7A and ATP7B, are also indicated. Ceruloplasmin (CP) is the main copper transport protein in the blood. Transport of copper to the fetus and neonate is vital for normal development and is regulated by ATP7A in the placenta and ATP7B in the mammary gland.

1.2.1 Menkes Disease

Menkes disease is an X-linked disorder characterized by growth failure, brittle hair, hypopigmentation, arterial tortuosity, and neuronal degeneration due to loss-of-function mutations in the gene encoding ATP7A (Mercer et al., 1993; Vulpe et al., 1993). The pleiotropic features of this disease are the result of impaired activity of specific cuproenzymes resulting from impaired ATP7A function. The neurologic features are present in early infancy, revealing a critical role for ATP7A and copper in neuronal

development (Mercer, 1998). Magnetic resonance imaging of the brain reveals deficient myelination with cerebellar and cerebral atrophy (Geller et al., 1997; Leventer et al., 1997), and neuropathologic examination demonstrates focal degeneration of the graymatter and neuronal loss most prominent in the hippocampus and cerebellum (Barnard et al., 1978). Studies in a murine model of Menkes disease suggest a role for ATP7A and copper in axon extension and synaptogenesis during development (El et al., 2005). ATP7A mediates the availability of an NMDA receptor-dependent, releasable pool of copper in hippocampal neurons, and the absence of ATP7A activity in Menkes disease markedly affect NMDA receptor–mediated excitotoxicity in these neurons (Schlief et al., 2006). These data suggest a model whereby loss of ATP7A contributes to both seizures and neuronal degeneration in affected patients and raise the possibility of therapeutic approaches based on NMDA receptor blockade (Hardingham and Bading, 2003).

1.2.2 Wilson's Disease

Wilson's disease is an autosomal recessive disorder resulting in hepatic cirrhosis and progressive basal ganglia degeneration due to loss-of-function mutations in the gene encoding the copper-transporter ATP7B (Bull et al., 1993; Tanzi et al., 1993). The resulting impairment in biliary copper excretion leads to copper accumulation in hepatocyte, copper-mediated liver damage, activation of cell-death pathways, leakage of copper into the plasma, and eventual copper overload in all tissues (Fig. 1.2) (Gitlin, 2003). Although ATP7B is expressed in some regions of the brain, in Wilson's disease copper overload in extrahepatic tissues is due to excess accumulation from the plasma following liver injury because this is entirely reversed following liver transplantation

(Schumacher et al., 2001). Ceruloplasmin is an essential ferroxidase that contains greater than 95% of the copper present in plasma. This protein is synthesized in hepatocytes and secreted into the plasma following the incorporation of six copper atoms in the late secretory pathway. In Wilson's disease, loss of function of ATP7B results in synthesis of apoceruloplasmin that is rapidly degraded in the plasma (Fig. 1.2). As a result, the serum ceruloplasmin concentration is a useful diagnostic indicator of Wilson's disease (Hellman and Gitlin, 2002).

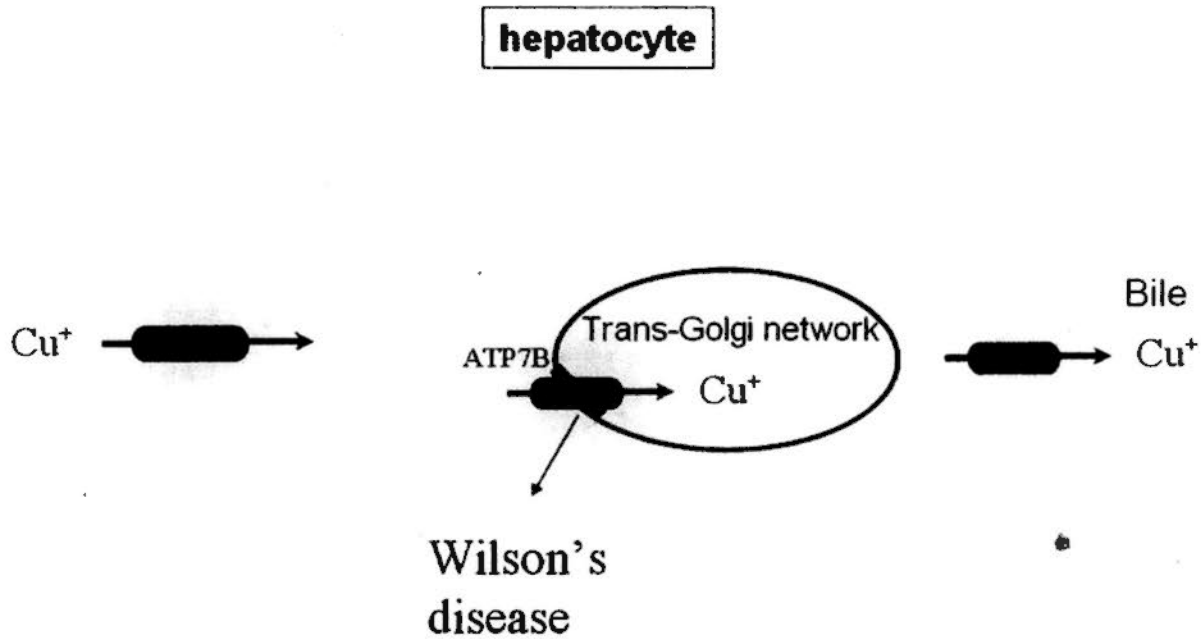

Fig. 1.2. Pathogenesis of Wilson's disease (Modified from Kim et al., 2008). Proposed model of the proposed pathways and proteins relevant to copper metabolism in human hepatocyte. Copper transport to the trans-Golgi network (TGN) is shown as the process mediating intracellular homeostasis by ATP7B. Dysfunction of ATP7B results in cytosolic copper accumulation with associated cellular damage.

1.2.3 Alzheimer's disease

Alzheimer's disease (AD) is the most common form of neurodegenerative dementia. The formation of senile plaques precipitated in the brain is a pathological marker of the disease (Barnham et al., 2004). Their core element of AD is an aggregated form of an acid peptide molecule involving 39 - 43 amino acid residues, which is termed the Aβ peptide (Fig. 1.3), a fragment of amyloid precursor protein (APP). This peptide is generally accepted to be neurotoxic and, as such, is a therapeutic target as well as a diagnostic marker. The cores of Alzheimic plaques consist of aggregated Aβ peptides and have been described as metal sinks because of their high metal content: Cu, 0.44 mM; Zn, 1 mM; Fe, 1 mM (Curtain et al., 2001). In vitro, each of these metals is capable of inducing aggregation of the peptide (Cherny et al., 1999), which has a high affinity for Cu^{2+} and complexation results in altered morphology of the aggregated Ab fibrils.

10 20 30 40

DAEFRHDSGY EVGGQKLVFF AEDVGSNKGA IIGLMVGGVV IA

Fig. 1.3. Sequences of the Aβ peptides (Donnelly et al., 2007).

Emerging evidence suggested that AD might be characterized by copper deficiency as recent data indicated that AD patients had higher levels of copper in the plasma but lower levels in the brain (Bayer and Multhaup, 2005). In a transgenic mouse model of AD, an increase in neuronal copper levels (induced either by genetic manipulation or by copper supplementation of diet) led to a significant decrease in brain Aβ levels (Bayeret al., 2005; Phinney et al., 2003). In addition, a recent study of 33 patients revealed a negative correlation between plasma copper levels and cognitive decline which was interpreted in terms of a mild copper deficiency in most AD patients (Kessler et al., 2006;

Pajonk et al., 2005). Although the mechanism leading to these changes is not understood, the observations suggested that copper supplements might have therapeutic potential. A clinical trial of daily supplementation via the salt Cu^{2+} orotate is currently underway in Germany (http://www.alzheimer-bayer.de/alzh st1.html) (Pajonket al., 2005).

1.3 Copper homeostasis in eukaryotic cells

Over the past few decades, critical progress was made in the identification of genes encoding proteins which function in copper uptake, intracellular distribution, efflux and in the regulation of the copper homeostasis machinery (Kimet al., 2008a; Puiget al., 2002a). Many of the structural, functional and regulatory details have been strikingly conserved from microbes to humans. Fig. 1.4 shows a model for copper homeostasis in a typical mammalian cell.

1.3.1 Cellular uptake of copper

Ctr1 is an integral membrane protein that functions as a major copper importer at the plasma membrane. Genetic, biochemical and structural studies support a model in which Ctr1 homotrimerizes to form a central region of low electron density through which copper may traverse the plasma membrane (Aller and Unger, 2006; Dancis et al., 1994). The genetic requirement for a metalloreductase in yeast for Ctr1-mediated high affinity copper uptake, in addition to other data (Kimet al., 2008a), all support the transport of Cu^{+} rather than Cu^{2+}. Conserved methionine residues are present in the Ctr1 extra-cellular domain as Met-X-Met or Met-X2-Met and, while not essential for activity, are needed for high affinity of Cu^{+} import. Additionally, a conserved Met motif, Met-X3-Met present in the Ctr1 second transmembrane domain, is essential for Cu^{+}

import (Puig et al., 2002). These and other experimental results are consistent with thioether-Cu^{+} coordination to Ctr1 at one or more steps in the import process.

Unlike many other high affinity metal transporters (such as ATP7A/B, see below), Ctr does not require ATP for copper uptake (Lee et al., 2002; Petris, 2004). Its transport ability is stimulated by extracellular K^{+} and probably facilitated by the extremely low intracellular concentration of free copper; while the concentration of intracellular total free copper ion concentration is approximate 10 to 100 micromolar. And several orders of magnitude lower are due to an instant association of imported copper with chaperones, scavengers and other proteins (Rae et al., 1999).

In yeast, three copper transporters termed yCtr1, yCtr2 and yCtr3 have been described. The yCtr1 and yCtr3 are functionally redundant, plasma membrane-integrated, high-affinity copper transporters. Extracellular copper, usually Cu^{2+}, has to be reduced to Cu^{+} by plasma membrane reductases encoded by FRE1 and FRE2 before being imported by yCtr1 and yCtr3 (Petris, 2004; Rutherford and Bird, 2004). Any excess copper is sequestered in the vacuole (somewhat analogous to the mammalian lysosome), a storage container of yeast for substances intended for recycling/degradation, including valuable metabolites such as phosphate, selected amino acids, metals, and sequestered toxins (Huang and Klionsky, 2002). Since yCtr2 is localized in the vacuolar membrane and upon copper depletion, imports copper from the vacuole to the cytoplasm, it plays an important role in yeast copper homeostasis (Rees et al., 2004). The function of all these copper importers was characterized by specific mutagenesis and by targeted gene disruption.

1.3.2. Copper delivery to secretory compartments

Many Cu-dependent proteins traverse the secretory pathway *en route* to the plasma membrane, intracellular membranes or secretion from cells. These include secreted rather than intracellular forms of lysyl oxidase and Cu/Zn SOD, tyrosinase, blood clotting factors and the multicopper ferroxidases ceruloplasmin and hephaestin. The Atox1 Cu chaperone, which is composed of βαββαβ folds, coordinates to a solvent-exposed Cu^{+} atom for delivery to the secretory compartment (Anastassopoulou et al., 2004; Wernimont et al., 2000). Cu^{+} is transferred from the surface of Atox1 to a metal binding domain repeat with the consensus sequence of GMTCXXC in the N terminus of the Cu^{+}-transporting ATPases ATP7A and ATP7B (Pufahl et al., 1997). This transfer occurs via a series of interprotein ligand exchange reactions, ultimately leading to the movement of Cu^{+} across the membrane of the secretory compartment (ATP7A and ATP7B), across the basolateral membrane of IECs (ATP7A) or out of hepatocytes and into the bile (ATP7B). Though much progress has been made in understanding the catalytic mechanisms used by Cu^{+}-transporting ATPases, what is not clear at present are the mechanisms by which Cu^{+} is transferred from the N-terminal Cu^{+} binding domain of the transporters to the transmembrane domain for transfer across the membrane. Whereas mutations in the genes encoding ATP7A and ATP7B cause Menkes disease and Wilson's disease, respectively (and similar states in mouse knockout models (Huster et al., 2006; Lutsenko et al., 2007), loss of the gene encoding Atox1 in mice resulted in perinatal lethality. This likely reflects the central role this Cu chaperone plays in delivering Cu^{+} to both the ATP7A and ATP7B transporters, and perhaps other intracellular targets that have not yet been identified.

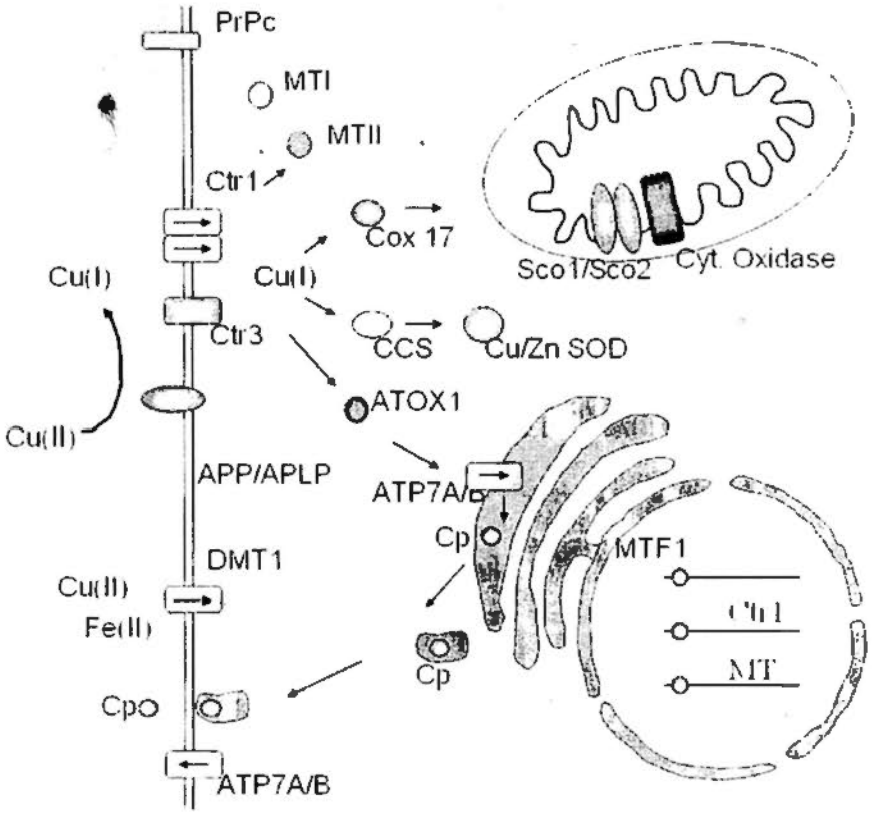

Fig. 1.4. Cellular copper homeostasis (Modified from Balamurugan and Schaffner, 2006). Model of copper trafficking in polarized cell reveals copper entry via Ctr1 followed by distribution to the copper chaperones. The copper chaperone for superoxide dismutase (CCS) delivers copper to Cu/Zn superoxide dismutase (SOD), Atox1 delivers copper to one of the Atpases (ATP7A/ATP7B) in the late Golgi and Cox17, and Sco1 and Cox17 are involved in the pathway of copper trafficking to mitochondria and cytochrome oxidase (Cox). The Atpases transport copper into the secretory pathway for incorporation into newly synthesized cuproproteins and for export from the cell. Metallothionein (MT) serves to chelate most available copper and is critical for cell survival in copper excess. MTF1 served as a transcription factor to modulate the regulation of MT and Ctr1.

1.3.3. Controlling cytosolic copper

Without the Cu cofactor, Cu/Zn SOD is catalytically inactive for superoxide disproportionation, and thus organisms lacking either Ctr1 or SOD are deficient in oxidative stress protection (De Freitas et al., 2000). Indeed, Δsod1 yeast accumulated DNA mutations, and SOD⁻ mice developed hepatocellular carcinoma, presumably as a result of oxidative damage of DNA. Importantly, mutant forms of Cu/Zn SOD that cause a familial form of amyotropic lateral sclerosis are more prone to unfolding and aggregation when metal-free, which underscores the importance of deciphering the mechanisms for metal loading of this enzyme.

Copper delivery to Cu/Zn SOD requires the Cu chaperone for SOD called CCS (copper chaperon for SOD). Though CCS bears strong structural similarity to Cu/Zn SOD, CCS is catalytically inactive and delivers Cu to Cu/Zn SOD by directly docking with the apo or zinc-loaded monomer (Furukawa et al., 2004; Lamb et al., 2001). In an oxygen-dependent mechanism accompanied by Cu/Zn SOD intramolecular disulfide bond formation, and a series of ligand exchange reactions between CCS and Cu/Zn SOD, Cu^{2+} is transferred from CCS to four histidine ligands of Cu/Zn SOD, with water as the fifth ligand bound to Cu^{2+} in square pyramidal coordination geometry. In addition to their residency in the cytoplasm, both CCS and Cu/Zn SOD are also localized to the mitochondrial IMS, where active Cu/Zn SOD is thought to protect cells from significant quantities of superoxide given off from the incomplete reduction of oxygen during mitochondrial electron transport (Field et al., 2003).

1.3.4. Copper delivery to mitochondria

In addition to delivery of Cu^{2+} to cytosolic proteins and to the secretory compartment, Cu^{2+} must be targeted to mitochondria, where cytochrome oxidase uses Cu^{2+} for oxidative phosphorylation. Genetic studies in microbes, and the mapping of mutated genes that are responsible for defects in cytochrome oxidase assembly, have also identified many proteins involved in cytochrome oxidase copper binding in mitochondria (Cobine et al., 2006). These proteins include Cox17 in the mitochondrial inter-membrane space, Cox11 in the mitochondrial inner membrane, and Sco1 and Sco2, structurally similar proteins that play a more proximal role in copper delivery to cytochrome oxidase. Defects in Sco1 and Sco2 caused catastrophic defects in cytochrome c oxidase assembly and resulted in severe human disease (Leary et al., 2004).

1.4. Detoxification/elimination

1.4.1. Metallothioneins: a safeguard of the cell

Even though copper export and import are subject to elaborate control mechanisms, there can be conditions where copper is imported in excess. For example, Drosophila Ctr1, the major larval copper importer, is regulated at the transcriptional level while in other species the Ctrs are regulated posttranscriptionally. However, because Ctrs are not active transporters both down-regulation mechanisms may not be fast enough to cope with a sudden increase in ambient copper concentration (Petris et al., 2003; Selvaraj et al., 2005). Therefore, an important aspect of metal homeostasis is the sequestration of intracellular toxic heavy metals, especially copper, a task that is mainly performed by intraceullar proteins, such as metallothioneins (Kagi, 1991).

Metallothioneins constitute a group of low molecular weight, cysteine-rich proteins with high metal binding capacity (Baskin et al., 1998; Kagi, 1991; Palmiter, 1998; Quaife et al., 1998; Schwartz et al., 1998; Thomas and Palmiter, 1998). They are found in all eukaryotes as well as in some prokaryotes and mainly function as intracellular metal scavengers/metal storage proteins (Ecker et al., 1986; Turner and Robinson, 1995). Typically, metallothionein genes are expressed at a basal level but their transcription is strongly induced upon heavy metal load (Andrews, 2000).

Among the approximately 60 amino acids of a typical vertebrate metallothionein, close to one third are cysteines. All mammals contain four major members of the metallothionein family, termed MT-I to MT-IV (or MT-1 to MT-4) (Kagi, 1991; Palmiter, 1998). In mouse, each type is represented by one member, while in humans, MT-I has expanded into a gene family of its own with over 12 genes (some are pseudogenes). MT-I and MT-II are expressed at all stages of development in most, if not all cell types. Their transcriptions are responsive to adverse conditions, especially heavy metal load, oxidative stress, ionizing radiation and a number of other stress conditions (Durnam and Palmiter, 1987; Palmiter, 1998). MT-III is constitutively expressed, predominantly in neurons but also in glia and male reproductive organs, and its elimination in the mouse increased susceptibility to seizures (Aschner et al., 1997). MT-IV expression is confined to differentiated squamous epithelia and the MT-IV gene, which also contains a metal response element (MRE) in the promoter region, is at least partially metal responsive (Quaife et al., 1994).

1.4.2. Metallothioneins and ATPase transporters handle excess cellular copper

Metallothioneins can store copper but they are not suitable to eliminate an excess of it from the cell. For this, there are the aforementioned ATP7 transporters, which in some multicellular organisms redistribute copper from one cell to the others but do not affect total body copper. In vertebrates, as mentioned before, there is nevertheless a specific way of eliminating excess copper from the organism utilizing the liver-specific ATP7B Wilson transporter, which upon copper load translocates from the Golgi to the plasma membrane to export copper into the so-called canaliculi, the smallest bile transport channels that ultimately lead into the gall bladder (Camakaris et al., 1999; Petris et al., 2002).

1.4.3 Transcriptional regulation of copper homeostasis

As mentioned, the expression of metallothioneins is regulated at the transcriptional level. Upon heavy metal load, specific metal-responsive transcription factors bind to metallothionein gene promoters to boost their expression. The cis-acting element on the metallothionein gene promoter is called metal-responsive element (MRE) and its associated binding protein or trans-acting transcriptional factor is known as MRE-binding transcription factor, MTF1.

MTF-1 is a unique transcription factor which is able to handle both extremes, namely, copper load and copper starvation. At high copper level, it activates metallothionein genes for more metallothionein to sequester extra copper ions, while at low copper level MTF-1 activates the gene for the copper importer Ctr1 to remove copper ions. The upstream region of the Ctr1 gene, which mediates transcriptional induction upon copper

scarcity, includes a segment with three uniquely spaced, strong MREs that is highly conserved among several Drosophila and other animal species. These MREs are bound by MTF-1 both at low and high copper, and due to their specific arrangement, possibly in conjunction with auxiliary factors, confer activity upon copper starvation. While Drosophila Ctr1 is predominantly, if not exclusively, regulated at the transcriptional level (Selvarajet al., 2005), yeast and human Ctrs are regulated posttranscriptionally, whereby excessive copper concentration was reported to stimulate rapid protein degradation and/or endocytosis (Guo et al., 2004; Petriset al., 2003). Each of these mechanisms, whether transcriptional or posttranscriptional, allows for a fine tuning of Ctr1 levels and thus of copper import by controlling the amounts of copper transporters and metallothionein.

1.5 Copper in the environment

Soluble copper compounds (those that dissolve in water), that are most commonly used in agriculture, are more likely to be health threatening. The concentration of copper in air ranges from a few nanograms in a cubic meter of air (ng/m3) to about 200 ng/m3. Near smelters, which process copper ore into metal, concentrations may reach 5000 ng/m^3. The average concentration of copper in lakes and rivers is 4 ppb (Craig et al., 2007a). The average copper concentration in groundwater is similar to that in lakes and rivers; however, monitoring data indicated that some ground water, contained higher levels of copper. This copper is generally strongly attached to particles in the water. Lakes and reservoirs recently treated with copper compounds to control algae or receive cooling water from a power plant may have high concentrations of dissolved copper. Once in natural water, much of this copper soon attaches to particles or converts to

forms that cannot easily enter the body.

Although copper is important, it is toxic when concentrations exceed that of natural concentrations (<0.05 mmol/L). At concentrations even found in natural waters, the ionic form of copper is very poisonous towards photosynthesis and growth of unicellular algae (Contreras et al., 2009). Copper is one of the world's most widely used metals, with the electrical industry probably making use of it the most. It reaches aquatic systems through anthropogenic sources such as industrial, mining, plating operations, usage of copper salts to control aquatic vegetation or influxes of copper containing fertilizers (Nussey et al., 1995). Copper has an unclear mode of action on aquatic organisms, but toxicity is largely attributable to Cu^{2+} (Sandrini et al., 2009), that forms complexes with other ions and many useful proteins (Nusseyet al., 1995). Changes in the amount of free Cu^{2+} in solution will affect the amount of copper that is bioavailable and hence become toxic (Welsh et al., 2008). A reduction in water dissolved oxygen, hardness, temperature, pH, and chelating agents can change the Cu^{2+} toxicity (Nusseyet al., 1995). Organic and inorganic substances can easily complex the cupric form of copper, which is the most common speciation of this metal, and it's then adsorbed on to particulate matter. The chemical speciation of copper ions strongly depends on the pH of water. Copper, in water, precipitates at high pH (alkaline) and is thus not toxic, whilst at low pH (acidic) it is mobile, soluble and toxic (Nusseyet al., 1995). The main difference in copper toxicity between mammals and fish concerns environmental uptake, occurring almost exclusively through the gills in fish. This organ is the important site of toxic insult and important in the start of compensatory responses (Pelgrom et al., 1995).

1.6. Biomarkers

Traditionally, chemical analysis was the principal approach in assessing environmental impacts and setting water quality standards (Hallare et al., 2005; Kohler et al., 2007). It measures ambient contamination concentrations to assess the pollution level, and also the health status of aquatic organisms in the environment (Hallare et al., 2005). Nevertheless, chemical analysis does not show the bioavailablity of environmental pollutants and thus only little information can be provided on the potential or actual biological effects or environmental damage caused by the contaminants (Hook and Fisher, 2001). Using the water quality parameters collected merely from chemical analysis to portray the biological and ecological condition of the aquatic system, in many cases, inaccurate predications are resulted (Adams, 2002).

Therefore, an idea of using the molecular biomarker for prompt assessment of water cytotoxicity was also proposed earlier. Biomarkers have been defined by Nation Research Council as 'xenobiotically induced variations in cellular or biochemical components or proceses, structures, or functions that are measurable in a biological system or sample' in 1987. They are classified as marker of exposure to a toxicant, markers of effects and markers of susceptibility to the effects of exposure. The use of biomarkers in environmental pollution assessment enables monitoring of stress responses ranging from biochemical to the population and community level (Lagadic et al., 1994).

As to the biomarkers for monitoring the copper contamination, it has been found several proteins had the potential to act as biomarkers, such as catalase, heat shock proteins (HSPs), and metallothionein (MT) (Airaksinen et al., 2003; Dang et al., 1999). However, most of these proteins were not specifically responsed to the copper

contamination. For example, the MT can be induced by other metals, including cadmium, lead (Chan, 1995). And the heat shock proteins can also regulated by many other factors (Chen et al., 2004). Therefore, it is important to find several proteins, which can be act as biomarkers to specially monitor the copper contamination.

The potential for multiple markers, using high throughput methods such as proteomics, transcriptomics and other methods is being investigated. Proteomics technology offers significant potential for the identification of novel Cu biomarkers particularly in relation to the analysis of Cu-transporting or Cu-binding proteins in both healthy individuals and those with Cu-related conditions (Park et al., 2009; Smyth et al., 2009). There are specific technological problems associated with the investigation of metalloproteins, including analysis at low concentrations and the inherent instability in response to environmental changes. Consequently, isolation of Cu-containing proteins in physiological conformations is particularly challenging. The ability of these techniques to screen the entire proteome of a cell may ultimately facilitate the identification of biomarker(s) with no obvious role in Cu metabolism. Potentially, a protein-product substantially down-stream from processes clearly related to Cu metabolism may provide an unexpected component of the 'suite' of Cu biomarkers. Ultimately, a combination of 'standard' proteomics and transcriptomics technologies in conjunction with a range of innovative metal detection techniques will be required to drive the search for robust copper biomarkers.

1.7. Effects of copper on fish

Copper is an essential micronutrient and Cu^{2+} acts as a co-factor in multiple enzymatic processes but is potentially toxic to aquatic organisms. While copper ions are

present in all aquatic environments, multiple anthropogenic activities may result in elevated concentrations, increased exposure, and potential toxicity to aquatic organisms.

1.7.1. Copper toxicity in fish

At the cellular level, Cu^{2+} inhibits the sodium/potassium-ATPase, caused lipid peroxidation, and produced morphological damage, leading to disturbances in sodium the vertebral column occurred. According to (Lewis and Dickson, 1971), damage to the gill and head area of fish, could probably cause mucous to accumulate on the gill area and the formation of edema of gill filaments. This could then lead to respiratory problems, which in turn affects the fish even more negatively resulting in stress and eventually death. A decrease in heart rate (bradycardia), ventilation increases and anaemia may occur, whilst the locomotor activity increases, although glycogen content of liver and muscle is reduced. Copper exposure could also reduce fish growth, often with impacts to specific growth rates most evident during initial exposure times (Clearwater et al., 2002). It also interferes with branchial ion transport and affects various blood parameters such as plasma ion concentrations, hematologic parameters, and enzyme activities in blood and liver (Sappal et al., 2009). Cu^{2+} may also cause immunosuppression, vertebral deformities and neurological disorders in tilapia (Bettini et al., 2006).

1.7.2. Mechanism of acute copper toxicity in fish

The mechanism of acute copper toxicity to fish is well known and can be easily explained by direct target organ effects of Cu^{2+}. Copper concentrations of the order of

10–150 μg/l (0.16–2.3 μmol/l) or more are acutely toxic to fish in soft water (e.g. 24 h LC_{50} for rainbow trout, *Oncorhynchus mykiss*, is 90 μg/l total Cu, (Taylor et al., 2000). Toxicity is generally reduced by increasing water hardness, addition of humic substances, and changes in pH so that both free Cu^{2+} ions at low pH and cationic hydroxides at high pH ($CuOH^{+}$ and $Cu_2OH_2^{2+}$) cause toxicity (Grosell et al., 2007).

The primary target organ for aqueous exposure is the gill epithelium, which suffers an acute oedema and epithelial lifting during exposure. This oedema is probably initiated by Cu^{2+}-dependent inhibition of the branchial Na^+K^+-ATPase (Li et al., 1998) leading to solute accumulation in the epithelial cells and the consequent osmotic influx of water into the cells. This initial disruption is then followed by a general loss of ionoregulatory control by the gill, efflux of electrolytes from the blood over the gill epithelium, resulting in cardiovascular collapse and death (Pelgrom et al., 1995; Pilgaard et al., 1994). A moderate hypoxia due to gill injury probably also contributes to the latter stages of toxicity. The acute toxicology for dietary exposures to Cu has somewhat different etiology, but the end point is the same. It may involve protracted vomiting, resulting in ionoregulatory and acid–base disturbances, and eventually leading to severe lesions of the foregut which ultimately cause death via gastro-intestinal haemorrhage (Handy et al., 1999).

1.7.3 Mechanism of chronic copper toxicity in fish

Environmental quality standards (EQS) protect fresh waters from acute Cu contamination (e.g. in the EU the EQS for Cu is 1 μg/l in soft freshwater) and it is rare for Cu concentrations to exceed more than a few μg/l (or 0.1 μmol/l) in fresh waters

(Brix et al., 2001). Chronic effects of Cu around the EQS are, therefore, more environmentally relevant. Chronic toxicity estimates vary between fish species, life stage, and water quality; but values between 2 and 14 μg/l (0.03 - 0.22 μmol/l) are typical for freshwater fish (Brixet al., 2001). Arguably the longest and most comprehensive chronic effects study to date is that of (Mckim and Benoit, 1971) which explored sub-lethal effects over 18 months in brook trout (*Salvelinus fontinalis*). Some studies reported a maximum acceptable toxicant concentration between 17.4 and 9.5 μg/l of total copper in relatively soft water. In a subsequent study on the same species (Mckim and Benoit, 1971) reported 'no adverse effect' of 9.4 μg/l (0.15 μmol/l) total Cu based on survival, growth, and reproductive end points. There are relatively few chronic toxicity data for dietary Cu exposures, the lethal dose for rainbow trout is higher than 10 g Cu/kg food and sub-lethal effects occur between 1000 and 500 mg Cu/kg food (Handyet al., 1999; Kamunde et al., 2001).

The notion that responses to chronic Cu exposure are more a matter of physiological and metabolic adjustment, rather than a consequence of simple target organ toxicity are illustrated by adjustment to Cu homeostasis itself in the organs of fishes. Aqueous Cu accumulates in several tissues during chronic exposure including the gill, liver, kidney; and to a lesser extent in the muscle (McGeer et al., 2000; MCKIMet al., 1971). Whilst these target tissues are broadly the same as acute exposures, in chronic exposure fish have more time to down-regulate Cu uptake across the gills and re-distribute newly acquired Cu to the liver for excretion (Grosell et al., 1997; Grosell et al., 1998) to minimize toxic effects. The above work by Grosell's group also showed that fish shares important similarities with mammals: (i) fish regulates whole body Cu status using the

liver as central compartment for controlling excretion and circulating Cu concentrations, and (ii) hepatic excretion of Cu is stimulated by chronic sub-lethal exposure. Whole body Cu status in fish is also a function of body size. Adult fish are able to regulate tissue Cu concentrations to lower levels than smaller juvenile fish of the same species (e.g. muscle, (Grosellet al., 2007). Both the temporal adjustment of Cu distribution and excretion, and apparent body-mass dependence of these events suggested a well regulated physiological process in fish.

In addition to the control of whole body Cu status itself, many other physiological processes are modified during chronic Cu exposure. They include altered cellularity (both cell type and turnover) in the gut or gill epithelium (Berntssen et al., 1999), transient changes in ionoregulatory physiology, modified redox status (Baker et al., 1998), altered immunity (Dethloff and Bailey, 1998), reduced swimming speeds to preserve metabolic scope for aerobic metabolism, or modified aerobic metabolism to preserve swimming performance, and altered reproductive strategy.

1.7.4 Copper and oxidative damage

Many of these responses are in part due to Cu's high reactivity with H_2O_2 and potential to undergo redox reactions to form reactive oxygen species (ROS), a process known as the Fenton reaction. The resulting cellular damage can be in the form of membrane lipid peroxidation, DNA damage, and protein carbonyl production (Powell et al., 2005). Like other organisms, fish combat elevated levels of ROS with protective ROS-scavenging enzymes, such as superoxide dismutase (SOD) and catalase (CAT) that convert the superoxide anions into H_2O_2 and further into H_2O and O_2, respectively. Once

these enzymes are overwhelmed by excessive ROS production, irreversible cellular damage and death can occur.

In turn, ROS effect in cells has also evolved a complex mechanism, known as DNA repair system, to reduce the yield of mutations and chromosomal aberrations. This complex cellular system acts at three levels: (a) arresting the cell cycle to allow time for DNA repair; (b) triggering the signal transduction events to activate the repair components; and (c) directly reversing, excising or tolerating DNA damage via constitutive and induced activities (Begley and Samson, 2004). If DNA damage is not repaired, cells undergo complex enzymatic reactions that might lead to apoptosis, necrosis or other forms of cell death (Nyberg et al., 2002).

1.8 Fish models

1.8.1 Tilapia

Nile tilapia is one of the most important freshwater finfish in world aquaculture, and a very important species in global capture fisheries (Balirwa, 1992). Among the numerous regions now inhabited by Nile tilapia, many are under threat from metal pollutants including copper (Khallaf et al., 2003). Nile tilapia was found to be a good bioindicator as it could withstand the adverse conditions within the minimum period (4 weeks) of active biomonitoring (Birungi et al., 2007). Active biomonitoring is a good tool for monitoring water quality as it integrates responses to combinations of all contaminants thereby indicating overall effect in a water body.

In Hong Kong, tilapia is very common and widely distributed in inland waters, kei wais and estuarine regions (Shen et al., 1998). The tilapia (*Tilapia mossambica*) was introduced from East Africa into local reservoirs in the 1950s. Nowadays, they are widely distributed in local water courses and *Tilapia mossambica*, also known as *Oreochromis mossambicus*, is the dominant species found in local watercourses, especially the rehabilitated areas. The Shing Mun River is one of the major contaminated rivers and estuarine regions in Sha Tin (population over 580000) with two major industrial estates: Fo Tan and Tai Wai. Comparing different sites in Hong Kong, Fo Tan was found to have a relatively high metal contents in tilapia with up to 449 ppm (dry weight) copper (Zhou et al., 1998). Sediments collected from Fo Tan was also mostly polluted by copper, zinc, nickel, cadmium and chromium (Zhou et al., 1998, HKEPD, 1995). Another independent study also found high copper contents in liver and gills of tilapia collected from Fo Tan (Shen et al., 1998). No significant differences in metal contents were found in male and female tilapia, mean wet weight copper content was 328 ppm (standard deviation was 181 ppm) in liver of tilapia collected in Shing Mun River (Shen et al., 1998).

Tilapia was also found to be a copper resistant fish with 24 h and 96 h half lethal concentrations (LC50) of 2.8 ppm and 1.5 ppm respectively, after comparing with other species of fish as shown in table 1.2. For example, carp is a copper sensitive species with its 24 h and 96 h LC50 value of only 200 ppb and 50 ppb respectively (Lam et al., 1998). Liver and gill metallothionein mRNA levels in tilapia were also found to be sensitive biomarker of metal exposures with both injection and aqueous exposures (Lam et al., 1998; Cheung et al., 2004).

Table 1.2. The LC50 values of Cu^{2+} to different species of fish

Fish Species	LC 50 values	References
Tialpia (*Oreochromis mossambicus*)	2.8 ppm (24 h) and 1.5 ppm (96 h)	Lam et al., 1998
Common Carp (*Cyprinus carpio*)	200 ppb (24 h) and 50 ppb (96 h)	Lam et al 1998
Rainbow trout (*Oncorhynchus mykiss*)	20 ppb (96 h)	Eyckmans et al., 2010
Gibel carp (*Carassius auratus gibelio*)	150 ppb (96 h)	Eyckmans et al., 2010
Sea bream (*Sparus sarba*)	2.36 ppm (24 h) and 1.36 ppm (96 h)	Wong et al., 1999
Zebrafish (*Danio rerio*)	64 ppb (96 h)	Chen and Chan, upublished data

Until now, there have been some researches about the ecotoxicology of copper study in Tilapia. It was found that chronic dietary copper has more toxicity than waterborne copper exposure (Shaw and Handy, 2006). The tilapia recovering from dietary Cu exposure needed 63 days, but recovering from waterborne Cu exposure just needed 10 days. And some studies focused on copper uptake in tilapia larvae found that the copper concentration accumulated in tilapia larvae become steady for 96 h exposed in copper (Wu et al., 2007). Gills were the first organ to be targeted by heavy metal exposure: liver was the major site of accumulation, biotransformation and excretion of xenobiotic compounds, and intestines were also the important tissue in copper uptake. For example, it was found that the concentrations in liver and gill were much higher than that in the muscle after different copper concentration exposure (Table 1.3). As to metal interaction in tilapia, it was found that external Ca^{2+} and Na^{+} would enhance of Cu^{2+} resistance in fish, but reversely, exposure to sub-lethal concentrations of Cu^{2+} would decrease the content of Ca^{2+}, and increase the content of Na^{+} (Wu et al., 2007). It was thought that this interaction might be related to competition in binding with the same metal

transporter.

Table 1.3. Mean copper concentrations in the tissues of *Tilapia zillii* exposed to copper for 14 days (Ay et al., 1999)

Exposure (ppb)	Muscle (ppm)	Gill (ppm)	Liver (ppm)
Control	5.38	7.58	29.7
0.5	4.33	39.4	158.8
1	5.79	71.4	228.1

1.8.2 Zebrafish

The zebrafsh (*Danio rerio*) has traditionally been used as both an animal model for molecular genetics of development and aquatic toxicology research (Hill et al., 2005). It offers a significant advantage since they have small size and easy to expose them to different concentrations of chemicals in the laboratory with large numbers of individuals per experiment. Furthermore, embryonic development is external, outside the mother, providing access to all phases of development and making it possible to observe morphological changes associated with exposure to toxicants in the environment. Embryo-larvae of zebrafish is proven to be a sensitive and reliable model to study the toxic effects of sediments and pollutants such as metal ions and other chemicals (Li et al., 2004; Chan et al., 2006; Fraysee et al., 2006). Zebrafish is also proposed as a model for human disease (Perry et al., 2010).

In the zebrafish ovary, maturation of the oocytes is accompanied by accumulation of copper in the yolk, reaching amounts of 3.5 ng/oocyte by the late vitellogenic stages (Riggio et al., 2003). After fertilization, copper concentrations increased at 512-cell stage but declined gradually to normal level similar to 2-cell stage at 5 h post-fertiliazation, suggesting that there is excretion and possibly metal exchange with

the environment (Riggio et al., 2003). With this type of approach we may study the mechanisms by which copper enters the organism in early development, and whether certain levels may disturb the development of specific body structures.

Besides, many genes previously known from other organisms to be critical for copper homeostasis and transport were identified in the zebrafish, either by in silico examination of the genome or expressed sequence tag databases or by deliberate cloning of homologs. To date, only a handful of copper related genes have been characterized by mutation, but zebrafish offers the possibility of analyzing embryonic genes by inhibiting translation with antisense morpholinos, as was the case for the Ctr-1 high-affinity copper transporter (Mackenzie et al., 2004) or lysyl oxidase (Craig et al., 2007b). Transporters, chaperones, and other regulatory proteins (such as the metal-response transcription factor-1 and metallothionein genes) were studied in embryos and larvae only in terms of their expression (Chan et al., 2006; Chen et al., 2002; Chen et al., 2004). Likewise, most proteins that require copper as a cofactor for their activity are found in the fish, and some of these are characterized. Therefore, given the great genetic potential of the zebrafsh, it should be possible to approach the identifcation of the molecules and proteins involved. Such findings would also have immediate application to human physiology since, as mentioned above, copper homeostasis genes seem to be highly conserved throughout multicellular organisms.

1.9 Aims of this study

Previous studies showed that the mechanism of copper toxicity was mainly related to the oxidative effects on cellular molecules, and the studies of copper toxicity mainly

focused on several well known proteins and genes, such catalase, metallothionein, Cu/Zn SOD, etc (Table 1.3) (Kimet al., 2008a). A complete map of the mechanism of copper toxicity is still lacking. The use of proteomic approaches, which allow the large scale mining of the interesting proteins, would help us to a get more concrete proteins' profile related to copper toxicity. Tilapia is a metal tolerant species, and reversely, the zebrafish is metal sensitive. It is believed that by comparing the proteomic profile of tilapia and zebrafish's proteins, it would also help us to understand the mechanism of copper tolerance and sensitivity of the two species of fish.

The copper homeostasis and transportation pathways have been revealed principally, and several important copper binding proteins and transporters have been also identified (Table 1.4). However, a full picture of copper homeostasis remains unclear because other copper related proteins are still unknown, and many copper-binding proteins for copper transfer to mitochondria, and nuclear are not studied yet (Michelle and Thiele, 2008). In fact, copper ion is known to be able to bind with many proteins if not all in the cell, therefore, it is important to identify additional novel copper-related proteins and uncover the functions and relationships of copper-binding proteins and confirm if they bind copper specifically or non-specifically. Metalloproteomics refers to the identification and detailed characterization of metal-binding proteins and their metal binding motifs. Since most metals pass through the liver for detoxification, hepatocytes are ideal for the study of proteins involved in intracellular heavy metal metabolism. Determining this distinct proteome in the liver will help uncover novel components of copper transport and extend our understanding of the cellular mechanisms of copper intoxication.

Table 1.4. Example of copper binding proteins and copper homeostasis proteins (Kim et al., 2008).

Protein	Function
Amyloid precursor protein (APP)	Protein involved in neuronal development and potentially Cu metabolism; cleavage leads to generation of Aβ peptide that aggregates in senile plaque associated with Alzheimer's disease
Atox1	Metallochaperone that delivers Cu to ATP7A and ATP7B Cu^{+} transporters
ATP7A	Cu^{+}-transporting P-type ATPase expressed in all tissues except liver
ATP7B	Cu^{+}-transporting P-type ATPase expressed primarily in the liver
Carbon monoxide dehydrogenase to acetyl-CoA synthase	Moorella thermoacetica bifunctional enzyme; reduces CO2 to CO with subsequent assembly of acetyl-CoA
Ceruloplasmin	Serum ferroxidase that functions in Fe3+ loading onto transferrin
Coagulation factors V and VIII	Homologous pro-coagulants present on the surface of platelets, where they nucleate the assembly of multiprotein proteolytic complexes involved in blood coagulation
CCS	Metallochaperone that delivers Cu to Cu/Zn SOD
CopZ	Archaeoglobus fulgidus [2Fe-2S] and Zn2+-containing Cu chaperone
Cox17	Metallochaperone that transfers Cu to Sco1 and Cox11 for cytochrome oxidase Cu loading in mitochondria
Ctr1	High-affinity Cu^{+} transporter involved in cellular Cu uptake
Cu/Zn SOD (SOD1)	Antioxidant enzyme, catalyzes the disproportionation of superoxide to hydrogen peroxide and dioxygen
Cytochrome c oxidase	Terminal enzyme in the mitochondrial respiratory chain, catalyzes the reduction of dioxygen to water
Dopamine β-hydroxylase (DBH)	Oxygenase, converts dopamine to norepinephrine
Ethylene receptor (ETR1)	Member of a plant receptor family that uses a Cu cofactor for ethylene binding and signaling
Hemocyanin	Oxygen transport protein found in the hemolymph of many invertebrates such as arthropods and molluscs
Hephaestin	Transmembrane multi-Cu ferroxidase; involved in iron efflux from enterocytes and macrophages
Glucose oxidase	Pentose phosphate pathway oxidoreductase that catalyzes the oxidation of D-glucose into D-glucono-1, 5-lactone and hydrogen peroxide
Laccase	Phenol oxidase involved in melanin production
Lysyl oxidase	Catalyzes formation of aldehydes from lysine in collagen and elastin precursors for connective tissue maturation
Metallothionein	Cysteine-rich small-molecular-weight metal-binding and detoxification protein
Peptidylglycine-α-amidating mono-oxygenase (PAM)	Catalyzes conversion of peptidylglycine substrates into α-amidated products; neuropeptide maturation
Prion protein (PrP)	Protein whose function is unclear but binds Cu via the N-terminal octapeptide repeats
Steap proteins/Fre1/Fre2	Family of metalloreductases involved in Fe3+ and Cu^{2+} reduction
Tyrosinase	Monophenol mono-oxygenase; melanin synthesis
XIAP	Inhibitor of apoptosis through binding and catalytic inhibition of several caspases

While measured concentrations of chemical contaminants were generally below acutely toxic levels for fish, potential sub-lethal toxic effects resulting in, e.g. energy reallocation or behavioral abnormalities are of our major concerns to study the toxic effects of copper ions. Sub-lethal effects are difficult to detect in the field, but they may decrease the evolutionary fitness of fish populations (Scholz et al., 2000; Sorensen, 1991; De Vlaming et al., 2000; Sandahl et al., 2005). As copper contamination in the environment is getting more and more serious, it is also important to verify several biomarkers of effects genes to monitor the copper contamination in fish. Existing biomarker genes include catalase, heat-shock proteins, MTs, and the like, all may act as biomarkers of effects or exposures to copper stress (Airaksinen et al., 2003; Dang et al., 1999). However, these genes' regulation was found not very specific to the copper contamination, but also related to other chemicals, such as cadmium, dioxin, et al. Therefore, it is necessary to find some other biomarkers and develop a novel biomarkers' system to monitor the copper contamination together, and make the results more sensitive, comprehensive and specific. In a nutshell, the aims of this thesis research are to identify copper-related proteins and copper binding proteins in fish models using a proteomic approach. Further more, gene expression study of in vitro and in vivo experiments was also used to verify the responses of the identified proteins at their gene expression level with sensitive real-time PCR.

Specific objectives of this project are:

1. To identify novel proteins related to mechanism of copper tolerance using in vitro cell model and exposure experiments on tilapia;
2. To identify novel copper binding proteins and proteins related to detoxification and

intoxication mechanism of copper toxicity using in vivo fish exposure experiments using tilapia;

3. To identify novel proteins related to mechanism of copper sensitive using in vitro cell model of zebrafish;
4. Understand how copper ions affect the gene expression of copper transporters.

Chapter 2

Changes in the protein expression profiles of the Hepa-T1 cell line when exposed to Cu^{2+}

2.1. Introduction

Copper is an essential element, but it can have a number of potentially toxic effects on cells. It has been well-characterized that excessive copper levels lead to the production of hydroxyl radicals (OH·), which can damage phospholipids and enzymes (Huster et al., 2007; Turski and Thiele, 2009). Both prokaryotic and eukaryotic cells have developed a tight cellular control mechanism for copper homeostasis, with a complex machinery of proteins that bind the metal ion and thus control its uptake, transport, sequestration, and efflux of copper (Harrison et al., 2000; O'Halloran and Culotta, 2000; Puiget al., 2002a).

Despite the identification of many copper-related proteins, the full picture of copper homeostasis remains unclear because the functions and relationships of these proteins are still unknown, and many copper-binding proteins still need to be investigated (Turski and Thiele, 2009). Therefore, it is important to identify additional novel copper-related proteins and uncover the functions and relationships of copper-binding proteins. Some of these, such as catalase, heat-shock proteins, MTs, and the like, may be suitable to act as biomarkers of effects for monitoring copper contamination in the environment (Airaksinen et al., 2003; Dang et al., 1999). In recent years, a number of new techniques, such as transcriptomics-based DNA microarrays (Lange and Ghassemian, 2005) and proteomics, have been developed to evaluate environmentally induced protein changes in living organisms. Proteins are the primary effector molecules of all living systems,

and therefore virtually any adaptive response to environmental, physiological or pathological conditions will be reflected by alterations in protein activity, location and concentration (Bradley et al., 2002; Shepard et al., 2000).

Tilapia (e.g. *Oreochromis niloticus*) is commonly found in local ponds, rivers and estuarine regions, and are relatively (e.g., compared with carp) resistant to copper (Lam et al., 1998). We have used this fish model specie to study the induction of MT gene expression by metal ions. In this section, we would like to explore other biomarkers of effects from copper intoxication and a tilapia cell-line from liver (Hepa-T1) is chosen for this study to uncover proteins up-regulated and down-regulated by copper intoxication.

2.2. Materials and methods

2.2.1 Cell culture

Hepa-T1 is an adherent tissue hepatocyte cell line with epithelial-like morphology isolated from tilapia. It was purchased from the Cell Bank at the Riken BioResource Centre (Japan) and maintained in a standard culture medium comprising 50% L-15 medium, 35% DMEM and 15% Hams F12 and supplemented with 1.5 g/l sodium bicarbonate, 15 mM HEPES, 0.01 mg/ml insulin, 50 ng/ml EGF, 5% heat-inactivated fetal bovine serum and 1% penicillin/streptomycin, according to the supplier's protocol.

2.2.2. Cytotoxicity assay

Hepa-T1 was first seeded on 96-well plates with a cell density of 10×10^4 per well and incubated overnight. The medium was then removed, and the cells were exposed to media with different concentrations of Cu^{2+} (copper chloride, $CuCl_2 \cdot 2H_2O$, analytical grade) for 96 h. After metal exposure, the medium with Cu^{2+} was removed, and a 100 µl

medium with 10% alamar Blue was added into the wells and incubated for 1 hour. The culture plate was wrapped with aluminum foil during incubation to avoid photolysis of the alamarBlue. Fluorescence was measured with a Tecan Polarion microplate fluorescence reader (Tecan) with an excitation wavelength of 485 nm and an emission wavelength of 595 nm. The fluorescence readings of the wells with cells were corrected with blank readings without cells. The percentage of cytotoxicity was calculated using the fluorescence readings of the control and treatment.

After determination of the 96 h LC50, the Hepa-T1 were divided into three groups: a control group without the addition of metal and two metal-exposed groups to which were added two different concentrations of Cu^{2+} (20% and 50% of the 96 h LC50 values). After 96 h, the cells were lysed with trypsin briefly, washed with a PBS buffer and collected in a 15 mL falcon tube. They were then centrifugated at 1,500 Xg for 3 min. The suspension was discarded, and the cell pellets were washed with PBS three times by re-suspension and centrifugation. The harvested cells were then stored at -80°C until use.

2.2.3. Annexin-V/PI assay and cell cycle analysis

The Hepa-T1 cells were treated with 120 μM and 300 μM of Cu^{2+} for 96 h. The apoptotic and necrotic rates were determined with an Annexin-V-Fluos staining kit (BioSource International Inc., USA). The cells were incubated in Annexin-V-FITC and a PI labeling solution for 30 min after staining and were then washed and analyzed using a BD FACSCanto Flow Cytometer (BD Bioscience, NJ, USA). To analyze the distribution of Hepa-T1 in the cell cycle under different treatment conditions, the cells were briefly trypsinized, washed with PBS and fixed in 75% ethanol at 4°C for at least

18 h. They were then incubated for 30 min in a DNA-staining buffer that contained 200 μg/ml ribonuclease A (Sigma-Aldrich) and 5 μg/ml propidium iodide (PI, Sigma-Aldrich). For each sample, 10,000 PI stained cells were captured, and those in different phases of the cell cycle were expressed as a percentage of the total number of cells counted.

2.2.4 Isolation of the cytosolic fraction

The treated Hepa-T1 cells were thawed at room temperature and suspended in a 200 uL lysis buffer (25 mM tris-HCl, 2 mM DTT, 20 μM PMSF, pH 7.4). They were then lysed by ultrasonic fragmentation at 4°C for 10 min, followed by quick freezing in liquid nitrogen and re-thawing at room temperature three times to lyse them completely (Specter et al., 1997). The sample was then centrifugated at 1,500 Xg for 10 min. The supernatant was further centrifugated at 105,000 Xg for 60 min to collect its cytosolic fraction (Spector et al., 1997). All centrifugations were processed at 4°C. Finally, the protein concentration was determined using Bradford protein assay (Bio-Rad) with bovine serum albumin as the standard, and that of each sample was then adjusted to 2 mg/ml and stored at -80°C in aliquots.

2.2.5. Two-dimensional gel electrophoresis (2-DE)

The cytosolic samples were mixed with a rehydration buffer comprising 8 M urea, 2 M thiourea, 4% CHAPS, 0.5% ampholyte (pH 3-10, GE Health), 50 mM dithiothreitol and 0.01% bromophenol blue as the tracking dye. The isoelectric focusing (IEF) step was carried out using Ettan IPGphor (GE Health). Precast immobilized pH gradient (IPG) strips (ready-strip IPG strips, pH range 3-10, 13 cm long, GE Health) were rehydrated

with 250 uL (50 ug) of total protein and incubated for 12 h at 20°C with 30 V, followed by IEF steps of 2 h at 500 V, 1 h at 1000 V, gradient elevating to 8000 V for 2.5 h and 8000 V continued for 1 h. After the IEF steps, the IPG strips were incubated at room temperature for 15 min in an equilibration buffer (50 mM Tris-HCl [pH 8.8], 6 M urea, 30% glycerol, 2% sodium dodecyl sulfate [SDS], 1% DTT) that contained 0.01% bromophenol blue. A second equilibration step was carried out for another 15 min under the same conditions, except that the dithiothreitol was replaced with 135 mM iodoacetamide. The equilibrated strips were then loaded onto 12% polyacrylamide (14 × 16 cm, 1 mm thick) with SDS and a stacking gel of 2 cm of 4% polyacrylamide gel placed on top. The IPG strips were sealed with 1% low melting point agarose to ensure good contact with the gel. The second dimension of the SDS-polyacrylamide gel electrophoresis (SDS-PAGE) was carried out using an SE 600 Ruby Electrophoresis Unit (GE Health) at room temperature with a Tris-Glycine buffer (25mM Tris, 192 mM glycine and 0.5% SDS) at a constant power of 50 uA per gel until the tracking dye had reached the bottom of the gel. After separation, the proteins were visualized by staining the gels with silver stain, as recommended by the manufacturer (GE Health).

The 2-DE images were scanned and analyzed using ImageMaster 2-D Elite software. The image spots were initially automatically outlined and matched, and then manually edited. The intensity volume of each spot was processed bybackground subtraction and total spot volume normalization, and the resulting spot volume percentage was used for comparison.

2.2.6. In-gel digestion and protein identification

The protein spots of interest were manually excised from the 2-DE gel. Each protein

sample was further processed by enzymatic digestion with trypsin to generate peptide fragments (Cayatte et al., 2006). The tryptic peptides were mixed with acyano-4-hydroxycinnamic acid (CHCA) of 4 mg/mL in 50% ACN and 0.1% TFA, spotted onto the target plate and allowed to dry. MALDI-TOF MS was performed with a 4700 Proteomics Analyzer (TOF/TOF™) (Applied Biosystems, USA) equipped with a 355 nm Nd:YAG laser. The instrument was operated in a positive ion reflection mode of 20 kV accelerating voltage and in a batch mode of acquisition control. Reflector spectra were obtained over a mass range of 800-3000 Da. All of the mass spectra were internally calibrated with ACTH peptide and peaks of trypsinized alcohol dehydrogenase. Peptide mass mapping was carried out using the MASCOT program (Matrix Science, London) with the Swiss-Prot database and GPS explorer software (Applied Biosystems). During the database search, one missed cleavage *per* peptide was set as the maximum allowance, and a mass tolerance of 0.5 Da and an MS/MS tolerance of 0.1 Da were also used according to predefined optimized protocols. Other possible variations, such as carbamidomethylation for cysteine and oxidation for methionine, were also taken into account. Tryptic autolytic fragments and notable contamination were removed from the dataset manually before the database fragment search.

2.2.7. Real-time quantitative polymerase chain reaction (PCR)

The changes in identified protein expression following the administration of Cu^{2+} with different concentrations of copper ions were verified using real-time quantitative PCR methods. A real-time quantitative PCR was performed in a thin-wall 8-tube strip with the Chromo 4™ Four-Color Real Time System (MJ Research®); the GAPDH (Glyceraldehyde 3-phosphate dehydrogenase) gene was used as the internal control for

standardization.

Total RNAs were extracted using the TRIzol reagent (Invitrogen, Carlsbad, CA) from the 1×10^8 Hepa T1 cells with or without metal treatment, and cDNAs were synthesized using ImProm-II™ Reverse Transcription (Promega). SYBR® Green PCR Master Mix (Applied Biosystems) was used for the real-time PCR analysis. The sequences of the forward and reverse primers for the identified genes are shown in Table 1. The PCR primer sets for these genes were designed by using the online real-time PCR Primer Design tool (https://www.genscript.com/ssl-bin/app/primer), and the primers were synthesized by In Vitrogen. The amplification condition of the real-time quantitative PCR for the genes was optimized before further investigation and analysis. The Ct value is the number of PCR cycles required to be higher than the predetermined threshold value of 0.002 for SYBR® Green intensity. The Ct value of GAPDH for each sample was subtracted from the corresponding Ct value of each gene as ΔCt, and the value was normalized against the respective control treatment as ΔΔCt. The relative expression of each gene was calculated as the equation: Relative fluorescence = $2^{\Delta\Delta Ct}$.

Table 2.1. Nucleotide sequences of primers used in the real-time quantitative PCR assay.

Gene	Primer	Sequence
Cytochrome P450 1A (CYP1A)	Forward	5'-ATCTGYGGHATGTGCTTYGGCCGRCGCTA-3'
	Reverse	5'-TGCCACTGRTTGATGAAGACRCAKGTGTC YTTGG-3'
Vitellogenin (Vtg)	Forward	5'-GAATGTGAATGGGCTGGAAATAC-3'
	Reverse	5'-TTTGTTTGATCTGGATGTCAGCTT-3'
NADH dehydrogenase subunit 4L	Forward	5'-TTTATTGCCCTTTCCCTCTG-3'
	Reverse	5'-CGAGCAGTAGCGACGAGTAG-3'
Cytochrome c oxidase subunit II	Forward	5'-TAATTCTCATTGCCCTTCCC-3'
	Reverse	5'-TAAGAGTCGAAGCCGAGGTC-3'
Glyceraldehyde 3-phosphate dehydrogenase	Forward	5'-ACCACGAAAAGTACGACAGGTCA-3'
	Reverse	5'-CGGCCATCTCTCCACATTTTAC-3'
Actin	Forward	5'-GTGACGTCGACATCCGTAAG-3'
	Reverse	5'-TGATCTCCTTCTGCATCCTG-3'
Interleukin-1 alpha	Forward	5'-AGAGCATTGTGGAAGCACAG-3'
	Reverse	5'-TGGAGAAGAACCAAGCTCCT-3'
Growth hormone (GH1)	Forward	5'-TTTCACCAAGGCTGTCTGAG-3'
	Reverse	5'-GTTGCCTCCCAGACTTTGAT-3'
SUMO-1	Forward	5'-ATGTCAGACACGGAGACCAA-3'
	Reverse	5'-TCCTGACCGATCACTTTGAG-3'
ATP synthase subunit beta	Forward	5'-TGAGGCTCTCAGGGAGATTT-3'
	Reverse	5'-GGTTACCCAGGCACTTCACT-3'
Myoglobin	Forward	5'-CTGGGATTTCTCAGGGTGAT-3'
	Reverse	5'-GTGTATTGGCCAGTGGTTTG-3'
Zic family member 1	Forward	5'-CGAGCTTGTGACCCATCTAA-3'
	Reverse	5'-GCTTTGAATGGCTTTCCTTC-3'
Zinc finger protein 60	Forward	5'-GACGGTACCGGTCACTACCT-3'
	Reverse	5'-TCTGTTGATGCCGTTCATCT-3'
MHC class II antigen	Forward	5'-CTCCGAACATCCCAGAACTT-3'
	Reverse	5'-TACCAGTCCAGTTGCTCAGG-3'
Insulin-like growth factor-I	Forward	5'-TCAGATACACGGTGCCAAAT-3'
	Reverse	5'-GCGGCTCACACTCTTACAAA-3'
Proteasome	Forward	5'-GTCTGCAACTGTAGGGCTGA-3'
	Reverse	5'-TCCAGCAATGGAGATACCAA-3'
Parvalbumin beta	Forward	5'-ATTGAGGAGGAGGAGCTGAA-3'
	Reverse	5'-CATCACCATCACTGTCACCA-3'
Metallothionein (MT)	Forward	5'-TGCAAGAGCTGCAAGAAGAG-3'
	Reverse	5'-TGTCGCATGTCTTTCCTTTG-3'

2.2.8. Functional classification

The functional classification of the proteins modulated by Cu^{2+} treatment among the different metabolic pathways and subcellular locations was based on Ingenuity Pathways Analysis (IPA) (Ingenuity Systems, http://www.ingenuity.com). IPA mapped each modulated protein to its corresponding gene object (e.g., genes, mRNAs and

proteins) in the Ingenuity Pathways Knowledge Base (IPKB). These gene objects, called "focus genes," were overlaid onto a global molecular network developed from information contained in the IPKB and were used as the starting point to generate the anticipated biological networks based on their connectivity. The functional analysis of each network identified the biological functions and/or diseases that were most significant to the genes in that network. The networks associated with biological functions and/or diseases were considered for analysis. The genes mapped to the biological networks available in the IPKB were ranked by scores indicating the probability that a collection of genes equal to or greater than the number in the network could be achieved by chance alone. A score of 3 indicates that there is a 1/1000 chance that the focus genes are in the network due to random chance. Therefore, genes with scores of 3 or higher can be said not to have been generated by random chance with a 99.9% confidence level. A score of 3 was thus used as the cutoff for identifying gene networks significantly affected by Cu^{2+}.

2.2.9. Statistics

Statistical analyses of the gene expression levels and metal treatments were performed as described in Kennel et al. (2004). For proteomic analysis, the mean protein intensity of the control group was compared to that of each treatment group using the one way Annova Test. Statistical tests were performed at the $p < 0.05$ and $p < 0.01$ levels of significance using Imagemaster Plus (version 7.2, GE Health).

2.3. Results

2.3.1. Copper toxicities

The median lethal concentration (LC50) of Cu^{2+} on the Hepa T1 cell line at 96 h was determined using alamarBlue assay. The dose response curves with 96 h LC50 were plotted using SigmaPlot 10 (Fig. 2.1): that of $CuCl_2$ was 597 μM (95 % confidence interval: 513 uM to 696 uM) and that of $CuSO_4$ was 818 μM (95 % confidence interval: 655 uM to 1023 uM). $CuCl_2$ seemed to be more toxic than $CuSO_4$ and was thus used in this project. Flow cytometry measurement was used to quantify the extent of apoptosis and necrosis in the total cell population, and significant differences were observed between the control and the $CuCl_2$-treated cells. After incubation with different concentrations (120 μM and 300 μM) of $CuCl_2$ for 96 h, the percentage of Annexin-V+/PI+ cells (apoptosis) increased to 1.3% and 3.2%, respectively, compared to 0.0% in the control group. The percentage of Annexin-V-/PI+ cells (necrosis) increased to 10.7% and 18.4%, respectively, compared to 0.0% in the control group. These results demonstrate that $CuCl_2$ primarily induces cell necrosis rather than apoptosis. To determine whether $CuCl_2$ stimulates Hepa-T1 proliferation, the cell cycle distribution was also measured after exposure to different concentrations (120 μM and 300 μM) of $CuCl_2$. It was found that $CuCl_2$ treatment reduced the number of cells in the G0/G1 phase, but increased the percentage of cells in the S and G2/M phases (Fig. 2.2), thus indicating that copper can induce the proliferation of Hepa-T1.

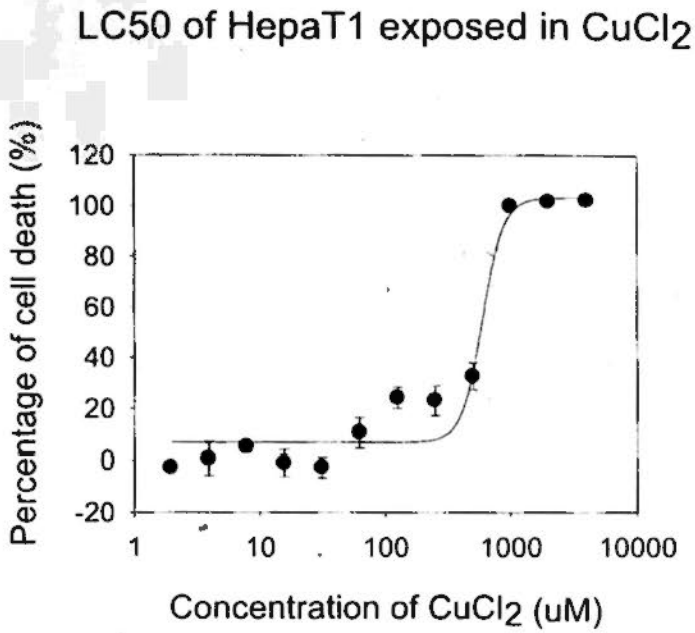

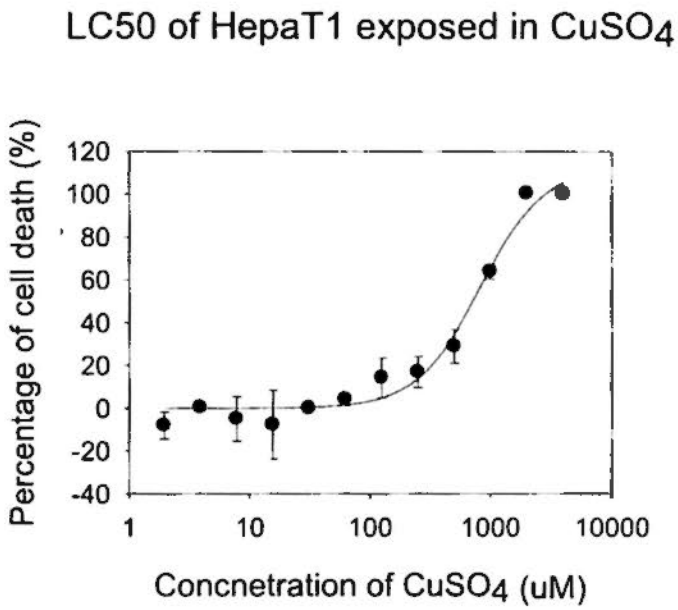

Fig. 2.1. Cytotoxicity (%) of Hepa-T1 cells after $CuCl_2$ and $CuSO_4$ exposure in different concentrations (in log scale) for 96 h. The 96 h LC50 values of $CuCl_2$ and $CuSO_4$ on Hepa-T1 cells were determined as 597 μM and 818 μM. The 96 h LC50 values were calculated using Sigmaplot with non-linear regression.

A

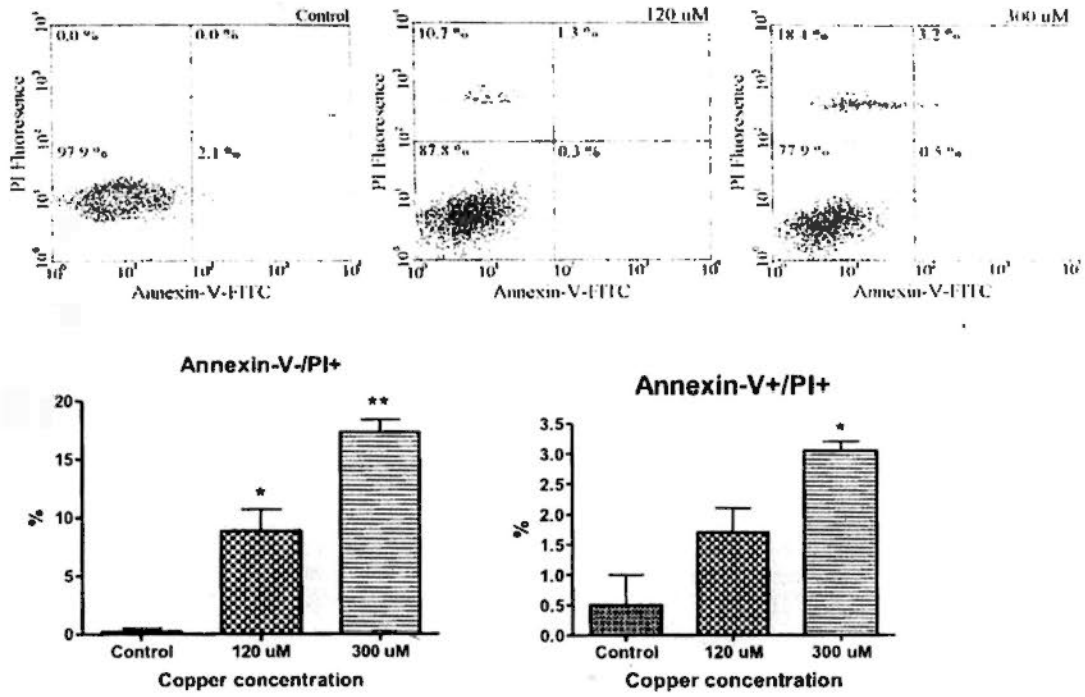
Control
120 uM
300 uM
PI Fluorescence
Annexin-V-FITC
Annexin-V-/PI+
Annexin-V+/PI+
%
Control
120 uM
300 uM
Copper concentration

B

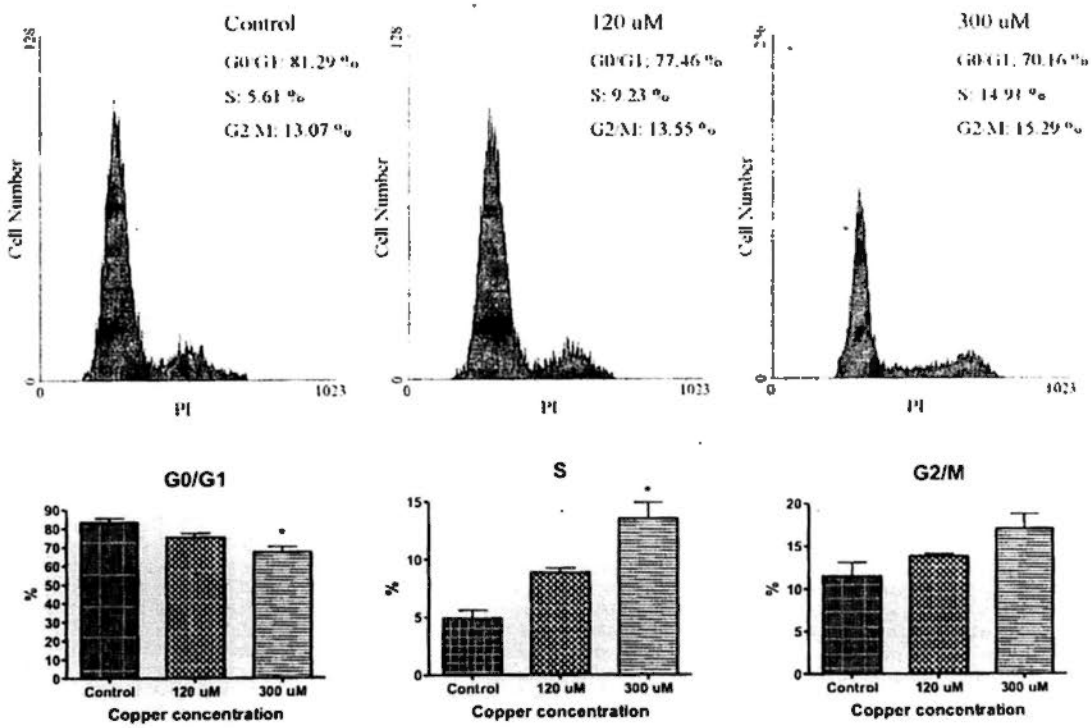
Control
G0/G1: 81.29 %
S: 5.61 %
G2/M: 13.07 %
120 uM
G0/G1: 77.46 %
S: 9.23 %
G2/M: 13.55 %
300 uM
G0/G1: 70.16 %
S: 14.98 %
G2/M: 15.29 %
Cell Number
PI
G0/G1
S
G2/M
%
Control
120 uM
300 uM
Copper concentration

Fig. 2.2. CuCl2-induced apoptosis and necrosis with Annexin-V-FITC and PI staining. Panel A. The upper panel shows the detection of $CuCl_2$-induced apoptosis and necrosis with Annexin-V-FITC and PI staining. The Hepa T1 cells were exposed to different concentrations of $CuCl_2$ for 96 h. After being stained with Annexin-V-FITC and PI, the cells were analyzed using flow cytometry. LL: Annexin-V-/PI-cells (normal); LR: Annexin-V+/PI-cells (early apoptosis); UR: Annexin-V+/PI+ cells (late apoptosis); UL: Annexin-V-/PI+ cells (necrosis). The data shown are representative of three independent experiments. Statistic analysis of the apoptosis cells and necrosis cells among the total population was shown in bar graph (% of cells in each phase relative to the total population). **Panel B**. The lower panel shows the flow cytometry analysis of the cell cycle. After $CuCl_2$ exposure for 96 h, the cells were collected, fixed and incubated with PI as described in Materials and Methods section. The cells were then subjected to flow cytometry analysis, and 10,000 cells in each sample were counted. Quantitative analysis of the distribution of cells in cell cycle was shown in bar graph (% of cells in each phase relative to the total population). G0/G1: cells in quiescent or early G1 phase; S: cells in DNA synthesis phase; G2/M: G2 and mitotic population. These figures show the representative results of three experiments. (*$p<0.05$, **$p<0.01$, derived from Mann-Whitney test).

2.3.2. 2-DE gel analysis of cytosolic proteins

The cytosolic proteins extracted from the control cells and $CuCl_2$-treated (120 μM and 300 μM) Hepa-T1 cells were analyzed by 2-DE. Approximately 2,000 protein spots were detected on the 2-DE gels. A representative protein profile of the Hepa-T1 cells treated with 120 μM of $CuCl_2$ is shown in Fig. 2.3. In total, 125 proteins were found to be regulated by $CuCl_2$ exposure with a clear dose-response, of which 93 were identified using mass spectrometry protein identification (MALDI-TOF MS and/or MS/MS). The details of each indentified protein, including the identification number on the gel, the accession number, the protein name and the ratio of treatment to control for each dose level, are listed in Table 2.2. In most cases, the experimental Mw and pI values from the 2-D gels were in agreement with the theoretical Mw and pI values of the proteins. Thus, the protein spots were identified with a high degree of confidence.

The magnitude of the ratio changed from 0.00051 down-regulation (Ig heavy chain, Spot No. 3298) to 201.2 up-regulation (Preprotein translocase subunit secG, Spot No. 3205). Of the proteins identified, few (e.g., Spot Nos. 1983 and 2089) were located in an unexpected position on the gel, based on their Mw and pI theoretical values. Any changes in Mw and pI can most probably be attributed to posttranslational protein modifications, such as proteolytic cleavage, glycosylation and phosphorylation. Furthermore, a number of different protein spots were identified as being the same protein. For example, Spot Nos. 2154 and 2340 were identified as a growth hormone precursor. They may be degradation products or different isoforms of the same protein. Thus, out of the original 125 spots selected for identification, a total of 93 individual proteins were identified.

2.3.3. Verification of gene expression by quantitative PCR

To verify the regulation of the proteins identified after copper exposure, real-time quantitative PCR was used to analyze that regulation at the level of mRNA accumulation. A total 18 genes that had their sequences in the tilapia database were chosen for this analysis. Those chosen are shown in Table 2.2 in yellow. As can be seen in Fig. 2.3B, except for cytochrome P450IA (CYP1A1) and Small ubiquitin-related modifier I precursor (Sumo-1), the regulation of most of the genes at the RNA level was in accordance with the regulation of the proteins shown in Fig. 2.4A. This result further confirms our confidence in the proteins identified through the proteomic approaches. Interestingly, the fold regulation of the genes was lower than that of the protein regulation, which suggests that, in addition to gene regulation, there are also various levels of regulation during protein synthesis, e.g., translational, post-translational and post-transcriptional regulation. For instance, CYP1A may be affected by the transcriptional activities of the Aryl-hydro carbon (Ah) receptor, which may be inhibited by copper ions. However, the mRNA produced may be enhanced by translational control to produce more proteins.

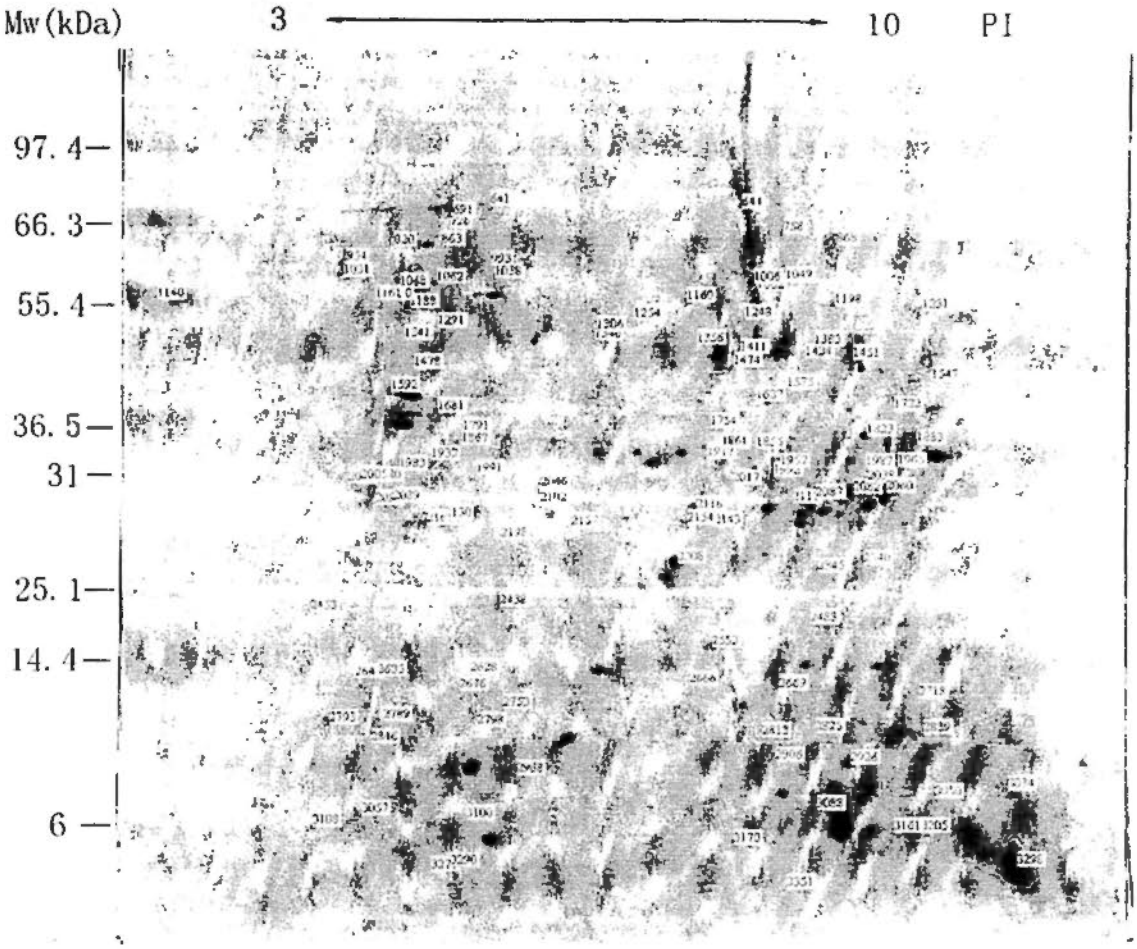

Fig. 2.3. 2-DE gel images of the cytosolic proteins obtained from the Hepa T1 cell line in the 120 μM CuCl2 treatment group. The total cytosolic proteins were loaded and separated using IPG strips (pH 3-10)/SDS-PAGE (12% acrylamide). The gels were stained by silver staining. The green cycled spots represent the matched spots in these three gels, and the spot numbers refer to the proteins with a modified accumulation level after $CuCl_2$ treatment that were selected for mass spectrometry identification (the details are summarized in Table 2.2).

A

B

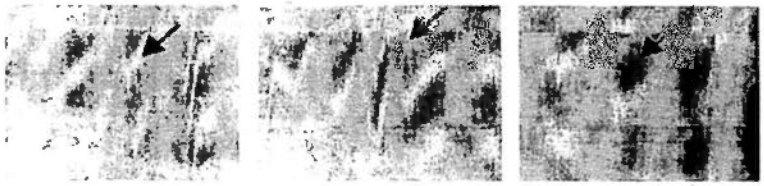
Control
120 uM
300 uM

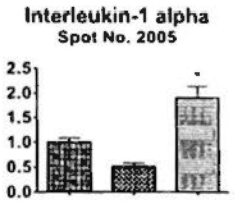
Interleukin-1 alpha
Spot No. 2005
2.5
2.0
1.5
1.0
0.5
0.0

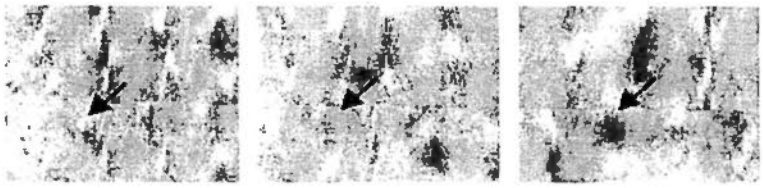
Control
120 uM
300 uM

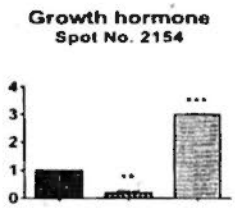
Growth hormone
Spot No. 2154
4
3
2
1
0


Control
120 uM
300 uM

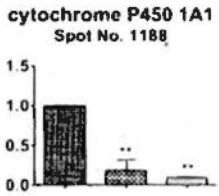
cytochrome P450 1A1
Spot No. 1188
1.5
1.0
0.5
0.0


Control
120 uM
300 uM

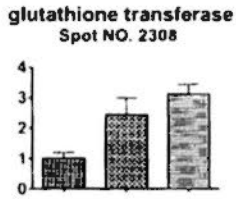
glutathione transferase
Spot NO. 2308
4
3
2
1
0

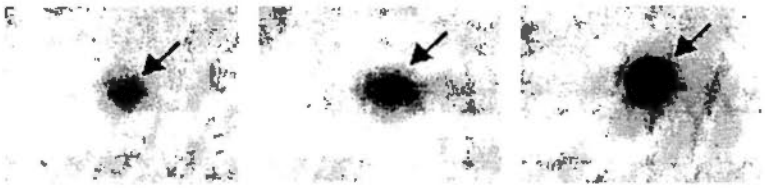
Control
120 uM
300 uM

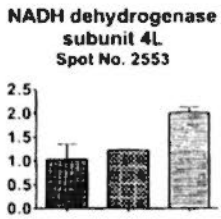
NADH dehydrogenase
subunit 4L
Spot No. 2553
2.5
2.0
1.5
1.0
0.5
0.0


Control
120 uM
300 uM

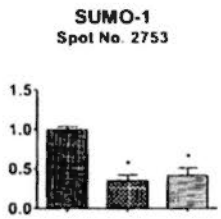
SUMO-1
Spot No. 2753
1.5
1.0
0.5
0.0

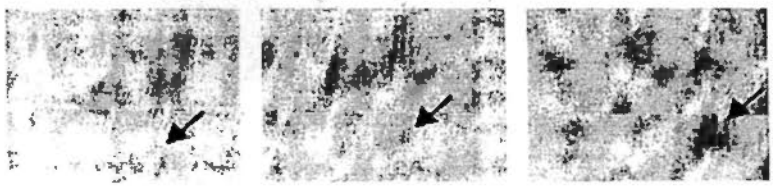
Control
120 uM
300 uM

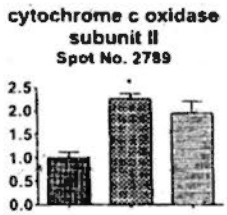
cytochrome c oxidase
subunit II
Spot No. 2789
2.5
2.0
1.5
1.0
0.5
0.0


Control
120 uM
300 uM

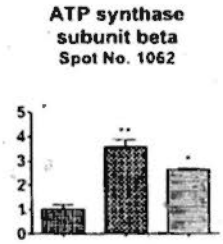
ATP synthase
subunit beta
Spot No. 1062
5
4
3
2
1
0

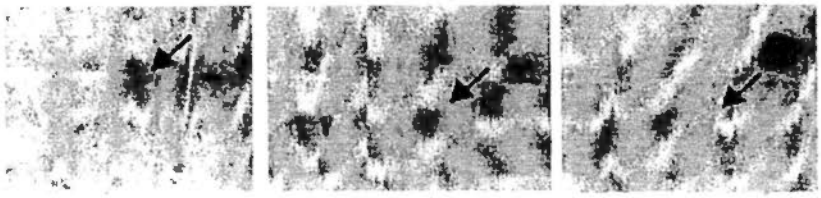
Control
120 uM
300 uM

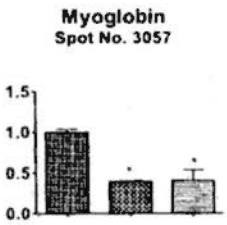
Myoglobin
Spot No. 3057
1.5
1.0
0.5
0.0

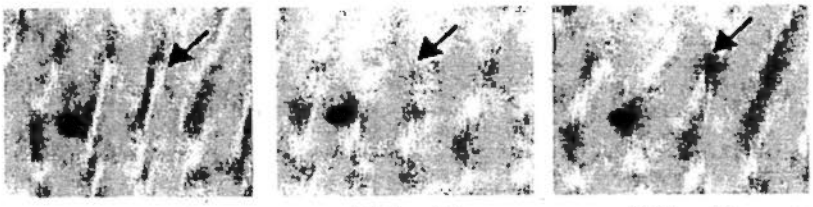
Control
120 uM
300 uM

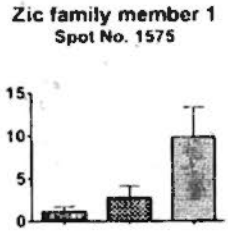
Zic family member 1
Spot No. 1575
15
10
5
0


Control
120 uM
300 uM

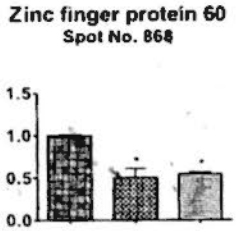
Zinc finger protein 60
Spot No. 868
1.5
1.0
0.5
0.0

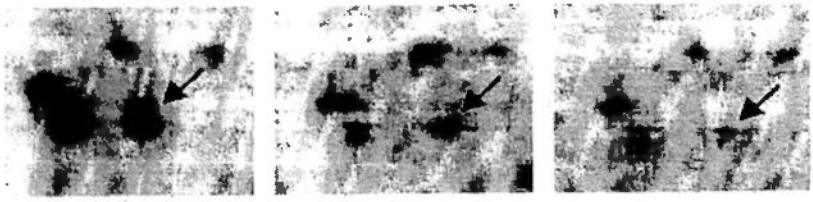
Control
120 uM
300 uM

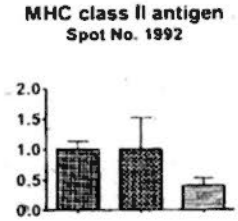
MHC class II antigen
Spot No. 1992
2.0
1.5
1.0
0.5
0.0

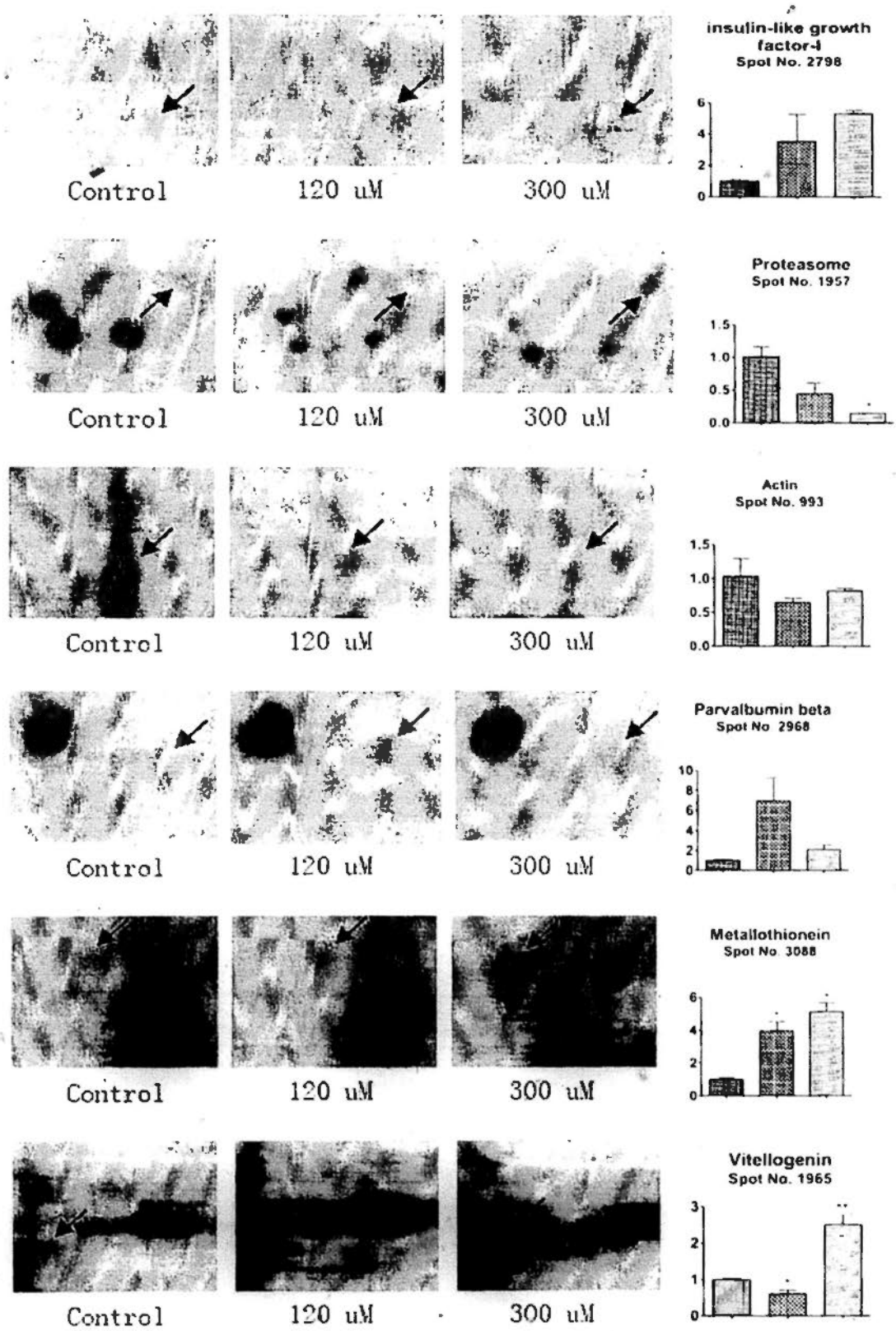

Fig. 2.4. Effects of increasing the $CuCl_2$ concentration on the regulation of proteins and

their related genes with tilapia sequences in the database. (A) Zoom-in regions of typical 2-DE demonstrate the effect of increasing the $CuCl_2$ concentration on the regulation of these proteins. (B) Real-time quantitative PCR results of the genes' regulation through the effects of increasing the $CuCl_2$ concentration on Hepa-T1 cells. The concentrations of $CuCl_2$ increase from left to right (the left column is the control group; the middle column is the 120 uM $CuCl_2$ treatment group; and the right column is the 300 uM $CuCl_2$ treatment group) (*$p < 0.05$, **$p < 0.01$, ***$p < 0.001$, derived from the Mann-Whitney test of individual gene regulation.)

2.3.4. Protein function analysis

Functional classification, according to cellular processes and the subcellular location of the identified proteins, was performed using IPA (Ingenuity Systems, http://www.ingenuity.com). The 93 differentially expressed proteins (Table 2.2) were searched with their corresponding access numbers for their exact gene counterparts in IPA. These gene counterparts and their respective levels of change were then uploaded to the IPA module. IPA mapped the 68 modulated proteins at the $CuCl_2$ high-dose level for their corresponding gene objects (e.g., genes, mRNAs and proteins) in the IPKB. The focus genes for 64 of the 68 modulated proteins were overlaid onto a global molecular network developed from information contained in the IPKB. The networks of these focus genes were then algorithmically generated based on their connectivity. Biological pathways were assigned to each network and ranked according to the significance of the biological function for that network. Four of the ten networks identified were found to be highly significant, in that they had more of the identified proteins present than would be expected by chance (Table 2.3, Fig. 2.5).

The toxic and biological functions of these focus genes were also analyzed by IPA. As the cell line was derived from tilapia liver, we focused only on hepatoxicity. Five toxic functions were identified as significant ($p < 0.05$): liver hepatomegaly, liver damage, liver hypertrophy, liver proliferation and liver necrosis. Lipid metabolism (16%

of the identified proteins) was identified as the main biological function affected. Furthermore, the proteins were also classified into 14 groups according to their functions, which were then analyzed using IPA software (Table 2.3). Twenty-two of the 93 were found to function as enzymes, which suggested that Cu^{2+} exerts its toxicity primarily by affecting enzymes.

2.4. Discussion

The aim of the study reported herein was to identify novel proteins that are related to the mechanisms of copper toxicity and detoxification, as well as protein biomarkers of effects for the biomonitoring of copper stress. As with other types of biological stress, the adaptation to environmental pollution involves changes in protein expression that can be produced specifically in response to a particular contaminant or in a dose-dependent manner. This study is the first of its kind to explore the temporal changes in protein expression in tilapia that are associated with copper intoxication in liver cells. The levels of more than 100 cytosolic proteins were affected by 300 μM of $CuCl_2$, of which 93 were identified by MALDI-TOF MS combined with MS/MS. The relationship between some of these proteins, including metallothionein, catalase and cytochrome C oxidase (Atli et al., 2006; Chan et al., 2006; Craig et al., 2007), and copper intoxication has been confirmed, which also confirms the reliability of our results. IPA has also been identified as a powerful tool for analyzing networks of proteins. Using IPA and IPKB, the regulated proteins were found to be involved in ten networks, four of which had three or more focus genes and are considered to be "major" networks.

The first network contains 21 focus genes that are involved in connective tissue development and functioning, skeletal and muscular system development and

functioning, and tissue development. In this network, the growth hormone (GH) and insulin-like growth factor I (IGF-1) genes seem to play central roles in the regulation of other genes for growth and development. Growth hormone is a polypeptide hormone that stimulates growth and cell reproduction in vertebrates, and IGF-1 is a major hormonal regulator of growth and development in somatic tissues. The induction of GH and IGF-1 in this study supports the theory that copper may stimulate the growth of Hepa-T1, which is also supported by the flow cytometry experiment in which it was found that $CuCl_2$ induces the proliferation of Hepa-T1. In bony fish, the IGF-1 released from the liver under the control of pituitary GH is the main endocrine regulator of growth, maintenance and development, and the amount of IGF-1 circulating regulates the synthesis and release of GH (Eppler et al., 2007b). In human beings, a decline in GH-1 and IGF-1 contributes to increased oxidative stress in the hippocampus, which means that these two hormones may be mediated by increasing the cellular redox potential, thus resulting in a reduction in the oxidative stress caused by the Cu^{2+} ions.

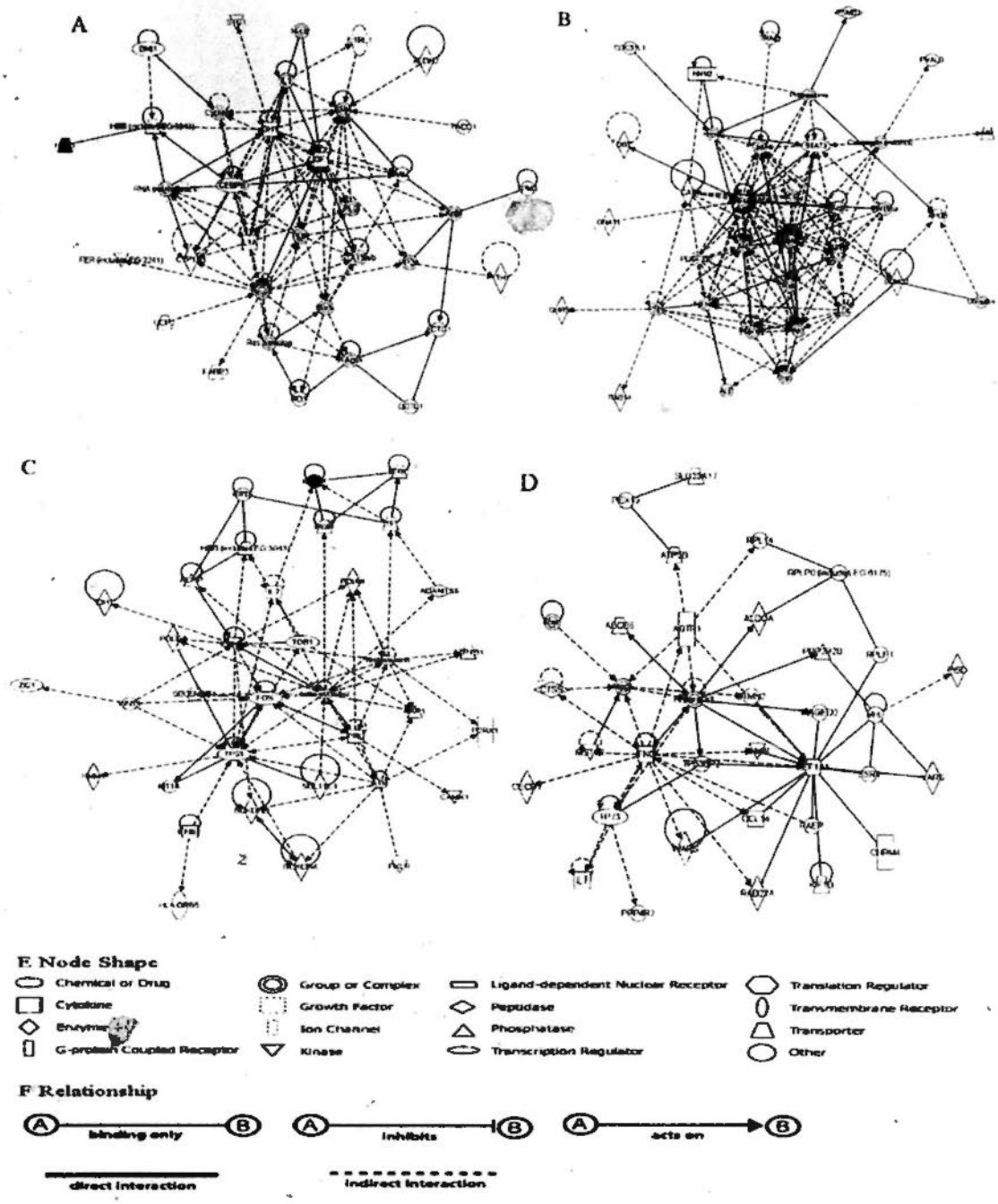

Fig. 2.5. Dynamic pathway/network modeling of the Hepa T1 proteome afforded by integration of the protein/gene data to the Ingenuity Pathway Analysis software from Ingenuity Systems. The intensity of the shading increases with the magnitude of the change. In the online color version, green represents a decrease, and red indicates an increase. The shaded or colored nodes are derived from the 2D-MALDI-TOF MS/MS identified protein data set, whereas the white nodes are inserted by the IPA program. The complete gene product names are listed in Table 2.2. A: Network 1; B: Network 2; C: Network 3; D: Network 4; E: Nodes are displayed using various shapes that represent the functional class of the gene product; F: Relationship between nodes.

Another branch of network 1 is involved in vimentin (VIM), actin (ACTIN) and tropomyosin (TPM3), which are associated with the structure/functioning of the cytoskeleton. $CuCl_2$ is found to reduce the expression of actin and to induce that of TPM3 and VIM. Actin is one of the most abundant proteins in cells, being a fundamental component of the cytoskeleton in muscle and non-muscle cells. It represents 12-15% of the total protein in most non-muscle cells and about 30% of that in muscle cells (Kekic and Dos Remedios, 1999). It is also present in all eukaryotic cells, and most organisms have several genes encoding this protein. The actin monomer (G-actin) is a soluble, globular protein with 43 kDa of molecular mass that polymerizes to form insoluble filaments (F-actin). Oxidative stress can cause severe F-actin disruption in different cell types. The Cu^{2+} treatment of cultured human intestinal Caco-2 cells decreases F-actin staining (Ferruzza et al., 1999), and hemocytes of *M. galloprovincialis* exposed to Cu^{2+} also suffer a drastic decrease in actin filaments (Fagotti et al., 1996). The oxidative-stress mediated alteration of Cu^{2+} homeostasis has been proposed as a probable mechanism of actin cytoskeleton disruption (Dalle-Donne et al., 2001; Gomez-Mendikute et al., 2002).

High Cu^{2+} concentrations activate a number of proteases, which can hydrolyze the actin filaments and the proteins anchoring them to the cell membranes. Post-translational modifications opposite to those previously discussed for the putative tropomyosin isoform may yield myosin isoforms with little variation in their *pI*s, some of which may appear under oxidative stress. Iinterestingly, tropomyosin 3, which is also an important cytoskeleton protein, was found to be up-regulated in this study. There are different tropomyosin isoforms that interact with actin, both in muscle and non-muscle cells, and they may have different responses to Cu^{2+}. Thus, in this study, the exposure of Hepa-T1

to Cu^{2+} induced TPM3 and repressed actin, which suggests that metal ions can alter the cytoskeleton ultra structure and cell adhesion dynamics.

The second network demonstrates several of the responses that are involved in the functions of lipid metabolism, molecular transport, and small biochemical signalling molecules, these were the top three functions in which the most differentially expressed genes were involved, including a number of major genes. The down-regulation of apolipoprotein may indicate the repression of lipid metabolism by $CuCl_2$, as apolipoprotein B is the primary apolipoprotein of low-density lipoproteins and is responsible for carrying cholesterol to the tissues (Richardson et al., 2005). A similar result was also reported by Huster et al. (2007), who found that copper can down-regulate lipid metabolism, particularly cholesterol biosynthesis. In addition, two important genes, proteasome subunit (prosome, macropain, beta type, 7).and ubiquitin, act on aprolipoprotein both directly and indirectly. It is possible that apolipoprotein is involved in the ubiquitin-proteasome pathway, which is essential for many fundamental cellular processes, including the cell cycle, apoptosis, angiogenesis and differentiation (Orlowski and Dees, 2003). The down-regulation of proteasome subunit, which has also been confirmed in a recent study (Milacic et al., 2008), likely reduces the expression of apolipoprotein and leads to necrosis in Hepa-T1, as shown in Fig. 2.2A.

The main functions of the third network are related to cellular growth and proliferation, cancer, and reproductive system disease Interestingly, we found a number of metal-binding proteins and transporters in this network, which indicates that these proteins may also be involved in these functions. Selenium-binding protein 1 (SELENBP1) has been found to be related to multiple types of cancer (Huang et al., 2006). Selenium is an essential nutrient that exhibits potent anti-carcinogenic properties,

and deficiency in it may cause certain carcinogenic diseases. The other important metal-binding proteins found in this network were MTs. Many experimental data suggest that MTs may provide protection against metal toxicity, be involved in the regulation of physiological metals (e.g., Zn^{2+} and Cu^{2+}) and provide protection against oxidative stress (Lam et al., 1998; Cheuk et al., 2008). Recent studies have also found increased MT expression in certain types of cancer (Ostrakhovitch et al., 2007). Therefore, the induction of SELENBP1 and MTs by $CuCl_2$ indicates that $CuCl_2$ may pose a risk by inducing cancer or cell growth and those metal-binding proteins may play an anti-cancer role.

The fourth network contains several nodes exhibiting changes that may be related to DNA replication, recombination and repair. The Rplp0 protein is a type of ribosome protein that is reported to be involved in DNA repair (Lindstrom, 2009). The up-regulation of the ribosome protein by copper has been found in other organisms (McIntosh and Bonham-Smith, 2005), which indicates that copper may influence DNA repair. In the left branch of this network, elongation factor 1-alpha (EEF1A1) takes the central role in regulating other genes and is responsible for the enzymatic delivery of aminoacyl tRNA to the ribosome. Recently, it was also proposed that it regulates DNA replication and repair by binding with proliferating cell nuclear antigen (PCNA) (Toueille et al., 2007). The up-regulation of EEF1A1 has also been reported to be in response to the inhibition of mitochondrial DNA expression in chicken cells (Wang and Morais, 1997), which indicates that its down-regulation should stimulate DNA replication. This conclusion further confirms the flow cytometry results in this study, which showed cell division (Fig 2.2). Tryptophanyl-tRNA synthetase (WARS) was found to be down-regulated, which may catalyze the aminoacylation of rRNA by its

cognate amino acid. Network 4 also shows that WARS can bind with EEF1A1, which indicates that the down-regulation of these two genes may also influence protein transcription after $CuCl_2$ exposure.

2-DE gel electrophoresis proved to be a reliable and powerful tool for evaluating molecular changes in Hepa-T1 cells after the administration of Cu^{2+} ions, although the technique does have certain limitations. For example, proteins with a high molecular weight or with pI values that fall at the extremities of the pH gradients (i.e., very acidic or basic proteins) are difficult to resolve in gel. Furthermore, it is well-known that certain classes of protein or those of low abundance are underrepresented in classic 2-DE (Gorg et al., 2004; Rabilloud et al., 2002). The analysis of low-abundance proteins could probably be improved by fractionation and purifying the various cell types before proteomic analysis (Ahmed and Rice, 2005). The use of the IPA tool also allowed us to overcome these limitations. More specifically, the identification of the altered protein spots, the analysis of networks and the description of the functional relationships between gene products reported in the literature all provided clues as to the other gene products that are also altered by Cu^{2+} treatment, but cannot be detected by 2-DE. The combination of protein profiles and IPA investigation may help to identify new genes that are altered by Cu^{2+} treatment and provide further insights into the toxic mechanisms of Cu.

In conclusion, 93 proteins were found to be differentially expressed, some of which may be suitable as biomarkers of effects to monitor copper contamination in the environment, especially the 18 that were further confirmed by real-time quantitative PCR. Some of these 18 proteins, including metallothionein, glutathione transferase and cytochrome c oxidase, are well-known biomarkers for metal contamination. In addition,

other proteins were also found to be significantly induced or reduced in the mRNA level of the Hepa-T1 cell line after copper exposure, including growth hormone (120 μM, $p < 0.01$; 300 μM, $p < 0.001$), interleukin-1 alpha (300 μM, $p < 0.05$), ATP synthase subunit beta (120 μM, $p < 0.01$; 300 μM, $p < 0.05$), zinc finger protein 60 (120 μM, $p < 0.05$; 300 μM, $p < 0.05$), proteosome (300 μM, $p < 0.05$) and vitellogenin (120 μM, $p < 0.05$; 300 μM, $p < 0.01$). These six proteins may be new biomarkers for copper contamination, and we are currently examining them in an in vivo tilapia fish exposure test to determine the lowest observable effect levels and no observable effect levels of copper concentrations in water. A multiple biomarker monitoring system may also help to detect copper contamination more accurately and specifically.

Table 2.2. Differentially expressed proteins in the cytosolic fraction of Hepa-T1 after $CuCl_2$ treatments at 120 and 300 μM.

No.	Protein Name	Access No.	MW (Observed as dalton/Calculated KDa)	PI Obs./Cal.)	Matched genes	120 μM	300 μM
Cytokine							
2005	Interleukin-1 alpha precursor	IL1A_RAT	30953/32.3	5.47/4.2	IL1A	5.51	14.42
2154	Growth hormone precursor	Q5J3Q3_ACASC	23222/29.2	6.96/7.0	GH-1	1.5	3.28
Enzyme							
1188	Cytochrome P450 1A1	gi|13620980	34148/57	4.87/4.6	CYP2C19	1.83	3.53
1356	Cat eye synrdrome chromosome region, candidate 1	gi|76780837	57945/47.8	5.87/7.1	CECR1	3.74	10.23
1917	Retinal arylalkylamine N-acetyltransferase	gi|3978551	27875.4/35.1	7.72/7.2	AANAT	7.23	11.46
1983	Catalase	gi|9972785	59906/33.7	8.12/4.5	CAT	4.86	6.48
2046	Allantoicase	ALLC_DANRE	44580/31	7.26/5.7	ALLC	1.08	13.93
2099	RAB14, member RAS oncogene family	gi|41393147	24091/30.4	5.84/4.3	RAB14	1.1	2.67
2130	Phosphomannomutase	Q2N6Y7_9SPHN	31940/29.8	5.11/5.0	PMM1	1.5	2.14
2308	GST-e/GST-5; glutathione transferase	gi|1125671	24369/26.3	6.32/7	CHST7	19.13	42.42
2483	Probable short chain dehydrogenase/reductase	Q2L012_BORA1	26031/23.3	7.79/8.1	DHRS3	9.31	23.23
2553	NADH dehydrogenase subunit 4L	Q8HMU7_GYMKI	10767/19.7	6.95/7.2	ND4L	1.66	2.54
2753	Small ubiquitin-related modifier 1 precursor (SUMO-1)	gi|82117159	11536/13.2	5.51/5.3	SUMO1	2.01	8.5
2789	Cytochrome c oxidase subunit II	gi|1552409	16737/12.6	4.7/4.3	COX2	1.38	29.05
758	Dihydrolipoamide branched chain transacylase E2	gi|61806604	54239/71	8.91/8.0	DBT	0.35	0.03
1038	Aldehyde dehydrogenase 2 precursor	gi|20339358	57354.9/60.1	6.05/5.3	ALDH2	0.52	0.23
1068	Prephenate dehydrogenase	gi|89099146	40393/60.1	5.73/4.5	prephenate dehydrogenase	0.65	0.22
1291	Tyrosine hydroxylase 1 (EC 1.14.16.2)	O42428_LATCA	56304/55.4	5.56/4.8	TH	0.78	0.14
1411	Guanin nucleotide binding protein, alpha 11	gi|148227192	42451/49.7	5.75/7.5	GNA11	0.72	0.31
1451	Phosphatidylserine decarboxylase proenzyme	PSD_BORBR	32739/49.7	9.05/8.5	PISD	0.9	0.46
1823	Rab and DnaJ domain-containing protein	RABJ_DANRE	31378/36.5	8.95/8.6	RBJ	0.8	0.44
1855	Tryptophanyl-tRNA synthetase (EC 6.1.1.2)	Q2B8Z6_9BACI	37103/36.5	6.92/7.5	WARS	0.44	0.26

1861	Aldolase-1	gi|6624225	36242/36.5	7.81/7.3	ALDOA	0.52	0.32
1883	Isocitrate dehydrogenase 1 (NADP−), soluble	gi|41393155	48807/36	7.62/9.1	IDH1	0.95	0.44
Transporter							
1062	ATP synthase subunit beta, mitochondrial precursor	ATPB_CYPCA	55329/60.1	5.05/4.8	ATP5B	1.11	3.04
2143	Uncoupling protein 2A	Q2PXW8_ONCMY	33018/29.8	9.67/7.3	UCP2	1.37	2.27
2345	Sodium/potassium-transporting ATPase subunit beta-1	AT1B1_ANGAN	35285/26.8	8.76/8.2	ATP1B1	2	2.87
2793	Fatty acid binding protein 3, muscle and heart	gi|23308625	14872/12.6	5.74/3.8	FABP3	3.18	4.58
3170	Alpha globin	gi|22135540	15634.2/6.6	6.97/7.5	HBA1	59.63	169.5
3290	Hemoglobin subunit beta	HBB_POGSC	16232/6.0	6.11/4.9	HBB	28.62	35.6
1383	Putative ABC transporter ATP-binding protein	gi|149917561	50338/51.6	5.63/8.1	ABCB6	0.4	0.15
1474	PMP1 protein	gi|3176094	32953/44.1	9.55/7.5	SLC25A17	0.27	0.2
2718	Apolipoprotein B	gi|854620	115969/12	5.24/7.6	APOB	0.81	0.059
3057	Myoglobin	MYG_MAKNI	15832/8.7	9.07/4.1	MB	0.97	0.15
Transcription regulator							
1346	Stat3 protein	gi|28277427	48512/53.5	7.15/6.4	Stat3	1.45	6
1575	Zic family member 1	gi|18859577	48937/40.3	8.7/7.9	ZIC1	1.14	2.59
1754	Retinal homeobox protein Rx3	RX3_DANRE	32911/40.2	9.45/7.2	RAX	1.26	6.01
2017	CCAAT/enhancer binding protein beta	gi|42476260	31325/32.3	8.61/7.4	CEBPB	1.27	2.72
868	Zinc finger protein 60	gi|3123237	84714/62.2	9.17/8.4	ZFP60	0.16	0.063
1082	Elongation factor 1-alpha	EF1A_DANRE	50306/58.6	9.16/7.7	EEF1A1	0.68	0.055
1231	Zinc finger protein 547	ZN547_PONAB	47449/55.4	8.81/9.0	ZNF547	0.15	0.065
1637	Polycomb complex protein BMI-1-A (polycomb group RING finger protein 4-A)	gi|158563842	37286/46.7	8.67/7.7	BMI1	0.64	0.38
Kinase							
1987	Stanniocalcin	gi|29170570	28689/33.7	8.62/8.6	STC1	2.08	2.25
2089	Ca^{2+}/calmodulin-dependent protein kinase	A60041	42448/30.4	6.16/4.5	Camk1	2.53	5.97
820	Protein-tyrosine kinase	gi|94969610	77029/66	6.35/4.3	FER	0.67	0.3
1160	Golgin-84	gi|2829746	60794/57	6.55/7.0	GOLGA5	0.7	0.4
1248	Pyruvate kinase	gi|21715946	48750/55.4	6/7.5	PKLR	0.3	0.13
transmembrane receptor							

641	Putative ST2L protein	gi|23477183	67268/79.8	5.84/5.3	ILRL1	1.65	4.24
1992	MHC class II antigen (Fragment).-	Q70XU1_BARIN	26810/32.3	6.43/7.8	HLA-DR B5	0.81	0.23
Growth factor							
2798	Insulin-like growth factor-I	gi|7649259	13584/12.6	9.63/5.2	IGF1	1.02	10.44
G protein coupled receptor							
1732	Type-1-like angiotensin II receptor 1	AGTRL_XENLA	41903/40.2	9.20/8.8	AGTR1	1.42	3.78
Ion channel							
2839	P2x4 receptor	gi|2245576	14461/11.4	8.71/9.0	P2RX1	0.83	0.49
Nuclear receptor							
1031	Pregnane X receptor	gi|185134293	52960/60.1	5.87/4	NR1I2	1.31	5.44
Peptidase							
1957	Proteasome (Prosome, macropain) subunit, beta type, 7.	Q7T002_BRARE	27774/35.1	6.95/7.8	PSMB7	0.59	0.32
1478	Peptidase U62, modulator of DNA gyrase	gi|154151929	48436/47.8	5.53/4.5	SNORD6 2A	0.051	0.022
Cytoskeleton							
1592	Tropomyosin 3	Q803M1_BRARE	28827/44	4.76/4.4	MSDB	2.01	3.68
1791	Vimentin	gi|6226787	52517/36.5	5.13/5.1	TPM3	1.17	18.61
2628	Coactosin-like 1	gi|85719983	10187/16.1	5.48/5.1	COTL1	1.68	9.65
644	Keratin, type I cytoskeletal 9	gi|81175178	62323/70.1	5.19/7.5	KRT9	0.64	0.28
993	Actin, cytoplasmic 1	ACTB1_DANRE	42088/61.6	5.3/5.3	ACTG1	0.14	0.1
1006	Rdx protein	gi|29436484	52265/61.6	8.41/7.7	RDX	0.56	0.1
Metal binding protein							
1254	Selenium-binding protein 1	SBP1_BOVIN	53092/55.4	6.03/6.6	SELENB P1	1.16	3.32
2968	Parvalbumin beta	PRVB_MERME	11346/9.6	4.69/5.5	PVALB	2.57	6.16
3088	Metallothionein	MT_PSEAM	7185/8.1	8.05/8.2	MT1A	3.54	15.3
Others							
954	Similar to transforming acidic coiled coil 1a	gi|125827335	84820/63.2	4.7/4	TACC1	1.76	4.74
1150	HORMA domain-containing protein 1	HORM1_DANRE	41529/60.1	5.97/4.8	HORMA D1	1.29	2.09
1341	Serine/threonine-protein phosphatase 4 regulatory subunit	P4R2A_DANRE	46513/53.5	4.35/4.5	PPP4R2	1.42	3.3

	2-A						
1681	Phytanoyl-CoA dioxygenase domain-containing protein 1	PHYD1_DANRE	33405/42.1	5.39/4.8	PHYHD1	2.66	4.53
1991	Rplp0 protein	gi|29124460	34689.1/33.7	5.73/5.1	RPLP0	2.14	18.03
1965	Vitellogenin	gi|16151381	54419/33.7	7.77/8.9	VTG	2.34	4.16
2060	Hsp90 co-chaperone Cdc37-like 1	CD37L_DANRE	36986/31	5.36/8.8	Rplp0	1.72	2.41
2635	TCR-alpha V segment 1-7	gi|26984612	13621/14.4	4.97/4.3	TRA@	1.57	4.22
3298	Ig heavy chain	gi|195714	13187/6	9.23/9.8	IGHA1	0.96	0.0005
Unmatched proteins							
691	Conserved hypothetical protein	D90207	58607/75.4	6.91/4.9		3.07	3.19
1161	Unnamed protein product	gi|47206711	50785/57	5.8/4.3		1.35	2.67
1306	Nitrilase/cyanide hydratase and apolipoprotein N-acyltransferase	gi|115350687	30714/55.4	6.14/6.2		3.21	10.55
1867	Unknown (protein for IMAGE:5409354)	gi|145337930	35317/36.5	6.8/5		1.19	12.04
2020	Peptide chain release factor 2	gi|110802702	41256/32.3	5.22/4.4		8.41	31.32
2647	Rieske [2Fe-2S] region	Q4NIU1_9MICC	13129/14.4	4.74/4.2		57.67	58.19
2666	Helix-turn-helix motif	Q26UA8_XANP2	10126/14.4	6.26/7.0		1.54	126.5
2669	Oocyte protease inhibitor-1	gi|27461227	9552.6/14.4	8.27/7.8		1.87	5.07
2676	2',3'-cyclic-nucleotide 3'-phosphodiesterase isoform 2 g RICH 70	gi|2121265	13409/13.8	4.1/4.9		1.39	6.8
3100	4Fe-4S ferredoxin, iron-sulfur binding domain protein	gi|156937863	9771/7.8	5.63/5.1		7.3	13.44
3205	Preprotein translocase subunit secG	SECG_IGNH4	6308/6.0	9.69/9.0		48.65	201.2
3351	Ice-structuring protein LP	ANP1_LYCPO	6978/6	8.48/8.0		8.26	19.8
863	CG31104 CG31104-PA	gi|24650005	50075/62.2	5.52/4.9		0.61	0.14
1198	Eukaryotic translation enlongation factor 1 gammar	gi|27545277	50948/55.4	6.97/8.4		0.59	0.44
1547	Similar to gag-pol polyprotein precursor; hypothetical protein, partial	gi|156538901	40155/45.9	8.65/9.1		0.11	0.089
3034	Novel protein	gi|55962650	14682/9.0	6.92/10		0.08	0.0055

Note: The matched genes are the identified proteins that can be found in the Ingenuity Pathways Knowledge Base (IPKB) with Ingenuity Pathway Analysis (IPA) software. Related genes are found for only 68 of the 93 differential proteins. The proteins in yellow have their sequences in the tilapia database, which were chosen for real-time quantitative PCR analysis.

Table 2.3. The Four networks of differential proteins identified by Ingenuity Pathway Analysis.

ID	Molecules in Network	Score	Focus Molecules	Top Functions
1	***ACTG1***, Actin, ***ALDH2***, ***BMI1***, **CEBPB**, **COTL1**, Cyclin A, **CYP1A1**, ERK, F Actin, **FABP3**, ***FER (includes EG:2241)***, **GH1**, **HBA1**, **HBB (includes EG:3043)**, **IGF1**, IL1, **IL1A**, **IL1RL1**, Insulin, N-cor, PI3K, PLC, PP2A, Ras homolog, ***RDX***, RNA polymerase II, Rock, STAT5a/b, **STC1**, **TACC1**, ***TH***, **TPM3**, **UCP2**, **VIM**	47	21	Connective Tissue Development and Function, Skeletal and Muscular System Development and Function, Tissue Development
2	Akt, ALP, Ap1, ***APOB***, Calcineurin protein(s), **CAT**, **CDC37L1**, Creb, **DBT**, **DHRS3**, ERK1/2, FSH, ***GNA11***, hCG, Hsp90, IFN Beta, IL12, Jnk, LDL, ***MB***, NFkB, **NR1I2**, P38 MAPK, PDGF BB, Pkc(s), Proteasome, ***PSMB7***, **PVALB**, **RAB14**, Ras, **STAT3**, **SUMO1**, Tgf beta, **TRA@**, Ubiquitin	27	14	Lipid Metabolism, Molecular Transport, Small Molecule Biochemistry
3	ACPP, ADAMTS5, AKP1, ATP, **ATP1B1**, BCKDHA, BCKDHB, beta-estradiol, **CAMK1**, ERBB2, FOS, **HBB (includes EG:3043)**, ***HLA-DRB5***, ***IDH1***, IFNB1, ***IGHA1***, IL7, ***KRT9***, **MT1A**, ***P2RX1***, PDIA4, PIGR, ***PKLR***, **PMM1**, POLE2, PRL, **SELENBP1**, SULT1E1, testosterone, TF, TFRC, TOB1, TP53, WNT1, **ZIC1**	24	13	Cellular Growth and Proliferation, Cancer, Reproductive System Disease
4	***ABCB6***, **AGTR1**, ***ALDOA***, **ATP5B**, CCL18, **CECR1**, CHRM4, CTSS, ***EEF1A1***, Histone h3, IFNG, IL7, KIF1B, MAGED2, Mapk, MST1R, PAEP, PEX19, PI4KB, ***PISD***, PPP2R2B, **PPP4R2**, RAB27A, Rac, RPL14, RPLP1, **RPLP0 (includes EG:6175)**, ***SLC25A17***, SSR1, STMN2, TP73, TP53BP2, VARS, VHL, ***WARS***	20	11	DNA Replication, Recombination, and Repair, Carbohydrate Metabolism, Lipid Metabolism

Note: The proteins in bold are those modulated by $CuCl_2$ and identified by 2-DE/MS. Those underlined are up-regulated proteins, and those typed in italic are down-regulated proteins. Abbreviations of proteins can be found in Table 2.2. These proteins are called "focus genes." A score of > 3 is considered significant ($p < 0.001$). Abbreviations for other genes are showed as below: ACPP: Prostatic acid phosphatase; ADAMTS5: ADAM metallopeptidase with thrombospondin type 1 motif, 5; AKP1: alkaline phosphatase 1; AKT1: v-akt murine thymoma viral oncogene homolog 1; ALP: alkaline phosphatase 1; Ap1: activator protein 1; ATP: ATPase; BCKDHA: branched chain keto acid dehydrogenase E1, alpha polypeptide; BCKDHB: branched chain keto acid dehydrogenase E1, beta polypeptide; CCL18: chemokine (C-C motif) ligand 18; CHRM4: cholinergic receptor, muscarinic 4; Creb: cAMP response element binding; CTSS: cathepsin S; ERBB2: v-erb-b2 erythroblastic leukemia viral oncogene homolog 2; ERK: extracellular signal-regulated kinase; FSH: Follicle-stimulating hormone; FOS: v-fos FBJ murine osteosarcoma viral oncogene homolog; hCG: Human chorionic gonadotropin; Hsp90: heat shock protein 90; IFN Beta: Interferons Beta; IFNG: interferon, gamma; IL1: Interleukin-1; IL7: Interleukin-7; IL12: Interleukin-12; Jnk: c-Jun N-terminal kinase; KIF1B: kinesin family member 1B; LDL: Low-density lipoprotein; MAGED2: Melanoma antigen family D, 2; MAPK: mitogen-activated protein kinase; MST1R: Macrophage stimulating 1 receptor; NFkB: nuclear factor kappa-light-chain-enhancer of activated B cells; N-cor: Nuclear receptor co-repressor; PAEP: Progestagen-associated endometrial protein; PEX19: Peroxisomal biogenesis factor 19; PDGF BB: Platelet-derived growth factor beta polypeptide homodimer; PDIA4: protein disulfide isomerase family A, member 4; PIGR: polymeric immunoglobulin receptor; PI3K:

Phosphoinositide 3-kinase. PI4KB: Phosphatidylinositol 4-kinase, catalytic, beta; POLE2: polymerase (DNA directed), epsilon 2; PP2A: Protein Phosphatase 2; Pkc: Protein kinase C; PLC: Phospholipase C; PPP2R2B: Protein phosphatase 2 (formerly 2A), regulatory subunit B, beta isoform; PRL: prolactin, RAB27A. RAB27A, member RAS oncogene family; Rac. Rho family of GTPases; Rock: Rho-associated, coiled-coil containing protein kinase. RPL14: Ribosomal protein L14, RPLP1. Ribosomal protein, large, P1, SSR1. Signal sequence receptor, alpha; STAT5a/b: Signal transducer and activator of transcription 5A/B. STMN2: Stathmin-like 2, SULT1E1 sulfotransferase family 1E, estrogen-preferring, member 1, TF: transferrin; TFRC: transferrin receptor; Tgf beta. Transforming growth factor beta; TOB1. transducer of ERBB2, 1; TP53: tumor protein p53; TP53BP2: Tumor protein p53 binding protein, 2; TP73: tumor protein P73; VARS: Valyl-tRNA synthetase; VHL Von Hippel-Lindau tumor suppressor; WNT1: wingless-type MMTV integration site family, member

Chapter 3

Identification of hepatic copper-binding proteins from tilapia

3.1 Introduction

Biosynthesis of "cuproproteins" is dependent on the high-affinity uptake of copper ions from natural environments, regulatory proteins, and other auxiliary proteins. Even so, the mechanism underlying copper homeostasis is still not fully understood (Turski and Thiele, 2009). It is therefore important to identify all copper-binding proteins and uncover their functions and relationships using a proteomic approach. Some identified proteins may be useful biomarkers of effects that allow for monitoring the impact of copper contamination in the environment (Correi et al., 2002; Kehoe et al., 2000). Metalloproteomics refers to the identification and detaile characterization of metal-binding proteins and their metal-binding motifs. Because most metals pass through the liver for detoxification, hepatocytes are ideal for the study of proteins involved in intracellular heavy metal metabolism. Determining the properties of this distinct proteome in the liver will help uncover novel components of copper transport and the toxic mechanisms of copper ion.

We have previously reported copper toxicity and accumulation in tilapia (*Oreochromis niloticus*), and have used the Hepa-T1 hepatocyte cell-line of tilapia to identify novel copper-affected proteins using differential proteomic approaches (Chen and Chan, 2009). Feral tilapia fish collected in the field were found to have high copper content in the liver (Lam et al., 1998; Shen et al., 1998; Zhou et al., 1998). We have also reported the identification of 93 proteins in Hepa-T1 exposed to copper ions which are mainly involved in lipid metabolism, tissue connective development, cell cycle control, etc. (Chen and Chan, 2009). However, we did not positively identify copper-binding

proteins in this *in vitro* study, nor did we carry out similar study *in vivo* using tilapia. This chapter reports a comprehensive assessment of the hepatic cuproproteins of tilapia *in vivo*. We first separated cytosolic proteins into different fractions by fast performance liquid chromatography (FPLC), greatly improving the resolution of our 2-dimensional gel electrophoresis (2-DE) separation in comparison with initial attempts using liver cytoplasm lysate (data not shown). The fractions after FPLC with higher copper concentration were then loaded on copper immobilized metal affinity chromatography (Cu-IMAC) to separate the copper-binding proteins and were subsequently analyzed using 2-DE and proteomic analysis. We hoped to obtain some novel copper-binding proteins and uncover the copper transportation pathway and biomarkers that enable to monitor the copper contamination in the aquatic environment.

3.2. MATERIALS AND METHODS

3.2.1. Tilapia

All-male adult tilapia (*Oreochromis aureus* × *Oreochromis niloticus*) were obtained from a hatchery in mainland China as fry and reared in 60 L glass aquaria, were supplied with dechlorinated, circulated, and aerated local tap water at 26-28 °C under a photoperiod of 14:10 h (day:night), and were fed with commercial fish food pellets in the laboratory for 2-3 years. The fish were treated with $CuCl_2$ by the two methods of copper injection and exposure. To maximize the induction of copper-binding proteins, the fish were intraperitoneally injected with different dosages of $CuCl_2$ solution (100 ppm $CuCl_2$ in 0.9 % NaCl) for 4 days: 0.5 mg/kg on day one, 0.5 mg/kg on day two, 1 mg/kg on day three, and 1 mg/kg on day four. They were then killed to remove their liver tissues on day five (Chan et al., 1989; Chan, 1994). The control group was injected

with 0.9 % NaCl only using the same injection regime. The volume of the solvent was calculated according to the weight of the fish. The liver samples were dissected before being stored at -80 °C for further use. To enable us to detect the regulation of the related genes, the tilapia were also exposed to four different sub-lethal concentrations of $CuCl_2$ (25 ppb, 50 ppb, 100 ppb, and 500 ppb) in several 10 L glass tanks for 96 h, including one control group exposed to tap water only. After aqueous exposure, the liver tissues were dissected and store at -80 °C.

3.2.3. Preparation of cytosolic fractions and protein determination

All steps were carried out at 4 °C. Pooled liver tissue from $CuCl_2$ injected tilapia were weighed and homogenized using a homogenizer in ice-cold 10 mM Tris-HCl (pH 7.4, 3 mL/g tissue) containing 2 % triton X-100, 14.4 mM mercaptoethanol, and 20 uM phenylmethanesulphonylfluoride (PMSF). Cellular debris were removed by centrifugation at 1,500 Xg for 10 min, and after centrifugation at 30,000 Xg for 1 h, the supernatant were stored at -80 °C. Protein concentration was determined by the Bradford method using bovine serum albumin as standard (Compton and Jones, 1985).

3.2.3. Gel filtration and atomic absorbance spectrometry (AAS)

The cytosolic proteins (20 mg) were separated according to their molecular weight using Superdex 75 (HiLoad 16/60 prep grad, GE Health) gel filtration chromatography on AKTA fast protein liquid chromatography (FPLC, GE Health)., Elution of cytosolic proteins was carried out using 10 mM Tris-HCl (pH 7.4) containing 100 mM NaCl, 14.4 mM mercaptoethanol, and 20 uM PMSF. Protein elution was monitored at 280 nM and

254 nM, respectively. Five mL of each fraction separated by a column was then collected. The column was calibrated with standard protein markers: 1 mg/mL BSA (67 kDa), 10 mg/mL albumin from chicken egg white (44 kDa), 1 mg/mL carbonic anhydrase (29 kDa), 10 mg/mL metallothionein (7 kDa), and 10 mg/mL glutathione (0.3 kDa). The copper concentration in alternate fractions separated by AKTA FPLC was analyzed by using AAS (Hitachi Z8100 FAAS) to find the copper-binding proteins containing fractions. Before AAS analysis, 1 mL of each 5 mL fraction was added to 14.5 uL 69 % HNO_3. The elution buffer was used as a blank. Then fractions (peaks) with higher copper concentrations were pooled together and analyzed by IMAC and 2-DE to search for the copper-binding or related proteins.

3.2.4. Western blot analysis

Fractions after FPLC at the same peaks were pooled together and analyzed with 12 % SDS-PAGE gel and visualized by silver staining with PlusOne silver staining kit (GE Health). Di-Golden pre-stained protein markers (10-220 kDa, HOU-BIO Tech, Hong Kong) were used for SDS-PAGE with a 16 kDa lysozyme marker as control for Western blot transfer. After transferring the proteins to a PVDF membrane (Millipore), the blot was blocked with blocking solution (5 % skim milk and 0.1 % Tween 20 in phosphate-buffered saline) then incubated with anti-MT (1:1000 dilution) antibody in blocking solution. The anti-MT antiserum was obtained from a custom-made product from rabbits injected with synthetic peptide of N-terminal amino acid sequence of fish MT, N-MDPCECSKTG-C (Chan, 1994) conjugated to limpet hemocyanin (GenWay Biotechnology, San Diego, USA). Horseradish peroxidase-conjugated secondary antibody (Santa Cruz) was used at 1:5000 dilution and super signal chemiluminescent

substrate (Pierce) was used for detection and signal enhancement. The fluoroimage was obtained using X-ray film (Fuji) and was digitally scanned using ImageMaster 2-D Elite software on a Molecular Imager (STORM 860, GE Health).

3.2.5. Immobilized metal affinity chromatography (IMAC)

Cu-IMAC columns were prepared by using 1 mL HiTrap Chelating HP columns (GE Health) and protein separation was performed on AKTA fast protein liquid chromatography (FPLC, GE Health). Copper was coupled to the column by applying a 50 mM $CuSO_4$, 0.5 M NaCl solution. Excess metal was removed with 4 mL binding buffer (20 mM Na_2HPO_4, 500 mM NaCl, 5 mM imidazole, pH 7.4). The pooled fractions with high copper peaks were first dialyzed with dialysis membrane (MWCO 3kDa) to remove mercaptoethanol before being loaded on the column for 1 h at 4 °C. The column was washed thoroughly with 10 column volumes of binding buffer to remove unbound proteins. The bound proteins were eluted with elution buffer (20 mM Na_2HPO_4, 500 mM NaCl, 50 mM imidazole, pH 7.4). Protein concentrations were determined using the BioRad protein assay (Comptonet al., 1985) and fractions were monitored by SDS-PAGE using protein ladder purchased from Biolabs as markers. Proteins after SDS-PAGE were visualized with silver stain by PlusOne silver staining kit (GE Health).

3.2.6. Two-dimensional gel electrophoresis (2-DE)

Samples from FPLC and IMAC were dialyzed with dialysis membrane (MWCO 3 kDa) and concentrated with Microcon centrifugal filter devices (MWCO 10 kDa). The concentrated samples were diluted to 1 mg/mL with iso-electric focusing (IEF)

rehydration buffer (7 M urea, 2M thiourea, 4 % CHAPS, 0.5% ampholyte (pH 3-10, GE Health), 50 mM dithiothreitol). IEF was preceded by rehydrating the 13 cm immobilized pH gradient (IPG) drystrips, pH 3-10 (GE Health), with rehydration buffer containing protein samples of up to 150 ug. The rehydrated strips were focused overnight with an IPGphor instrument (GE Health). The following steps were in accordance with previous study in chapter 2.

3.2.7. In-gel digestion and protein identification

The protein spots of interest were manually excised from the 2-DE gel. The in-gel digestion protocol was similar with that in chapter 2.

3.2.8. Real-time quantitative polymerase chain reaction (PCR)

The changes in identified protein expression following the administration of Cu^{2+} with different concentrations were verified using real-time quantitative PCR methods. A real-time quantitative PCR was performed in a thin-wall 8-tube strip with the Chromo 4™ Four-Color Real Time System (MJ Research®); the 18S gene was used as the internal control for standardization. The sequences of the forward and reverse primers for the identified genes are shown in Table 2.1. The other procedures were same to that in chapter 2.

Table 3.1. Nucleotide sequences for primers used in the real-time quantitative PCR assay. Primers were designed from the nucleotide sequence of genes reported in GenBank with accession numbers shown.

Gene	Accession No.	Nucleotide Sequence (F, forward; R, reverse)
Heat shock protein 70	FJ375325	F: 5'- TCCATCCTGACCATTGAAGAC -3'
		R: 5'- TTCTGGCTGATGTCCTTCTTG -3'
Calmodulin	AY513748	F: 5'- CAAAGAGCTTGGGACTGTCA -3'
		R: 5'- TTGCCGTCAGCATCTACTTC -3'
Ferritin	AY737022	F: 5'- CTACCTTGCCCTGGGTATGT -3'
		R: 5'- TCAGCCTGTTCCCTCTCTTT -3'
Glycogen phosphorylase	DQ010415	F: 5'- TCTCGCAATGCCTTATGAC -3'
		R: 5'- CAGAACGGCTTGGATGTAA -3'
18S	DQ397879	F: 5'- GCCGAGAAGACGATCAAACT -3'
		R: 5'- GCAGGTTCACCTACGGAAAC -3'
Cytochrome P450 aromatase type II	AF472621	F: 5'- CAGATATATTCTTCAAGGTTGGAT -3'
		R: 5'- CTTCAAGCAGGCTCTCCAT -3'
Cu/Zn-superoxide dismutase	AY491056	F: 5'- CGTGACTCCATCATTGGAAG -3'
		R: 5'- TACCGGTCTTCAGGCTCTCT -3'
Beta hemoglobin	AY522595	F: 5'- ACCTGTCCACCAATGCCG -3'
		R: 5'- TGGCTCAGGTTGGCATAGG -3'
Vimentin	Q92155	F: 5'- TTCTGGGTACGACTCGTTGA -3'
		R: 5'- ATCGAAACCACAACAACCAA -3'
Glutathione peroxidase	Q4RSM6	F: 5'- TATGTCTGCGTTTCCTGAGC -3'
		R: 5'- AACAACCCTCTCCAAGCAAC -3'

3.3. RESULTS

3.3.1. Copper and metallothionein distribution after FPLC

Cytosolic proteins from tilapia hepatocytes with or without heat treatment in the control and Cu^{2+} injection groups were separated by Superdex 75 with detection in the 254 nm and 280 nm, respectively (Fig. 3.1). A total of 5 peaks were resolved after FPLC separation in the control and Cu^{2+} injection group without heat treatment (Fig. 3.1A & B), while two major peaks with higher copper concentration were detected in the copper-injected samples. In addition, the copper concentration in peak 3 of the copper injection group was much higher than that of the control group.

It appeared that the copper-binding proteins should exist in these two peaks after FPLC and there should be some differentially expressed protein in the liver of tilapia after Cu^{2+} injection. To further confirm this hypothesis, the cytosolic proteins with heat treatment were also conducted with the same methods. It was found that there were only 4 peaks after FPLC separation in heat-treated cytosols with lower peak 2 and peak 3 in Fig 3.1A & B disappeared. As shown in Fig 3.1C & D, the copper in peaks 2 also got lower, and that in peak 3 disappeared, but accumulated near the peak 4 after heat treatment. This should be due to heat treatment will cause denaturalization of proteins in peak 2 and 3, then the copper binding with these proteins will be released, and redistributed. It seems that the heat treatment is one of factors to influence the copper distribution. At the same time, this result proved our previous hypothesis about copper binding proteins and differentially expressed proteins in peak 2 and 3.

To enable further analysis of the distribution and migration of copper, the distribution of MT in each peak after FPLC was studied by western blot. There was only a single band in peaks 2 and 3 in the western blot result (Fig. 3.2B). Interestingly, the

signals of peaks 2 and 3 disappeared after heat treatment and moved to peak 4. This should be due to the binding ability of MT with other proteins in peaks 2 and 3, or its polymerization. As MT is a heat-stable protein, when other proteins in peaks 2 and 3 were denatured after heat treatment, MT moved to peak 4 as monomer according it its molecular size of 7 kDa. In summary, it appeared that the copper-binding proteins should exist in these two peaks after FPLC and that there should be some differentially expressed protein in the liver of tilapia after Cu^{2+} injection. To identify the copper-binding proteins and the differentially expressed proteins, peak 2 and peak 3 from the Superdex 75 column chromatography were further analyzed with 2DE gel and Cu-IMAC combined with 2-DE gel.

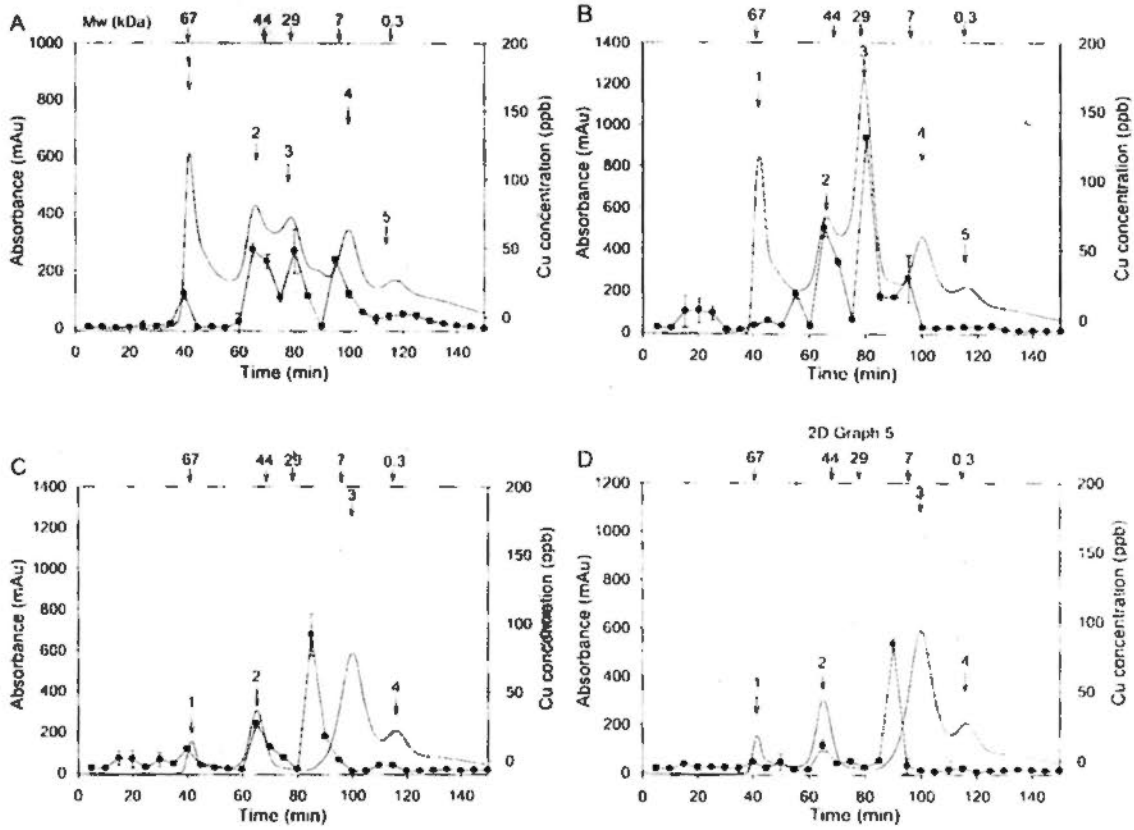

Fig. 3.1. Separation of cytosolic proteins by FPLC with Cu contents determined in different fractions. The cytosols collected from liver of tilapia with or without copper injection were loaded on a Superdex 75 column, eluted with tris buffer at a flow rate of 1 ml/min; 5 ml fractions were collected and analyzed for Cu concentration by AAS. The solid lines are the results detected with 280 nm; the dotted lines are the results detected with 254 nm; and the solid lines with circle represent the Cu distribution in different fractions. A: control group without heat treatment; B: Cu injected group without heat treatment; C: control group with heat treatment; D: Cu injected group with heat treatment. Relative positions of molecular size markers for column calibration are shown on top of the profiles and the peaks pooled for SDS-PAGE and further studies are also marked.

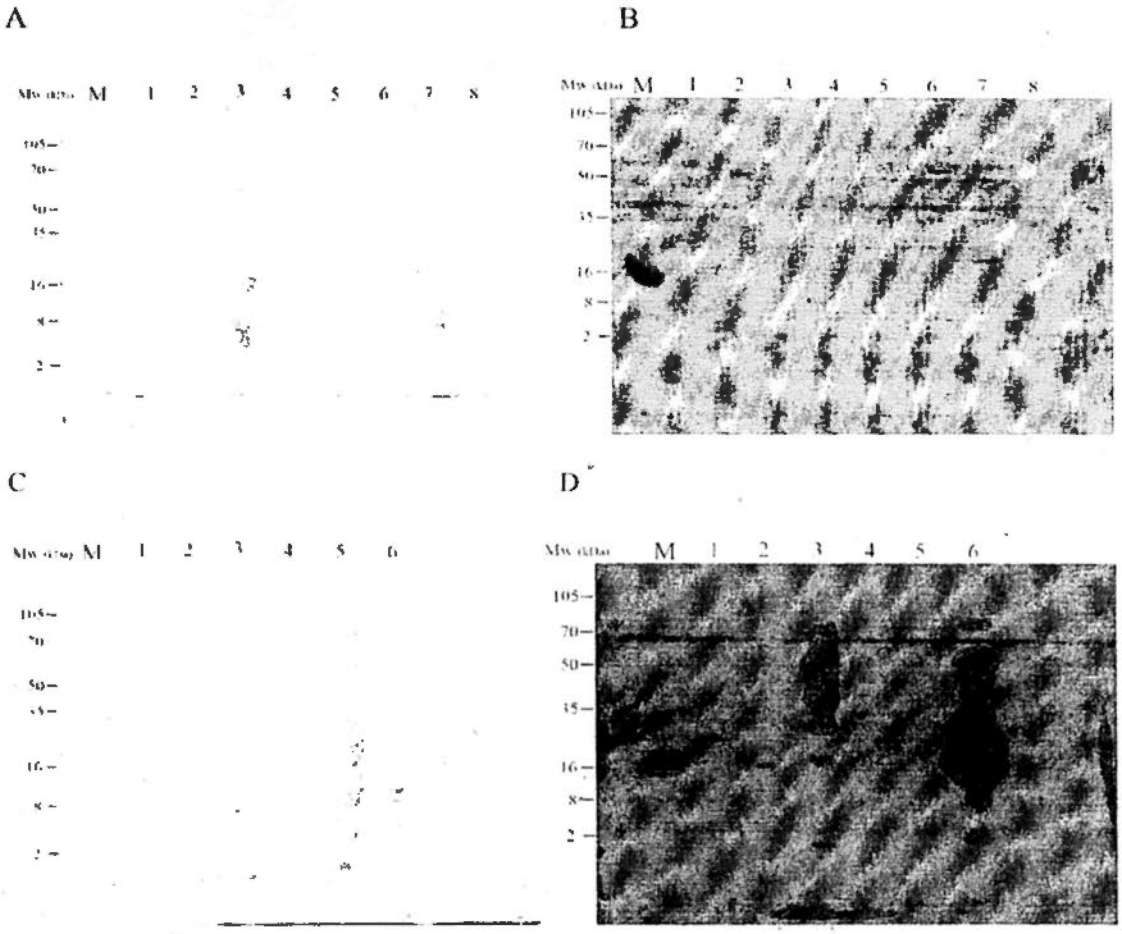

Fig. 3.2. SDS-PAGE of protein fractions from FPLC as shown in Fig. 3.1 and the fractions were also detected for metallothionein by western blot analysis. The left panels were result of SDS-PAGE stained with silver nitrate (panel A and C), and the right two panels were the western blot result from unstained gels (panel B and D). A: cytosolic proteins without heat treatment. The control group is shown from lanes 1 to 4 (lane 1: peak 1; lane 2: peak 2; lane 3: peak 3; lane 4: peak 4). The Cu injected group is shown from lanes 5 to 8 (lane 5: peak 1; lane 6: peak 2; lane 7: peak 3; lane 8: peak 4); B: cytosolic proteins with heat treatment. The control group is shown from lanes 1 to 3 (lane 1: peak 1; lane 2: fraction peak 2; lane 3: peak 3). The copper treatment group is shown from lanes 4 to 6 (lane 4: peak 1; lane 5: peak 2; lane 6: peak 3). Lanes marked with M were loaded with pre-stained markers with a 16 kDa lysozyme detected as positive control of western blot analysis.

3.3.2. Differentially expressed proteins

The two major peaks with high copper concentration after FPLC with Superdex 75 were analyzed by using 2-DE gel (Fig. 3.3). By comparing the control and Cu^{2+} injected groups, 66 and 49 spots were found to be differentially expressed in peaks 2 and 3, respectively (Fig. 3.3). These differentially expressed proteins were then identified by MALDI-TOF MS. A total of 44 proteins were identified in peak 2 and 36 in peak 3. The details of each identified protein, including the identification number on the gel, the accession number, the proteins' name and the regulation folds, are listed in Table 3.2 & 3.3. In most cases, the experimental Mw and pI values from 2D gels were in agreement with the theoretical Mw and pI values of the proteins. The results for the differentially expressed proteins in peaks 2 and 3 were also compared with the proteins found in our previous study of copper-affected proteins *in vitro* using the Hepa T1 cell-line (Chen and Chan, 2009). Most of the proteins in these two peaks, which were also listed in Table 3.2 & 3.3, were also regulated by Cu^{2+} *in vitro*. Although the regulation of these proteins by Cu^{2+} was almost well-matched, some proteins such as trypomyosin (No. 39) and paralbumin beta (No. 64) in peak 2 were not found in this study. Besides, there were some overlap between peak 2 and peak 3, such as heat shock protein 70 (No. 16, peak 2; No. 3, peak 3), and cytochrome P450 1A1 (No. 19, peak 2; No. 9, peak 3). Most of these overlap proteins' regulation was well-matched, except vimentin (No. 50, peak 2, down regulated; No. 15, peak 3, up regulated), which might be due to the the different isoforms of this protein.

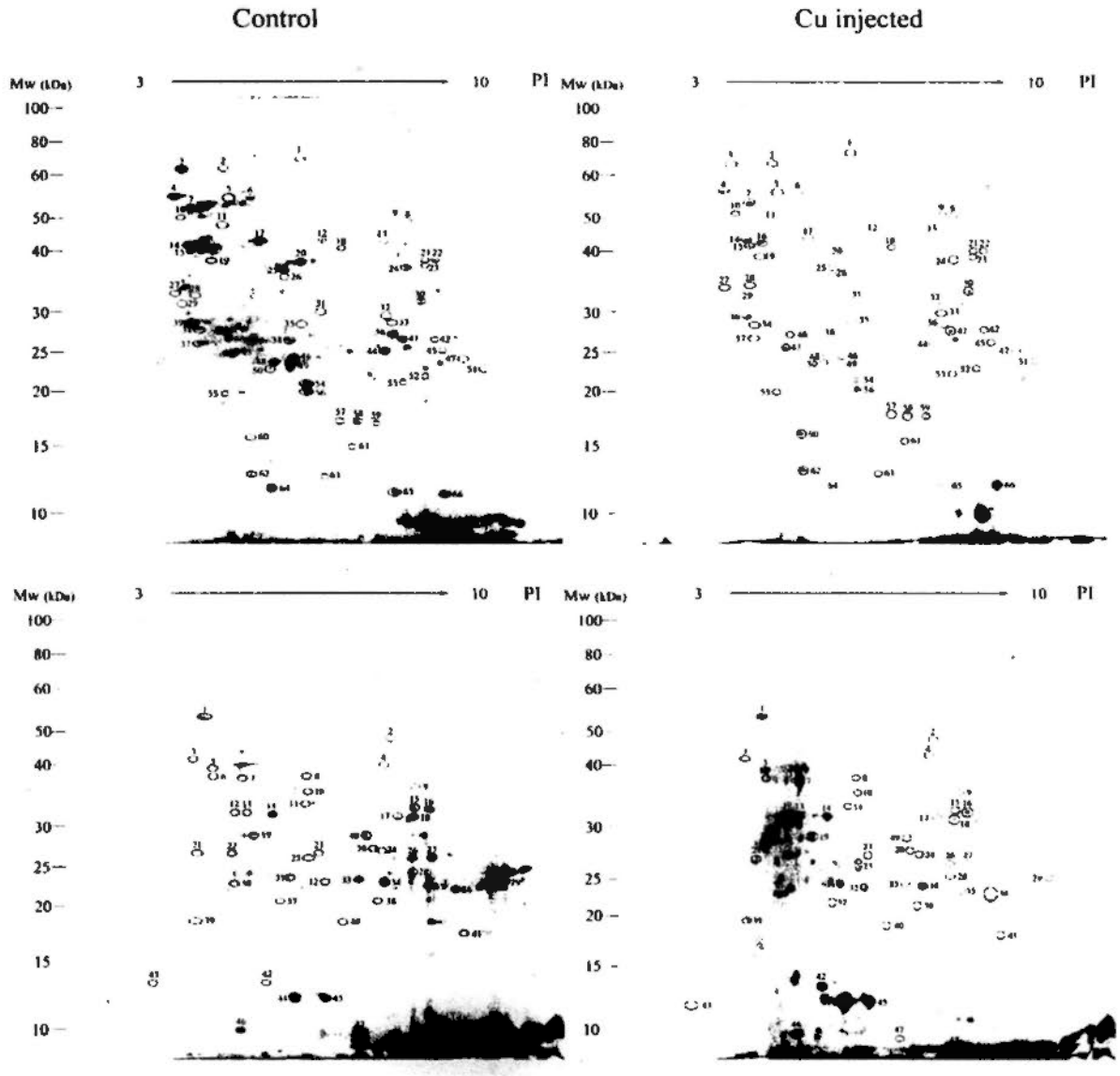

Fig. 3.3. 2D profiles of the control (left panels) and Cu injected (right panels) groups in peaks 2 (upper panels) and 3 (lower panels). Proteins were separated by 2-DE on a pH 3-10 gradient in the first dimension and by 12 % SDS-PAGE for the second dimension and were visualized by Coomassie Blue staining. The proteins identified by MALDI-TOF MS/MS analysis, as listed in Tables 3.2 and 3.3, are labeled. The spots with a red cycle were up-regulated and those with a green cycle were down-regulated.

Table 3.2. Differentially expressed proteins in peak 2 (Fig. 3.1) after FPLC separation comparing control and Cu injected groups

N	Protein Name	Accessing No.	MW/PI	Score Q	Ratio	M
		Chaperone				
15	Heat shock protein 5	gi|25742763	72476/5.07	*68/7*	1.98±0.26	U
16	Heat shock cognate 71 kDa protein	gi|1346318	71528/5.19	*63/7*	3.37±0.60	U
2	Glucose-regulated protein 78	gi|110226520	72363/4.97	*78/8*	0.31±0.02	
6	Heat shock 60 kD protein 1	gi|31044489	61389/5.56	*66/5*	0.28±0.12	U
7	Glucose-regulated protein 94	gi|110226526	92182/4.70	*89/24*	0.49±0.20	
		Enzyme				
19	Cytochrome P450 1A1	gi|209155992	59714/5.93	*34/4*	15.52±2.71	U
21	Cytochrome P450, subfamily 21A, poly peptide 1	gi|16923948	56257/9.18	*47/5*	4.45±1.48	
22	Catalase	gi|9622234	59794/8.12	*40/3*	3.11±0.97	U
28	ATP synthase subunit alpha	gi|14193440	6053/4.42	*48/2*	2.04±0.49	U
62	Cytochrome c oxidase subunit II	gi|12248168	25976/4.78	*59/4*	3.36±0.74	U
63	Cytochrome oxidase subunit I	gi|14599429	13890/6.43	*46/3*	5.78±1.43	U
66	NADH dehydrogenase subunit 5	gi|1707606	9312/8.12	*40/3*	4.24±2.06	U
8	Homogentisate 1,2-dioxygenase	gi|10441585	45208/6.37	*50/4*	0.39±0.14	
31	Glycogen phosphorylase	gi|67810419	42178/8.45	*71/10*	0.28±0.11	
32	Proteasome subunit, alpha type	gi|24119230	26339/8.72	*37/3*	0.34±0.18	D
35	Cysteine protease p32-beta	gi|1381643	30104/5.68	*58/5*	0.16±0.20	
44	Soluble guanylyl cyclase beta subunit	gi|157278046	70685/5.32	*48/5*	0.41±0.12	
48	Serine/threonine kinase 3	gi|13929032	56433/5.05	*47/5*	0.37±0.13	
49	Xanthine dehydrogenase	gi|14905703	148389/6.69	*48/7*	0.10±0.10	
		Transporter				
52	Beta globin	gi|22135542	16434/7.14	*65/3*	2.38±0.5	U
55	Mitochondrial uncoupling protein UCP	gi|13259162	33334/9.27	*73/5*	3.47±1.17	U
		Hormone				
30	Insulin-like growth factor I precursor	gi|60462010	20312/9.08	*48/4*	2.95±1.20	U
34	Novel protein	gi|126632503	8689/6.04	*72/5*	3.71±1.29	
14	Adiponectin	gi|27807433	26190/5.47	*59/4*	0.29±0.07	
38	Prolactin	gi|17367486	23670/7.08	*48/3*	0.34±0.19	
		Transcription factor				
59	Transportin 3	gi|41055198	105967/5.4	*35/3*	2.92±1.24	
36	similar to coiled-coil domain containing 57, partial	gi|109119249	118262/5.89	*58/10*	0.40±0.13	U
47	Transcription factor 1d	gi|26984176	11808/8.65	*46/2*	0.23±0.13	
		Metal-binding proteins				
57	Ferritin H-2	gi|185133949	20504/5.69	*66/5*	3.47±1.17	
58	Ferritin H-2	gi|185133949	20504/5.69	*61/5*	2.55±0.76	
64	Parvalbumin beta	gi|218931108	11433/4.41	*46/3*	0.28±0.05	U
		Cytoskeleton				
17	Actin	gi|42560193	42073/5.3	105/6	0.29±0.07	D
20	Myosin heavy chain	gi|3211972	5059/5.22	*57/3*	0.36±0.17	
25	Actin	gi|42560193	42073/5.3	*130/8*	0.34±0.05	D

39	Tropomyosin4-1	gi|28557136	28682/4.65	*89/11*	0.41±0.10	U
50	Vimentin	gi|860908	44613/4.75	*48/4*	0.15±0.06	U
65	Putative collagen alpha 1	gi|11095779	11047/5.7	*34/2*	0.27±0.09	
		Others				
18	Unnamed protein product	gi|21757857	37998/9.11	*75/5*	3.32±1.34	
24	Syndesmos	gi|14150147	23497/9.07	*62/4*	2.62±0.17	
1	Fragile X mental retardation 1	gi|23308667	64099/8.74	*41/3*	0.13±0.05	
5	Unnamed protein product	gi|47215577	102469/6.00	*65/14*	0.42±0.10	
12	MHC class I antigen	gi|2149390	37800/5.31	*43/3*	0.34±0.06	
29	IGFBP5	gi|263306	12996/6.1	*40/3*	0.39±0.12	
51	Immunoglobulin heavy chain variable region	gi|14289028	13649/9.06	*44/3*	0.10±0.08	

* In this table, "N" stands for spot no.; "Q" stands for number of peptides matched: "M" stands for a match with the data from our previous *in vitro* study; "U" stands for up-regulation and "D" stands for down-regulation as found in our previous *in vitro* study (Chen and Chan, 2009).

Table 3.3. Differentially expressed proteins in peak 3 after FPLC separation between control and Cu injected groups.

N	Protein Name	Accessing No.	MW/PI	Score/Q	Ratio	M
		Chaperone				
3	HSP70 protein	gi|157679184	69955/5.13	*53/7*	2.41±0.55	U
		Enzyme				
7	Dihydropyrimidinase-like 3	gi|66472750	61911/6.00	*58/7*	17.82±2.16	
16	Glyceraldehyde-3-phosphate dehydrogenase	gi|185133678	36030/ 7.81	*65/6*	3.92±0.45	
18	Glyceraldehyde 3-phosphate dehydrogenase isoform 1	gi|194241594	36170/8.69	*62/6*	4.16±1.47	
11	Putative zinc metallopeptidase; MEP4	gi|5281311	78652/8.21	*54/4*	5.36±1.32	
20	Methylmalonyl-CoA mutase	gi|22293511	54063/8.48	*67/5*	3.91±0.97	
24	Methylmalonyl-CoA mutase	gi|22293511	54063/8.48	*47/3*	3.87±2.01	
27	Glutathione S-transferase	gi|4630882	24500/8.16	*38/2*	3.54±1.07	U
30	Excision repair enzyme ERCC-1	gi|1763756	14465/5.89	*43/3*	12.39±1.14	
32	Stanniocalcin	gi|29170568	28487/8.27	*45/3*	2.87±0.75	U
34	Triosephosphate isomerase B	gi|82245450	27100/6.45	*69/4*	3.52±1.09	
38	1-Cys peroxiredoxin	gi|27497545	12161/8.72	*34/2*	4.38±1.86	
49	ATP synthase alpha subunit precursor	gi|162719	38967/9.57	*48/3*	3.07±1.31	U
4	Phosphoglucose isomerase-2	gi|158936941	61974/7.07	*51/8*	0.27±0.21	
48	Cytochrome P450	gi|6910928	7235/9.52	*52/3*	0.33±0.09	
		Transcription factor				
14	Zinc finger protein	gi|17368847	47796/6.5	36/2	5.52±1.10	D
23	ATP-dependent chromatin remodeling protein SNF2-related protein	gi|21105435	16830/4.78	54/4	3.59±0.85	
2	Cell division control proteins homolog	gi|1705675	34593/8.6	44/3	0.28±0.11	
		Transporter				
6	Na+/K+ ATPase alpha subunit isoform 5	gi|11096277	113858/5.17	*47/3*	4.74±0.64	U
8	V-ATPase subunit A	gi|14915706	68757/5.43	*32/3*	3.27±1.45	
12	Vacuolar protein sorting 26	gi|41053860	38255/6.3	*37/2*	5.30±0.42	
13	Apolipoprotein A-IV	gi|563320	28140/5.39	*45/3*	3.82±0.53	
19	Similar to transmembrane protein 74	gi|189530054	30997/6.00	*46/4*	3.62±1.52	
25	Beta hemoglobin A	gi|6230890	16347/7.96	*51/4*	2.98±1.66	U
36	copper-translocating P-type ATPase	gi|114764834	15554/10.38	*58/5*	5.02±0.53	
		Cytoskeleton				
15	Vimentin beta	gi|1353210	52165/5.26	33/3	2.89±1.12	U
35	Titin-like protein	gi|21238658	19460/4.45	*69/4*	3.52±1.07	
		Metal-binding protein				
22	Ca^{2+}-dependent activator protein for secretion	gi|1022782	25856/5.06	43/3	5.35±0.481	
41	Metallothionein	MT_PSEAM	7185/8.05	*45/3*	3.74±1.03	U
43	Calmodulin	gi|124271042	7535/4.32	*34/3*	2.62±0.82	U
		Hormone				
45	Growth hormone	gi|404398	19869/7.83	*34/3*	5.31±1.40	U
		Others				
1	Vitellogenin II	gi|157278415	191691/9.22	*43/3*	2.86±0.77	U

21	Ywhab1 protein	gi|56269288	32529/4.63	*62/6*	3.22±1.38	
40	T cell receptor alpha chain	gi|29691067	28086/5.64	*55/4*	2.69±0.72	
44	MHC class II beta chain	gi|309948	9752/7.93	*38/3*	5.08±0.09	D
17	Gamma-aminobutyric acid B receptor	gi|15741079	34037/7.07	*44/3*	0.20±0.15	

* In this table, "N" stands for spot no.; "Q" stands for number of peptides matched; "M" stands for a match with the data from our previous *in vitro* study; "U" stands for up-regulation and "D" stands for down-regulation as found in our previous *in vitro* study on the Hepa-T1 cell-line (Chen and Chan, 2009).

To further confirm the regulation of these genes, quantitative real-time PCR was adopted in the next experiment. Furthermore, the differentially expressed proteins can be divided into 8 groups according to their function, including chaperone, enzyme, transporter, hormone, transcription factor, metal-binding, cytoskeleton, and other proteins. Most of the differentially expressed proteins were enzymes.

3.3.3. Cu-IMAC separated proteins

After FPLC separation, two peaks with higher copper concentration were loaded on a Cu-IMAC column to separate the copper-binding proteins. The binding of proteins to the Cu-IMAC column was monitored by conventional SDS-PAGE and the BioRad protein assay. No protein was bound to a control column without copper ion added and there was a significant amount of protein bound to Cu-IMAC columns in the two peaks of copper-binding protein fractions (Fig. 3.4). Washes with 10 column volumes presumably removed all non-specifically bound proteins from the column. Following elution, the Cu-IMAC columns yielded 100-300 ug of copper-binding proteins which were all loaded for 2-DE analysis.

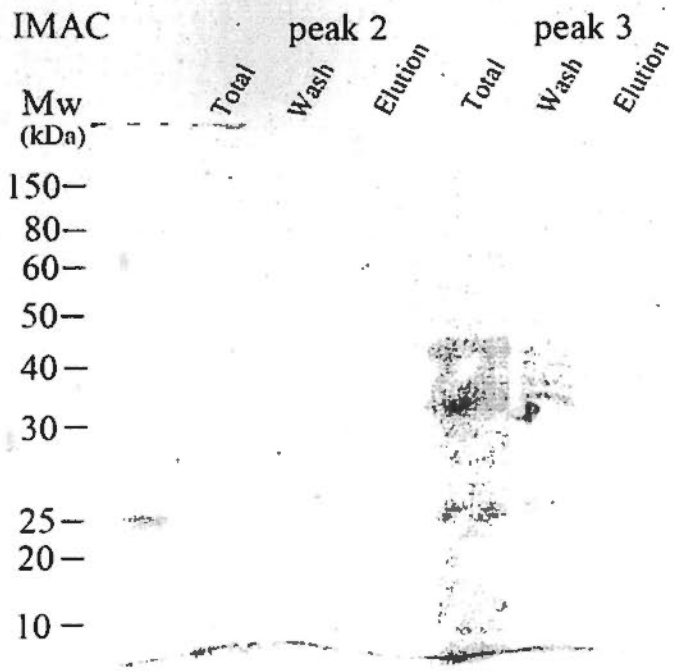

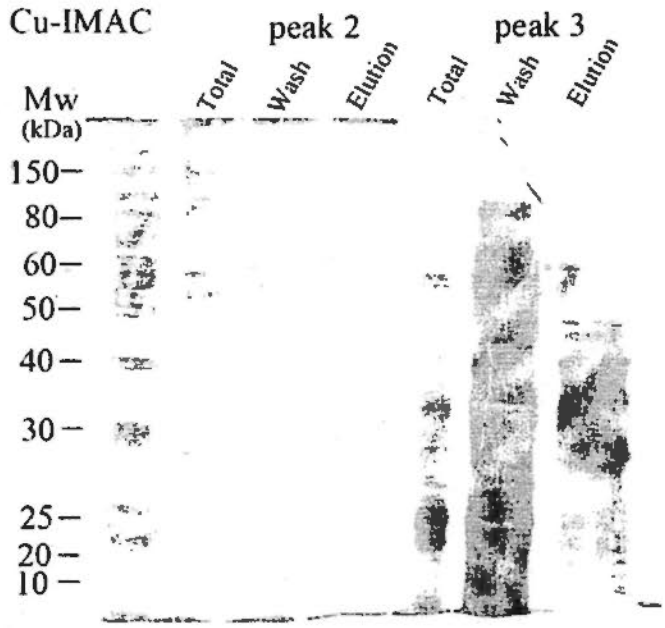

Fig. 3.4. SDS-PAGE separation of proteins in peak 2 and peak 3 bound to IMAC column without (left) and with (right), chelating copper ion. No visible protein in peak 2 (left) and peak 3 (right) found to be bound to IMAC without copper ions.

3.3.4. 2-DE separation and MS identification of proteins after Cu-IMAC separation

After Cu-IMAC separation of the copper-binding proteins in peaks 2 and 3, the copper-binding fractions in these two peaks were analyzed separately with 2-DE. As shown in Fig. 3.5, around 100 and 300 spots were found in the 2-DE gel for peak 2 and peak 3, respectively. The protein spots with higher concentration were chosen for peptide mass fringerprint (PMF) identification, including 36 spots in peak 2 and 51 spots in peak 3. The proteins identified are listed in Table 3.3 and comprise 25 proteins identified from peak 2 and 41 proteins from peak 3. A comparison of this part of the results with proteins identified in previous FPLC and *in vitro* studies showed that a total of 38 proteins found in peaks 2 and 3 can be differentially expressed. These differentially expressed copper-binding proteins should play an important role in copper transportation and detoxification. Therefore, they are summarized in Table 3.4. Six well known copper-binding proteins (ATP7A, Cytochrom c oxidase, and copper/zinc superoxide dismutase, etc.) and six other metal-binding proteins (transferrin, ferritin, calmodulin, etc.) were found, which made the results of IMAC separation more convincing. Also found were 17 novel differentially expressed copper-binding proteins: 3 cytoskeleton proteins (collagen, vimentin, myosin heavy chain), 6 enzymes (catalase, NADH dehydrogenase subunit 5, aldehyde dehydrogenase, etc.), 2 transporters (apolipoprotein and V-ATPase), 1 glycolipoprotein (vitellogenin), 1 hormone (insulin-like growth factor I), 1 transcription factor (STAT3), 1 cytokine (Interleukin-1 beta) and 2 other proteins (methionine-rich storage protein 1, Igfbp5 protein).

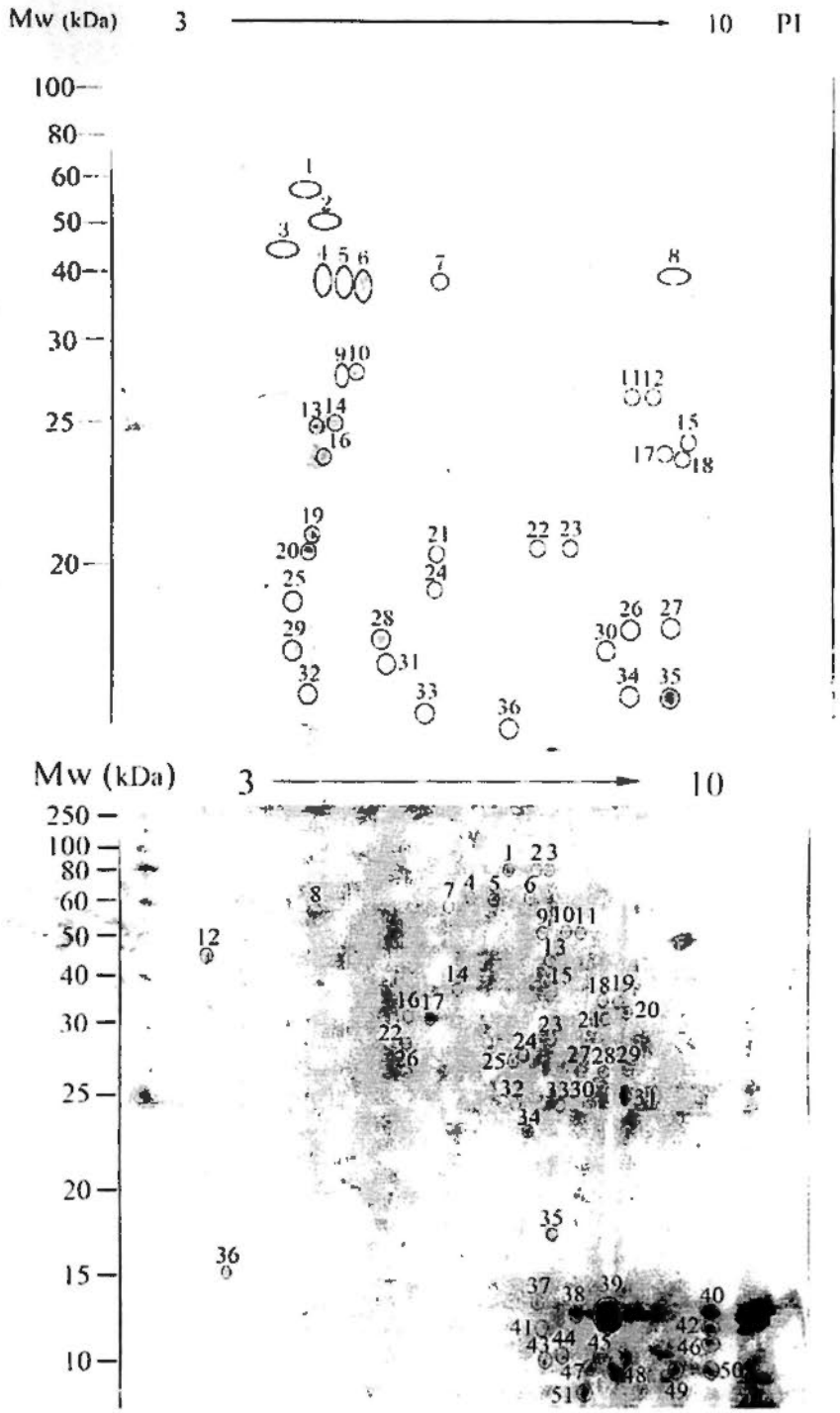

Fig. 3.5. 2D analysis of copper-binding proteins eluted from a Cu-IMAC column in peak 2 (upper panel) and peak 3 (lower panel) after FPLC separation. The proteins were separated by 2DE on a pH 3-10 gradient in the first dimension and by 12 % SDS-PAGE in the second dimension and were visualized by Coomassie Blue staining. The proteins identified by MALDI-TOF MS/MS analysis, as listed in Tables 3.4 and 3.5, are labeled.

Table 3.4. Copper-binding proteins in peak 2 (Fig. 3.1) eluted from Cu-IMAC column and identified by MALDI TOF MS

N	Protein Name	Accessing No.	MW/PI	Score/Q	M1	M2
1	Novel protein similar to human STAT1	gi|22316176	133796/7.02	*36/4*		
2	Procollagen type I alpha 1 chain	gi|15149946	49398/5.59	*33/3*		D
3	Histone deacetylase 3	gi|41055869	49644/5.23	*33/3*		
4	Hypoxia-inducible factor 1, alpha subunit	gi|41053885	60829/6.21	*32/2*		
5	Lysyl oxidase-like 3b	gi|220678603	16596/4.88	*30/2*		
6	Cathepsin D, Precursor	gi|25452827	43693/5.79	*33/3*		
8	3 beta-hydroxysteroid dehydrogenase 1	gi|47086447	42436/7.56	*57/5*		
9	Retinol dehydrogenase 1	gi|37620196	36852/9.15	*32/2*		
11	Igfbp5 protein	gi|13278235	14233/5.6	*51/3*		D
12	Stat3 protein	gi|28277427	48512/7.15	*49/3*	U	
13	Myosin heavy chain	gi|3211972	5059/5.22	*79/3*		D
14	Catalase	gi|9972785	59906/8.12	*50/4*	U	U
15	Stat3 protein	gi|28277427	48512/7.15	*49/3*	U	
16	Josephin domain containing 2	gi|41055888	21194/6.31	*50/3*		
18	Mitochondrial ribosomal protein S27	gi|57524611	46126/5.86	*55/5*		
20	Catalase	gi|223648824	60228/8.09	*70/9*	U	U
21	Transferrin	gi|11877338	66959/7.1	*36/3*		U
22	Ferritin, middle subunit	gi|209737542	20745/5.64	*42/3*		U
25	ATP7A	gi|12699501	24568/7.7	*40/3*		U
27	Splicing factor, arginine/serine-rich 8	gi|41054717	42117/4.77	*44/4*		
28	Alpha-2-HS-glycoprotein	gi|226358603	26374/5.46	*43/3*		
29	Proteasome beta 3 subunit	gi|193788711	23386/5.36	*40/3*	D	D
33	Serine/threonine kinase 38 like	gi|27370078	53969/6.5	*39/2*		
34	Beta hemoglobin A	gi|6230890	16347/7.96	*53/4*	U	U
35	Beta hemoglobin A	gi|6230890	16347/7.96	*53/4*	U	U

* In this table, "N" stands for spot no.; "Q" stands for number of peptides matched; "M1" stands for a match with the data from previous work done *in vitro* (Chen and Chan, 2009); "M2" stands for a match with data from the present study conducted *in vivo*; "U" stands for up-regulation and "D" stands for down-regulation.

Table 3.5. Copper-binding proteins in peak 3 (Fig. 3.1) eluted from Cu-IMAC column and identified by MALDI TOF MS.

N	Protein Name	Accessing No	MW/PI	Score/Q	M1	M2
1	Serotransferrin	gi|6136039	69551/6.12	32/4		U
2	Serotransferrin	gi|6136039	69551/6.12	36/4		U
3	Vitellogenin	gi|3123011	184635/9.08	49/3	U	U
4	Transferrin	gi|15387705	18400/6.09	61/5		U
6	Methionine-rich storage protein 1	gi|159526	88783/8.71	42/6		
9	Copper/zinc superoxide dismutase	gi|27462182	16170/5.64	43/3		
10	Kinesin-associated protein family member (kap-1)	gi|71984142	77506/5.49	70/8		
11	Kinesin-associated protein family member (kap-1)	gi|71984142	77506/5.49	67/7		
13	Prolactin receptor	gi|148224000	69365/5.07	44/4		
14	Phosphoribosylaminoimidazole carboxylase	gi|41053415	47684/6.99	38/3		
15	65kDa FK506-binding protein	gi|18034674	65178/5.38	50/4		
16	Apolipoprotein A-IV	gi|563320	28140/5.39	54/5		U
17	NADH dehydrogenase subunit 5	gi|24460002	31301/6.96	48/4	U	U
18	V-ATPase subunit A	gi|14915706	68757/5.43	34/3		U
19	Vps20-associated 1 like 1	gi|213513620	34757/8.31	65/6		
20	Glyceraldehyde-3-phosphate dehydrogenase	gi|21955965	36068/8.63	51/4		U
21	Insulin-like growth factor I precursor	gi|60462010	20312/9.08	58/5	U	U
24	Similar to catalase	gi|20070714	26096/8.66	44/3	U	U
28	Aldehyde dehydrogenase family member	gi|17551164	55933/6.23	68/6	D	
29	Aldehyde dehydrogenase family member	gi|17551164	55933/6.23	62/6	D	
30	Catenin, alpha	gi|18858485	101209/5.88	47/6		
32	Annexin II	gi|148233163	38752/8.59	66/6		
33	Dynamin	gi|487851	85334/5.97	62/8		
34	Stretchin-MLCK	gi|9623341	38845/6.3	62/5		
35	Calcium-regulating hormone Stanniocalcin	gi|9457238	20274.5/5.52	54/4	U	U
37	Beta hemoglobin A	gi|6230890	16347/7.96	101/4	U	U
38	Beta hemoglobin A	gi|6230890	16347/7.96	71/3	U	U
39	Beta globin	gi|22135544	16461/8.34	127/4	U	U
42	Novel protein similar to human titin	gi|29561775	2128176/6.46	34/31		D
43	Beta hemoglobin A	gi|6230890	16347/7.96	71/3	U	U
45	Probable glutathione peroxidase 8	gi|41055524	23907/9.6	45/4		
46	Vimentin beta	gi|1353210	52165/5.26	42/5	U	U,D
47	MHC class II B antigen	gi|15625266	9832/5.24	33/3	D	U
48	metallothionein B	gi|185132566	7114/8.24	58/4	U	U
49	Calmodulin	gi|124271042	7535/4.32	53/4	U	U
51	Amyloid precursor protein; APP	gi|257378	3156/8.59	45/3		

* In this table, "N" stands for spot no.; "Q" stands for number of peptides matched; "M1" stands for a match with the data from previous work done *in vitro* (Chen and Chan, 2009); "M2" stands for a match with the data from the present study conducted *in vivo*; "U" stands for up-regulation in the previous study; "D" stands for down-regulation in the previous study.

3.3.5. Verification of gene expression using quantitative real-time PCR

To verify the regulation of the gene for Cu^{2+} related proteins after copper exposure, real-time quantitative PCR was used to analyze regulation at the level of mRNA accumulation. A total of 27 genes with sequences available from the GenBank database (Table 3.1) were chosen for this experiment. Those chosen are also shown in Table 3.2 in italics. As shown in Fig. 3.6, other than proteasome, the regulation of most of the genes at the RNA level was in accordance with the regulation of the proteins *in vivo*. Aso, most genes' regulation *in vivo* well matched with previous 18 genes' regulation *in vitro*, except zinc finger protein 60. Interestingly, the fold regulation of the genes was some different from that of their protein regulation, indicating that in addition to gene regulation, there are various other levels of regulation during protein synthesis, e.g., translational, post-translational, and post-transcriptional regulation. Among these 27 genes, 12 genes were found significantly dosage dependent induced by copper ion, including 5 well known biomarkers for monitoring the copper contamination. The other 7 genes differentially expressed after copper exposure should be potential biomarkers that can be used to monitor copper contamination in the environment.

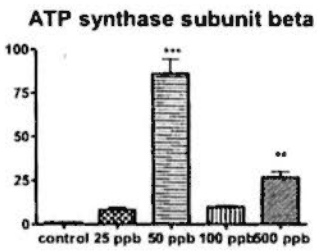
ATP synthase subunit beta
control 25 ppb 50 ppb 100 ppb 600 ppb

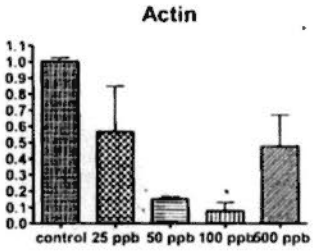
Actin
control 25 ppb 50 ppb 100 ppb 600 ppb

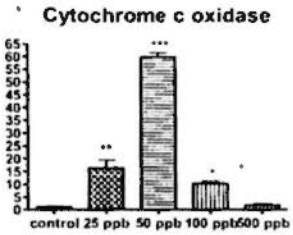
Cytochrome c oxidase
control 25 ppb 50 ppb 100 ppb 600 ppb

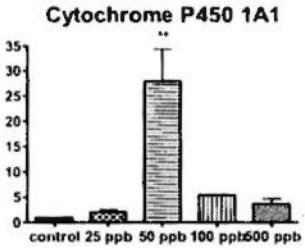
Cytochrome P450 1A1
control 25 ppb 50 ppb 100 ppb 600 ppb

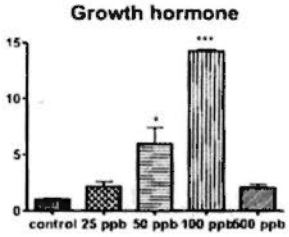
Growth hormone
control 25 ppb 50 ppb 100 ppb 600 ppb

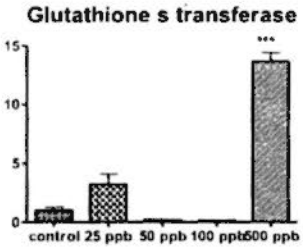
Glutathione s transferase
control 25 ppb 50 ppb 100 ppb 600 ppb

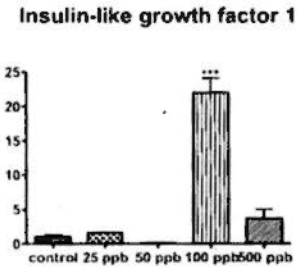
Insulin-like growth factor 1
control 25 ppb 50 ppb 100 ppb 600 ppb

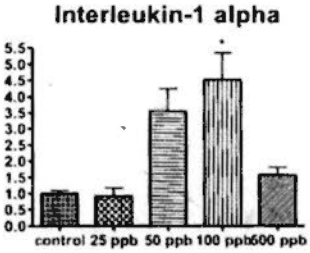
Interleukin-1 alpha
control 25 ppb 50 ppb 100 ppb 600 ppb

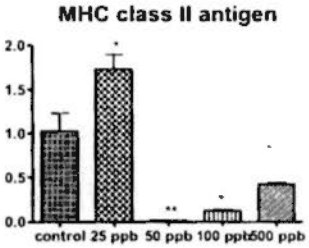
MHC class II antigen
control 25 ppb 50 ppb 100 ppb 600 ppb

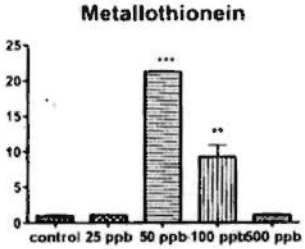
Metallothionein
control 25 ppb 50 ppb 100 ppb 600 ppb

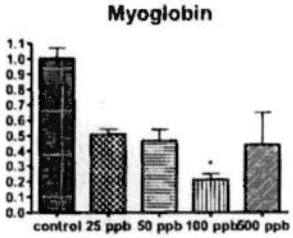
Myoglobin
control 25 ppb 50 ppb 100 ppb 600 ppb

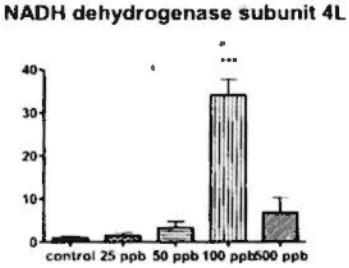
NADH dehydrogenase subunit 4L
control 25 ppb 50 ppb 100 ppb 600 ppb

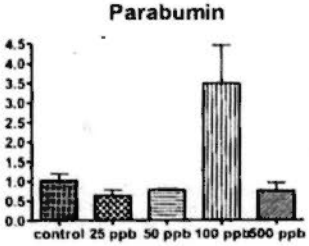
Parabumin
control 25 ppb 50 ppb 100 ppb 600 ppb

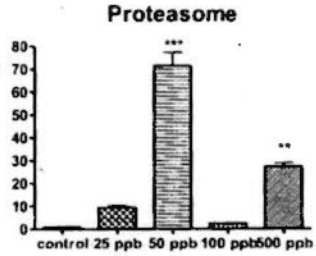
Proteasome
control 25 ppb 50 ppb 100 ppb 600 ppb

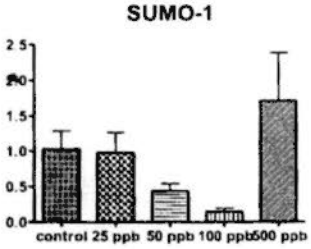
SUMO-1
control 25 ppb 50 ppb 100 ppb 600 ppb

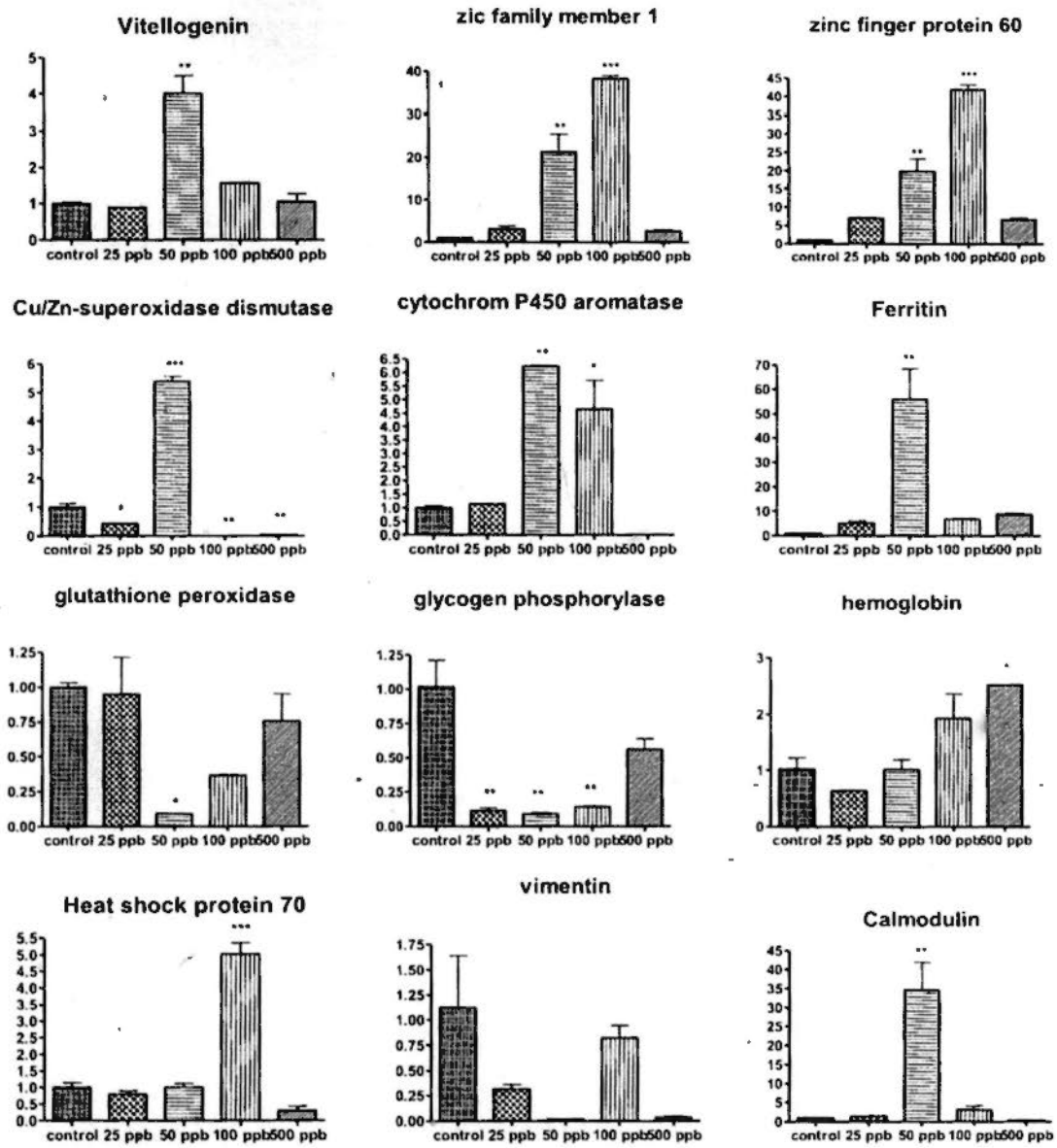

Fig. 3.6. Real-time quantitative PCR results for gene regulation in the liver of tilapia through the effect of exposures to increasing $CuCl_2$ concentrations. The concentrations of $CuCl_2$ increase from left to right including the control, 25 ppb, 50 ppb, 100 ppb, and 500 ppb. The y axis represents the fold regulation of these genes (*$p < 0.05$, **$p < 0.01$, ***$p < 0.001$, derived from the Mann–Whitney test of individual gene regulation).

3.4 DISCUSSION

We employed a Cu-IMAC column to isolate hepatic copper-binding proteins on a selective basis. The copper-IMAC strategy for isolating copper-binding proteins is ideal for the selective identification of high abundance proteins with affinity for copper. To make the Cu-IMAC more specific to the copper-binding proteins, in this study, FPLC separation was first combined with AAS detection of copper ion to confirm the distribution of these proteins. The fractions with higher copper concentration were then analyzed using differential proteomic approaches and the copper-binding proteins were separated or enriched by a Cu-IMAC column prior to using proteomic studies. Until now, PMF has been used to identify 50 and 43 differentially expressed proteins in peaks 2 and 3. These proteins can be divided into 8 groups according their function: chaperone, enzyme, transporter, etc. Furthermore, the Cu-IMAC column separated the copper-binding proteins in the copper ion-containing peaks. Twenty-five and 41 proteins were identified in peaks 2 and 3, respectively. They were differentially expressed as found in a previous *in vitro* study (chapter 2) and they play important roles in copper transportation and detoxification.

Table 3.6. Categories and functions of the differentially expressed copper-binding proteins in peaks 2 and 3.

Protein	Category	Biological Function	Regulation
Known copper-binding proteins			
ATP7A	Transporter	Copper-exporting ATPase activity	Induced
Cytochrome C oxidase family	Enzyme	Copper chaperone activity	Induced
Copper/zinc superoxide dismutase	Enzyme	Antioxidant defense	Induced
Titin	Cytoskeleton	Structure protein	Depressed
Metallothionein	Metal-binding protein	Metal-binding and storage	Induced
Amyloid precursor protein, APP	Unkown	Copper efflux	
Novel copper-binding proteins with differential expressions			
Collagen	Cytoskeleton	Structure protein	Depressed
Igfbp5 protein		Binding of insulin-like growth factors	Depressed
Stat3 protein	Transcription regulator	Transcription activators	Induced
myosin heavy chain	Cytoskeleton	Structure protein	Depressed
Catalase	Enzyme	Catalyze the decomposition of hydrogen peroxide to water and oxygen	Induced
Proteasome	Enzyme	Degrade unneeded or damaged proteins	Depressed
Vitellogenin	Yolk protein	Lipid metabolism and gonad development	Induced
Apolipoprotein A-IV	Transporter	Transport lipid	Induced
NADH dehydrogenase subunit 5	Enzyme	Quinone oxidoreductase	Induced
V-ATPase	Transporter	Proton transport	Induced
Glyceraldehyde-3-phosphate dehydrogenase	Enzyme	Metabolic mechanism	Induced
Insulin-like growth factor I	Hormone	Cell cycle and growth control	Induced
Aldehyde dehydrogenase	Enzyme	Catalyze the oxidation of aldehydes	Depressed
Vimentin	Cytoskeleton	Structure protein	Induced
Other metal-binding proteins			
Transferrin	Transporter	Iron ion delivery	Induced
Ferritin	Metal-binding protein	Iron storage protein	Induced
Beta globin	Transporter	Makeup of hemoglobin	Induced
Hemoglobin A	Transporter	Iron-containing oxygen-transport metalloprotein	Induced
Stanniocalcin	Kinase	Regulation of renal and intestinal calcium and phosphate transport	Induced
Calmodulin	Metal-binding protein	Calcium-binding protein; inflammation, metabolism, apoptosis	Induced

*As to the amyloid precursor protein, it was not found to be regulated in the differential expressed proteins, but it is a well known copper-binding protein which is related to Alzheimer's disease.

3.4.1. Proteins related to endocrine system

Chronic sub-lethal Cu^{2+} exposure causes a series of cellular and physiological changes in fish that enable them to survive. Cu^{2+} is also an endocrine-disrupting metal in the aquatic environment and has a number of normal neuro-endocrine roles in vertebrates (Handy, 2003). In our previous *in vitro* study on Hepa-T1, Cu^{2+} affected cell development by regulating growth hormone (GH) and insulin-like growth factor 1 (IGF1)(Chenet et al., 2009). In this study, these two hormones were also found to be regulated by Cu^{2+}, confirming that copper can stimulate fish growth by inducing growth hormone and growth factors to express. IGF1 was also found to have copper-binding ability. In bony fish, IGF1 released from the liver under the control of pituitary GH is the main endocrine of growth, maintenance, and development, and the amount of IGF1 in circulation regulates the synthesis and release of GH (Eppler et al., 2007). A previous study has also found that IGF1 has antioxidant effects against copper in rats with advanced liver cirrhosis (Garcia-Fernandez et al., 2005). This copper ion binding ability and up-regulation by Cu^{2+} may help us to establish how IGF1 is involved in the antioxidant mechanism for copper and the copper transportation pathway.

In addition, IGFBP5, one of the IGF-binding proteins, was found to be down-regulated and have copper-binding ability. Approximately 98 % of IGF1 is always bound to one of 6 binding proteins (IGFBP). IGFBP binds to IGF1 inside the liver, allowing growth hormone to act continuously on the liver to produce more IGF1 (Clemmons et al., 1995). This is important, because proliferation of the IGF1 + IGFBP complex allows for growth of the femur and muscle. Andress (1995) demonstrated that IGFBP5 bound to and was internalized by a 420 kDa membrane protein of mouse osteoblastic cells. Hence, copper might be related to the IGF1+IGFBP5 complex, which

plays an important role in the transfer of copper from the membrane to other organelles in the cell. My study showed that the regulation of IGF1 and IGFBP5 were different in that IGF1 was up-regulated by copper, whereas IGFBP5 was down-regulated. This should be attributable to the different functions of these two proteins. A previous study has shown that IGFBP5 can exert its biological activities in the absence of IGF1, indicating the existence of IGF-independent actions (Schneider et al., 2002). Because IGFBP5 is also localized in the nucleus (Schneideret al., 2002), Cu^{2+} may enter the nucleus by binding with IGFBP5. Chapman et al. (1999) found that IGFBP5 was a direct or indirect target for STAT3, which our study also found to have copper-binding ability, and STAT3 is a transcription factor in the nucleus which can regulate many aspects of cell growth, survival, and differentiation. Thus, it is hypothesized that Cu^{2+} may enter the nucleus via the IGF-IGFBP5-STAT3 pathway.

Other hormones found to be regulated by copper include prolactin (PRL) and adiponectin. PRL is a protein hormone that serves a number of vital functions involving metabolism, reproduction, and the maintenance of homeostasis in immune responses, osmotic balance, and angiogenesis, and is being increasingly used as a measure of neuroendocrine/dopaminergic function in environmental and occupational epidemiology studies. Meeker et al. (2009) found that the expression of PRL is inversely associated with arsenic, cadmium, copper, and lead manganese in the serum of adult men. Kelleher and Lonnerdal (2006) found that transient changes in PRL signaling play a role in the regulation of mammary gland Cu secretion during lactation by regulating the expression of three important copper transporters: Ctr1, Atp7A, and ATP7B. This study showed that PRL is also down-regulated by Cu in male tilapia. Sadineni et al. (2006) revealed that human PRL contains metal-binding sites which could bind with Cu^{2+}. While we did not

find PRL in our Cu-IMAC experiment, the PRL receptor was found to have copper-binding ability. Ali and Ali (1998) found that STAT5 is specifically activated by PRL treatment in HC11 cells, demonstrating that STAT5 is a physiological substrate downstream of PRLR. Cataldo et al. (2000) also demonstrated that STAT3 is preferably activated through PRLR in T-47D cells, which further confirmed the interaction between PRLR and STAT.

Adiponectin modulates a number of metabolic processes including glucose regulation and fatty acid catabolism. It plays a role in the suppression of the metabolic derangements that may result in type 2 diabetes, obesity, atherosclerosis, and non-alcoholic fatty liver disease (NAFLD). A recent study showed that copper bioavailability may be related to NAFLD (Aigner et al., 2008). Our results showed that adiponectin is suppressed by Cu^{2+} and may help to understand the mechanism of Cu^{2+} in NAFLD.

3.4.2 Copper transports in mitochondiral

Recent studies have demonstrated that steady-state levels in the mitochondiral matrix were nearly an order of magnitude above that predicted to be required for the activation of the abundant mitochondiral Cu-dependent enzyme cytochrom C oxidase (Kim et al., 2008). While there are likely to be additional Cu-dependent mitochondrial enzymes, with clues possibly arising from the bacterial Cu-binding proteome, these observations also suggest that mitochondria serve as Cu storage organelles. Until now, only cytochrome c oxidase (COX) and Sco1 have been found to be targeted by Cu^{2+} and to transport cytosolic Cu^{2+} into the mitochondria; little is known about how Cu^{2+} is delivered to and stored in the mitochondria. There should be some proteins that transport

and store Cu^{2+} in the mitochondria. This study found that cytochrome c oxidase subunit 2 has copper-binding ability and that two more enzymes located in the mitochondria - NADH dehydrogenase subunit 5 (ND5) and aldehyde dehydrogenase (ALDH) - have copper-binding ability. These two enzymes are both involved in the mitochondrial electron transport chain with ND5 located in the inner mitochondrial membrane, which may cooperate with cytochrom c oxidase to transfer the copper ion into the mitochondria, whereas ALDH is an enzyme that catalyses the oxidation of aldehydes located inside the mitochondria. Moreover, a previous study has shown that mitochondrion is an important target for copper to exert its toxicity by inducing reactive oxygen species (Belyaeva et al., 2008). In this study, COX2 and ND5 were up-regulated and ALDH was down-regulated by Cu^{2+}. These results indicate that Cu^{2+} may cause mitochondria dysfunction and lead to ROS effects on the cell.

3.4.3. Copper competes with iron and calcium

This study identified some iron and calcium related proteins after Cu-IMAC purification. This result agrees with that of a previous study whereby Cu^{2+} can compete with Fe^{2+} and Ca^{2+} in binding to the target proteins. Fe^{2+} and Cu^{2+} have several similarities including a facile ability to alternate between two common oxidation states. The metabolism of iron and copper are intimately linked and they can compete for a common intestinal transporter (e.g., divalent metal transporter 1, DMT1), function in concert in the same protein (e.g., cytochrome c oxidase), and serve as reactive centers of the same enzyme (e.g., copper in ceruloplasmin); they can also participate in each other's oxidation/reduction (McArdle et al., 2008). This study found that transferrin (TF), ferritin, and hemoglobin, which are important proteins for iron transportation and

storage, have copper-binding ability. TF, a glycoprotein that binds Fe^{2+} very tightly, can deliver iron ion into a vesicle inside the cell by binding with the transferrin receptor (TFR) in the cell membrane. The pH of the vesicle is then reduced by hydrogen ion pumps (H^+-ATPase), which were also found in the Cu-IMAC experiment (V-ATPase), causing transferrin to release Fe^{2+} and acquire other ferric ions for another cycle of iron transport. The metal is then reduced to ferrous iron (Fe^{2+}) and transported into the cytoplasm by DMT1 (McArdleet al., 2008). The excessive ferrous iron in the cytoplasm is stored in the ferritin, which is a buffer against iron deficiency and overload. Previous studies have found that several iron transporters (Ftr1, Fet3, Fet4) also have copper-binding ability and are involved in copper uptake and efflux (Allen et al., 2007; Puig and Thiele, 2002). In this study, the binding of iron binding proteins with Cu-IMAC further confirmed that Cu^{2+} may be involved in the pathway of iron transportation.

Turning to competition between copper and calcium, some studies have shown that competition between these two metals does indeed exist. Wu et al. (2003) found that a non-lethal concentration of Cu^{2+} significantly reduces the calcium content of tilapia larvae after exposure to copper ion for 72 H. Conversely, calcium pre-exposure can act as a protective agent against environmental copper toxicity for juvenile tilapia (Abdel-Tawwab et al., 2007). Sivaraja et al. (2006) found that a member of the S100 family of EF-hand calcium-modulated proteins, S100A13, can bind independently with both copper and calcium with almost equal affinity, indicating that copper and calcium interact with each other. This study found that two important calcium binding proteins – calmodulin (CaM) and stanniocalcin (STC) – have copper-binding ability. CaM modulates calcium homeostasis and protects cells from apoptotic stimuli. CaM also

mediates processes such as inflammation, metabolism, apoptosis, smooth muscle contraction, and intracellular movement. STC is a calcium/phosphate homeostatic hormone that is active in the regulation of renal and intestinal calcium and phosphate transport. Over-expression of STC causes inhibition of gill calcium transport, thereby reducing intestinal calcium uptake and stimulating phosphate re-absorption by renal proximal tubules. Our results show that these two proteins have copper-binding ability, which further confirms the existence of competition between copper and calcium and indicates that the induction of STC by copper ion might suppress calcium uptake in the liver of tilapia (Greenwood et al., 2009). Furthermore, STC is a hormone that targets mitochondria. High-affinity receptors for STC are present on the cytoplasmic membranes and on both the outer and inner mitochondrial membranes of nephrone cells and hepatocytes. In both cell types, STC is also present within the mitochondrial matrix and receptors presumably enable its sequestration (Ellard et al., 2007). STC may therefore play a role in transferring Cu^{2+} from cytoplasm to mitochondria. This should be an important pathway for copper ion delivery to the mitochondria for incorporation into COX.

3.4.4 Copper and lipid metabolism

Apolipoprotein is an important protein family which can serve as enzyme co-factors, receptors, and lipid transfer carriers that regulate the metabolism of lipoproteins and their uptake in tissue. Most apolipoproteins have already been well-studied and some have been found to be involved in copper detoxification and Alzheimer's disease. In contrast, the apolipoprotein E (ApoE) protein has antioxidant properties because it can bind with Cu^{2+} or Fe^{2+} (Zappasodi et al., 2008). APOE-ε4 appears to modulate the effect

of Cu^{2+} on altered AD brain activities, suggesting that the modulation of oxidative stress related to copper dysfunction may be one of the mechanisms that make APOE-ε4 a risk factor for AD (Zappasodi et al., 2008). Apolipoprotein B has also been found to bind with Cu^{2+} (Burkitt, 2001) and our previous *in vitro* study found that apolipoproteins B is down-regulated after Cu^{2+} exposure (Chen et al., 2009). In this study, apolipoproteins A-IV (apoA-IV) was up-regulated by Cu^{2+} and showed copper-binding ability in the Cu-IMAC experiment. Apolipoprotein A-IV can inhibit lipid peroxidation, thus demonstrating its potential anti-atherogenic properties. Wong et al. (2007) found that recombinant wild-type apoA-IV (100 ug/ml) inhibits the oxidation of LDL (50 ug protein/ml) with 5 uM CuSO4 ($P < 0.005$), but not with 100 uM CuSO4, suggesting that it may act by binding copper ions. Our results further confirm that apoA-IV can bind with copper and that excessive copper will induce the expression of apoA-IV to reduce lipid peroxidation. Furthermore, Cu^{2+} can bind with LDL to cause an oxidation effect and LDL will bind with apolipoprotein (Burkitt, 2001), indicating that LDL-APOA-IV may be involved in Cu^{2+} transportation. Amyloid precursor protein (APP) (Bayer et al., 2003) in Cu^{2+} efflux from cells also showed copper-binding ability in our experiment. Previous studies have found that apolipoproteins can directly interact with APP by binding with each other (Koldamova et al., 2001). Thus, it can be concluded that Cu^{2+} may efflux out of APOA-IV in conjunction with APP.

The other important protein involved in lipid metabolism, vitellogenin (VTG), was also found to have copper-binding ability. VTG, a very high-density lipoprotein, is a glycophospholipoprotein composed of 82 % apolipoprotein and 18 % lipid. (Ando and Yanagida, 1999) found that VTG is resistant to copper-induced oxidation and binds with Cu^{2+}. Vitellogenin also protects the copper-induced oxidation of VLDL because of its

antioxidant function. VTG also seems to serve as a transition metal-binding lipoprotein by which free-radical reactions in the oocytes are extensively depressed. Our study found that VTG is up-regulated by Cu^{2+} in terms of both protein and mRNA level, showing that copper may have an antioxidant function in fish by up-regulating the expression of VTG.

The cytoskeleton is a highly dynamic structure that not only forms the scaffold, the basis of cell morphology and plasticity, but plays a major role in transport and signaling (Frixione, 2000). The cytoskeleton comprises three major types of cytoplasmic structural proteins: microtubules, actin, and intermediate filaments (IFs). My previous *in vitro* study found that copper may influence the cell cytoskeleton by regulating actin, vimentin, and tropomoysin (Chen and Chan., 2009). Here, these proteins and their mRNA were also regulated by Cu^{2+} *in vivo*. Several other cytoskeleton proteins were identified to be differentially expressed including down-regulation of myosin heavy chain, alpha tubulin, titin-like protein, and collagen. This result further confirms that Cu^{2+} exerts its toxicity by disrupting the cell cytoskeletons reported previously (Pribyl et al., 2008; Rodriguez-Ortega et al., 2003).

3.4.5 Copper and cytoskeleton proteins

In the Cu-IMAC experiment, some of these cytoskeleton proteins were found to have copper-binding ability, such as collagen, vimentin, and myosin heavy chain. Collagen is the main protein of connective tissue in animals and is the most abundant protein, making up about 25 % to 35 % of the whole-body protein content. Prior studies have found that collagen cross-links with lysyl oxidase cuproenzymes, an important copper-bonding protein, in the notochord sheath of zebrafish (Gansner and Gitlin, 2008).

Copper deficiency and inhibition of lysyl oxidase will lead to disruption of the notochord sheath by influencing the expression of collagen. Vimentin is a member of the intermediate filament family of proteins and myosin is a motor protein that is responsible for actin-based motility (Norlen et al., 2007). The finding of copper-binding ability in these three proteins may indicate that copper ion transfer from lysyl oxidase to collagen, and then to vimentin and myosin, eventually influences the cell cytoskeleton and locomotion.

3.4.6 Function of other potential copper binding proteins

This study is the first to identify many proteins as copper-binding proteins which may play interesting roles in copper transportation and detoxification, including glyceraldehyde-3-phosphate dehydrogenase (GAPDH), catalase (CAT), and proteasome. GAPDH has recently been implicated in several non-metabolic processes including transcription activation, the initiation of apoptosis, and ER to Golgi vesicle shutting. GAPDH can move between the cytosol and the nucleus (Zheng et al., 2003) so that Cu^{2+} may also enter or exit from the nucleus by binding with GAPDH. CAT is an important protein that is related to the ROS effect and has been found to be up-regulated by Cu^{2+} in a previous study (Craig et al., 2007). Here, this protein was also up-regulated by Cu^{2+} and shown to have copper-binding ability for copper detoxification. The ubiquitin-proteasome pathway plays an essential role in multiple cellular processes including cell cycle progression, apoptosis, and differentiation. Recent studies have also shown that copper complexes can act as inhibitors of the 20S proteasome for cancer therapy (Hindo et al., 2009; Milacic et al., 2009).

3.4.7 Biomarkers

While our previous *in vitro* study (Chapter 2) identified 18 proteins as potential biomarkers, there was a need to confirm these results via an *in vivo* study. This study also confirmed that most of these potential biomarkers are differentially expressed at the protein level *in vivo*. This study found 9 additional interesting proteins for which the sequences have been entered in the tilapia database, and thus a total of 27 Cu^{2+} related genes were thus detected by real-time PCR for mRNA regulation after exposure to a wide range of concentrations of Cu^{2+} *in vivo* (Fig. 3.5). All of genes' regulation was all in accordance with protein regulation, and the regulation of 18 genes *in vivo* matched well with that for the same genes *in vitro,* except zinc finger protein 60 and protesome. Among these genes, well-characterized biomarkers such as cytochrom P450 1A1, cytochrome c oxidase, metallothionein, glutathione-S-transferase, and heat shock protein 70 were found. Seven genes were found to be novel biomarkers of effects for copper contamination in the aquatic environment including interleukin 1-alpha, growth hormone, NADH dehydrogenase, zic family member 1, zinc finger protein 60, ferritin, vitellogenin, and calmodulin.

3.5 Conclusion

In summary, the study reported here examined copper-binding proteins and their regulation in tilapia after copper exposure using chromatography (FPLC & Cu-IMAC) in combination with proteomic approaches. Fig 3.7 illustrates the copper transportation pathways in the hepatocyte based on our results and proteins reported in other studies (Hernandez and Allende, 2008). Cu^{2+} entering the cell can act on the cytoskeleton before moving to the nucleus and mitochondria to control cell motion, growth and metabolism.

Exposure to excessive Cu^{2+} can therefore cause defects in cytoskeleton formation, cellular growth, mitochondria, iron metabolism, and lipid metabolism. According to the functions of the cuproproteins identified in this study, copper may exert its toxicity by inducing endocrine disruption, mitochondria dysfunction, ion competition, lipid metabolism, and cytoskeleton disruption. Our results also suggest that Cu^{2+} may be transferred from cytoplasm to cytochrome C oxidase in mitochondria by binding with stanniocalcin, and that NADH dehydrogenase subunit 5 and aldehyde dehydrogenase may play a role in copper transportation and storage inside the mitochondria. These findings may help us to understand Cu^{2+} transport and storage in the liver of tilapia and perhaps in other fish species or even other vertebrates in general.

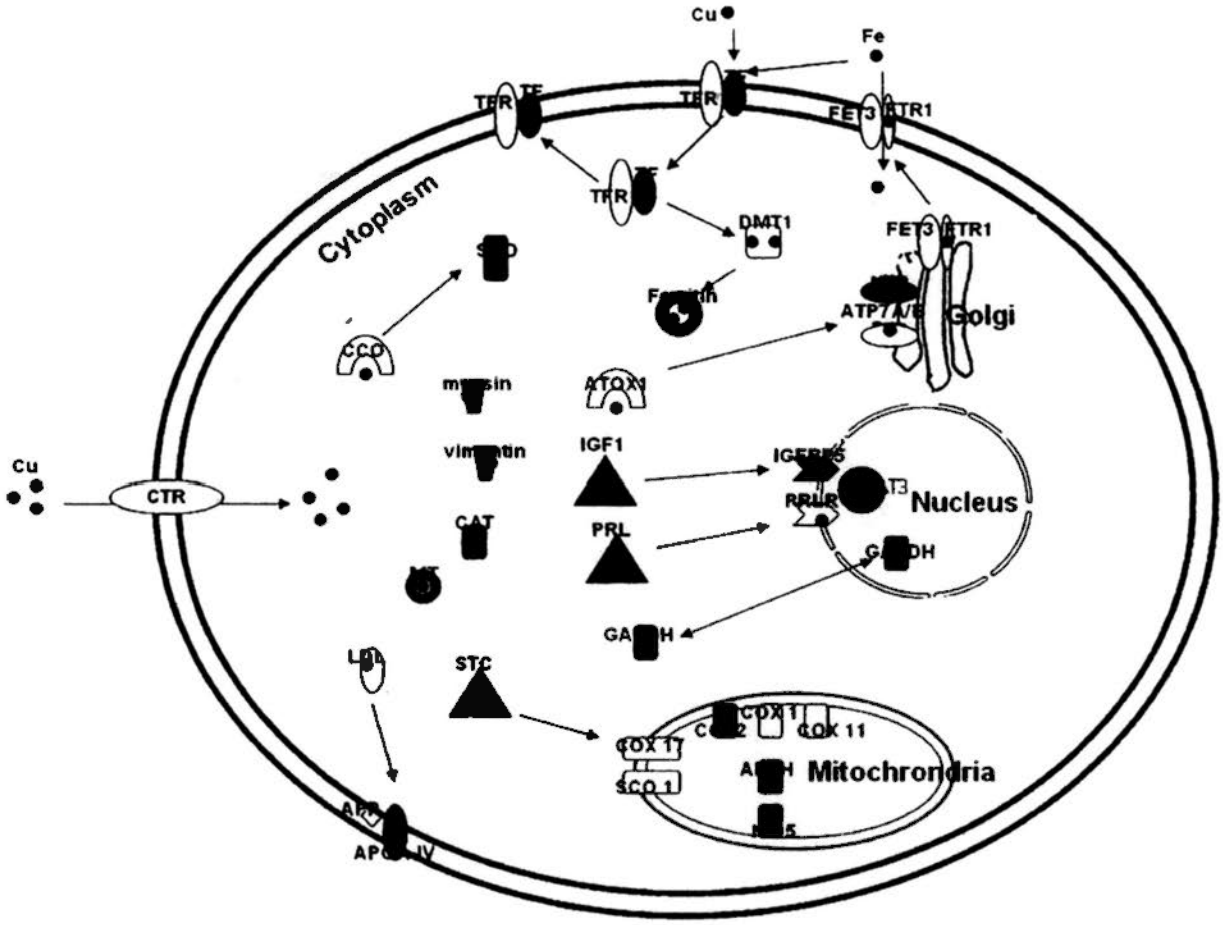

Fig. 3.7. Proposed copper transportation pathways in tilapia hepatocyte. Up-regulated proteins are shaded red, whereas the down-regulated proteins are shaded in green, proteins without regulation are shaded in white. Proteins shaded blue are those reported in other studies (Hernandezet al., 2008). These proteins are mainly involved in endocrine disruption, mitochondria dysfunction, ion competition, lipid metabolism, and cytoskeleton disruption. In addition, our results suggest that Cu^{2+} may be transferred from cytoplasm to cytochrome c oxidase in mitochondria by binding with stanniocalcin, and that NADH dehydrogenase subunit 5 and aldehyde dehydrogenase may play a role in copper transportation and storage inside the mitochondria. Abbreviations: ALDh, aldehyde dehydrogenases; APOA-IV, apolipoprotein A-IV; APP, amyloid precursor protein; ATP7A/B, ATPase, Cu transporting alpha/beta polypeptide; ATX1, copper transport protein ATOX1; CAT, catalase; CCO, copper chaperone for SOD1; COX 1/2/11/17, cytochrome c oxidase 1/2/11/17; CTR, high-affinity copper uptake protein; DMT1, divalent metal transporter 1; FET3, iron transport multi-copper oxidase; FTR1, iron transporter 1; GAPDH, glyceraldehyde 3-phosphate dehydrogenase; IGF1, insulin–like growth factor 1; IGFBP5, IGF-binding protein 5; LDL, low-density lipoprotein; MT, metallothionein; ND5, NADH dehydrogenase subunit 5; PRL, prolactin; PRLR, prolactin receptor; SCO1, SCO cytochrome oxidase deficient homolog 1; SOD, Cu/Zn superoxidase dismutase; STAT3, signal transducer and activator of transcription 3; STC, stanniocalcin; TF, transferrin; TFR: transferrin receptor.

Chapter 4

Differentially expressed proteins in the ZFL cell exposed to Cu^{2+}

4.1 Introduction

In the Chapter 2 and 3, I have used tilapia as a model to study the mechanism of copper toxicity *in vivo* and *in vitro*. It has been found some interesting proteins, and revealed that the copper tolerance of tilapia may be related to several proteins involved in lipid metabolism, tissue connective development and cell cycle control. Besides, in Chapter 3, I also indentified some interesting copper binding proteins, and hypothesized a transportation pathway according our results and several previous studies. These results would help us to understand the mechanism of copper tolerance in tilapia more clearly. In the other hand, the mechanism of copper toxicity to the copper sensitive species is still unclear. Therefore, in this chapter, I am interested to study the copper toxicity to the copper sensitive species.

In this chapter, the zebrafish (*Danio rerio*) is chosen as a model since it is more sensitive to copper toxicity than tilapia. The 96 h LC50 of Cu^{2+} to zebrafish adult is 0.064 ppm, but that of tilapia is 1.52 ppm (Wu et al. 2003). Also, the zebrafish has been used as a model in several toxicological studies (Amanuma et al., 2000; Craig et al., 2007). These studies have demonstrated that many physiological mechanisms between zebrafish and mammals are highly conserved. Therefore, in this chapter, we will also use proteomic approaches to analyze the molecular effects of copper exposure on zebrafish hepatocytes (ZFL cell-line), and identify some differentially expressed proteins, which can help us to understand the mechanism of copper sensitivity of zebrafish, comparing with that of tilapia which is regarded as a copper tolerant specie.

4.2. Materials and methods

4.2.1 Cell culture

ZFL is an adherent tissue hepatocyte cell line with epithelial-like morphology isolated from zebrafish (*Danio rerio*). It was purchased from the Cell Bank at American Type Culture Collection (ATCC® number CRL-2643TM) and maintained in a standard culture medium comprising 50% L-15 medium, 35% DMEM and 15% Hams F12 and supplemented with 1.5 g/l sodium bicarbonate, 15 mM HEPES, 0.01 mg/ml insulin, 50 ng/ml EGF, 5% heat-inactivated fetal bovine serum and 1% penicillin/streptomycin, according to the supplier's protocol.

4.2.2. Cytotoxicity assay.

The 96 h LC50 of CuCl2 to ZFL was determined according to the methods described as previously (Section 2.2.2)

4.2.3. Annexin-V/PI assay and cell cycle analysis.

See Section 2.2.3.

4.2.4 Isolation of the cytosolic fraction.

See Section 2.2.4.

4.2.5. Two-dimensional gel electrophoresis (2-DE) and protein identification

See Section 2.2.5 and 2.2.6.

4.3 Results

4.3.1. Copper toxicities

The median lethal concentration (LC50) of Cu^{2+} on the ZFL cell line at 96 h was determined using alamarBlue assay. The dose response curves with 96 h LC50 were plotted using GraphPad Prism 5.0 (Fig. 4.1): that of $CuCl_2$ was 362.4 μM (95 % confidence interval: 322 uM to 408 uM). Comparing with the 96 h LC50 of Cu^{2+} to Hepa T1 (tilapia hepatocyte), which was 598 uM, it was further confirmed that zebrafish was more sensitive than tilapia after exposed to Cu^{2+}. Flow cytometry measurement was used to quantify the extent of apoptosis and necrosis in the total cell population, and significant differences were observed between the control and the $CuCl_2$-treated cells. After incubation with different concentrations (100 μM and 200 μM) of $CuCl_2$ for 96 h, the percentage of Annexin-V+/PI+ cells (apoptosis) increased to 3.3 % and 3.0 %, respectively, compared to 0.9 % in the control group. The percentage of Annexin-V-/PI+ cells (necrosis) increased to 6.0 % and 7.4 %, respectively, compared to 1.4 % in the control group. These results demonstrated that $CuCl_2$ primarily induced cell necrosis rather than apoptosis.

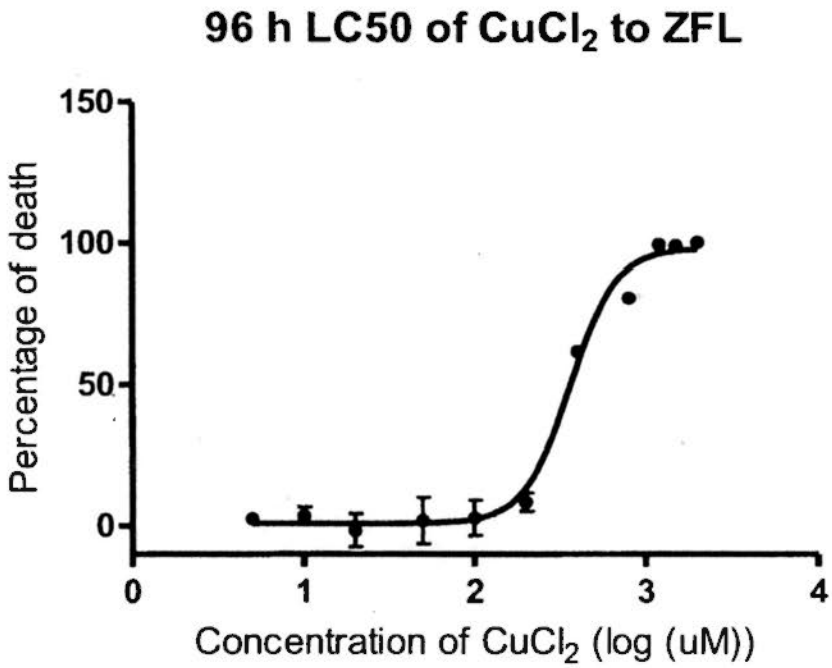

Fig. 4.1. Cytotoxicity (%) of ZFL cells after $CuCl_2$ exposure in different concentrations (in log scale) for 96 h. The 96 h LC50 of $CuCl_2$ on ZFL cells was determined as 362.4 μM. The 96 h LC50 values were calculated using Sigmaplot with linear regression.

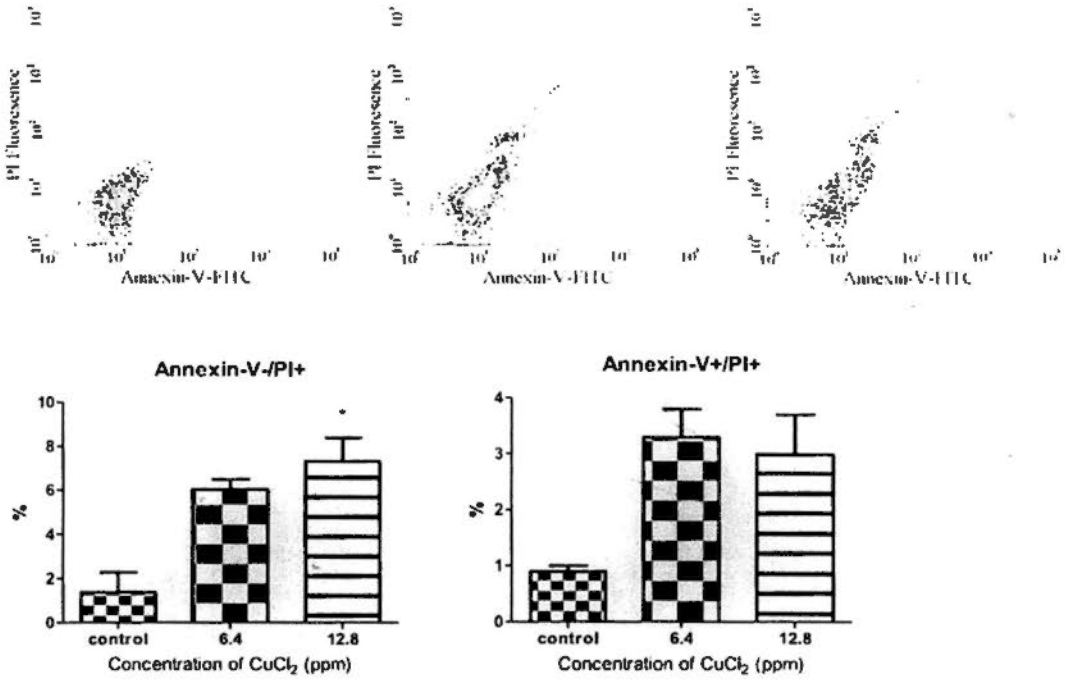

Fig 4.2. Flow cytometer detection of $CuCl_2$-induced apoptosis and necrosis with Annexin-V-FITC and PI staining. The ZFL cells were exposed to different concentrations of $CuCl_2$ for 96 h. After being stained with Annexin-V-FITC and PI, the cells were analyzed using flow cytometry. LL: Annexin-V-/PI-cells (normal); LR: Annexin-V+/PI-cells (early apoptosis); UR: Annexin-V+/PI+ cells (late apoptosis); UL: Annexin-V-/PI+ cells (necrosis). The data shown are representative of three independent experiments. Statistic analysis of the apoptosis cells and necrosis cells among the total population was shown in bar graph (% of cells in each phase relative to the total population).

4.3.2. 2-DE gel analysis of cytosolic proteins

The cytosolic proteins extracted from the control cells and $CuCl_2$-treated (100 μM and 200 μM) ZFL cells were analyzed by 2-DE. Approximately 2,000 protein spots were detected on the 2-DE gels. A representative protein profile of the ZFL cells treated with 120 μM of $CuCl_2$ is shown in Fig. 4.3. In total, 90 proteins were found to be regulated by $CuCl_2$ exposure with a clear dose-response, of which 72 were identified using mass spectrometry protein identification (MALDI-TOF MS and/or MS/MS). The details of each indentified protein, including the identification number on the gel, the accession number, the protein name and the ratio of treatment to control for each dose level, are listed in Table 4.1. In most cases, the experimental Mw and pI values from the 2-D gels were in agreement with the theoretical Mw and pI values of the proteins. Thus, the protein spots were identified with a high degree of confidence.

Control

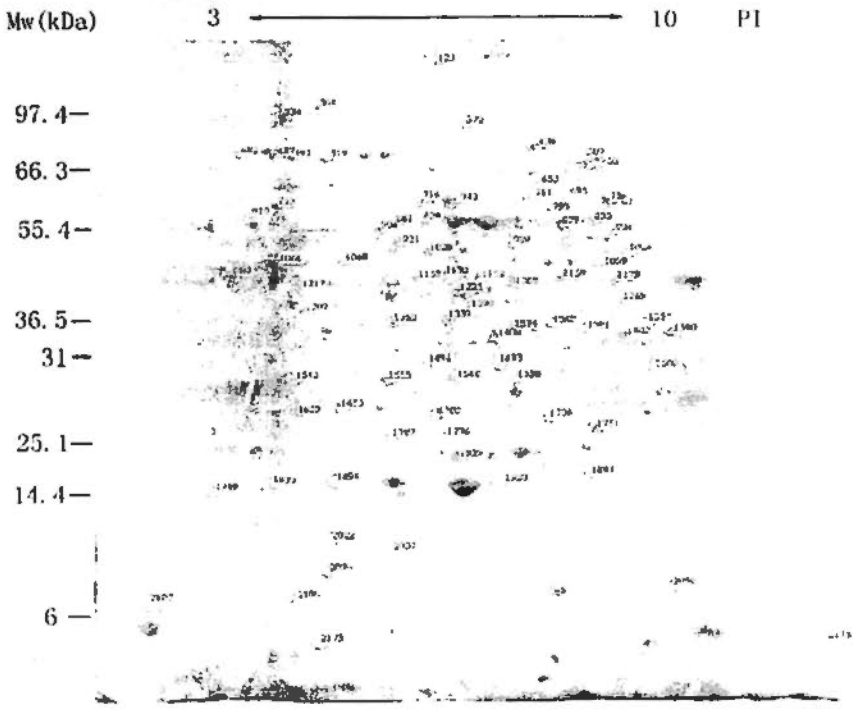

100 uM

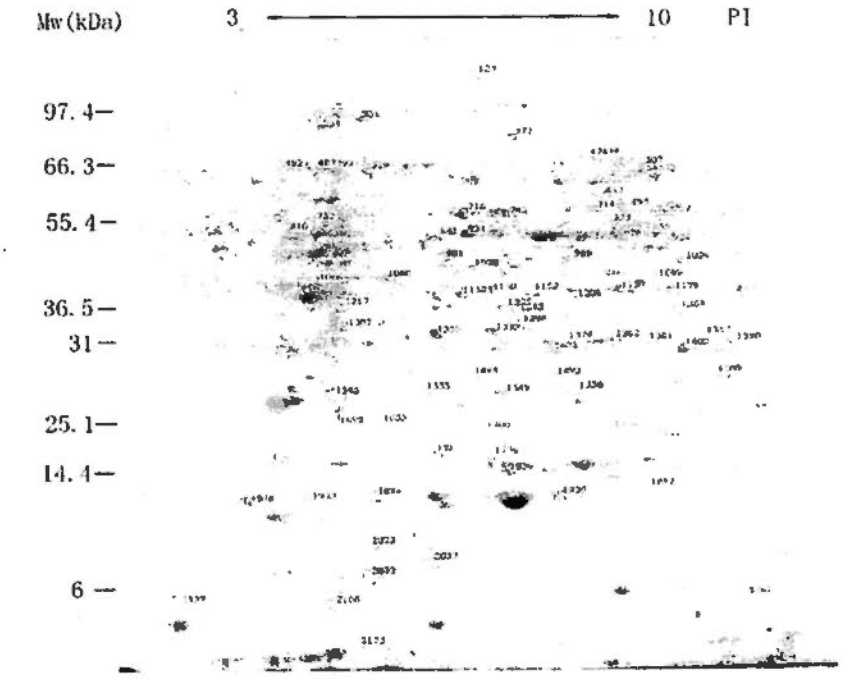

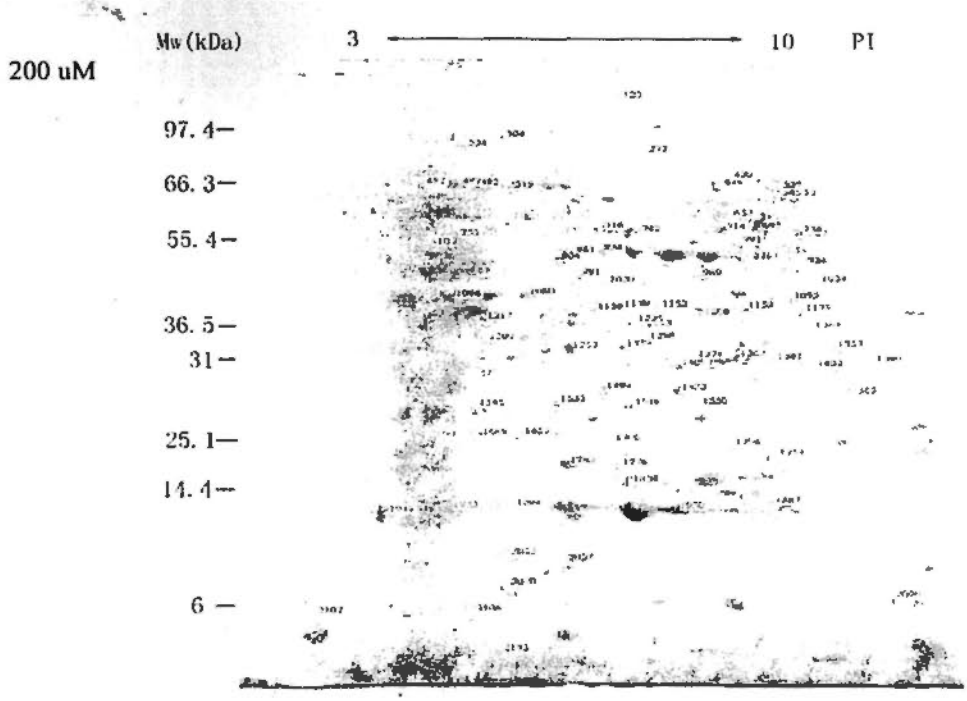

Fig. 4.3. A sample of 2-DE gel images of the cytosolic proteins obtained from the ZFL cell line in the control, 100 uM, and 200 uM treatment groups. The total cytosolic proteins were loaded and separated using IPG strips (pH 3-10)/SDS-PAGE (12% acrylamide). The gels were stained by silver staining. The cycled spots represent the matched spots in these three gels, and the spot numbers refer to the proteins with a modified accumulation level after $CuCl_2$ treatment that were selected for mass spectrometry identification (the details are summarized in **Table 4.1**).

The magnitude of the ratio changed from 0.26 down-regulation (guanine nucleotide binding protein, Spot No. 123) to 18.6 up-regulation (metallothionein, Spot No. 2175). Of the proteins identified, few (e.g., Spot Nos. 1060 and 1653) were located in an unexpected position on the gel, based on their Mw and pI theoretical values. Any changes in Mw and pI can most probably be attributed to posttranslational protein modifications, such as proteolytic cleavage, glycosylation and phosphorylation. Furthermore, a number of different protein spots were identified as being the same protein. For example, Spot Nos. 834, 835 and 861 were identified as enolase 1 alpha. They may be degradation products or different isoforms of the same protein. Interestingly, a fructose-bisphosphate aldolase C (Spot No. 1390) was up-regulated by Cu^{2+}, but reversely, its isoform fructose-bisphosphate aldolase A was down-regulated by Cu^{2+}. These results meant that the different isoforms of fructose-bisphosphate aldolase have different functions when exposed to Cu^{2+}. Thus, out of the original 90 spots selected for identification, a total of 72 individual proteins were identified.

Table 4.1. Differentially expressed proteins in the cytosolic fraction of ZFL after $CuCl_2$ treatments at 100 and 200 uM.

No	Protein Name	Accessing No.	MW	PI	S	100	200	M
Chaperone								
474	stress-induced-phosphoprotein 1	gi|56090148	62151	6.43	100	1.64	1.82	
482	Heat shock protein 5	gi|39645428	72120	5.04	218	1.32	1.76	U
487	HSC70 protein	gi|1865782	71479	5.18	70	1.49	2.13	U
492	Heat shock protein 8	gi|28279108	71386	5.32	91	1.46	2.78	U
Enzyme								
695	glucose-6-phosphate dehydrogenase-like	gi|292626911	60077	6.39	68	1.13	1.50	U
714	glucose-6-phosphate dehydrogenase-like	gi|292626911	60077	6.39	112	2.05	2.95	U
736	cytochrome P450 1A	gi|13365614	45713	5.26	43	1.39	2.61	U
924	fumarate hydratase, mitochondrial precursor	gi|41055718	55000	8.98	77	1.54	2.04	
1130	4-hydroxyphenylpyruvate dioxygenase	gi|51230599	44857	5.84	130	1.36	1.68	
1208	fructose-bisphosphate aldolase C	gi|35902900	39698	6.21	99	1.02	2.52	D
1179	serine/threonine protein kinase	gi|40363564	28817	8.56	36	1.74	1.89	D
1159	thioredoxin/glutathione reductase	gi|29165346	21246	8.55	42	1.49	1.91	
1362	Ldhb protein	gi|28277619	36398	6.4	52	1.10	1.66	
1374	uroporphyrinogen decarboxylase	gi|18859531	42024	6.05	45	1.06	1.82	
1493	GST	gi|1125671	24369	6.32	40	1.43	1.71	U
1494	Cu/Zn superoxide dismutase	gi|157152709	16088	5.85	26	1.68	2.36	U
1887	cytochrome c oxidase subunit II	gi|28882001	26207	4.65	36	1.10	1.51	U
1933	lactoylglutathione lyase	gi|47085917	20404	5.23	69	2.19	2.64	
2022	peroxiredoxin-1	gi|61806512	22207	6.42	120	3.23	3.47	U
2070	NADH dehydrogenase subunit 4L	gi|16357243	10494	6.47	40	1.57	1.66	U
545	transketolase	gi|31872040	68681	6.81	109	0.76	0.48	
552	transketolase	gi|31872040	68681	6.81	127	0.56	0.36	
716	tyrosine kinase	gi|472720	11472	5.26	34	0.56	0.56	D
751	aldehyde dehydrogenase 1A2	gi|18858265	57117	5.89	114	0.66	0.64	D
834	Enolase 1, (alpha)	gi|37590349	47392	6.16	149	0.59	0.48	
855	Enolase 1, (alpha)	gi|37590349	47392	6.16	122	0.84	0.58	
861	Enolase 1, (alpha)	gi|37590349	47392	6.16	80	0.47	0.38	
1020	Ornithine aminotransferase	gi|189526312	49142	6.58	52	0.52	0.51	
1024	isocitrate dehydrogenase 2 ($NADP^+$)	gi|41054651	50944	8.35	40	0.52	0.43	D
1275	cathepsin D precursor	gi|22651403	43607	6.23	73	0.44	0.39	
1390	fructose-bisphosphate aldolase A	gi|41282154	40237	8.45	54	0.38	0.33	D
1402	malate dehydrogenase	gi|47085883	35804	8.4	99	0.64	0.59	
1420	proteasome subunit beta type-9	gi|18859275	23650	4.72	30	0.54	0.32	D
1706	putative tyrosinase enzyme	gi|21449828	7364	6.49	22	0.70	0.63	
Transcription factor								
793	Stat3 protein	gi|28277427	48512	7.15	36	1.50	1.55	U
1653	zinc finger protein, subfamily 1A, 1	gi|18859581	59988	6.1	49	1.65	1.66	U
519	IGF2BP2	gi|169158244	51855	8.66	46	0.34	0.27	D
1307	eukaryotic translation initiation factor 3, subunit 2 beta	gi|55742565	36727	5.22	50	0.64	0.50	

Metal binding proteins								
1353	annexin A1a	gi|32308156	38020	6.26	71	1.46	1.61	
1408	transferrin	gi|27464846	38582	6.28	35	2.31	2.68	U
2175	MT	MT_PSEAM	7185	8.1	40	10.5	18.6	U
1217	calcium-binding protein 39	gi|50344946	40057	6.22	40	0.65	0.47	
Cytoskeleton								
753	Bactin1 protein	gi|28279111	42073	5.3	66	0.73	0.62	D
810	kinesin-like protein 2	gi|6503041	44358	6.88	43	0.53	0.47	
904	keratin 18	gi|30410758	48573	5.53	80	0.61	0.52	D
1158	novel protein similar to human titin (TTN)	gi|27884115	75693	5.56	30	0.51	0.49	D
1782	cardiac myosin light chain-1	gi|55926111	21925	4.87	43	2.71	2.79	D
Transporter								
334	transitional endoplasmic reticulum ATPase	gi|41393119	90006	5.14	106	0.60	0.50	
1060	ATP-binding cassette sub-family B member 8	ABCB8_DANRE	77693	9.66	36	1.83	2.67	U
1243	V-type ATPase subunit G-like protein	gi|7861924	7546	5.83	30	2.03	2.63	U
1269	novel protein similar to human transporter 2, ATP-binding cassette, subfamily B	gi|26788068	79478	8.23	34	1.45	1.74	U
1776	ATPase, Na^+/K^+ transporting, beta 2b polypeptide	gi|18858317	34340	8.5	34	1.51	1.78	U
Cytokine								
1553	insulin-like growth factor I	gi|4261848	2025	6.69	23	0.27	0.18	U
1930	Interleukin-1 beta	gi|83416463	5908	4.51	32	1.55	4.69	U
Lipoprotein								
878	low density lipoprotein receptor-related protein	gi|41152012	39391	6.67	43	1.60	1.87	
2107	Vitellogenin	gi|21952780	18686	9.37	33	1.52	1.71	U
372	apolipoprotein E	gi|6688892	5078	4.03	45	0.56	0.46	D
Others								
653	CDC23	gi|41055558	67885	5.99	45	1.51	1.79	U
1339	mitochondrial uncoupling protein 4	gi|41054379	35188	10.2	37	1.40	1.80	U
1548	potassium channel tetramerisation domain containing 12.2	gi|77404244	31229	6.25	77	1.49	1.60	
1550	voltage-dependent anion-selective channel protein 1	gi|47777306	30665	6.23	112	2.25	2.46	
2037	MHC class IIB antigen	gi|62825852	8451	9.13	35	1.11	1.83	U
2090	cold inducible RNA binding protein	gi|62955567	18443	8.75	63	1.61	2.25	
304	Mvp protein	gi|29179488	95061	5.48	72	0.81	0.56	
742	Sb:cb825 protein	gi|27881963	55119	6.32	66	0.63	0.62	
763	G-protein coupled receptor 173	gi|18859427	44250	9.44	35	0.39	0.32	
1099	Sjogren syndrome antigen B	gi|41054695	46225	6.68	78	0.21	0.16	
1225	crk-like protein	gi|47087217	33916	6.01	59	0.68	0.56	
1509	guanine nucleotide-binding protein subunit beta-2-like 1	gi|18859301	35565	7.6	103	0.57	0.50	
1545	Gag-Pol polyprotein-like	gi|292611256	199035	8.48	62	0.49	0.38	D
1949	RAB14, member RAS oncogene family	gi|41393147	24091	5.84	24	0.81	0.66	U

* In this table, "N" stands for spot no.; "S" stands for score of the protein calculated by MASCOT software, when "S" > 54, the protein was significant identified; "M" stands for a match with the data from previous work done in tilapia; "U" stands for up-regulation and "D" stands for down-regulation.

The differentially expressed proteins can be divided into 9 groups according to their function, including chaperone, enzyme, transcription factor, metal-binding, cytoskeleton, transporter, cytokine, lipoprotein and other proteins, and 42 % of the differentially expressed proteins were enzymes. The results of the differentially expressed proteins in cytosolic fraction of ZFL were also compared with the proteins found in our previous study of copper-affected proteins using tilapia Hepa T1 cells. More than 50 % of the differential proteins were also regulated by Cu^{2+} in tilapia, which were shown in the last column of Table 4.1. Also, the functions of the differential expressed proteins in zebrafish were involved in lipid metabolism (Spot No. 2107, vitellogenin; Spot No. apolipoprotein E), cytoskeleton (Spot No. 753, beta-actin; Spot No. 904, keratin), cell proliferation (Spot No. 1553, insulin-like grow factor 1), etc. These functions were also similar to that of differential expressed proteins in the tilapia, which meant that the mechanism of copper toxicity to zebrafish and tilapia was highly conserved.

Even though, there were some differences in the differentially expressed proteins between zebrafish and tilapia. Firstly, Cu^{2+} can regulate more proteins in tilapia (125 proteins) than zebrafish (90 proteins). Secondly, the fold induction and depression of differentially expressed proteins by Cu^{2+} in tilapia were mostly higher than that in zebrafish. Thirdly, the regulation trend of several proteins in zebrafish was different from that in tilapia. For example, serine/threonine protein kinase (Spot No. 1179) was found up-regulated in zebrafish but down-regulated in tilapia. And insulin-like growth factor 1 (Spot No. 1553) was found down-regulated in zebrafish but up-regulated in tilapia. At last, some well identified proteins in tilapia were not found in zebrafish after exposed Cu^{2+}, such as growth hormone and catalase. These four differences between

reactions of zebrafish and tilapia to Cu^{2+} may help us to uncover the mechanism of copper sensitivity in zebrafish and tolerance in tilapia.

4.3. Discussion

In the present study, copper effects on zebrafish ZFL cells were investigated. Several studies have reported the effects of metal exposure in zebrafish (Craig et al., 2007; Gonzalez et al., 2006; Paris-Palacios and Biagianti-Risbourg, 2006). Regarding copper, there was no report describing the changes in proteins expression in zebrafish exposed to Cu^{2+}. The present work was intended as a preliminary qualitative study of the changes in protein expression induced by copper in the zebrafish liver cell line (ZFL) to study the mechanism of copper toxicity to zebrafish, and identified several proteins related to the copper sensitivity of zebrafish.

Proteomic is an efficient method to identify new proteins as well as to investigate the ecological risk assessments (Dail et al., 2008; Rodriguez-Ortega et al., 2003b). It may be useful in providing insights into the molecular mechanisms underlying copper-induced responses in zebrafish liver cell. As is known, toxic effects of Cu^{2+} are generally attributed to its high affinity for thiol groups and to its capacity in participating in redox reactions to form reactive oxygen species. In fact, several authors reported an increased ROS formation after copper exposure in different aquatic species (Pourahmad et al., 2003; Sandrini et al., 2009). In the present study, exposure for 96 h to 200 uM Cu^{2+} (50 % 96 h LC50) significantly induced several ROS generation related proteins in ZFL cells, such as thioredoxin/glutathione reductase (Spot No. 1159), Glutathione S-transferase (GST) (Spot No. 1493), Cu/Zn superoxide dismutase (Cu/Zn SOD) (Spot No. 1494), peroxiredoxin-1 (Spot No. 2022), et al (Sandrini et al., 2009; Craig et al.,

2007). Also, these several important ROS related proteins can be found in the Hepa T1 cell line after exposed to 300 uM Cu^{2+} (50 % 96 h LC50 of Cu^{2+} to Hepa T1). But interestingly, the regulation folds of these proteins in zebrafish were much lower than that in tilapia. For example, 200 uM Cu^{2+} just induced GST at 1.71 folds in ZFL, but 120 uM and 300 uM Cu^{2+} could induced GST at 19.13 and 42.42 folds in Hepa T1, respectively. It was known that these four ROS related proteins were important proteins which had antioxidant effect to the free oxygen inside the cell. The lower induction of these four proteins in zebrafish would help us to revealed sensitivity of zebrafish to Cu^{2+}. Besides, one of the most important ROS related proteins, catalase, was absent in ZFL exposed to Cu^{2+}, but up-regulated in Hepa T1, which also confirmed that the sensitivity of zebrafish should be due to lower antioxidant ability. Anyway, the induction of the ROS related proteins in ZFL can further confirmed that the toxicity of copper was probably related to ROS effect.

One of the main targets of metal toxicity is the mitochondrion, and there is a close relationship between metal-induced oxidative stress and proper mitochondrial function, as seen in mammals and fish (Craig et al., 2007; Belyaeva et al. 2008). Many studies have examined the *in vitro* impact of metals on mitochondrial respiration and energetics in fish (Manzl et al., 2003; Manzl et al., 2004). In this study, several mitochondrion inner proteins were found differentially expressed in ZFL after 96 h exposure to Cu^{2+}, including cytochrome c oxidase subunit II (COX2) (Spot No. 1887), NADH dehydrogenase subunit 4L (ND4L) (Spot No. 2070), aldehyde dehydrogenase (Spot No. 751). Comparing with Hepa T1, these three proteins were also found differentially expressed after Cu^{2+} exposure, and the regulation trends were also well matched. This

result further confirmed that copper toxicity to the mitochondrion. However, the induction of COX2 in the Hepa T1 (300 uM induced 29.05 folds) is much higher than that in zebrafish (200 uM induced 1.51 folds) after exposed to Cu^{2+}. This should be due to the copper binding ability of COX2, which was found in chapter 3. Recent studies demonstrate that steady state Cu levels in the mitochondrial matrix are nearly an order of magnitude above that predicted to be required for the activation of the abundant mitochondrial Cu-dependent enzyme cytochrome oxidase (eg. COX17, COX11) (Craig et al., 2007). COX2 should play an important role in copper transportation inside the mitochondrion. Therefore, the higher induction of COX2 in Hepa T1 may accelerate copper transportation in mitochondrion and help the cell to process the detoxification of Cu^{2+}.

It is important to note that Cu^{2+} can induce different members of heat shock protein 70 (Hsp70), including heat shock protein 5 (Spot No. 482), heat shock protein 70 (Spot No. 487), and heat shock protein 8 (Spot No. 492). Heat shock proteins inductions are markers of multiple stress exposures, and the Hsp70 family comprises the most important proteins responsive to toxic compounds including Cu^{2+} (Piano et al., 2004; Rodriguez-Ortega et al., 2003). Induction of heat shock/stress proteins is a key feature of a universal mechanism of cellular defense to injury known as the "stress response", which means that the ZFL cell may protect itself from Cu^{2+} by induction of Hsp70. Interestingly, Hsp70 was not found regulated in the Hepa T1 cell after Cu^{2+} exposure, but induced in vivo as the results showed in the chapter 3. According to previous studies and our previous data, Hepa T1 cell is much more resistant to Cu^{2+} than the zebrafish and tilapia adult (Sandrini et al., 2009; Cheuk et al., 2008; Chen and Chan, 2009).

Therefore, the Cu^{2+} could cause stress response in vivo but not in vitro to tilapia. In view of these data, it is concluded that Cu^{2+} can induce more stress response to ZFL than the Hepa T1 cell.

In this study, two interesting proteins were firstly identified to be related to Cu^{2+} toxicity in the ZFL cell, which were potassium channel tetramerisation domain containing 12.2 (Spot No. 1548) and voltage-dependent anion-selective channel protein 1 (VDAC1) (Spot No. 1550). Potassium channel tetramerisation domain is the N-terminal, cytoplasmic tetramerisation domain (T1) of voltage-gated K^+ channels, which belongs to most diverse group of the ion channel family. It defines molecular determinants for subfamily-specific assembly of alpha-subunits into functional tetrameric channels (Gan et al., 1996; Perney et al., 1992). Voltage-dependent anion channels are a class of porin ion channel located on the outer mitochondrial membrane (Li et al., 2001). In addition to its function as a channel protein for solutes or ions, VDAC1, which acts as a major mitochondrial outer-membrane anion transporter, also functions as a gatekeeper in mitochondria-mediated apoptosis (Daoudal and Debanne, 2003). It was reported that opening of voltage-gated ion channels located in the cell membrane is mandatory when an excitatory synapse becomes activated (Liu et al., 2008). Here, we showed the up-regulation of potassium channel tetramerisation domain containing 12.2 and VDAC1 in the ZFL cell after copper exposure, which should be due to the stimulation of Cu^{2+} to the cell. However, how the Cu^{2+} stimulated the ion channel needs to be further studied.

Taken together, the study in the chapter showed the differentially expressed proteins

profile in the ZFL cell after exposed to Cu^{2+}. According the these results and previous data, the mechanism of Cu^{2+} toxicity to the ZFL is highly conserved with that of Hepa T1, which were both involved in lipid metabolism, cytoskeleton, and cell proliferation. However, as zebrafish is a copper sensitive species, there were also some differences in differentially expressed proteins between ZFL and Hepa T1 cell. The most differences of the differentially expressed proteins between these two cell lines after copper exposure were involved in the ROS effect, mitochondrion function and stress response. As discussed previously, the copper ion would induce more proteins related antioxidant and mitochondrial copper transportation in Hepa T1 than ZFL, which would act to protect Hepa T1 from Cu^{2+} toxicity. Also, Cu^{2+} would induce more stress effect to ZFL than Hepa T1 cell. These differences should help us to reveal the reason of copper sensitivity of zebrafish and tolerance of tilapia. At last, two interesting proteins were firstly found to be induced by Cu^{2+}, but the real mechanism of these two proteins related to is still unclear and need to be further studied.

Chapter 5

Regulation of copper transporters mRNA levels in zebrafish and tilapia after waterborne exposure to copper ion

5.1. Introduction

In previous chapters, the mechanism of Cu^{2+} toxicity to tilapia and zebrafish was studied by proteomic approaches. From our previous studies, cytosolic fractions were used for copper binding protein analysis and thus copper transporters on plasma membranes were not studied. This chapter focuses on the regulation of copper transporters by Cu^{2+}. Previous chapters found that the Cu^{2+} sensitivity of zebrafish and tolerance of tilapia might be due to the regulation of several important proteins related to ROS effect, copper transport in mitochondrion, and stress response. However, these proteins' regulation by Cu^{2+} should happen after copper ion enter into the cell and copper transporters are responsible for copper uptake in cells. Copper transporters also play important roles in copper intoxication and detoxification.

Cu metabolism and export from the cell rely on important Cu-transporting ATPases. In mammals, there are two types of ATPases: ATP7A (Menkes disease gene) and ATP7B (Wilson's disease gene) that are associated with human genetic disorders of the same name (Kim et al., 2008; Madsen and Gitlin, 2007). The copper ATPases, ATP7A (ATPase, Cu^{+} transporting, alpha polypeptide) and ATP7B (ATPase, Cu^{+} transporting, beta polypeptide) are two copper transporters important for regulating copper levels in the body. ATP7A function is thought to be regulated mainly at the post-translational level by alterations in membrane transport of copper ions. Under acute conditions of elevated levels of copper ions, it has been shown that there is a change in the subcellular

localization of the protein from the trans golgi network to the cell periphery (Balamurugan and Schaffner, 2006). In the small intestine, the ATP7A protein helps control the absorption of copper from food, and in other organs or tissues, the ATP7A protein has a dual role and shuttles between two locations within the cell. The ATP7A protein normally resides in the Golgi apparatus, which modifies and transports newly produced enzymes and other proteins, it supplies copper to certain enzymes that are critical for the structure and function of bone, skin, hair, blood vessels, and the nervous system. When intracellular copper level is elevated, however, the ATP7A protein will move to the cell membrane and eliminates excessive copper ions from the cell. ATP7B is an ATPase that transports copper ions. This protein functions as a monomer, exporting copper ions out of the cells, such as the efflux of hepatic copper ions into the bile (Kim et al., 2008; Madsen and Gitlin, 2007; Balamurugan and Schaffner, 2006).

To study the regulation of copper transporters of Cu-ATPAses in tilapia and zebrafish, the nucleotide sequences of ATP7A & B cDNAs were investigated by using Reverse Transcription-PCR. Further more, real-time PCR was used to determine the mRNA levels of metallothein (MT), ATP7A and 7B in tilapia and zebrafish exposed to copper ions in vivo and in vitro.

5.2. Materials and Methods

5.2.1 Fish and cell culture

To compare the regulation of ATP7A & B in tilapia and zebrafish, the *in vitro* and *in vivo* experiments were both conducted. In the in vitro experiment, the Hepa T1 (tilapia

hepatocyte) and ZFL (zebrafish hepatocyte) was chosen. Hepa T1 and ZFL cells were treated with two dosage of sterile $CuCl_2$ solution as shown in chapter 2 & 4. As to the *in vivo* experiment, the liver and gill in the tilapia and zebrafish larvae were examined. The administrations with copper ions of tilapia can be referred to chapter 3.

To prepare zebrafish larvae, firstly, adult zebrafishs were raised and maintained in a closed flow-through culture system at 28 ± 0.5 ∘ C with a photoperiod of 14 h light and 10 h dark. The zebrafish were fed twice a day with dry flakes supplemented with liver brine shrimps once a day. Spawning is triggered once the light is turned on in the morning and is complete within 30 min. At 4–5 h post-fertilization (hpf), embryos were collected and rinsed several times with culture medium to remove residues on the egg surface. Healthy embryos at blastula stage were then selected for subsequent experiments. Zebrafish larvae (5 day post-fertilization) were treated with three dosages of waterbone exposure $CuCl_2$ according to its 96 h LC50 value, which was calculated by observation the death percentage of larvae exposed to different concentration of $CuCl_2$.

5.2.2. First strand cDNA synthesis

Exposed samples with control fishes were collected and homogenized in TRIZOL® reagent (Invitrogen, Carlsbad, CA, USA). Total RNAs were isolated according to the manufacturer's protocol. RNA qualities were confirmed spectrophotometrically. Single-stranded cDNA was synthesized from 2 μg total RNA using an oligo (dT) 20 primer and the SuperScript™ III RT kit (Invitrogen, Carlsbad, CA, USA) by reverse transcription according to the manufacturer's manual.

5.2.3. Cloning and sequencing of cDNAs for tilapia ATP7A & B

Several degenerative primers were designed using conserved domains after multiple alignments of full-length or partial cDNA sequence of ATP7A & B reported from other species (Fig. 5.1). For amplifying partial sequences of these two genes in tilapia, RT-PCR was carried out using 2 μM of each primer and hepatic cDNA as a template with the following conditions: 2 min at 94 °C, 10 cycles of 94 °C for 30 s, 48 °C for 30 s, and 72 °C for 60 s, 10 cycles of 94 °C for 30 s, 50 °C for 30 s, and 72°C for 60 s, 10 cycles of 94 °C for 30 s, 52 °C for 30 s, and 72°C for 60 s, 10 cycles of 94 °C for 30 s, 54 °C for 30 s, and 72°C for 60 s, and 7 min at 72°C. Information of primers used in this study is shown in Table 1. The RT-PCR products were purified from 1 % agarose gel using the Gel Extraction kit (Qiagen, Hilden, Germany), ligated into pCR2.1. TA plasmid vector, and transformed into competent E. coli (Invitrogen). The plasmid DNA was isolated from bacterial cultures using the Plasmid Purification kit (Promega, Madison, WI, USA).

A

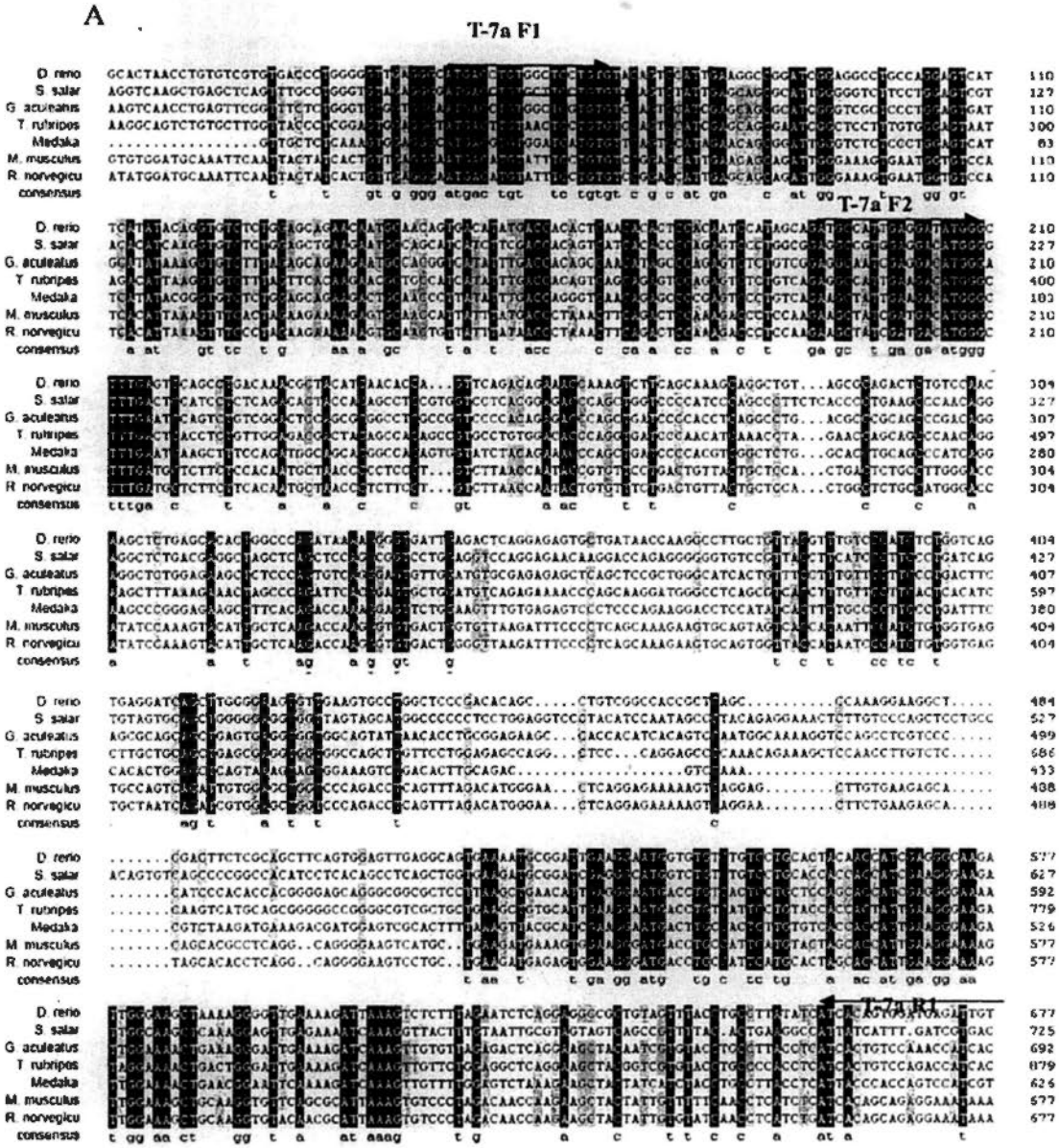
T-7a F1
T-7a F2
T-7a R1
D. rerio
S. salar
G. aculeatus
T. rubripes
Medaka
M. musculus
R. norvegicu
consensus

B

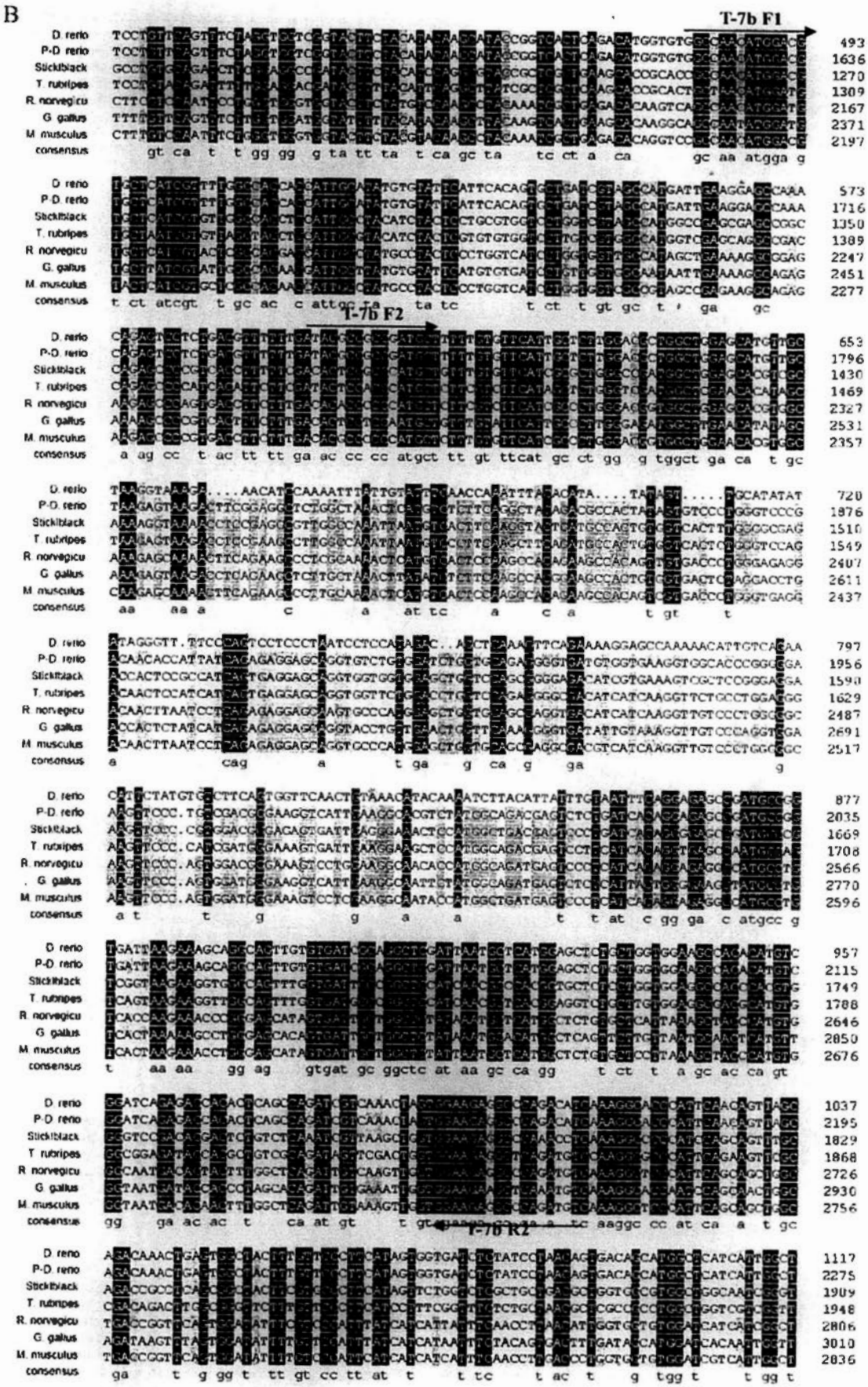
T-7b F1
T-7b F2
T-7b R2
D. rerio
P-D. rerio
Stickleback
T. rubripes
R. norvegicu
G. gallus
M. musculus
consensus

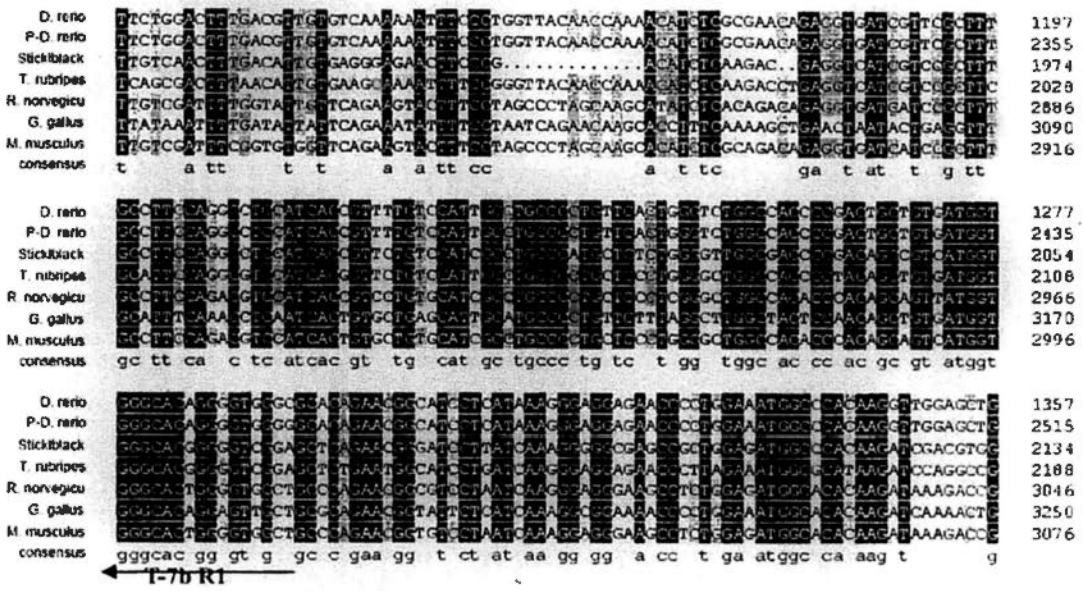

Fig. 5.1. Conserved regions of ATP7A & B from the alignment of nucleotide sequences obtained from NCBI. Locations of degenerative primers are shown with arrows. A: ATP7a; B: ATP7B.

5.2.4. 5'- and 3'-RACEs for ATP7A & B in tilapia

For rapid amplification of cDNA end (RACE), the forward and reverse primers were designed from the partial cDNA sequence (Table 5.1). The 5' and 3' end sequences of each gene were obtained using the GeneRacer^{TM} kit (Invitrogen). The temperature conditions for RACE were set as specified by the manufactures of the kit.

5.2.5. Tissue distribution

The tissue distribution of mRNAs from these two genes in tilapia was explored by quantitative real time RT-PCR by using β-actin as control gene. Six different tissues (brain, gill, intestine, kidney, liver and heart) were carefully dissected from the acclimated fish (n=3). Total RNA in each tissue was isolated from the pooled tissues of 3

fish, and cDNA was synthesized using the method described above. And the expression level of these two genes in the liver was taken as control.

5.2.6. Copper accumulation in ZFL and zebrafish larvae

ZFL cells were exposed (96 h) to different concentrations CuCl2 (0, 100 and 200 uM), as described above. After trypsinization, cells (6 groups of 2×10^6 cells per group) were centrifuged (3min) at 1500 rpm. Pellet was resuspended in PBS and centrifuged for three times. The new pellet was dried (60 °C) and completely digested in 50 uL of HNO3 (Suprapur; Merck) for 24 h. Copper concentration in digested samples was measured by AAS, as described above. Results were expressed as fg Cu/cell.

Zebrafish larvae were also exposed to 4 concentration of CuCl2 (0, 0.17, 0.34 and 0.67 uM), with 30 larvae in each triplicate. After exposed for 96 h, the larvae were collected and weighted the wet weight. Then the samples were also digested and measured the copper concentration by AAS with the same method to ZFL.

5.2.7. Real-time quantitative polymerase chain reaction (PCR)

Control and Cu-induced expression levels of ATP7A & B and MT were checked using quantitative real-time RT-PCR with the cDNA of each sample as a template. Information of primers used for the real-time RT-PCR is given in Table 5.1. The other procedures were same to that in chapter 2.

Table 5.1. PCR Primers used in the studies of ATP7A and 7B cDNAs and gene expression

Gene	Oligo name	Sequences (5′→3′)	Remarks
T-ATP7A	T-7a F1	ATGACNTGTGNHTCCTGTGT	Conserved
	T-7a F2	GCHATBGADGAYATGGGVTTTGA	region
	T-7a R1	CCAATCTTBCCYTCRATGGT	amplification
	T-7A 3' F1	CTCTTGGAGTGGAGGGTATGAC	3' end region
	T-7A 3' F2	TGACACCCACAGCCCAACAGGAA	amplification
	T-7A 3' F3	AACCGTTTCGTCGCCATCTGA	
	T-7A 3' F4	CAAAGGCTCCCATCCAGCAGTAT	
	T-7A5' R1	CGATGGTGGTAATACAGGAGTGAC	5' end region
	T-7A5' R2	CGTTAGGGAGGGAACAAAGGT	amplification
	T-7A F1	ATTAGGTCCACATAGCAGAGTTC	Full length
	T-7A F2	TGTGGCTAACAGTTTGCTTCA	amplification
	T-7A R1	GCTATCTTTGGAATGGGTTGGACT	
	T-7A RT-F	CCAACAGGAAGCATTGAAGA	Real-time
	T-7A RT-R	TGTCTGTGGCAGGTTCTCTC	PCR
T-ATP7B	T-7b F1	GCCAACATGGAYGTGCTHATCGT	Conserved
	T-7b F2	CCNCCVATGCTBTTTGTVTTCAT	region
	T-7b R1	GCNCCVACCCCHGTGCCCACCAT	amplification
	T-7b R2	TTTGABRTYTGGGCCTCTTCCAC	
	T-7B 3' F1	GCTGGAACAGATAGCCAAGAGCAA GA	3' end region amplification
	T-7B 3' F2	GCAGGTGGATGTGGAGCTGGTTCA	
	T-7B 3' F3	ACACCCGCTGGGAGCCGCTATTA	
	T-7B5' R1	TGACCCTCCCATCGACTGGAAACT	5' end region
	T-7B5' R2	CTCCACATCCACCTGCTCCTCACT	amplification
	T-7B5' R3	CTCCCTTCACGCACTCGGCTA	
	T-7B RT-F	GCCACTTCCATAGCCTTCA	Real-time
	T-7B RT-R	GGGATTGACTTTTGCCTTCT	PCR
ZF-ATP7	ZF 7A F	GGCTCGACTTCTCGCAGCT	Real-time
A	ZF 7A R	ATTCCGCATTTTCACTGCCT	PCR
ZF-ATP7	ZF 7B F	CACCACTCCTCGTCACCCT	
A	ZF 7B R	TTTCCCTTACCTGACCCTGA	
ZF-MT	ZF MT F	GCCAAGACTGGAACTTGCAAC	
	ZF MT R	CGCAGCCAGAGGCACACT	

5.3 Results

5.3.1 Cloning ATP7A & B in tilapia

ATP7A & B have not been previously reported in tilapia, it was therefore important to identify their mRNA (cDNA) sequence enabling the measurement of their tissue expression profile in normal and under excess Cu conditions. Until now, the full length cDNA of ATP7A obtained from tilapia (TiATP7A) was 5822 bp which contained an open reading frame of 4554 bp (1514 amino acids) and 5′ end 3′ untranslated regions of 269 and 999 bp respectively (as showed in appendix 5). The deduced TiATP7A protein sequence displayed 63 % identity with human ATP7A and 75 % with zebrafish ATP7A sequences. Also, a partial length cDNA of ATP7B from Tilapia (TiATP7B) of 4294 bp. The deduced protein sequence of TiATP7B displayed 59 % identity with the human ATP7B sequence.

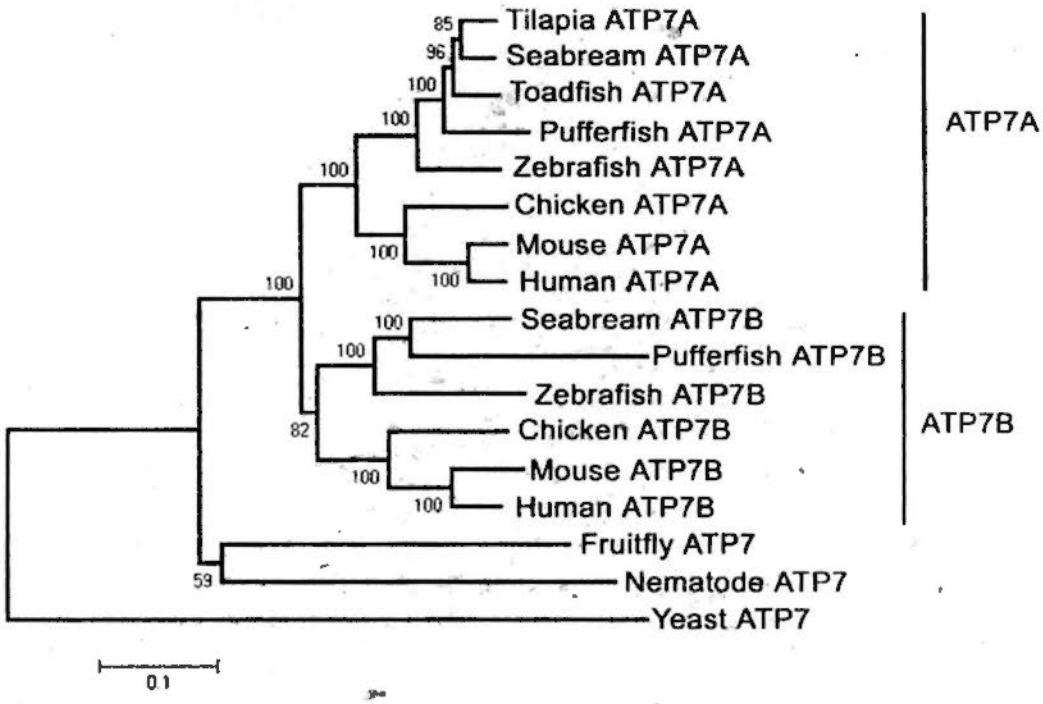

Fig. 5.2. A phylogenetic tree of Cu-ATPases. Human (*Homo sapiens*) ATP7A (NP_000043.3) and ATP7B (NP_000044), mouse (*Mus musculus*) ATP7A (NP_001103227.1) and ATP7B (NP_031537), chicken (*Gallus gallus*) ATP7A (XM 420307.2) and ATP7B (XM 417073.2), zebrafish (*Danio rerio*) ATP7A (NP_001036185) and ATP7B (Ensemble, ENSDARP00000029666), pufferfish (Tetraodon nigrovividis) ATP7A (Ensemble, GSTENG00017010001.1) and ATP7B (Ensemble, GSTENG00020077001.1), sea bream (*Sparus aurata*) ATP7A (ACX37119) and ATP7B (ACX37120), fruit fly (*Drosophila melanogaster*) ATP7 (FlyBase database, FBpp0271765), nematode (*Caenorhabditis elegans*) Cua-1 (NP_499778.1), and yeast Ccc2 (*Saccharomyces cerevisiae*) (AAC37425.1), were used to generate the neighbor-joining tree constructed using the program MEGA.

5.3.2 Tissue distribution patterns of ATP7A & B in tilapia and zebrafish

To check whether ATP7A & B of tilapia and zebrafish are ubiquitously expressed in the tissues, we measured mRNAs from 6 different tissues. In tialapia, as shown in Fig. 5.3, by comparing the gene's expression level in the liver, ATP7A's expression level in the gill (1.48 folds) is almost similar to the liver, but much higher in the kidney (3.61 folds) and intestine (3.32 folds), lower in the brain (0.64 folds), and almost null in the heart were found. As to ATP7B, this gene's expression level in the gill (0.35 folds), intestine (0.62 folds) and brain (0.18 folds) was lower than that in the liver, but also higher in the kidney (2.06 folds) and heart (2.03 folds).

As to the distribution of ATP7A & B in zebrafish (Fig. 5.4), ATP7A's expression level in the gill (0.67 folds) was a little lower than that of liver, but much higher in the heart (7.45 fold), kidney (11.33 folds) and intestine (28.68 folds), and almost not detected in the brain. The distribution pattern of ATP7B is almost similar to ATP7A in zebrafish, except with a lower expression in gill (0.26 folds), and higher expression in heart (7.45 folds).

ATP7A & B were found to express in liver, gill, heart, intestine and kidney of tilapia and zebrafish, their mRNA levels were higher in kidney and intestine. However, the expression levels of ATP7A & B were low in brain of tilapia, and not expressed in zebrafish. This difference should be one of reasons for the different response to the metal exposure in tilapia and zebrafish.

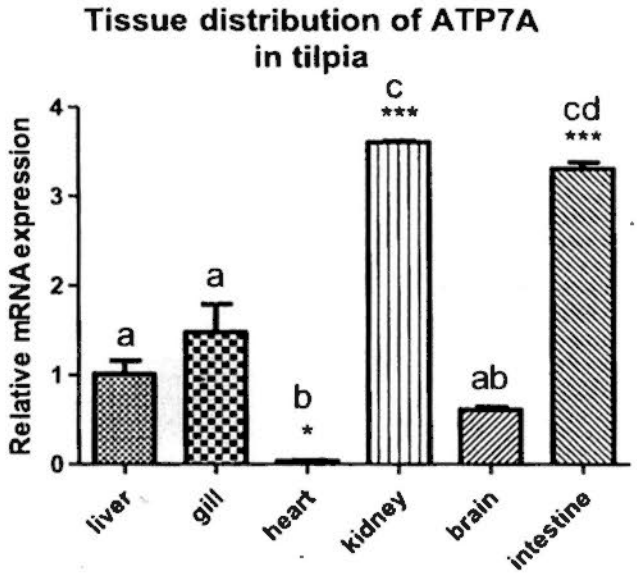

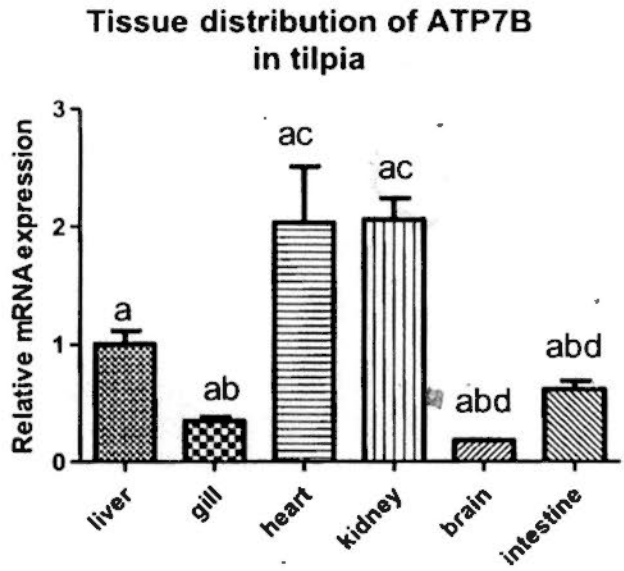

Fig. 5.3. Tissue distribution of ATP 7A & B mRNA in tilapia detected by real time PCR. Values are means±S.D. N= 3. Bars with asterisk indicates significant difference from the liver (*$p < 0.05$, **$p < 0.01$, ***$p < 0.001$; ANOVA, Tukey's test). Bars bearing different lettering are significantly different ($p<0.05$, ANOVA, Tukey's test).

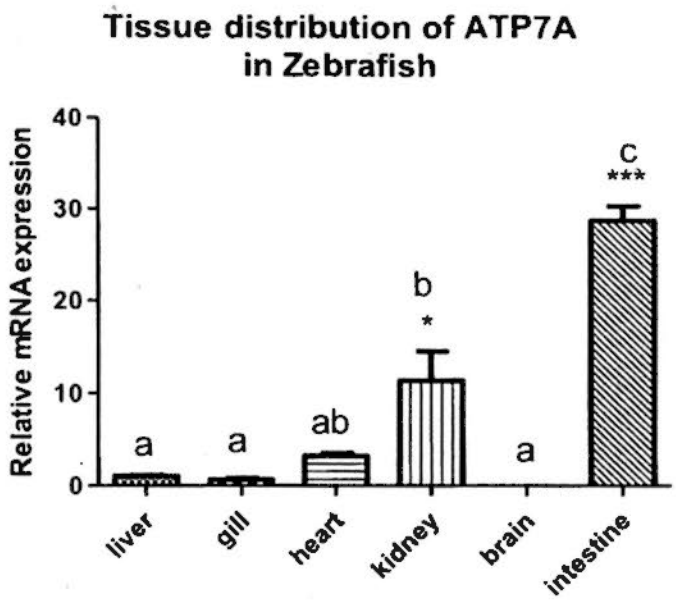

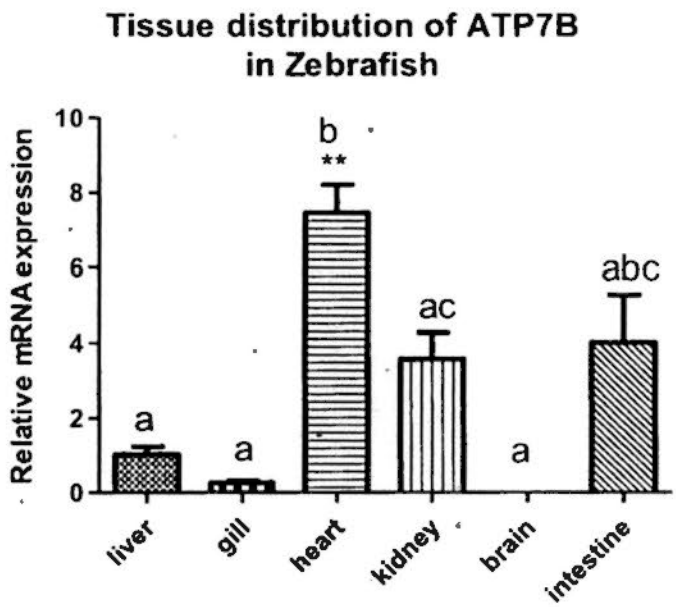

Fig. 5.4. Tissue distribution of ATP 7A & B mRNA in zebrafish detected by real time PCR. Values are means±S.D. N= 3. Bars with asterisk indicates significant difference from the liver (*$p < 0.05$, **$p < 0.01$, ***$p < 0.001$; ANOVA, Tukey's test). Bars bearing different lettering are significantly different ($p<0.05$, ANOVA, Tukey's test).

5.3.3 Copper accumulation in ZFL and zebrafish larvae

Firstly, the 96 h LC50 of $CuCl_2$ to zebrafish larvae was determined to be 85.73 ppb (1.34 uM) (Fig 5.5). The copper accumulation in ZFL and zebrafish larvae after Cu exposure was shown in Fig. 5.6. It was found that higher Cu concentration can induce higher accumulation in ZFL and zebrafihs larvae. These results were similar with our lab's previous data about the Cu accumulation in tilapia's tissues. However, the copper accumulation in zebrafish larvae was much lower than that of tilapia after exposed to similar concentration of Cu^{2+}. This should be due to the regulation of ATP7A & B and MT, which would be discussed in the following section.

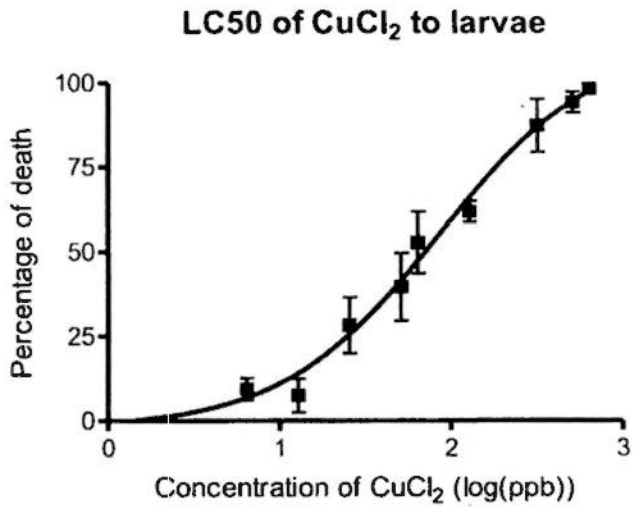

Fig. 5.5. Cytotoxicity (%) of zebrafish after $CuCl_2$ exposure in different concentrations (in log scale) for 96 h. The 96 h LC50 of $CuCl_2$ on zebrafish larvae was determined as 85.73 ppb (1.34 uM). The 96 h LC50 values were calculated using Graphpad prism 5 with linear regression.

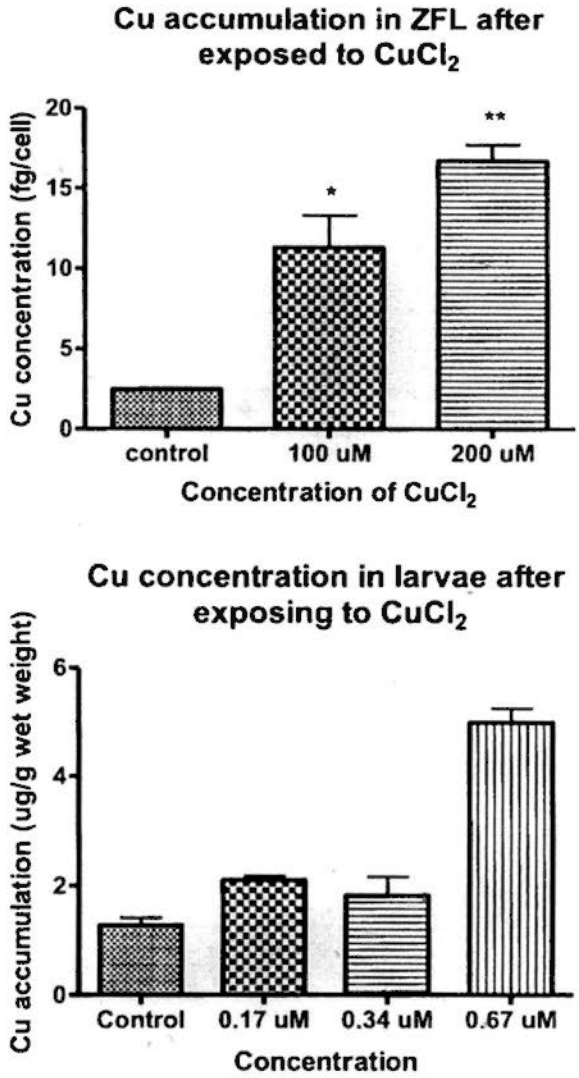

Fig 5.6. Copper levels in ZFL (left panel) and zebrafish larvae (right panel) after exposed to different concentration of Cu^{2+}. Values are means ± S.D. N = 3. Bars with asterisk indicates significant difference from control (*$p < 0.05$, **$p < 0.01$, ***$p < 0.001$; ANOVA, Tukey's test).

5.3.4. Cu-modulated expression of ATP7A & B and MT in tilapia and zebrafish

After getting the full sequence of ATP7A & B, we were interested in studying these two genes' regulation in tilapia and zebrafish after Cu^{2+} exposure. To make our result more significant, metallothionein (MT) was also chosen in this study, because MT is also an important copper binding protein, which plays a role in metal storage and detoxification. Here, these three genes' regulation was studied with both in vivo and in vitro. As the results showed in Fig. 5.7, 5.8 and 5.9, 300 uM Cu^{2+} could induce most ATP7A (8.14 folds), ATP7B (8.98 folds) and MT (5.12 folds) in Hepa T1. In ZFL groups, 200 uM Cu^{2+} can induce more ATP7A (1.90 folds) and MT (3.38 folds) than the other two dosages, and ATP7B was maxism induced in 100 uM Cu^{2+} (3.83 folds). Obviously, 300 uM Cu^{2+} can induced more ATP7A, ATP7B and MT in Hepa T1 cell than ZFL treated with 200 uM Cu^{2+}. Similar to the in vitro result, the expressions of ATP7A, ATP7B and MT were up-regulated in tilapia's liver and gill after exposed to different concentration of Cu^{2+}, so did in zebrafish larvae. Also, the regulation folds of these three genes in tilapia's liver and gill by Cu^{2+} were higher than that in zebrafish larvae. These results would help us to further understand the differences between tilapia and zebrafish treated with Cu^{2+}.

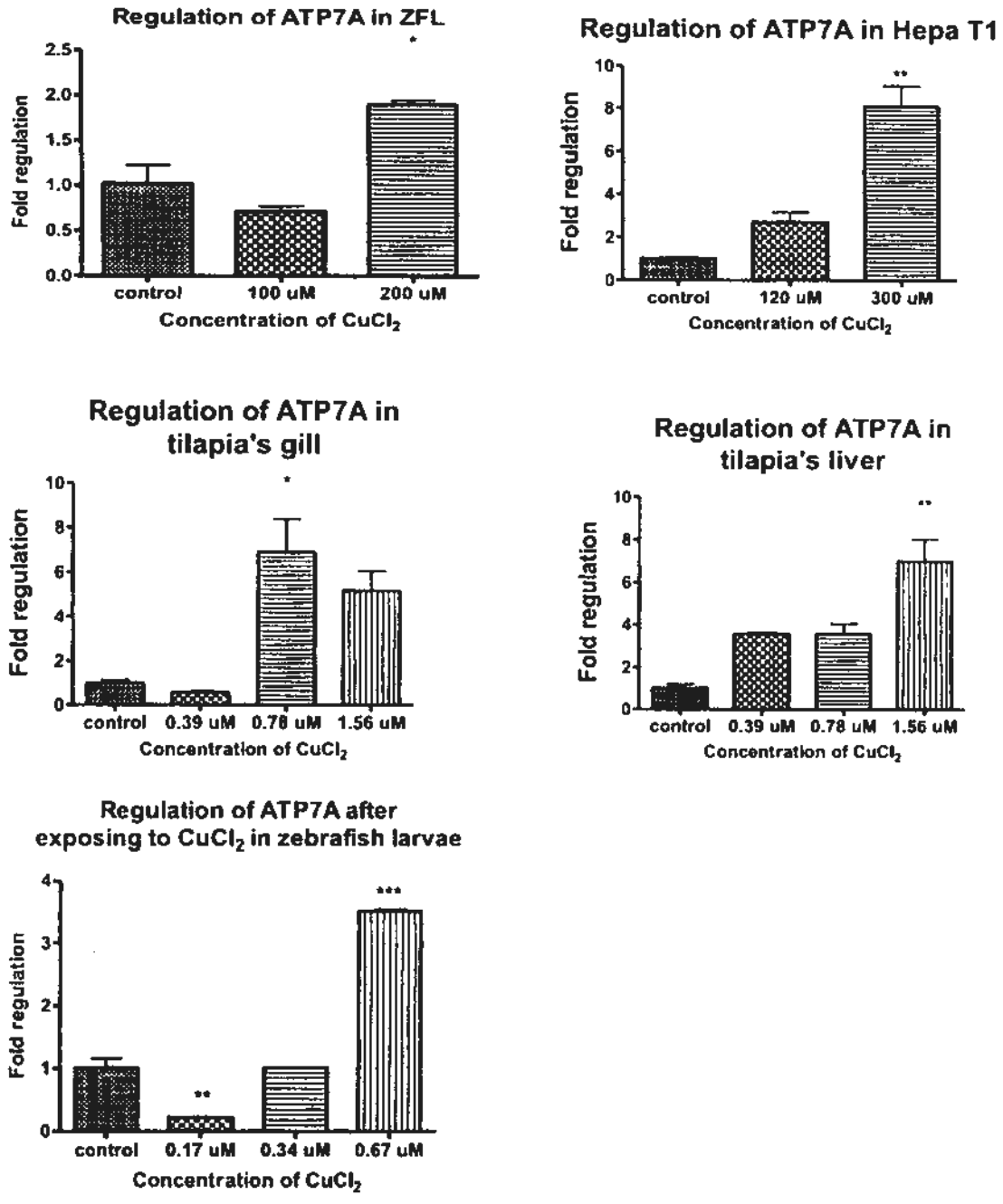

Fig. 5.7 Fold induction of ATP7A mRNA levels in tilapia and zebrafish exposed to $CuCl_2$. The y axis represents the fold regulation of these genes (*$p < 0.05$, **$p < 0.01$, ***$p < 0.001$; ANOVA, Tukey's test).

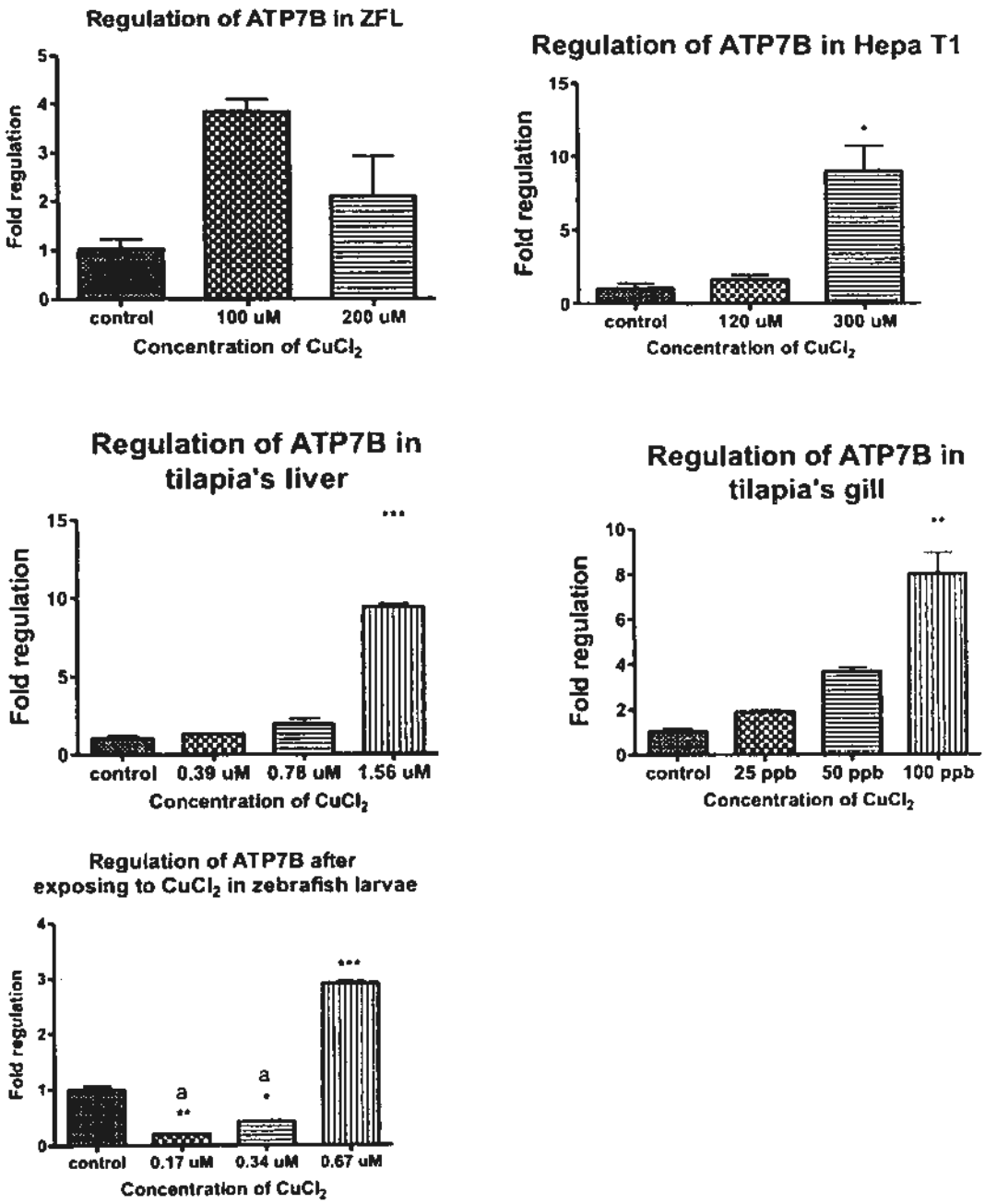

Fig. 5.8 Fold induction of ATP7B mRNA levels in tilapia and zebrafish exposed to $CuCl_2$. The y axis represents the fold regulation of these genes (*$p < 0.05$, **$p < 0.01$, ***$p < 0.001$; ANOVA, Tukey's test).

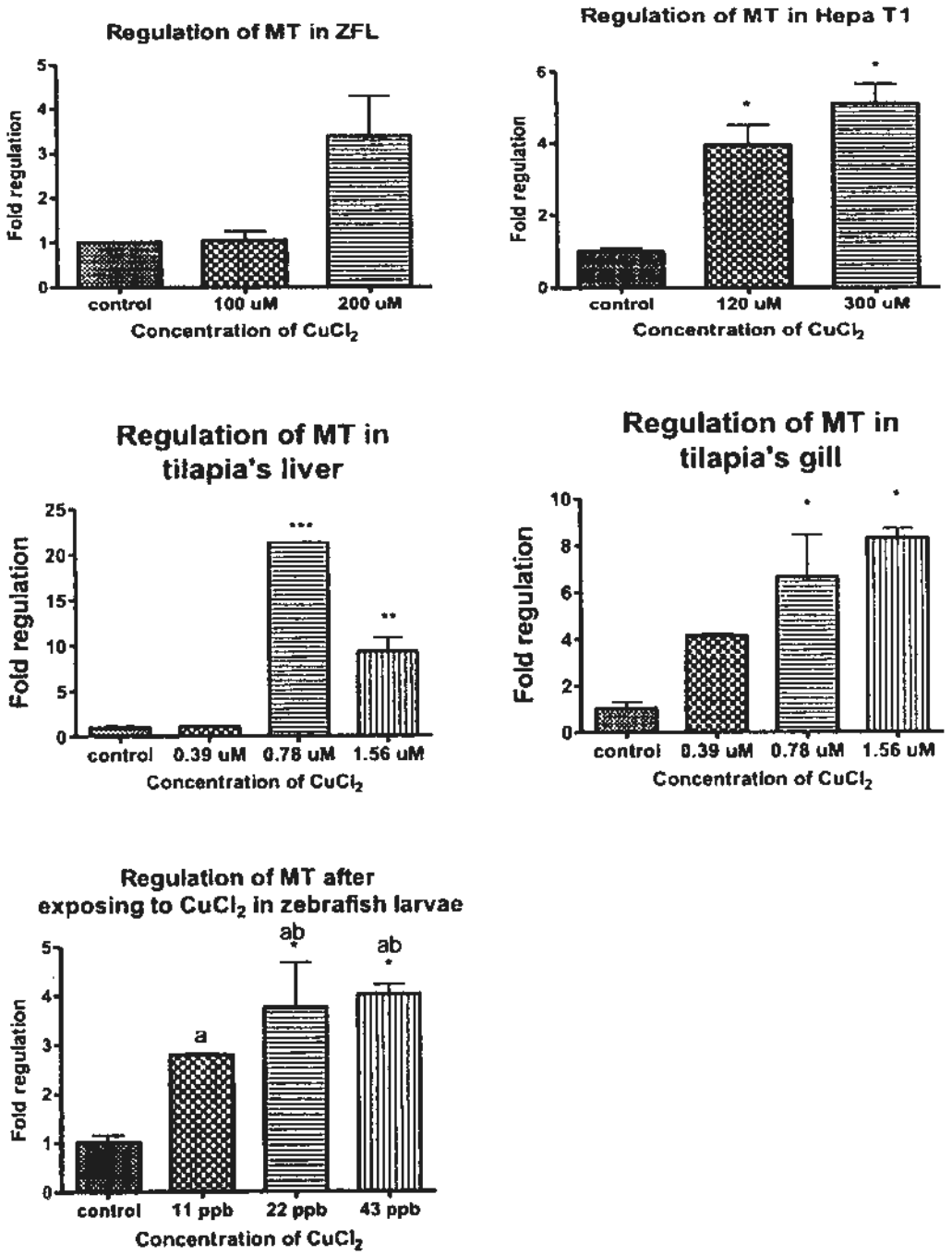

Fig. 5.9. Fold induction of MT mRNA levels in tilapia and zebrafish exposed to $CuCl_2$. The y axis represents the fold regulation of these genes (*$p < 0.05$, **$p < 0.01$, ***$p < 0.001$; ANOVA, Tukey's test).

5.4. Discussion

5.4.1. Tissue expression profile

In mammals, the functional diversity of ATP7A and ATP7B is apparent from their differential tissue expression patterns and disease outcomes in Wilson's and Menkes Diseases. In human adults, very low levels of ATP7A mRNA are found in the liver, although it is ubiquitously expressed during development (Lutsenko et al., 2008); whereas, ATP7B expression is more delimited with high levels of expression in liver, kidney and intestine, but to a lesser extent in brain (Kuo et al., 1997).

In tilapia and zebrafish, the expression profiles of ATP7A and ATP7B are to a certain extend similar to those found in mammals (Fig. 5.3), except that the expression of ATP7A in liver was higher than anticipation. The distribution of ATP7A is reflective of its role in delivery of Cu to cuproenzymes eg. peptidyl-α-monooxygenase (El Meskini et al., 2003), tyrosinase (Petris et al., 2000) and lysyl oxidase (Tchaparian et al., 2000). Recently, several studies showed that ATP7A could be also found in liver of mammals (Lenartowicz et al., 2010), therefore our result of ATP7A's expression in the liver is not uncommon.

Interestingly, the ATP7A & B's expression levels in intestine were higher than that in gill, even though lower expression of ATP7B in the intestine and gill, which should be due to the function of this gene (Minghetti et al., 2010). Gill and Intestine are two important organs with important pathways for uptake of waterborne and diet-borne Cu^{2+}. Previous studies demonstrated that dietary uptake is the major source of copper for fish under optimal growth conditions (Clearwater et al., 2002; Minghetti et al., 2010), and waterborne copper for fish health would be significant at times when the dietary source of copper become inadequate (Minghetti et al., 2010). Shek and Chan (manuscript in

preparation) determined that copper accumulation in intestine had high copper concentration than in gill of tilapia after exposed to different concentration of $CuCl_2$. Here, my result of ATP7A & B's expression in gill and intestine further confirmed the role of gill and intestine played in the copper uptake. Since ATP7A but lower ATP7B was expressed in both tilapia intestine and gill, ATP7A is implicated as the probable candidate for basolateral Cu transport in fish.

Also, the expression levels of ATP7A & B in kidney were both at a higher level. The kidneys have one of the highest copper concentrations among organs (Shek and Chan, unpublished data) and show tight homeostatic control of their copper content. Compared with other tissues, the renal copper content is less affected by systemic copper deficiency or overload (Lutsenko et al., 2007). Currently, little is known about renal copper transport and regulation. Our results about expression of ATP7A & B in kidney might indicate that renal cells require Cu-ATPase function to maintenance of intracellular copper and also the whole body's copper levels.

5.4.2. Inductions of ATP7A and 7B in tilapia and zebrafish

In this study, Cu-ATPase mRNA expression was measured in tilapia and zebrafish after Cu^{2+} exposure. It was found that Cu^{2+} exposure could induce ATP7A & B and MT in tilapia and zebrafish *in vivo* and *in vitro* in a dose dependent manner. Cu homeostasis in fish is tightly regulated, and as in higher vertebrates. In mammals, excessive amount of Cu^{2+} is accumulated in the liver and excreted in the bile (Madsen and Gitlin, 2007; Balamurugan and Schaffner, 2006). Likewise, in zebrafish, elevated Cu load was observed in the larvae and ZFL after exposed to increased waterborne Cu (Fig. 5.4).

Also, MT was up-regulated in zebrafish larvae and ZFL, which also indicated that the metal accumulation in larvae and cell after Cu^{2+} exposure.

In a recent study in zebrafish, Craig et al. (2009) reported that intestinal and liver ATP7A mRNA was increased after exposure to 8 ug/L Cu in the water. Their result is in-line with the results obtained in the present study. ATP7B is an important copper transporter in the hepatocyte, which can efflux the excess copper out of liver to bile. In the present study, we also observed induction of hepatic ATP7B expression in tilapia and zebrafish after Cu exposure. Therefore, it can be concluded that increased ATP7A & B would help to remove Cu from the cell, and the excessive Cu^{2+} would also be stored in the several metal binding proteins, such as MT.

By comparing the regulation of ATP7A & 7B and MT in tilapia and zebrafish, it was found that the regulation of these three genes in tilapia was higher than that of zebrafish *in vitro* and *in vivo*. It is possible that the copper tolerance of tilapia might be due to higher regulation of ATP7A & 7B and MT, which can help tilapia to excrete or regulate the excessive Cu^{2+} entering into the organism.

In summary, in this study we obtained the full length sequence of ATP7A and partial sequence of ATP7B in tilapia, and found that ATP7A in tilapia was highly conserved with human and other teleost fish's ATP7As, which meant that the toxicity of Cu^{2+} to tilapia was conserved with zebrafish and human. The expression of tilapia and zebrafish Cu-ATPase (TiATP7A and TiATP7B) mRNAs were consistent with the available physiological evidence from various fish species for the involvement of ATP-dependent

(ATP7A-B-like) Cu-transporters under conditions of both normal and excess Cu exposure. To study the mechanism of copper tolerance (tilapia) and copper sensitive (zebrafish) by comparing the regulation of ATP7A & B and MT, we demonstrated that tilapia has a higher fold induction of these genes for better metal homeostatsis. Further investigations with RNAi or morpholino knock down approaches are needed to confirm the functions or roles of those transporters that may play in copper homeostasis.

Chapter 6

Comparative toxicity of Cu_2O nanoparticle and $CuCl_2$ to zebrafish larvae and ZFL

6.1. Introduction

Nanotechnology is one of the fastest growing sectors of the high-tech economy. There are more than 200 separate consumer products alone using nanomaterials with personal, commercial, medical, and military uses (Brumfiel, 2006). Engineered nanomaterials with dimension of 100 nm or less, provide us a wide range of novel applications in the electronics, healthcare, cosmetics, technologies and engineering industries. The exploitation of properties inherent to materials at the nanoscale (< 100 nM) has initiated innovative approaches to technologies which shape our world. Lack of toxicological data on nanomaterials makes it difficult to determine if there is a risk associated with nanomaterial exposure. Thus, there is an urgent need to develop rapid, accurate and efficient testing strategies to assess health effect of these emerging nanomaterials.

In previous chapters, we have studied the toxic effects of soluble copper, and in this chapter herein we report the use of zebrafish larvae and zebrafish cell-line, ZFL, for the study of copper nanoparicles. The primary target of this study was to determine if copper nanoparticles were toxic to zebrafish larvae comparing with copper ions. And if so, we would like to determine if the observed toxicity is solely due to dissolution of particles. Therefore, the behavior of copper nanoparticles in natural water was examined and the acute toxicity of nanoparticulate copper was compared to that of soluble copper using zebrafish larvae and zebrafish liver cell (ZFL). Metallothionein (MT), copper

transporters (Ctr1, ATP7A and 7B), superoxide dismutase (SOD) and glutathione sulfur transferase (GST) were used as biomarkers of exposure and effects to examine the concentrations of nano-copper particles and copper ions required to induce biochemical stress response.

6.2. Materials and Methods

6.2.1 Preparation of Cu_2O NPs stock suspension

In a typical synthesis of Cu_2O, a mixture of 0.20 g cupric acetate ($Cu(CH_3COO)_2 \cdot H_2O$)) (ACROS, 99 %) and 8.20 g hexadecylamine (HDA) (IL, 99 %) was heated to 85 °C to make a homogeneous solution. Then, the mixture in an open glass bottle was directly placed in the muffle furnace of 210 °C for 50 min. After the reaction, the resulting powder was easily collected by centrifuge and was rinsed with 70 °C toluene for 5 times to remove the hexadecylamine, and then dried in a vacuum at 80 °C for 4 h.

6.2.2 ZFL and zebrafish larvae culture

The culture of ZFL and zebrafish larvae can be referred to Chapters 4 & 5.

6.2.3 Toxicity study of Cu2O NP to ZFL and zebrafish larvae

The 96 h LC 50 value of Cu_2O NP to ZFL and zebrafish larvae can be referred to Chapters 4 & 5.

6.2.4 Annexin-V/PI assay of ZFL exposed to Cu2O NP

Referred to Chapter 4.

6.2.5. Copper accumulation in zebrafish larvae and ZFL exposed to Cu_2O NP

Referred to Chapter 5.

6.2.6. Real-time quantitative polymerase chain reaction (PCR)

To compare the toxicity of $CuCl_2$ and Cu_2O NP, 7 important genes related to copper transportation and ROS effect were chosen in this chapter, including ATP7A & B, Ctr1, MTF-1, MT, GST, and Cu/Zn SOD. The sequences of these 7 genes for real-time quantitative PCR were shown in Table 6.1. And the concreted procedures can be referred to chapter 2.

Table 6.1. PCR Primers used in this chapter.

Gene	Primers	Sequences (5' to 3')
ATP7A	Forwards	GGCTCGACTTCTCGCAGCT
	Reverse	ATTCCGCATTTTCACTGCCT
ATP7B	Forwards	CACCACTCCTCGTCACCCT
	Reverse	TTTCCCTTACCTGACCCTGA
Ctr1	Forwards	AATGTGGAGCTGCTTTTTGC
	Reverse	AACACAGCCAACAAGAACACG
MT	Forwards	CCTGCGAATGTGCCAAGA
	Reverse	TTGCTGCAACCAGATGGG
Cu/Zn SOD	Forwards	ATCAAGAGGGTGAAAAGAAGC
	Reverse	AAAGCATGGACGTGGAAAC
MTF1	Forwards	CCTCCTACAATCAGCATCGC
	Reverse	CCTGTTGTTCGGGGTTTTG
GST	Forwards	CTATACATGCGGCGAAGCT
	Reverse	GGCATTGCTCTGGACGAT

6.3 Results

6.3.1 Toxicity of Cu_2O NP

The Cu_2O NP was firstly constructed with the size smaller than 50 nM, showed as Fig 6.1, and used in the following experiments. The median lethal concentration (LC50) of Cu2O NP on the ZFL cell line and zebrafish larvae at 96 h was determined using alamarBlue assay and calculation of percentage of death, respectively. The dose response curves with 96 h LC50 were plotted using Graphpad Prism 5 (Fig. 6.2): 110 ppm (1545 uM Cu) in ZFL cell and 242 ppb (3.39 uM Cu) in zebrafish larvae.

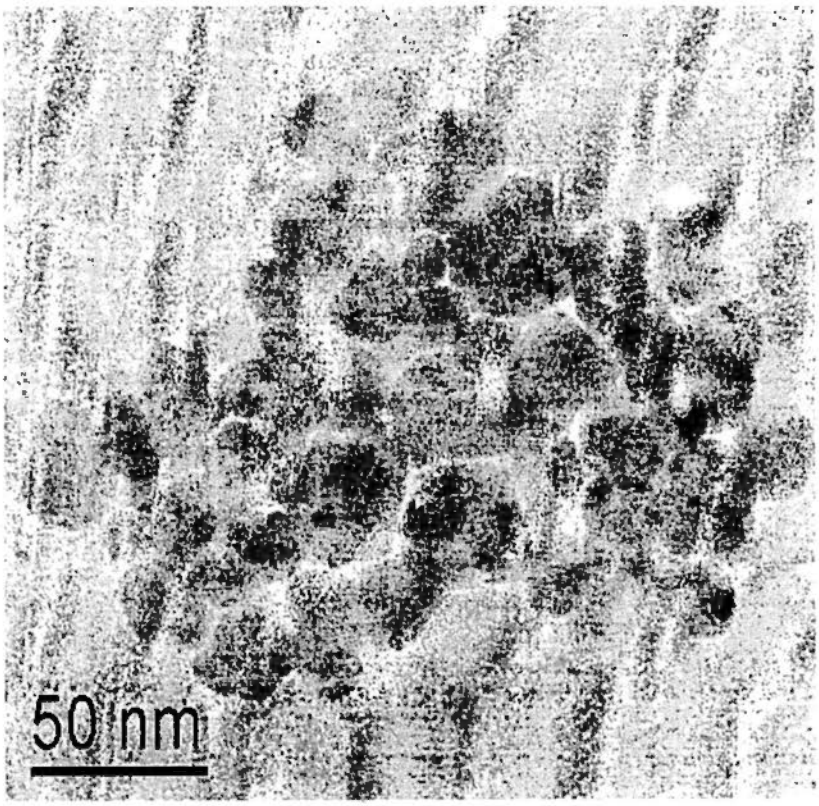

Fig. 6.1 SEM micrograph of nanocopper particles dispersed in water showing the wide disparity in particle aggregation states.

Comparing with previous data in Chapter 4 about $CuCl_2$ to ZFL (360 uM) and zebrafish larvae in Chapter 5 (1.34 uM), it was found that $CuCl_2$ is more toxic than Cu_2O NP, also it can be concluded that the ZFL cell was more resistant to Cu toxicity than zebrafish larvae. To further study the toxicity of Cu_2O NP, flow cytometry measurement was used to quantify the extent of apoptosis and necrosis in the ZFL exposed to two concentrations Cu_2O NP (50 ppm and 25 ppm), and significant differences were observed between the control and the Cu2O NP treated cells. After incubation with different concentrations of Cu_2O NP for 96 h, the percentage of Annexin-V^+/PI^+ cells (apoptosis) increased to 1.6 % and 2.4 %, respectively, compared to 0.9 % in the control group. The percentage of Annexin-V-/PI^+ cells (necrosis) increased to 5.9 % and 10.0 %, respectively, compared to 1.4 % in the control group (Fig. 6.3). Similar to $CuCl_2$, These results demonstrate that Cu_2O NP primarily induces cell necrosis rather than apoptosis, and the toxicity of 50 ppm Cu_2O NP was equal to that of 12.8 ppm (200 uM) $CuCl_2$ to ZFL.

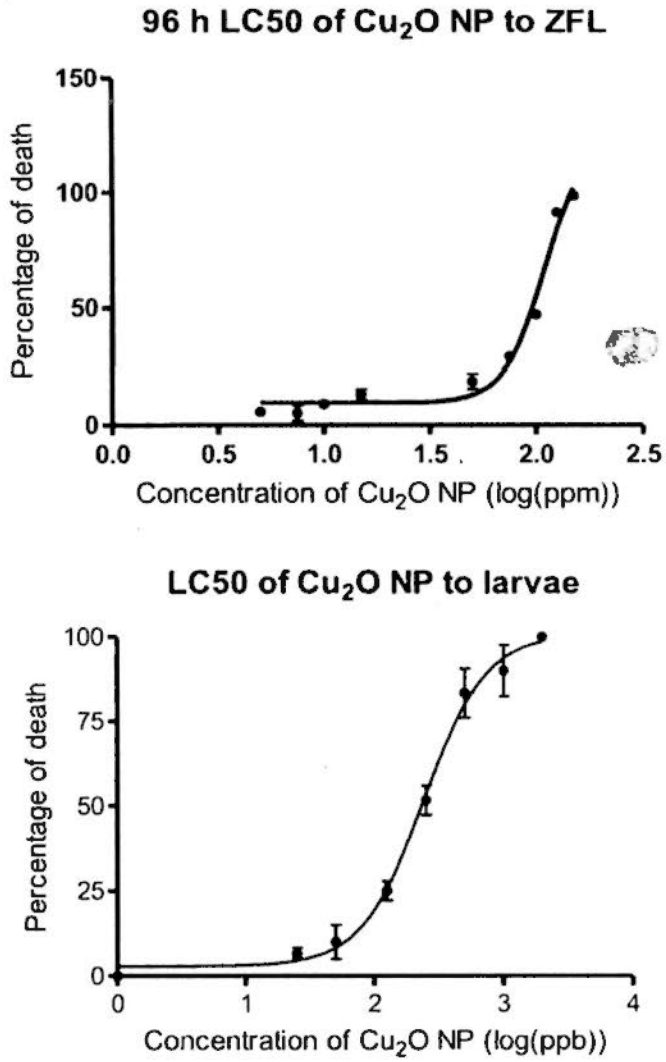

Fig. 6.2 Cytotoxicity (%) of ZFL and zebrafish after Cu_2O NP exposure in different concentrations (in log scale) for 96 h. The 96 h LC50 of Cu_2O NP on ZFL cells (upper panel) and zebrafish larvae (lower panel) was determined as 110 ppm and 242 ppb. The 96 h LC50 values were calculated using Graphpad prism 5 with linear regression.

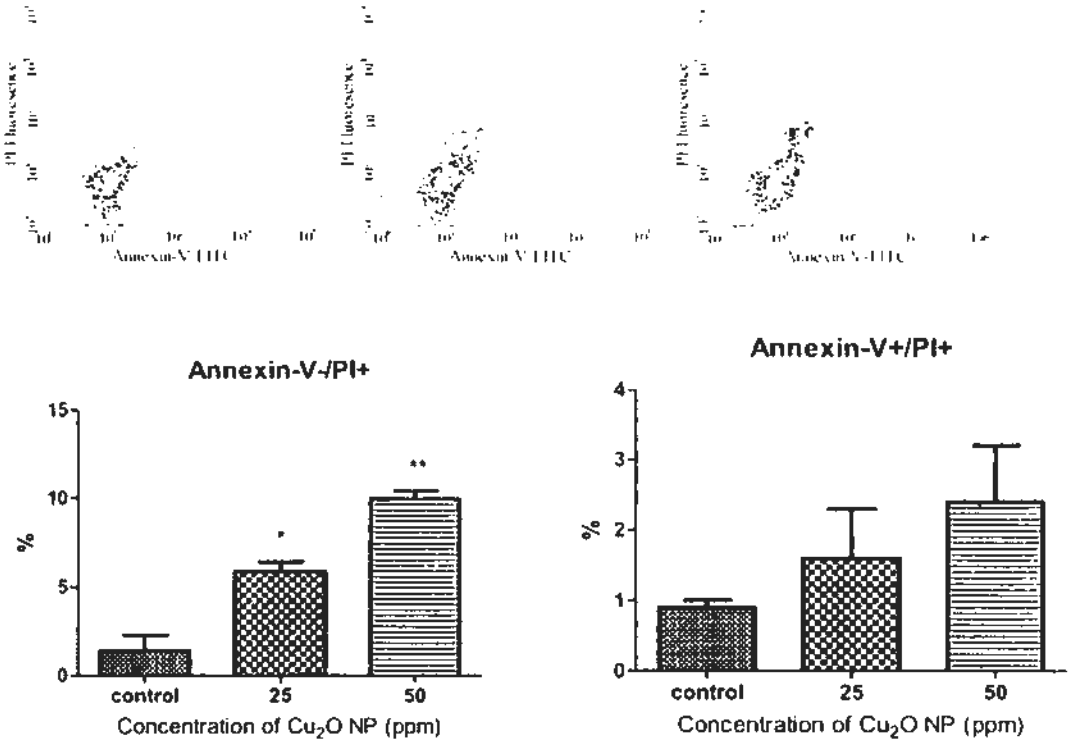

Fig. 6.3. Flow cytometer detection of Cu2O NP-induced apoptosis and necrosis with Annexin-V-FITC and PI staining. The ZFL cells were exposed to different concentrations of $CuCl_2$ for 96 h. After being stained with Annexin-V-FITC and PI, the cells were analyzed using flow cytometry. LL: Annexin-V-/PI-cells (normal); LR: Annexin-V+/PI-cells (early apoptosis); UR: Annexin-V+/PI+ cells (late apoptosis); UL: Annexin-V-/PI+ cells (necrosis). Statistic analysis of the apoptosis cells and necrosis cells among the total population was shown in bar graph (% of cells in each phase relative to the total population).

6.3.2 Copper accumulation in ZFL and zebrafish larvae

The copper concentrations in ZFL and zebrafish larvae after exposure to copper ions and Cu_2O NP are shown in Fig. 6.4. It was found that higher Cu_2O NP concentrations can induce higher copper contents in ZFL and zebrafihs larvae, and such a trend was similar to the copper accumulation after $CuCl_2$ treatment. However, the copper accumulation in zebrafish larvae after exposed to Cu_2O NP was both higher than that after exposed to $CuCl_2$, but almost at the same level in ZFL. It is interesting to note that the concentration of Cu_2O NP (50 ppm in vitro and 125 ppb in vivo) used in ZFL and zebrafish larvae was much higher than $CuCl_2$ (12.8 ppm in vitro and 43 ppb *in vivo*), but the copper accumulation in ZFL and zebrafish larvae in Cu_2O NP treatment groups (19.1 fg Cu/cell and 7.14 ug/g wet weight) was not much higher than that in the $CuCl_2$ treatment groups (16.7 fg Cu/cell and 4.99 ug/g wet weight). The possible reasons for these results could be involved in the insolubility of Cu_2O NP and a tight copper transportation system of Cu homeostasis in the organism. To further study the differences between Cu_2O NP and $CuCl_2$, the regulation of seven genes involved in copper transportation and ROS effect was studied.

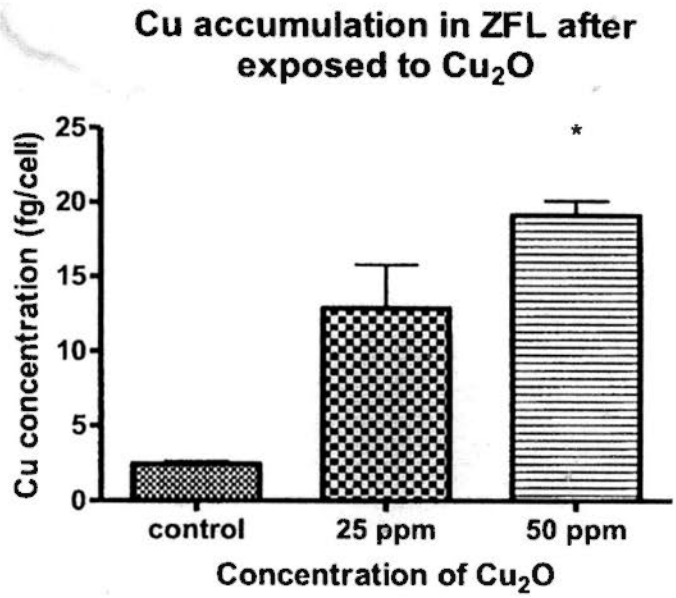

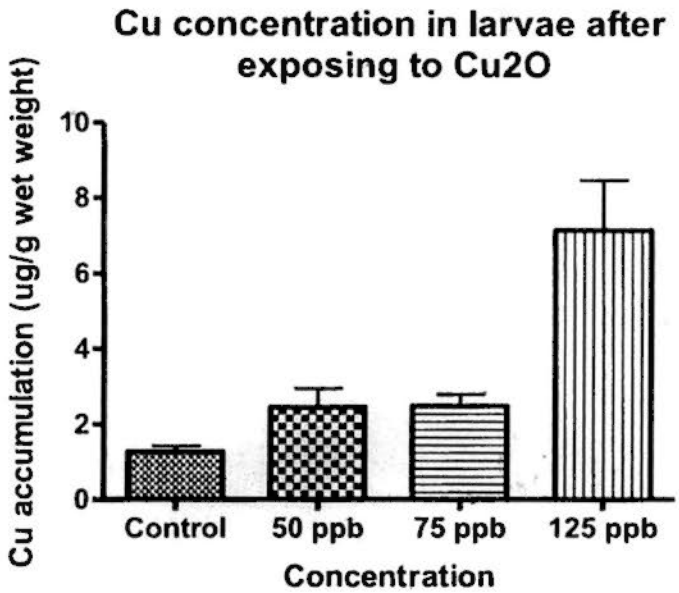

Fig 6.4. Copper levels in ZFL (left panel) and zebrafish larvae (right panel) after exposed to different concentration of Cu_2O NP. Values are means±S.D. N= 3. Bars with asterisk indicates significant difference from control (*$p < 0.05$, **$p < 0.01$, ***$p < 0.001$; ANOVA, Tukey's test).

6.3.3 Regulation of genes after Cu_2O NP and $CuCl_2$ exposure

After comparing the copper accumulation in ZFL and zebrafish larvae exposed to two chemicals, we conducted the real time quantitative PCR to test seven genes' regulation after exposure (Fig 6.5 and Fig 6.6). As the result showed, Cu_2O and $CuCl_2$ can induce the copper transoporters (Ctr1, ATP7A & B) and MT at the same level in ZFL. And these results can help to explain the result of copper accumulation *in vitro*. Furthermore, we also detect other three genes' regulations as showed in this slide. It was found that Cu_2O NP and $CuCl_2$ can also induce GST and SOD at the same level, which means that they cause equal ROS effect to ZFL. And MTF1 seems not change after exposure.

As to the effects on zebrafish larvae, the results were different from the ZFL. Firstly, 125 ppb Cu_2O NP could induce much more copper transporters and MT than 43 ppb CuCl2. As to the regulation of other three genes' regulation, Cu_2O NP could also regulate GST and SOD more strongly than $CuCl_2$, even through the down-regulation of GST. However, the Cu_2O NP and $CuCl_2$ can induced the MTF1 at the same level. These results would help us to further understand the toxic mechanism of Cu_2O NP and $CuCl_2$.

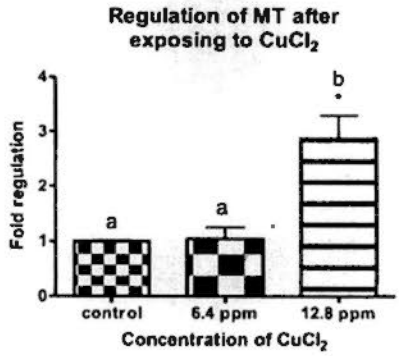
Regulation of MT after exposing to $CuCl_2$
Fold regulation
a
a
b
*
control
6.4 ppm
12.8 ppm
Concentration of $CuCl_2$

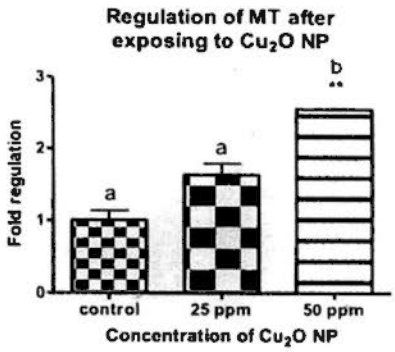
Regulation of MT after exposing to Cu_2O NP
Fold regulation
a
a
b
**
control
25 ppm
50 ppm
Concentration of Cu_2O NP

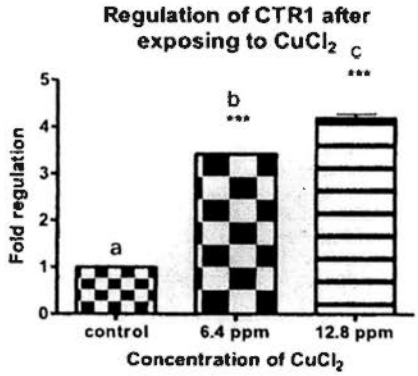
Regulation of CTR1 after exposing to $CuCl_2$
Fold regulation
a
b
***
c
***
control
6.4 ppm
12.8 ppm
Concentration of $CuCl_2$

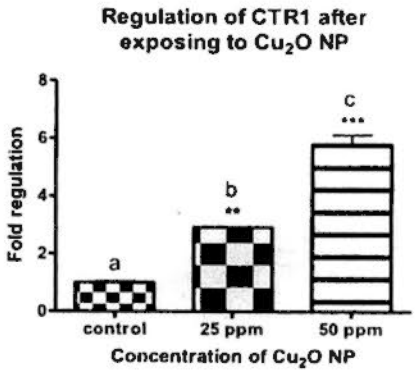
Regulation of CTR1 after exposing to Cu_2O NP
Fold regulation
a
b
**
c
***
control
25 ppm
50 ppm
Concentration of Cu_2O NP

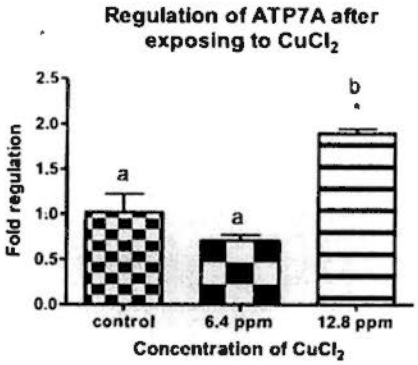
Regulation of ATP7A after exposing to $CuCl_2$
Fold regulation
a
a
b
*
control
6.4 ppm
12.8 ppm
Concentration of $CuCl_2$

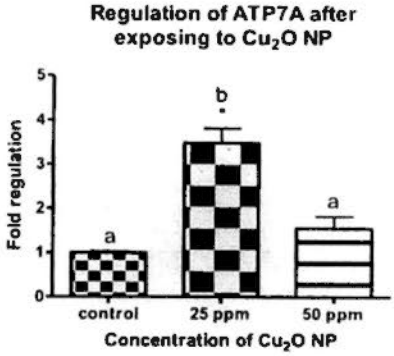
Regulation of ATP7A after exposing to Cu_2O NP
Fold regulation
a
b
*
a
control
25 ppm
50 ppm
Concentration of Cu_2O NP

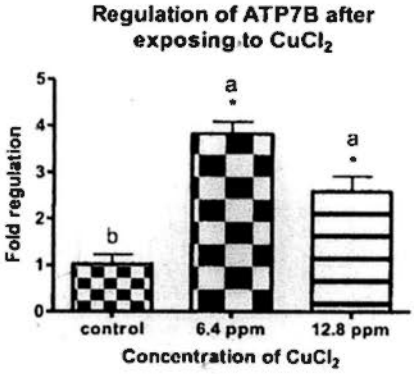
Regulation of ATP7B after exposing to $CuCl_2$
Fold regulation
b
a
*
a
*
control
6.4 ppm
12.8 ppm
Concentration of $CuCl_2$

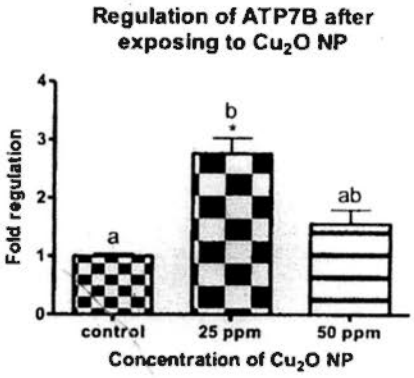
Regulation of ATP7B after exposing to Cu_2O NP
Fold regulation
a
b
*
ab
control
25 ppm
50 ppm
Concentration of Cu_2O NP

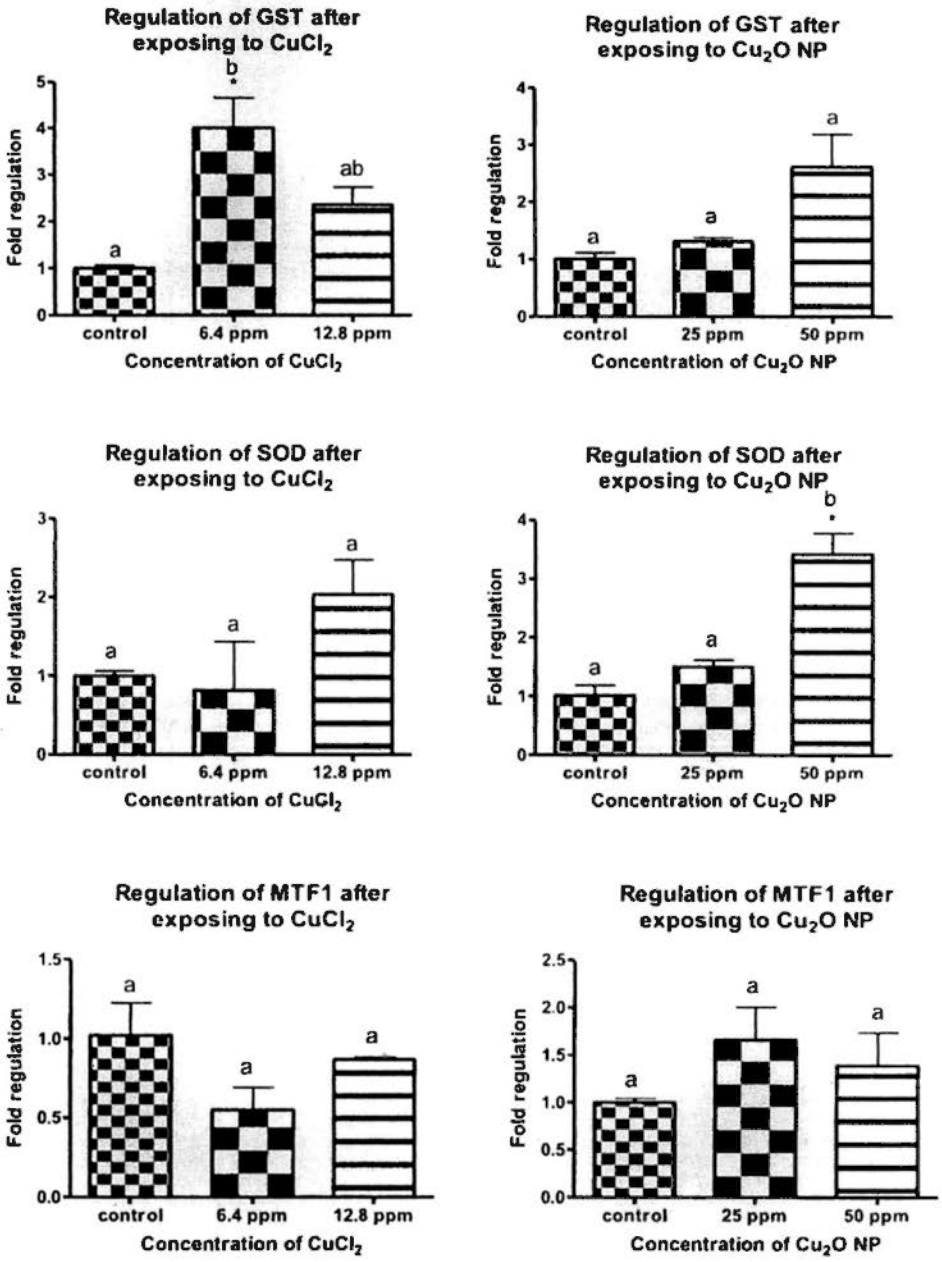

Fig. 6.5 Fold induction of seven genes in mRNA levels in ZFL exposed to $CuCl_2$ (left panel) and Cu_2O NP (right panel). The y axis represents the fold regulation of these genes (*$p < 0.05$, **$p < 0.01$, ***$p < 0.001$; ANOVA, Tukey's test). Bars bearing different lettering are significantly different ($p<0.05$, ANOVA, Tukey's test).

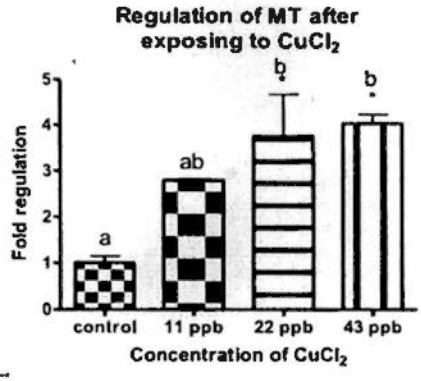
Regulation of MT after exposing to $CuCl_2$
Fold regulation
a
ab
b
b
control
11 ppb
22 ppb
43 ppb
Concentration of $CuCl_2$

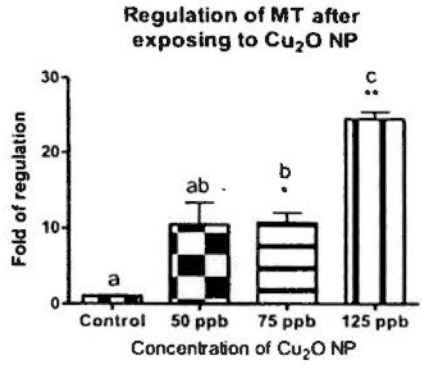
Regulation of MT after exposing to Cu_2O NP
Fold of regulation
a
ab
b
c
Control
50 ppb
75 ppb
125 ppb
Concentration of Cu_2O NP

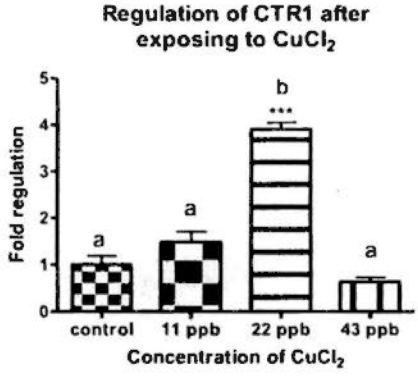
Regulation of CTR1 after exposing to $CuCl_2$
Fold regulation
a
a
b
a
control
11 ppb
22 ppb
43 ppb
Concentration of $CuCl_2$

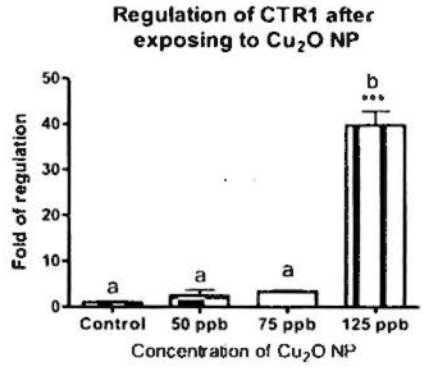
Regulation of CTR1 after exposing to Cu_2O NP
Fold of regulation
a
a
a
b
Control
50 ppb
75 ppb
125 ppb
Concentration of Cu_2O NP

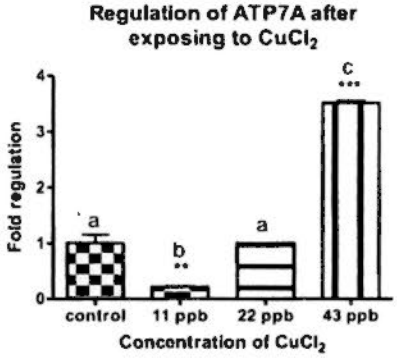
Regulation of ATP7A after exposing to $CuCl_2$
Fold regulation
a
b
a
c
control
11 ppb
22 ppb
43 ppb
Concentration of $CuCl_2$

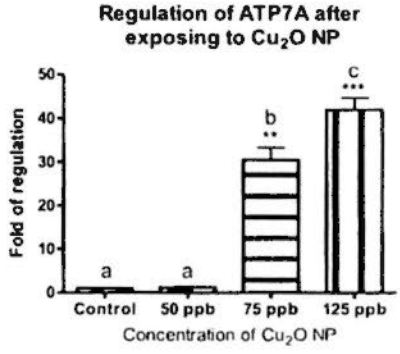
Regulation of ATP7A after exposing to Cu_2O NP
Fold of regulation
a
a
b
c
Control
50 ppb
75 ppb
125 ppb
Concentration of Cu_2O NP

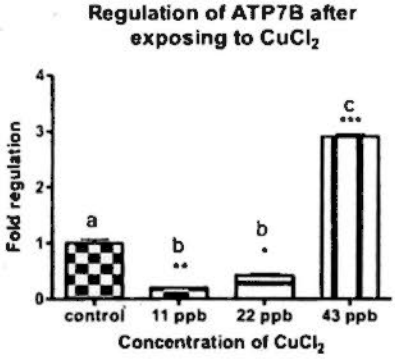
Regulation of ATP7B after exposing to $CuCl_2$
Fold regulation
a
b
b
c
control
11 ppb
22 ppb
43 ppb
Concentration of $CuCl_2$

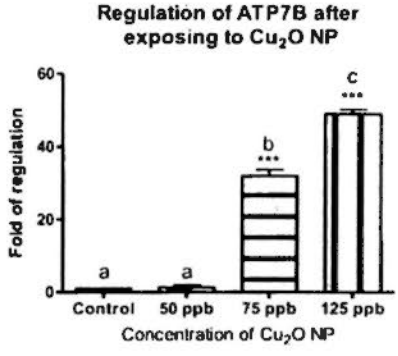
Regulation of ATP7B after exposing to Cu_2O NP
Fold of regulation
a
a
b
c
Control
50 ppb
75 ppb
125 ppb
Concentration of Cu_2O NP

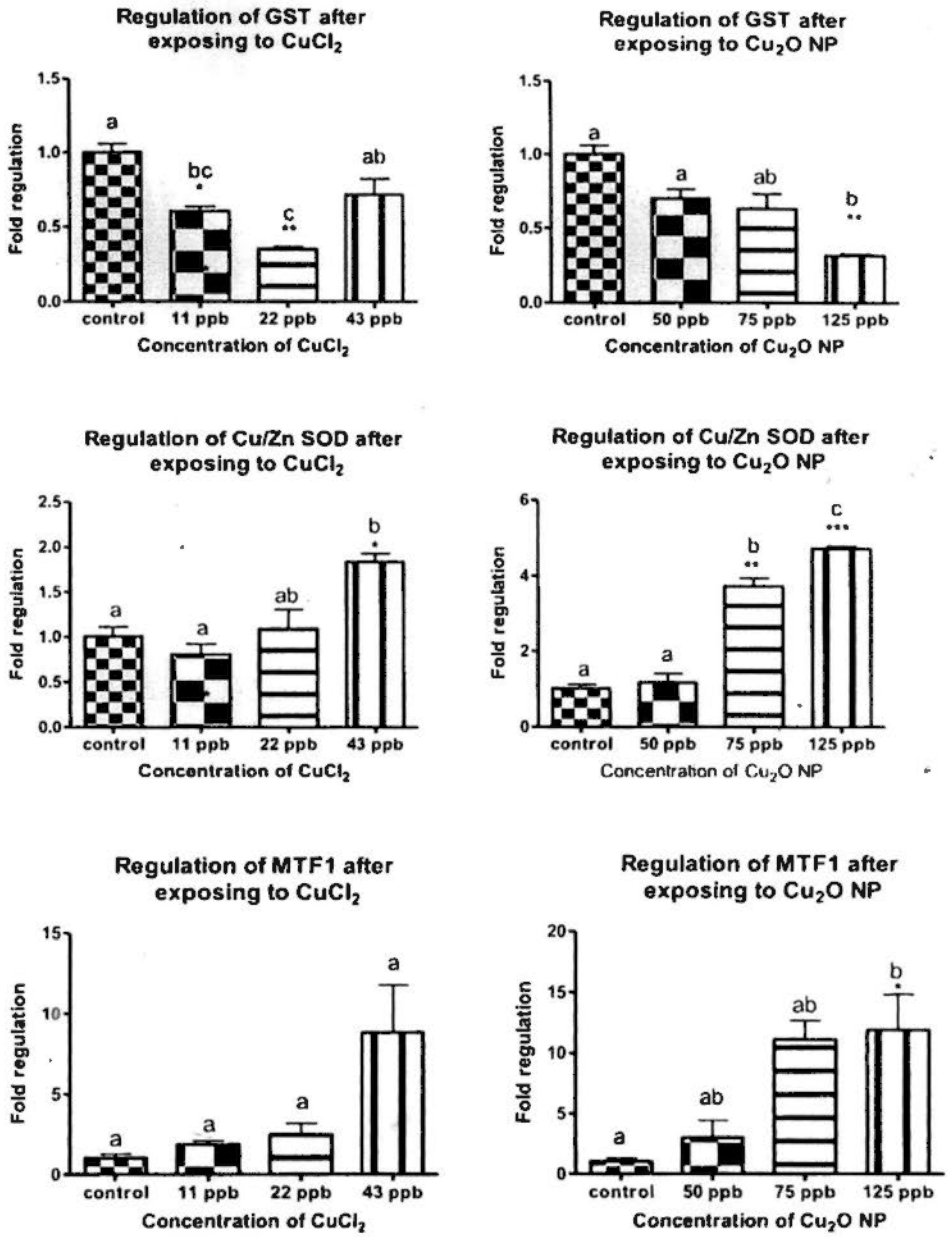

Fig. 6.6. Fold induction of seven genes in mRNA levels in zebrafish larvae exposed to $CuCl_2$ (left panel) and Cu_2O NP (right panel). The y axis represents the fold regulation of these genes (*$p < 0.05$, **$p < 0.01$, ***$p < 0.001$; ANOVA, Tukey's test). Bars bearing different lettering are significantly different ($p<0.05$, ANOVA, Tukey's test).

6.4 Discussion

The manufacture and use of metal oxide nanoparticles is continuously expanding due to their wide applications and unique physicochemical properties. Since they have a very small size (<0.1 um in diameter), they readily contaminate the environment and may pose a risk to humans (Griffitt et al., 2007). Thus, it becomes increasingly important to investigate and identify their possible toxicological effects and to identify which particles pose the greatest harm to human health. Since inhalation is a significant route of exposure to metal oxide nanoparticles, we have studied the impact of Cu_2O nanoparticle on ZFL and zebrafish larvae, also compare the toxicity with $CuCl_2$ to understand the toxic mechanism of un-soluble copper form with the help of biomarker genes' expressions.

Comparing the 96 h LC50 values of Cu_2O NP and $CuCl_2$, it was found that the toxicity of Cu_2O NP was lower than that of $CuCl_2$. This result was well matched with previous studies on the toxicities of copper NPs and soluble Cu ions (Griffitt et al., 2007; Lanone et al., 2009). Besides, the results of copper accumulation showed that Cu_2O NP exposures caused similar level of copper accumulation ZFL exposed to $CuCl_2$, and even much higher than zebrafish larvae exposed to $CuCl_2$. We hypothesized that the difference between toxicity of Cu_2O NP and $CuCl_2$ to ZFL and zebrafish larvae should be due to the property of Cu_2O NP and the copper transportation pathway, which was also studied using real time quantitative PCR.

In other study, it was found that copper entered into the eukaryotes with the form of Cu^+, which is the substrate for the Ctr1. Most Cu^+ would be transported into the cell by

binding with Ctr1 (Balamurugan and Schaffner, 2006). After that the cytosolic Cu ions will be transferred to different organelles, such as transfer golgi, mitochondria. Part of the intracellular copper ions will also be stored in MT which functions as metal detoxification (Balamurugan and Schaffner, 2006; Lutsenko et al., 2007). And the excessive cupric ion will be efflux out of cell by translocation using ATP7A & B excreted from transfer golgi. Our results also showed that Cu_2O NP and $CuCl_2$ could induce MT, Ctr1, ATP7A & B. The induction of these four genes in ZFL exposed to Cu_2O NP and $CuCl_2$ was almost at the same level. The similar accumulation of copper in ZFL exposed to Cu_2O NP and $CuCl_2$ well matched with the induction of MT. And the induction of Ctr1 and ATP7A & B by Cu_2O NP and $CuCl_2$ revealed that Cu^+ uptake and efflux by ZFL from Cu_2O NP and $CuCl_2$ similarly, even through the higher concentration of copper was found in cells exposed to Cu_2O NP. Also, the copper ion accumulated in the ZFL caused equal ROS effect, as indicated by similar fold inductions of GST and SOD genes by Cu_2O NP and $CuCl_2$.

In zebrafish larvae, most of the biomarker genes were induced by Cu_2O NP and $CuCl_2$, except down-regulation of GST mRNA levels was observed. But interestingly, Cu_2O NP could induce much more MT, Ctr1, ATP7A & B mRNAs than CuCl2. Firstly, the higher induction of MT would be related to higher accumulation of copper in zebrafish larvae (Fig. 6.4). Secondly, higher induction of Ctr1 would result in much more copper ion enter into the zebrafish larvae. The higher induction of Ctr1 and MT by Cu_2O NP in zebrafish larvae was much different from that in ZFL. This should be due to the differences between ZFL cell and zebrafish larvae. The ZFL is a hepatocyte, which can only utilize the soluble copper, but the Cu_2O NP with lower solubility and made it

hard to enter into ZFL cells. Turn to zebrafish larvae, larval uptake of copper would either be from waterborne by gill and dietary uptake by intestine (Minghetti et al., 2010). It was reported that copper NP can be utilized by gill of zebrafish not only by dissolution (Griffitt et al., 2007). It was also found that Cu_2O NP can be increased to dissolve into Cu^{2+} and Cu^{+} by changing the pH and salt components in the sea water (Palmer and Bénézeth, 2008). The circumstance in the intestine, which is different from the circumstance in vitro, would also help the dissolution of Cu_2O NP for better copper uptake. Even though the higher induction of Ctr1 in zebrafish larvae, Cu_2O NP could also induce more ATP7A & B, which would help the organism to efflux out of the excessive copper ion and keep the ion homeostasis. Therefore, copper accumulation in the zebrafish larvae exposed to Cu_2O NP is no much higher than that exposed to $CuCl_2$, compared with the difference between the inductions of copper transporters and MT

As to the regulation of GST, Cu/Zn SOD, MTF1, Cu_2O NP could also regulate GST and Cu/Zn SOD stronger than $CuCl_2$ in zebrafish larvae, indicating that Cu_2O NP induced more ROS effect to larvae. However, the difference between Cu_2O NP and $CuCl_2$ in regulating GST and Cu/Zn SOD was well matched with the difference between Cu accumulation in larvae exposed to Cu_2O NP and $CuCl_2$. This result indicated that higher copper accumulation in zebrafish larvae would cause higher ROS effect, which was also reported by other studies (Craig et al., 2007; Sandrini et al., 2009).

The widespread uses of nanomaterials have resulted in uncertainties regarding their environmental impacts. As partial dissolution of metal nanoparticles may occur, it is important to distinguish the toxic effects of nanoparticles from dissolved metals and

determine the no observable effect levels (NOELs) and lowest observable effect levels (LOELs) of these materials in water by using biomarkers gene expressions in zebrafish. In this study, Cu_2O NP and $CuCl_2$ induced the mRNA levels of Ctr1 and ATP7A & 7B dose-dependently, meaning that these three genes can be potential biomarkers to monitor the copper contamination in the environment. Furthermore, as determined by using Ctr1, ATP7A and ATP7B gene expression, the NOELs of $CuCl_2$ and nano-Cu_2O were 11 ppb and 50 ppb whereas the LOELs of $CuCl_2$ and nano-Cu_2O were 43 ppb and 125 ppb.

In conclusion, we have characterized the toxicity of Cu_2O NP, and compared with that of $CuCl_2$. We have shown that (1) the LC50 values of CuCl2 were significantly lower (more toxic) than that of Cu_2O NP *in vivo* and *in vitro*, (2) the *in vitro* toxicity and biomarker gene expression pattern of Cu_2O NP on ZFL cells were similar to $CuCl_2$; (3) Cu_2O NP induced copper transporters of zebrafish larvae *in vivo*, more stronger than $CuCl_2$; (4) Cu_2O NP can regulate GST, SOD more stronger than CuCl2, but showed similar effects on MTF-1 gene expressions *in vivo*; (5) Copper transporters (CTR1, ATP7A & 7B) are potential biomarkers of copper exposures and effects. We have also concluded that copper nanoparticles exert a toxic effect on zebrafish larvae separate from the well understood effects of soluble copper. This research highlights the need for integrated toxicological assessment and suggests that existing regulations for soluble copper may not adequately address the safety concerns associated with metallic nanoparticles. Zebrafish embryo-larvae system and ZFL cell models are useful to determine the toxic effects of nanoparticles with the help of biomarker gene expressions.

Chapter 7

General Conclusions

Copper is an essential nutrient for almost all eukaryotic organisms to carry out biological processes such as free radical detoxification, mitochondria respiration, iron metabolism, neuropeptides maturation, connective tissue formation, pigmentation, and oxygen carrier in hemocyanin (Flemming and Trevors, 1989). The regulation of copper is very important to keep the normal cell functions, and copper content needs precise control. If free copper ions present in the cells, it is lethal to cell by blocking transporters and enzymes, affecting transcription, or generating free radicals (Turski and Thiele, 2009, Balamurugan and Schaffner, 2006). There are two well known human being diseases, Menkes disease and Wilson's disease, which are related to genetic disorders of copper removal and uptake using specific metal transporters, ATP7A and 7B genes differentially expressed in liver and intestine, respectively for body removal and uptake of copper ions. Consequently, the Menkes disease is caused by copper deficiency, but reversely, the Wilson disease is caused by copper overload (Gitlin, 2003; Kim et al., 2009).

For copper homeostasis, it was thought to be related to many other important cellular proteins. And copper deficiency will cause enzyme defects, but reversely, copper overloading will cause ROS effect to cell, which would lead to damage to DNA, RNA, lipid, proteins, and result in cell apoptosis (Craig et al., 2007; Sandrim et al., 2009). Until now, it has been found several important copper transporters or copper related proteins as showed in Table 1.3, which can play an important role in the copper transportation and detoxification. However, expcept these proteins, are there any other proteins also involved in the copper transportation or detoxification? How can copper

exert its toxicity effect, such as ROS effect? What is the mechanism of copper tolerance and sensitivity? And is there any differences between soluble copper and un-soluble copper? To answer these queries, we conducted a serial of experiment in this study.

To study the mechanism of copper toxicity, a differentially expressed proteomics anaylsis on tilapia liver cell cell (Hepa T1) was conducted. In this part, 93 proteins were found to be differentially expressed, some of which may be suitable as biomarkers of effects to monitor copper contamination in the environment, especially the 18 that were further confirmed by real-time quantitative PCR. By using the IPA software analysis, it was found that these differentially expressed proteins were mainly involved in lipid metabolism, connective tissue development and cell cycle development. Therefore, it can be concluded that copper may also exert its toxicity effect by regulating these proteins, and cause blocking of these functions, except ROS effect. In addition, other proteins were also found to be significantly induced or reduced in the mRNA level of the Hepa-T1 cell line after copper exposure, including growth hormone (120 μM, $p < 0.01$; 300 μM, $p < 0.001$), interleukin-1 alpha (300 μM, $p < 0.05$), ATP synthase subunit beta (120 μM, $p < 0.01$; 300 μM, $p < 0.05$), zinc finger protein 60 (120 μM, $p < 0.05$; 300 μM, $p < 0.05$), proteosome (300 μM, $p < 0.05$) and vitellogenin (120 μM, $p < 0.05$; 300 μM, $p < 0.01$). These six proteins may be new biomarkers for copper contamination using tilapia as bioindicator.

The copper transportation should be involved in many proteins which can bind with copper ion. Therefore, to study some novel copper binding proteins, tilapia was further used as a model. Because of its copper tolerance, tilapia should contain more copper

binding proteins. This study used FPLC & IMAC to separate the copper binding proteins from liver cytosolic fraction, then analyzed with proteomic approaches. As the result showed, some proteins with copper binding ability were differentially regulated by copper ion, which should be important proteins involved in copper transportation. According to the functions of the cuproproteins identified in this study, copper may exert its toxicity by inducing endocrine disruption, mitochondria dysfunction, ion competition, lipid metabolism, and cytoskeleton disruption. Our results also suggest that Cu^{2+} may be transferred from cytoplasm to cytochrome c oxidase in mitochondria by binding with stanniocalcin, and that NADH dehydrogenase subunit 5 and aldehyde dehydrogenase may play a role in copper transportation and storage inside the mitochondria. Based on our results and proteins reported in other studies (Hernandez and Allende, 2008), a copper transportation pathway was hypothesized as shown in Fig 2.6. These findings may help us to understand Cu^{2+} transport and storage in the liver of tilapia and perhaps in other fish species or even other vertebrates in general.

Besides, we also examined the 27 genes' regulation *in vivo* by real-time quantitative PCR, including 18 genes found in the *in vitro* experiment. According to my results, the inductions of most genes were well matched *in vivo* and *in vitro*. Especially, several genes were found to be regulated by copper ion dosage dependently, which should act as novel biomarkers of effects for copper contamination in the aquatic environment. These genes include interleukin 1-beta, growth hormone, insulin-like growth factor 1, NADH dehydrogenase, zic family member 1, zinc finger protein 60, ferritin, vitellogenin, and calmodulin. From this study, zic family member 1 (zic1) is found to be significantly induced by Cu^{2+}. Zic1 is a member of ZIC family of C2H2-type zinc finger proteins,

which have been implicated as regulators of a number of critical developmental processes, including neurulation, regulation of cell proliferation and liver regeneration (Jochheim-Richter et al., 2006; Keller and Chitnis, 2007). The up-regulation of zic1 in liver implies that Cu^{2+} may disrupt the process of liver regeneration. Information regarding zinc finger 60, which is also significantly induced by Cu^{2+}, is less known and worthy of further investigation.

Because the tolerance of tilapia and zebrafish to copper was different, these two fishes were used as models to study the mechanism of copper tolerance and copper sensitivity. ZFL, a zebrafish cell line, was used as an model firstly. According to differentially expressed proteins profile in the ZFL cell after exposed to Cu^{2+}, most differentially expressed proteins in ZFL were well matched with that in Hepa T1, indicating that the mechanism of Cu^{2+} toxicity to the ZFL is highly conserved with that of Hepa T1. However, there were also some differences in differentially expressed proteins between ZFL and Hepa T1 cell. The major difference of the differentially expressed proteins between these two cell lines after copper exposure were involved in the ROS effect, mitochondrion function and stress response. As discussed previously, copper ion would induce more proteins related antioxidant and mitochondrial copper transportation in Hepa T1 than ZFL, which would act to protect Hepa T1 from Cu^{2+} toxicity. Also, Cu^{2+} would induce more stress effects to ZFL than Hepa T1 cell. These differences should help us to explain the copper sensitivity of zebrafish and tolerance of tilapia.

Besides, I also compared the regulation of three important copper binding proteins,

ATP7A & B and MT, in tilapia and zebrafish *in vivo* and *in vitro*. In this study I obtained the full length sequence of ATP7A and partial sequence of ATP7B in tilapia, and found that ATP7A in tilapia was highly conserved with human and other teleost fish's ATP7As, indicating that the toxicity of Cu^{2+} to tilapia was conserved with zebrafish and human. Real time quantitative PCR was conducted to study these three genes' regulation. As the results showed, copper can induce more ATP7A & B and MT in tilapia than zebrafish *in vivo* and *in vitro*. It is concluded that tilapia has a higher fold induction of these genes for better metal homeostatsis. However, further investigations with RNAi or morpholino knock down approaches are needed to further confirm the functions or roles of these transporters and MT play in copper homeostasis.

As the contamination of copper can be in soluble and unsoluble forms and the development of nanotechnology make the contamination of copper nanoparticles get more and more serious, we also compared the toxicity of $CuCl_2$ and Cu_2O NP in this study. It was found that the toxicity of Cu_2O NP was lower than that of $CuCl_2$. By detecting several genes' regulation in zebrafish, it was found that the regulation of copper transporters was different *in vivo* and *in vitro*. These results help us to understand that the copper ion inside the cell was tightly controlled. Also, we have concluded that copper nanoparticles exert a toxic effect on zebrafish larvae separate from the well understood effects of soluble copper. This research highlights the need for integrated toxicological assessment and suggests that existing regulations for soluble copper may not adequately address the safety concerns associated with metallic nanoparticles. All in all, zebrafish embryo-larvae system and ZFL cell models are useful to determine the toxic effects of nanoparticles with the help of biomarker gene expressions.

In summary, this study profiles the proteins regulated by copper ion in the tilapia and zebrafish, and also found several copper binding proteins which may involved into the copper transportation pathway. Besides, we also studied the mechanism of copper tolerance and copper sensitivity by comparing two species of fish, zebrafish and tilapia, and concluded that the copper tolerance of tilapia should be due to higher induction of ATP7A & B, MT and several proteins related to ROS effect, mitochondrion function. Also, we study the toxitiy of soluble and un-soluble copper, and found that the copper ion was tightly regulated by the copper transportation system. At last, this study found several proteins were dosage dependently regulated by copper exposure, and may be potential biomarker for monitoring of copper contamination in the environment by using fish model.

References

Abdel-Tawwab, M., Mousa, M., Ahmad, M. H. and Sakr, S. (2007). The use of calcium pre-exposure as a protective agent against environmental copper toxicity for juvenile nile tilapia, Oreochromis niloticus (L.). *Aquaculture* **264**, 236-246.

Ahmed, N. and Rice, G. E. (2005). Strategies for revealing lower abundance proteins in two-dimensional protein maps. *J Chromatogr B* **815**, 39-50.

Aigner, E., Theurl, I., Haufe, H., Seifert, M., Hohla, F., Scharinger, L., Stickel, F., Mourlane, F., Weiss, G. and Datz, C. (2008). Copper availability contributes to iron perturbations in human nonalcoholic fatty liver disease. *Gastroenterology* **135**, 680-8.

Airaksinen, S., Rabergh, C., Lahti, A., Kaatrasalo, A., Sistonen, L. and Nikinmaa, M. (2003). Stressor-dependent regulation of the heat shock response in zebrafish, Danio rerio. *Comp Biochem Phys A* **134**, 839-846.

Ali, S. and Ali, S. (1998). Prolactin receptor regulates Stat5 tyrosine phosphorylation and nuclear translocation by two separate pathways. *J Biol Chem* **273**, 7709-7716.

Allen, M. D., Del, C. J., Kropat, J. and Merchant, S. S. (2007). FEA1, FEA2, and FRE1, encoding two homologous secreted proteins and a candidate ferrireductase, are expressed coordinately with FOX1 and FTR1 in iron-deficient Chlamydomonas reinhardtii. *Eukaryot Cell* **6**, 1841-52.

Aller, S. G. and Unger, V. M. (2006). Projection structure of the human copper transporter CTR1 at 6-A resolution reveals a compact trimer with a novel channel-like architecture. *Proc Natl Acad Sci U S A* **103**, 3627-32.

Amanuma, K., Takeda, H., Amanuma, H. and Aoki, Y. (2000). Transgenic zebrafish for detecting mutations caused by compounds in aquatic environments. *Nat Biotechnol* **18**, 62-65.

Anastassopoulou, I., Banci, L., Bertini, I., Cantini, F., Katsari, E. and Rosato, A. (2004). Solution structure of the apo and copper(I)-loaded human metallochaperone HAH1. *Biochemistry-US* **43**, 13046-53.

Ando, S. and Yanagida, K. (1999). Susceptibility to oxidation of copper-induced plasma lipoproteins from Japanese eel: protective effect of vitellogenin on the oxidation of very low density lipoprotein. *Comp Biochem Physiol C Pharmacol Toxicol Endocrinol* **123**, 1-7.

Andress, D. L. (1995). Heparin modulates the binding of insulin-like growth factor (IGF) binding protein-5 to a membrane protein in osteoblastic cells. *J Biol Chem* **270**, 28289-96.

Andrews, G. K. (2000). Regulation of metallothionein gene expression by oxidative stress and metal ions. *Biochem Pharmacol* **59**, 95-104.

Aschner, M., Cherian, M. G., Klaassen, C. D., Palmiter, R. D., Erickson, J. C. and Bush, A. I. (1997). Metallothioneins in brain--the role in physiology and pathology. *Toxicol Appl Pharmacol* **142**, 229-42.

Atli, G., Alptekin, O., Tukel, S. and Canli, M. (2006). Response of catalase activity to Ag^{+}, Cd^{2+}, Cr^{6+}, Cu^{2+} and Zn^{2+} in five tissues of freshwater fish Oreochromis niloticus. *Comp Biochem Phys C* **143**, 218-224.

Ay, O., Kalay, M., Tamer, L. and Canli, M. (1999). Copper and lead accumulation in tissues of a freshwater fish Tilapia zillii and its effects on the branchial Na, K-ATPase activity. *B Eenviron Contam Tox* **62**, 160-168.

Baker, R., Handy, R. D., Davies, S. J. and Snook, J. C. (1998). Chronic dietary exposure to copper affects growth, tissue lipid peroxidation, and metal composition of the grey mullet, Chelon labrosus. *Mar Environ Res* **45**, 357-365.

Balamurugan, K. and Schaffner, W. (2006). Copper homeostasis in eukaryotes: Teetering on a tightrope. *BBA-Mol Cell Res* **1763**, 737-746.

BALIRWA, J. S. (1992). The evolution of the fishery of oreochromis-niloticus (Pisces, cichlidae) in lake victoria. *Hydrobiologia* **232**, 85-89.

Barnard, R. O., Best, P. V. and Erdohazi, M. (1978). Neuropathology of Menkes' disease. *Dev Med Child Neurol* **20**, 586-97.

Barnham, K. J., Masters, C. L. and Bush, A. I. (2004). Neurodegenerative diseases and oxidative stress. *Nat Rev Drug Discov* **3**, 205-14.

Bartsch, H. and Nair, J. (2004). Oxidative stress and lipid peroxidation-derived DNA-lesions in inflammation driven carcinogenesis. *Cancer Detect Prev* **28**, 385-91.

Baskin, D. G., Seeley, R. J., Kuijper, J. L., Lok, S., Weigle, D. S., Erickson, J. C., Palmiter, R. D. and Schwartz, M. W. (1998). Increased expression of mRNA for the long form of the leptin receptor in the hypothalamus is associated with leptin hypersensitivity and fasting. *Diabetes* **47**, 538-43.

Bayer, T. A. and Multhaup, G. (2005). Involvement of amyloid beta precursor protein (AbetaPP) modulated copper homeostasis in Alzheimer's disease. *J Alzheimers Dis* **8**, 201-6; discussion 209-15.

Bayer, T. A., Schafer, S., Simons, A., Kemmling, A., Kamer, T., Tepest, R., Eckert, A., Schussel, K., Eikenberg, O., Sturchler-Pierrat, C., Abramowski, D., Staufenbiel, M. and Multhaup, G. (2003). Dietary Cu stabilizes brain superoxide dismutase 1 activity and reduces amyloid Abeta production in APP23 transgenic mice. *Proc Natl Acad Sci U S A* **100**, 14187-92.

Begley, T. J. and Samson, L. D. (2004). Reversing DNA damage with a directional bias. *Nat Struct Mol Biol* **11**, 688-90.

Belyaeva, E. A., Dymkowska, D., Wieckowski, M. R. and Wojtczak, L. (2008).

Mitochondria as an important target in heavy metal toxicity in rat hepatoma AS-30D cells. *Toxicol Appl Pharmacol* **231**, 34-42.

Berntssen, M., Hylland, K., Bonga, S. and Maage, A. (1999). Toxic levels of dietary copper in atlantic salmon (*Salmo salar L.*) parr. *Aquatic Toxicol* **46**, 87-99.

Bertinato, J. and L'Abbe, M. R. (2004). Maintaining copper homeostasis: regulation of copper-trafficking proteins in response to copper deficiency or overload. *J Nutr Biochem* **15**, 316-22.

Bettini, S., Ciani, F. and Franceschini, V. (2006). Recovery of the olfactory receptor neurons in the african tilapia mariae following exposure to low copper level. *Aquat Toxicol* **76**, 321-8.

Birungi, Z., Masola, B., Zaranyika, M. F., Naigaga, I. and Marshall, B. (2007). Active biomonitoring of trace heavy metals using fish (*Oreochromis niloticus*) as bioindicator species. The case of Nakivubo wetland along Lake Victoria. *Physics Chem Earth* **32**, 1350-1358.

Bradley, B. P., Shrader, E. A., Kimmel, D. G. and Meiller, J. C. (2002). Protein expression signatures: an application of proteomics. *Mar Environ Res* **54**, 373-377.

Brix, K. V., DeForest, D. K. and Adams, W. J. (2001). Assessing acute and chronic copper risks to freshwater aquatic life using species sensitivity distributions for different taxonomic groups. *Environ Tox Chem* **20**, 1846-1856.

Brumfiel, G. (2006). Consumer products leap aboard the nano bandwagon. *Nature* **440**, 262-262.

Bull, P. C., Thomas, G. R., Rommens, J. M., Forbes, J. R. and Cox, D. W. (1993). The Wilson disease gene is a putative copper transporting P-type ATPase similar to the Menkes gene. *Nat Genet* **5**, 327-37.

Burkitt, M. J. (2001). A critical overview of the chemistry of copper-dependent low density lipoprotein oxidation: roles of lipid hydroperoxides, alpha-tocopherol, thiols, and ceruloplasmin. *Arch Biochem Biophys* **394**, 117-35.

Camakaris, J., Voskoboinik, I. and Mercer, J. F. (1999). Molecular mechanisms of copper homeostasis. *Biochem Biophys Res Commun* **261**, 225-32.

Cataldo, L., Chen, N. Y., Yuan, Q., Li, W., Ramamoorthy, P., Wagner, T. E., Stseca, R. P. and Chen, W. Y. (2000). Inhibition of oncogene STAT3 phosphorylation by a prolactin antagonist, hPRL-G129R, in T-47D human breast cancer cells. *Int J Oncol* **17**, 1179-1185.

Cayatte, C., Pons, C., Guigonis, J. M., Pizzol, J., Elies, L., Kennel, P., Rouquie, D., Bars, R., Rossi, B. and Samson, M. (2006). Protein profiling of rat ventral prostate following chronic finasteride administration - Identification and localization of a novel putative androgen-regulated protein. *Mol Cell Proteomics* **5**, 2031-2043.

Chan, K. M. (1994). PCR-cloning of goldfish and tilapia metallothionein

complementary DNAs. *Biochem Biophys Res Commun* **205**, 368-374.

Chan, K. M. (1995). Metallothionein: Potential biomarker for monitoring heavy metal pollution in fish around Hong Kong. *Mar Pollut Bull* **31**, 411-415.

CHAN, K. M., DAVIDSON, W. S., HEW, C. L. and FLETCHER, G. L. (1989). Molecular-cloning of metallothionein cDNA and analysis of metallothionein gene-expression in winter flounder tissues. *Can J Zool* **67**, 2520-2527.

Chan, K. M., Ku, L. L., Chan, P. and Cheuk, W. K. (2006). Metallothionein gene expression in zebrafish embryo-larvae and ZFL cell-line exposed to heavy metal ions. *Mar Environ Res* **62Suppl. S**, S83-S87.

Chapman, R. S., Lourenco, P. C., Tonner, E., Flint, D. J., Selbert, S., Takeda, K., Akira, S., Clarke, A. R. and Watson, C. J. (1999). Suppression of epithelial apoptosis and delayed mammary gland involution in mice with a conditional knockout of Stat3. *Genes Dev* **13**, 2604-2616.

Chen, D. S. and Chan, K. M. (2009). Changes in the protein expression profiles of the Hepa-T1 cell line when exposed to Cu^{2+}. *Aquat Toxicol* **94**, 163-76.

Chen, J., He, Q. Y., Yuen, A. and Chiu, J. F. (2004). Proteomics of buccal squamous cell carcinoma: The involvement of multiple pathways in tumorigenesis. *Proteomics* **4**, 2465-2475.

Chen, W. Y., John, J., Lin, C. H. and Chang, C. Y. (2002). Molecular cloning and developmental expression of zinc finger transcription factor MTF-1 gene in zebrafish, Danio rerio. *Biochem Biophys Res Commun* **291**, 798-805.

Chen, W. Y., John, J., Lin, C. H., Lin, H. F., Wu, S. C., Lin, C. H. and Chang, C. Y. (2004). Expression of metallothionein gene during embryonic and early larval development in zebrafish. *Aquat Toxicol* **69**, 215-227.

Chenet, A. L., Courtillot, V., Fluteau, F., Gerard, M., Quidelleur, X., Khadri, S., Subbarao, K. V. and Thordarson, T. (2009). Determination of rapid Deccan eruptions across the Cretaceous-Tertiary boundary using paleomagnetic secular variation: 2. Constraints from analysis of eight new sections and synthesis for a 3500-m-thick composite section. *J Geophys Res* **114**.

Cherny, R. A., Legg, J. T., McLean, C. A., Fairlie, D. P., Huang, X., Atwood, C. S., Beyreuther, K., Tanzi, R. E., Masters, C. L. and Bush, A. I. (1999). Aqueous dissolution of Alzheimer's disease Abeta amyloid deposits by biometal depletion. *J Biol Chem* **274**, 23223-8.

Cheuk, W. K., Chan, P. and Chan, K. M. (2008). Cytotoxicities and induction of metallothionein (MT) and metal regulatory element (MRE)-binding transcription factor-1 (MTF-1) messenger RNA levels in the zebrafish (Danio rerio) ZFL and SJD cell lines after exposure to various metal ions. *Aquat Toxicol* **89**, 103-112.

Clearwater, S. J., Farag, A. M. and Meyer, J. S. (2002). Bioavailability and toxicity of dietborne copper and zinc to fish. *Comp Biochem Physiol C Toxicol Pharmacol* **132**,

269-313.

Clemmons, D. R., Busby, W. H., Arai, T., Nam, T. J., Clarke, J. B., Jones, J. I. and Ankrapp, D. K. (1995). Role of insulin-like growth factor binding proteins in the control of IGF actions. *Prog Growth Factor Res* **6**, 357-66.

Cobine, P. A., Pierrel, F. and Winge, D. R. (2006). Copper trafficking to the mitochondrion and assembly of copper metalloenzymes. *Biochim Biophys Acta* **1763**, 759-72.

Compton, S. J. and Jones, C. G. (1985a). Mechanism of dye response and interference in the Bradford protein assay. *Anal Biochem* **151**, 369-74.

Compton, S. J. and Jones, C. G. (1985b). Mechanism of dye response and interference in the bradford protein assay. *Aanl Biochem* **151**, 369-374.

Contreras, L., Mella, D., Moenne, A. and Correa, J. A. (2009). Differential responses to copper-induced oxidative stress in the marine macroalgae Lessonia nigrescens and Scytosiphon lomentaria (Phaeophyceae). *Aquat Toxicol* **94**, 94-102.

Correi, A. D., Livingstone, D. R. and Costa, M. H. (2002). Effects of water-borne copper on metallothionein and lipid peroxidation in the marine amphipod Gammarus locusta. *Mar Environ Res* **54**, 357-60.

Craig, P. M., Galus, M., Wood, C. M. and McClelland, G. B. (2009). Dietary iron alters waterborne copper-induced gene expression in soft water acclimated zebrafish (Danio rerio). *Am J Physiol Regul Integr Comp Physiol* **296**, R362-R373.

Craig, P. M., Wood, C. M. and McClelland, G. B. (2007). Oxidative stress response and gene expression with acute copper exposure in zebrafish (danio rerio). *Am J Physiol Regul Integr Comp Physiol* **293**, R1882-92.

Curtain, C. C., Ali, F., Volitakis, I., Cherny, R. A., Norton, R. S., Beyreuther, K., Barrow, C. J., Masters, C. L., Bush, A. I. and Barnham, K. J. (2001). Alzheimer's disease amyloid-beta binds copper and zinc to generate an allosterically ordered membrane-penetrating structure containing superoxide dismutase-like subunits. *J Biol Chem* **276**, 20466-73.

Dail, M. B., Shack, L. A., Chambers, J. E. and Burgess, S. C. (2008). Global Liver Proteomics of Rats Exposed for 5 Days to Phenobarbital Identifies Changes Associated with Cancer and with CYP Metabolism. *Toxicol Sci* **106**, 556-569.

Dalle-Donne, I., Rossi, R., Milzani, A., Di Simplicio, P. and Colombo, R. (2001). The actin cytoskeleton response to oxidants: From small heat shock protein phosphorylation to changes in the redox state of actin itself. *Free Radical Bio Med* **31**, 1624-1632.

Dancis, A., Haile, D., Yuan, D. S. and Klausner, R. D. (1994). The Saccharomyces cerevisiae copper transport protein (Ctr1p). Biochemical characterization, regulation by copper, and physiologic role in copper uptake. *J Biol Chem* **269**, 25660-7.

Dang, Z. C., Lock, R., Flik, G. and Bonga, S. (1999). Metallothionein response in gills of Oreochromis mossambicus exposed to copper in fresh water. *Am J Physiol Regul Integr Comp Physiol* **277**, R320-R331..

Daoudal, G. and Debanne, D. (2003). Long-term plasticity of intrinsic excitability: Learning rules and mechanisms. *Learn Memory* **10**, 456-465.

De Freitas, J. M., Liba, A., Meneghini, R., Valentine, J. S. and Gralla, E. B. (2000). Yeast lacking Cu-Zn superoxide dismutase show altered iron homeostasis. Role of oxidative stress in iron metabolism. *J Biol Chem* **275**, 11645-9.

Dethloff, G. M. and Bailey, H. C. (1998). Effects of copper on immune system parameters of rainbow trout (Oncorhynchus mykiss). *Environ Tox Chem* **17**, 1807-1814.

Donnelly, P. S., Xiao, Z. G. and Wedd, A. G. (2007). Copper and Alzheimer's disease. *Curr Opin Chem Bio* **11**, 128-133.

Durnam, D. M. and Palmiter, R. D. (1987). Analysis of the detoxification of heavy metal ions by mouse metallothionein. *Experientia Suppl* **52**, 457-63.

Ecker, D. J., Butt, T. R., Sternberg, E. J., Neeper, M. P., Debouck, C., Gorman, J. A. and Crooke, S. T. (1986). Yeast metallothionein function in metal ion detoxification. *J Biol Chem* **261**, 16895-900.

El Meskini, R., Culotta, V. C., Mains, R. E. and Eipper, B. A. (2003). Supplying copper to the cuproenzyme peptidylglycine alpha-amidating monooxygenase. *J Biol Chem* **278**, 12278-12284.

El, M. R., Cline, L. B., Eipper, B. A. and Ronnett, G. V. (2005). The developmentally regulated expression of Menkes protein ATP7A suggests a role in axon extension and synaptogenesis. *Dev Neurosci* **27**, 333-48.

Ellard, J. P., McCudden, C. R., Tanega, C., James, K. A., Ratkovic, S., Staples, J. F. and Wagner, G. F. (2007). The respiratory effects of stanniocalcin-1 (STC-1) on intact mitochondria and cells: STC-1 uncouples oxidative phosphorylation and its actions are modulated by nucleotide triphosphates. *Mol Cell Endocrinol* **264**, 90-101.

Eppler, E., Shved, N., Moret, O. and Reinecke, M. (2007). IGF-I is distinctly located in the bony fish pituitary as revealed for Oreochromis niloticus, the Nile tilapia, using real-time RT-PCR, in situ hybridisation and immunohistochemistry. *Gen Comp Endocr* **150**, 87-95.

Eyckmans, M., Tudorache, C., Darras, V. M., Blust, R. and De Boeck, G. (2010). Hormonal and ion regulatory response in three freshwater fish species following waterborne copper exposure. *Comp Biochem Physiol C* **152**, 270-278.

Fagotti, A., DiRosa, I., Simoncelli, F., Pipe, R. K., Panara, F. and Pascolini, R. (1996). The effects of copper on actin and fibronectin organization in Mytilus galloprovincialis haemocytes. *Dev Comp Immunol* **20**, 383-391.

Ferenci, P. (2004). Pathophysiology and clinical features of Wilson disease. *Metab Brain Dis* **19**, 229-39.

Ferruzza, S., Scarino, M. L., Rotilio, G., Ciriolo, M. R., Santaroni, P., Muda, A. O. and Sambuy, Y. (1999). Copper treatment alters the permeability of tight junctions in cultured human intestinal Caco-2 cells. *Am J Physiol Regul Integr Comp Physiol* **277**, G1138-G1148.

Field, L. S., Furukawa, Y., O'Halloran, T. V. and Culotta, V. C. (2003). Factors controlling the uptake of yeast copper/zinc superoxide dismutase into mitochondria. *J Biol Chem* **278**, 28052-9.

FLEMMING, C. A. and TREVORS, J. T. (1989). Copper toxicity and chemistry in the environment - a review. *Water Air Soil Poll* **44**, 143-158..

Frixione, E. (2000). Recurring views on the structure and function of the cytoskeleton: a 300-year epic. *Cell Motil Cytoskeleton* **46**, 73-94.

Furukawa, Y., Torres, A. S. and O'Halloran, T. V. (2004). Oxygen-induced maturation of SOD1: a key role for disulfide formation by the copper chaperone CCS. *EMBO J* **23**, 2872-81.

Gan, L., Perney, T. M. and Kaczmarek, L. K. (1996). Cloning and characterization of the promoter for a potassium channel expressed in high frequency firing neurons. *J Biol Chem* **271**, 5859-5865.

Gansner, J. M. and Gitlin, J. D. (2008). Essential role for the alpha 1 chain of type VIII collagen in zebrafish notochord formation. *Dev Dyn* **237**, 3715-26..

Garcia-Fernandez, M., Castilla-Cortazar, I., Diaz-Sanchez, M., Navarro, I., Puche, J. E., Castilla, A., Casares, A. D., Clavijo, E. and Gonzalez-Baron, S. (2005). Antioxidant effects of insulin-like growth factor-I (IGF-I) in rats with advanced liver cirrhosis. *BMC Gastroenterol* **5**, 7-10.

Geller, T. J., Pan, Y. and Martin, D. S. (1997). Early neuroradiologic evidence of degeneration in Menkes' disease. *Pediatr Neurol* **17**, 255-8.

Gitlin, J. D. (2003). Wilson disease. *Gastroenterology* **125**, 1868-77.

Gomez-Mendikute, A., Etxeberria, A., Olabarrieta, I. and Cajaraville, M. P. (2002). Oxygen radicals production and actin filament disruption in bivalve haemocytes treated with benzo(a)pyrene. *Mar Environ Res* **54**, 431-436.

Gonzalez, P., Baudrimont, M., Boudou, A. and Bourdineaud, J. P. (2006). Comparative effects of direct cadmium contamination on gene expression in gills, liver, skeletal muscles and brain of the zebrafish (Danio rerio). *Biometals* **19**, 225-235.

Gorg, A., Weiss, W. and Dunn, M. J. (2004). Current two-dimensional electrophoresis technology for proteomics. *Proteomics* **4**, 3665-3685..

Greenwood, M. P., Flik, G., Wagner, G. F. and Balment, R. J. (2009). The corpuscles of

Stannius, calcium-sensing receptor, and stanniocalcin: responses to calcimimetics and physiological challenges. *Endocrinology* **150**, 3002-10.

Griffitt, R. J., Weil, R., Hyndman, K. A., Denslow, N. D., Powers, K., Taylor, D. and Barber, D. S. (2007). Exposure to copper nanoparticles causes gill injury and acute lethality in zebrafish (Danio rerio). *Environ Sci Tech* **41**, 8178-8186.

Grosell, M. H., Hogstrand, C. and Wood, C. M. (1997). Cu uptake and turnover in both Cu-acclimated and non-acclimated rainbow trout (Oncorhynchus mykiss). *Aquat Toxicol* **38**, 257-276.

Grosell, M. H., Hogstrand, C. and Wood, C. M. (1998). Renal Cu and Na excretion and hepatic Cu metabolism in both Cu acclimated and non acclimated rainbow trout (Oncorhynchus mykiss). *Aquat Toxicol* **40**, 275-291.

Grosell, M., Blanchard, J., Brix, K. V. and Gerdes, R. (2007). Physiology is pivotal for interactions between salinity and acute copper toxicity to fish and invertebrates. *Aquat Toxicol* **84**, 162-172.

Guo, Y., Smith, K., Lee, J., Thiele, D. J. and Petris, M. J. (2004). Identification of methionine-rich clusters that regulate copper-stimulated endocytosis of the human Ctr1 copper transporter. *J Biol Chem* **279**, 17428-33.

Handy, R. D. (2003). Chronic effects of copper exposure versus endocrine toxicity: two sides of the same toxicological process? *Comp Biochem Physiol A Mol Integr Physiol* **135**, 25-38.

Handy, R. D., Sims, D. W., Giles, A., Campbell, H. A. and Musonda, M. M. (1999). Metabolic trade-off between locomotion and detoxification for maintenance of blood chemistry and growth parameters by rainbow trout (Oncorhynchus mykiss) during chronic dietary exposure to copper. *Aquat Toxicol* **47**, 23-41.

Hardingham, G. E. and Bading, H. (2003). The Yin and Yang of NMDA receptor signalling. *Trends Neurosci* **26**, 81-9.

Hallare, A. V., Pagulayan, R., Lacdan, N., Kohler, H. R. and Triebskorn, R. (2005). Assessing water quality in a tropical lake using biomarkers in zebrafish embryos: Developmental toxicity and stress protein responses. *Environ Monit Assess* **104**, 171-187.

Harris, E. D. (2000). Cellular copper transport and metabolism. *Annu Rev Nutr* **20**, 291-310.

Harrison, M. D., Jones, C. E., Solioz, M. and Dameron, C. T. (2000). Intracellular copper routing: the role of copper chaperones. *Tren Biochem Sci* **25**, 29-32.

Hellman, N. E. and Gitlin, J. D. (2002). Ceruloplasmin metabolism and function. *Annu Rev Nutr* **22**, 439-58.

Hernandez, P. P. and Allende, M. L. (2008). Zebrafish (Danio rerio) as a model for studying the genetic basis of copper toxicity, deficiency, and metabolism. *Am J Clin*

Nutr **88**, 835S-9S.

Hill, A. J., Teraoka, H., Heideman, W. and Peterson, R. E. (2005). Zebrafish as a model vertebrate for investigating chemical toxicity. *Toxicol Sci* **86**, 6-19.

Hindo, S. S., Frezza, M., Tomco, D., Heeg, M. J., Hryhorczuk, L., McGarvey, B. R., Dou, Q. P. and Verani, C. N. (2009). Metals in anticancer therapy: copper(II) complexes as inhibitors of the 20S proteasome. *Eur J Med Chem* **44**, 4353-61.

Hook, S. E. and Fisher, N. S. (2001). Reproductive toxicity of metals in calanoid copepods. *Mar Bio* **138**, 1131-1140.

Huang, K. C., Park, D. C., Ng, S. K., Lee, J. Y., Ni, X. Y., Ng, W. C., Bandera, C. A., Welch, W. R., Berkowitz, R. S., Mok, S. C. and Ng, S. W. (2006). Selenium binding protein 1 in ovarian cancer. *Inter J Cancer* **118**, 2433-2440.

Huang, W. P. and Klionsky, D. J. (2002). Autophagy in yeast: a review of the molecular machinery. *Cell Struct Funct* **27**, 409-20.

Huster, D., Finegold, M. J., Morgan, C. T., Burkhead, J. L., Nixon, R., Vanderwerf, S. M., Gilliam, C. T. and Lutsenko, S. (2006). Consequences of copper accumulation in the livers of the Atp7b-/- (Wilson disease gene) knockout mice. *Am J Pathol* **168**, 423-34.

Huster, D., Purnat, T. D., Burkhead, J. L., Ralle, M., Fiehn, O., Stuckert, F., Olson, N. E., Teupser, D. and Lutsenko, S. (2007). High copper selectively alters lipid metabolism and cell cycle machinery in the mouse model of Wilson disease. *J Biol Chem* **282**, 8343-8355.

Jochheim-Richter, A., Rudrich, U., Koczan, D., Hillemann, T., Tewes, S., Petry, M., Kispert, A., Sharma, A. D., Attaran, F., Manns, M. P. and Ott, M. (2006). Gene expression analysis identifies novel genes participating in early murine liver development and adult liver regeneration. *Differentiation* **74**, 167-173.

Kagi, J. H. (1991). Overview of metallothionein. *Methods Enzymol* **205**, 613-26.

Kaler, S. G. (1998). Metabolic and molecular bases of Menkes disease and occipital horn syndrome. *Pediatr Dev Pathol* **1**, 85-98.

Kamunde, C. N., Grosell, M., Lott, J. and Wood, C. M. (2001). Copper metabolism and gut morphology in rainbow trout (Oncorhynchus mykiss) during chronic sublethal dietary copper exposure. *Can J Fish Aquat Sci* **58**, 293-305.

Kehoe, C. A., Faughnan, M. S., Gilmore, W. S., Coulter, J. S., Howard, A. N. and Strain, J. J. (2000). Plasma diamine oxidase activity is greater in copper-adequate than copper-marginal or copper-deficient rats. *J Nutr* **130**, 30-3.

Kekic, M. and Dos Remedios, C. G. (1999). Electrophoretic monitoring of pollutants: Effect of cations and organic compounds on protein interactions monitored by native gel electrophoresis. *Electrophoresis* **20**, 2053-2058.

Kelleher, S. L. and Lonnerdal, B. (2006). Mammary gland copper transport is stimulated by prolactin through alterations in Ctr1 and Atp7A localization. *Am J Phs-Reg Inte Comp Phys* **291**, R1181-R1191.

Keller, M. J. and Chitnis, A. B. (2007). Insights into the evolutionary history of the vertebrate zic3 locus from a teleost-specific zic6 gene in the zebrafish, Danio rerio. *Dev Genes Evolution* **217**, 541-547.

Kessler, H., Pajonk, F. G., Meisser, P., Schneider-Axmann, T., Hoffmann, K. H., Supprian, T., Herrmann, W., Obeid, R., Multhaup, G., Falkai, P. and Bayer, T. A. (2006). Cerebrospinal fluid diagnostic markers correlate with lower plasma copper and ceruloplasmin in patients with Alzheimer's disease. *J Neural Transm* **113**, 1763-9.

Khallaf, E. A., Galal, M. and Authman, M. (2003). The biology of Oreochromis niloticus in a polluted canal. *Ecotoxicology* **12**, 405-416.

Kim, B. E., Nevitt, T. and Thiele, D. J. (2008). Mechanisms for copper acquisition, distribution and regulation. *Nat Chem Biol* **4**, 176-85.

Koch, K. A., Pena, M. M. and Thiele, D. J. (1997). Copper-binding motifs in catalysis, transport, detoxification and signaling. *Chem Biol* **4**, 549-60.

Kodama, H., Murata, Y. and Kobayashi, M. (1999). Clinical manifestations and treatment of Menkes disease and its variants. *Pediatr Int* **41**, 423-9.

Koehler, H. R., Sandu, C., Scheil, V., Nagy-Petrica, E. M., Segner, H., Telecean, I., Stan, G. and Triebskorn, R. (2007). Monitoring pollution in river Mures, Romania, Part III: biochemical effect markers in fish and integrative reflection. *Envrion Monit Assess* **127**, 47-54.

Koldamova, R. P., Lefterov, I. M., Lefterova, M. I. and Lazo, J. S. (2001). Apolipoprotein A-I directly interacts with amyloid precursor protein and inhibits A beta aggregation and toxicity. *Biochemistry* **40**, 3553-60.

Kuo, Y. M., Gitschier, J. and Packman, S. (1997). Developmental expression of the mouse mottled and toxic milk genes suggests distinct functions for the Menkes and Wilson disease copper transporters. *Hum Mol Genet* **6**, 1043-1049.

Lagadic, L., Caquet, T. and Ramade, F. (1994). The role of biomarker in environmental assessment .5. inverterbrate populations and communities. *Ecotoxicology* **3**, 193-208.

Lam, K. L., Ko, P. W., Wong, J. and Chan, K. M. (1998). Metal toxicity and metallothionein gene expression studies in common carp and tilapia. *Mar Environ Res* **46**, 563-566.

Lamb, A. L., Torres, A. S., O'Halloran, T. V. and Rosenzweig, A. C. (2001) Heterodimeric structure of superoxide dismutase in complex with its metallochaperone. *Nat Struct Biol* **8**, 751-5.

Lange, B. M. and Ghassemian, M. (2005). Comprehensive post-genomic data analysis

approaches integrating biochemical pathway maps. *Phytochemistry* **66**, 413-451.

Lanone, S., Rogerieux, F., Geys, J., Dupont, A., Maillot-Marechal, E., Boczkowski, J., Lacroix, G. and Hoet, P. (2009). Comparative toxicity of 24 manufactured nanoparticles in human alveolar epithelial and macrophage cell lines. *Part Fib Tox* **6**.

Leary, S. C., Kaufman, B. A., Pellecchia, G., Guercin, G. H., Mattman, A., Jaksch, M. and Shoubridge, E. A. (2004). Human SCO1 and SCO2 have independent, cooperative functions in copper delivery to cytochrome c oxidase. *Hum Mol Genet* **13**, 1839-48.

Lee, J., Petris, M. J. and Thiele, D. J. (2002). Characterization of mouse embryonic cells deficient in the ctr1 high affinity copper transporter. Identification of a Ctr1-independent copper transport system. *J Biol Chem* **277**, 40253-9.

Lenartowicz, M., Wieczerzak, K., Krzeptowski, W., Dobosz, P., Grzmil, P., Starzynski, R. and Lipinski, P. (2010). Developmental Changes in the Expression of the Atp7a Gene in the Liver of Mice During the Postnatal Period. *J Exp Zool Part A* **313A**, 209-217.

Leventer, R. J., Kornberg, A. J., Phelan, E. M. and Kean, M. J. (1997). Early magnetic resonance imaging findings in Menkes' disease. *J Child Neurol* **12**, 222-4.

Lewis, A. F. and Dickson, R. C. (1971). Platelet aggregation: induction by means of a complex between endotoxin and copper (Cu 2+). *Can J Biochem* **49**, 1236-44.

Li, J., Quabius, E. S., Bonga, S., Flik, G. and Lock, R. (1998). Effects of water-borne copper on branchial chloride cells and Na+/K+-ATPase activities in Mozambique tilapia (Oreochromis mossambicus). *Aquat Toxicol* **43**, 1-11..

Li, X. X., Vander Heiden, M. G., Thompson, C. B. and Colombini, M. (2001). Bcl-x(L) facilitates the open configuration of VDAC. *Biophys J* **80**, 961..

Lindstrom, M. S. (2009). Emerging functions of ribosomal proteins in gene-specific transcription and translation. *Biochem Biophys Res Comm* **379**, 167-170.

Liu, X. Y., Yang, J. L., Chen, L. J., Zhang, Y., Yang, M. L., Wu, Y. Y., Li, F. Q., Tang, M. H., Liang, S. F. and Wei, Y. Q. (2008). Comparative proteomics and correlated signaling network of rat hippocampus in the pilocarpine model of temporal lobe epilepsy. *Proteomics* **8**, 582-603.

Lutsenko, S., Barnes, N. L., Bartee, M. Y. and Dmitriev, O. Y. (2007). Function and regulation of human copper-transporting ATPases. *Physiol Rev* **87**, 1011-1046.

Lutsenko, S., Gupta, A., Burkhead, J. L. and Zuzel, V. (2008). Cellular multitasking: The dual role of human Cu-ATPases in cofactor delivery and intracellular copper balance. *Arch Biochem Biophys* **476**, 22-32.

Lutsenko, S., LeShane, E. S. and Shinde, U. (2007). Biochemical basis of regulation of human copper-transporting ATPases. *Arch Biochem Biophys* **463**, 134-48.

Mackenzie, N. C., Brito, M., Reyes, A. E. and Allende, M. L. (2004). Cloning, expression pattern and essentiality of the high-affinity copper transporter 1 (ctr1) gene in zebrafish. *Gene* **328**, 113-120.

Madsen, E. and Gitlin, J. D. (2007). Copper and iron disorders of the brain. *Ann Rev Neuro* **30**, 317-337.

Manzl, C., Ebner, H., Kock, G., Dallinger, R. and Krumschnabel, G. (2003). Copper, but not cadmium, is acutely toxic for trout hepatocytes: short-term effects on energetics and ion homeostasis. *Tox Appl Pharm* **191**, 235-244.

Manzl, C., Enrich, J., Ebner, H., Dallinger, R. and Krumschnabel, G. (2004). Copper-induced formation of reactive oxygen species causes cell death and disruption of calcium homeostasis in trout hepatocytes. *Toxicology* **196**, 57-64.

McArdle, H. J., Andersen, H. S., Jones, H. and Gambling, L. (2008). Copper and iron transport across the placenta: regulation and interactions. *J Neuro endocrinol* **20**, 427-31.

McGeer, J. C., Szebedinszky, C., McDonald, D. G. and Wood, C. M. (2000). Effects of chronic sublethal exposure to waterborne Cu, Cd or Zn in rainbow trout. 1: Iono-regulatory disturbance and metabolic costs. *Aquat Toxicol* **50**, 231-243.

McIntosh, K. B. and Bonham-Smith, P. C. (2005). The two ribosomal protein L23A genes are differentially transcribed in Arabidopsis thaliana. *Genome* **48**, 443-454.

Mckim, J. M. and Benoit, D. A. (1971). Effects of long-term exposure to copper on survival growth, and reproduction of brook trout (*salvelinus fontinalis*). *J Fish Res Board Can* **28**, 655.

Meeker, J. D., Rossano, M. G., Protas, B., Diamond, M. P., Puscheck, E., Daly, D., Paneth, N. and Wirth, J. J. (2009). Multiple metals predict prolactin and thyrotropin (TSH) levels in men. *Environ Res* **109**, 869-873.

Mercer, J. F. (1998). Menkes syndrome and animal models. *Am J Clin Nutr* **67**, 1022S-1028S.

Mercer, J. F., Livingston, J., Hall, B., Paynter, J. A., Begy, C., Chandrasekharappa, S., Lockhart, P., Grimes, A., Bhave, M., Siemieniak, D. and Et, A. (1993). Isolation of a partial candidate gene for Menkes disease by positional cloning. *Nat Genet* **3**, 20-5.

Mercer, J. and Llanos, R. M. (2003). Molecular and cellular aspects of copper transport in developing mammals. *J Nut* **133Suppl. 1**, 1481S-1484S.

Milacic, V., Chen, D., Giovagnini, L., Diez, A., Fregona, D. and Dou, Q. P. (2008). Pyrrolidine dithiocarbamate-zinc(II) and -copper(II) complexes induce apoptosis in tumor cells by inhibiting the proteasomal activity. *Tox Appl Pharm* **231**, 24-33.

Milacic, V., Jiao, P., Zhang, B., Yan, B. and Dou, Q. P. (2009). Novel 8-hydroxylquinoline analogs induce copper-dependent proteasome inhibition and cell death in human breast cancer cells. *Int J Oncol* **35**, 1481-91.

Minghetti, M., Leaver, M. J. and George, S. G. (2010). Multiple Cu-ATPase genes are differentially expressed and transcriptionally regulated by Cu exposure in sea bream, Sparus aurata. *Aquat Toxicol* **97**, 23-33.

Norlen, L., Masich, S., Goldie, K. N. and Hoenger, A. (2007). Structural analysis of vimentin and keratin intermediate filaments by cryo-electron tomography. *Exp Cell Res* **313**, 2217-27.

Nussey, G., Van Vuren, J. H. and Du Preez, H. H. (1995). Effect of copper on blood coagulation of *Oreochromis mossambicus* (Cichlidae). *Comp Biochem Physiol C Pharmacol Toxicol Endocrinol* **111**, 359-67.

Nyberg, K. A., Michelson, R. J., Putnam, C. W. and Weinert, T. A. (2002). Toward maintaining the genome: DNA damage and replication checkpoints. *Annu Rev Genet* **36**, 617-56.

O'Halloran, T. V. and Culotta, V. C. (2000). Metallochaperones, an intracellular shuttle service for metal ions. *J Biol Chem* **275**, 25057-25060.

Orlowski, R. Z. and Dees, E. C. (2003). The role of the ubiquitination-proteasome pathway in breast cancer - Applying drugs that affect the ubiquitin-proteasome pathway to the therapy of breast cancer. *Breast Cancer Res* **5**, 1-7.

Ostrakhovitch, E. A., Olsson, P. E., von Hofsten, J. and Cherian, M. G. (2007). P53 mediated regulation of metalolothionen transcription in breast cancer cells. *J Cell Biochem* **102**, 1571-1583.

Pajonk, F. G., Kessler, H., Supprian, T., Hamzei, P., Bach, D., Schweickhardt, J., Herrmann, W., Obeid, R., Simons, A., Falkai, P., Multhaup, G. and Bayer, T. A. (2005). Cognitive decline correlates with low plasma concentrations of copper in patients with mild to moderate Alzheimer's disease. *J Alzheimers Dis* **8**, 23-7.

Palmiter, R. D. (1998). The elusive function of metallothioneins. *Proc Natl Acad Sci U S A* **95**, 8428-30.

Paris-Palacios, S. and Biagianti-Risbourg, S. (2006). Hepatocyte nuclear structure and subcellular distribution of copper in zebrafish Brachydanio rerio and roach Rutilus rutilus (Teleostei, Cyprinidae) exposed to copper sulphate. *Aquat Toxicol* **77**, 306-313.

Park, J. Y., Mun, J. H., Lee, B. H., Heo, S. H., Kim, G. H. and Yoo, H. W. (2009). Proteomic analysis of sera of asymptomatic, early-stage patients with Wilson's disease. *Proteom Clinic Appl* **3**, 1185-1190.

Pelgrom, S. M., Lamers, L. P., Lock, R. A., Balm, P. H. and Bonga, S. E. (1995). Interactions between copper and cadmium modify metal organ distribution in mature tilapia, Oreochromis mossambicus. *Environ Pollut* **90**, 415-23.

Pelgrom, S., Lock, R., Balm, P. and Bonga, S. (1995). Effects of combined waterborne cd and cu exposures on ionic composition and plasma-cortisol in tilapia, *Oreochromis mossambicus*. *Comp biochem phys c* **111**, 227-235.

Pena, M. M., Lee, J. and Thiele, D. J. (1999). A delicate balance: homeostatic control of copper uptake and distribution. *J Nutr* **129**, 1251-60.

Perney, T. M., Marshall, J, Martin, K. A., Hockfield, S. and Kaczmarek, L. K. (1992). Expression of the messenger-rnas for the kv3.1 potassium channel gene in the adult and developing rat-brain. *J Neurophys* **68**, 756-766.

Petris, M. J. (2004). The SLC31 (Ctr) copper transporter family. *Pflugers Arch* **447**, 752-5.

Petris, M. J., Smith, K., Lee, J. and Thiele, D. J. (2003). Copper-stimulated endocytosis and degradation of the human copper transporter, hCtr1. *J Biol Chem* **278**, 9639-46.

Petris, M. J., Strausak, D. and Mercer, J. (2000). The Menkes copper transporter is required for the activation of tyrosinase. *Hum Mol Genet* **9**, 2845-2851.

Petris, M. J., Voskoboinik, I., Cater, M., Smith, K., Kim, B. E., Llanos, R. M., Strausak, D., Camakaris, J. and Mercer, J. F. (2002). Copper-regulated trafficking of the Menkes disease copper ATPase is associated with formation of a phosphorylated catalytic intermediate. *J Biol Chem* **277**, 46736-42.

Phinney, A. L., Drisaldi, B., Schmidt, S. D., Lugowski, S., Coronado, V., Liang, Y., Horne, P., Yang, J., Sekoulidis, J., Coomaraswamy, J., Chishti, M. A., Cox, D. W., Mathews, P. M., Nixon, R. A., Carlson, G. A., St, G. P. and Westaway, D. (2003). In vivo reduction of amyloid-beta by a mutant copper transporter. *Proc Natl Acad Sci U S A* **100**, 14193-8.

Piano, A., Valbonesi, P. and Fabbri, E. (2004). Expression of cytoprotective proteins, heat shock protein 70 and metallothioneins, in tissues of *Ostrea edulis* exposed to heat and heavy metals. *Cell Stress Chaper* **9**, 134-142.

Pilgaard, L., Malte, H. and Jensen, F. B. (1994). Physiological - effects and tissue accumulation of copper in fresh - water rainbow trout (*Oncorhynchus mykiss*) under normoxic and hypoxic conditions. *Aquat Toxicol* **29**, 197-212.

Pourahmad, M., O'Brien, P. J., Jokar, F. and Daraei, B. (2003). Carcinogenic metal induced sites of reactive oxygen species formation in hepatocytes. *Toxicol In Vitro* **17**, 803-810.

Powell, C. L., Swenberg, J. A. and Rusyn, I. (2005). Expression of base excision DNA repair genes as a biomarker of oxidative DNA damage. *Cancer Lett* **229**, 1-11.

Pribyl, P., Cepak, V. and Zachleder, V. (2008). Cytoskeletal alterations in interphase cells of the green alga Spirogyra decimina in response to heavy metals exposure: II. The effect of aluminium, nickel and copper. *Toxicol In Vitro* **22**, 1160-8.

Pufahl, R. A., Singer, C. P., Peariso, K. L., Lin, S. J., Schmidt, P. J., Fahrni, C. J., Culotta, V. C., Penner-Hahn, J. E. and O'Halloran, T. V. (1997). Metal ion chaperone function of the soluble Cu(I) receptor Atx1. *Science* **278**, 853-6.

Puig, S. and Thiele, D. J. (2002a). Molecular mechanisms of copper uptake and

distribution. *Curr Opin Chem Biol* **6**, 171-80.

Puig, S. and Thiele, D. J. (2002b). Molecular mechanisms of copper uptake and distribution. *Curr. Opin. Chem. Biol* **6**, 171-80.

Puig, S., Lee, J., Lau, M. and Thiele, D. J. (2002). Biochemical and genetic analyses of yeast and human high affinity copper transporters suggest a conserved mechanism for copper uptake. *J Biol Chem* **277**, 26021-30.

Quaife, C. J., Findley, S. D., Erickson, J. C., Froelick, G. J., Kelly, E. J., Zambrowicz, B. P. and Palmiter, R. D. (1994). Induction of a new metallothionein isoform (MT-IV) occurs during differentiation of stratified squamous epithelia. *Biochemistry* **33**, 7250-9.

Quaife, C. J., Kelly, E. J., Masters, B. A., Brinster, R. L. and Palmiter, R. D. (1998). Ectopic expression of metallothionein-III causes pancreatic acinar cell necrosis in transgenic mice. *Toxicol Appl Pharmacol* **148**, 148-57.

Rabilloud, T., Luche, S. and Chevallet, M. (2002). Gel electrophoresis techniques in proteomic analysis. *Biofutur*, 11-19.

Rae, T. D., Schmidt, P. J., Pufahl, R. A., Culotta, V. C. and O'Halloran, T. V. (1999). Undetectable intracellular free copper: the requirement of a copper chaperone for superoxide dismutase. *Science* **284**, 805-8.

Rees, E. M., Lee, J. and Thiele, D. J. (2004). Mobilization of intracellular copper stores by the ctr2 vacuolar copper transporter. *J Biol Chem* **279**, 54221-9.

Richardson, P. E., Manchekar, M., Dashti, N., Jones, M. K., Beigneux, A., Young, S. G., Harvey, S. C. and Segrest, J. P. (2005). Assembly of lipoprotein particles containing apolipoprotein-B: Structural model for the nascent lipoprotein particle. *Biophys J* **88**, 2789-2800.

Riggio, M., Filosa, S., Parisi, E. and Scudiero, R. (2003). Changes in zinc, copper and metallothionein contents during oocyte growth and early development of the teleost *Danio rerio* (zebrafish). *Comp Biochem Phys C* **135**, 191-196.

Rodriguez-Ortega, M. J., Grosvik, B. E., Rodriguez-Ariza, A., Goksoyr, A. and Lopez-Barea, J. (2003a). Changes in protein expression profiles in bivalve molluscs (*Chamaelea gallina*) exposed to four model environmental pollutants. *Proteomics* **3**, 1535-43.

Rodriguez-Ortega, M. J., Grosvik, B. E., Rodriguez-Ariza, A., Goksoyr, A. and Lopez-Barea, J. (2003b). Changes in protein expression profiles in bivalve molluscs (*Chamaelea gallina*) exposed to four model environmental pollutants. *Proteomics* **3**, 1535-1543.

Rutherford, J. C. and Bird, A. J. (2004). Metal-responsive transcription factors that regulate iron, zinc, and copper homeostasis in eukaryotic cells. *Eukaryot Cell* **3**, 1-13.

Sadineni, V., Galeva, N. A. and Schoneich, C. (2006). Characterization of the metal-binding site of human prolactin by site-specific metal-catalyzed oxidation. *Anal Biochem* **358**, 208-215.

Sandrini, J. Z., Bianchini, A., Trindade, G. S., Nery, L. E. and Marins, L. F. (2009). Reactive oxygen species generation and expression of DNA repair-related genes after copper exposure in zebrafish (Danio rerio) ZFL cells. *Aquat Toxicol* **95**, 285-91.

Sappal, R., Burka, J.; Dawson, S. and Kamunde, C. (2009). Bioaccumulation and subcellular partitioning of zinc in rainbow trout (Oncorhynchus mykiss): cross-talk between waterborne and dietary uptake. *Aquat Toxicol* **91**, 281-90.

Schlief, M. L., West, T., Craig, A. M., Holtzman, D. M. and Gitlin, J. D. (2006). Role of the Menkes copper-transporting ATPase in NMDA receptor-mediated neuronal toxicity. *Proc Natl Acad Sci U S A* **103**, 14919-24.

Schneider, M. R., Wolf, E., Hoeflich, A. and Lahm, H. (2002). IGF-binding protein-5: flexible player in the IGF system and effector on its own. *J Endocrinol* **172**, 423-40.

Schumacher, G., Platz, K. P., Mueller, A. R., Neuhaus, R., Luck, W., Langrehr, J. M., Settmacher, U., Steinmueller, T., Becker, M. and Neuhaus, P. (2001). Liver transplantation in neurologic Wilson's disease. *Transplant Proc* **33**, 1518-9.

Schwartz, M. W., Erickson, J. C., Baskin, D. G. and Palmiter, R. D. (1998). Effect of fasting and leptin deficiency on hypothalamic neuropeptide Y gene transcription in vivo revealed by expression of a lacZ reporter gene. *Endocrinology* **139**, 2629-35.

Selvaraj, A., Balamurugan, K., Yepiskoposyan, H., Zhou, H., Egli, D., Georgiev, O., Thiele, D. J. and Schaffner, W. (2005). Metal-responsive transcription factor (MTF-1) handles both extremes, copper load and copper starvation, by activating different genes. *Genes Dev* **19**, 891-6.

Shaw, B. J. and Handy, R. D. (2006). Dietary copper exposure and recovery in Nile tilapia, Oreochromis niloticus. *Aquat Toxicol* **76**, 111-121.

Shen, L. H., Lam, K. L., Ko, P. W. and Chan, K. M. (1998). Metal concentrations and analysis of metal binding protein fractions from the liver of Tilapia collected from Shing Mun River. *Mar Environ Res* **46**, 597-600.

Shepard, J. L., Olsson, B., Tedengren, M. and Bradley, B. P. (2000). Protein expression signatures identified in Mytilus edulis exposed to PCBs, copper and salinity stress. *Mar Environ Res* **50**, 337-340.

Sivaraja, V., Kumar, T., Rajalingam, D., Graziani, I., Prudovsky, I. and Yu, C. (2006). Copper binding affinity of S100A13, a key component of the FGF-1 nonclassical copper-dependent release complex. *Biophys J* **91**, 1832-1843.

Smyth, R., Lane, C. S., Ashiq, R., Turton, J. A., Clarke, C. J., Dare, T. O., York, M. J., Griffiths, W. and Munday, M. R. (2009). Proteomic investigation of urinary markers of carbon-tetrachloride-induced hepatic fibrosis in the Hanover Wistar rat. *Cell Biol*

Tox **25**, 499-512.

Tanzi, R. E., Petrukhin, K., Chernov, I., Pellequer, J. L., Wasco, W., Ross, B., Romano, D. M., Parano, E., Pavone, L., Brzustowicz, L. M. and Et, A. (1993). The Wilson disease gene is a copper transporting ATPase with homology to the Menkes disease gene. *Nat Genet* **5**, 344-50.

Taylor, L. N., McGeer, J. C., Wood, C. M. and McDonald, D. G. (2000). Physiological effects of chronic copper exposure to rainbow trout (*Oncorhynchus mykiss*) in hard and soft water: Evaluation of chronic indicators. *Environ Toxicol Chem* **19**, 2298-2308.

Tchaparian, E. H., Uriu-Adams, J. Y., Keen, C. L., Mitchell, A. E. and Rucker, R. B. (2000). Lysyl oxidase and P-ATPase-7A expression during embryonic development in the rat. *Arch Biochem Biophys* **379**, 71-77.

Thomas, S. A. and Palmiter, R. D. (1998). Examining adrenergic roles in development, physiology, and behavior through targeted disruption of the mouse dopamine beta-hydroxylase gene. *Adv Pharmacol* **42**, 57-60.

Toueille, M., Saint-Jean, B., Castroviejo, M. and Benedetto, J. P. (2007). The elongation factor 1A: A novel regulator in the DNA replication/repair protein network in wheat cells? *Plant Physiol Biochem* **45**, 113-118.

Turner, J. S. and Robinson, N. J. (1995). Cyanobacterial metallothioneins: biochemistry and molecular genetics. *J Ind Microbiol* **14**, 119-25.

Turski, M. L. and Thiele, D. J. (2009). New Roles for Copper Metabolism in Cell Proliferation, Signaling, and Disease. *J Biol Chem* **284**, 717-721.

Uauy, R., Olivares, M. and Gonzalez, M. (1998). Essentiality of copper in humans. *Am J Clin Nutr* **67**, 952S-959S.

Valko, M., Morris, H. and Cronin, M. T. (2005). Metals, toxicity and oxidative stress. *Curr Med Chem* **12**, 1161-208.

Vulpe, C., Levinson, B., Whitney, S., Packman, S. and Gitschier, J. (1993). Isolation of a candidate gene for Menkes disease and evidence that it encodes a copper-transporting ATPase. *Nat Genet* **3**, 7-13.

Wang, H. and Morais, R. (1997). Up-regulation of nuclear genes in response to inhibition of mitochondrial DNA expression in chicken cells. *BBA-Gene Struct Express* **1352**, 325-334.

Welsh, P. G., Lipton, J., Mebane, C. A. and Marr, J. C. (2008). Influence of flow-through and renewal exposures on the toxicity of copper to rainbow trout. *Ecotoxicol Environ Saf* **69**, 199-208.

Wernimont, A. K., Huffman, D. L., Lamb, A. L., O'Halloran, T. V. and Rosenzweig, A. C. (2000). Structural basis for copper transfer by the metallochaperone for the Menkes/Wilson disease proteins. *Nat Struct Biol* **7**, 766-71.

Wong, P., Chu, L. M. and Wong, C. K. (1999). Study of toxicity and bioaccumulation of copper in the silver sea bream Sparus sarba. *Envrion Inter* **25**, 417-422.

Wong, W., Gerry, A. B., Putt, W., Roberts, J. L., Weinberg, R. B., Humphries, S. E., Leake, D. S. and Talmud, P. J. (2007). Common variants of apolipoprotein A-IV differ in their ability to inhibit low density lipoprotein oxidation. *Atherosclerosis* **192**, 266-274.

Wu, S. M., Ho, Y. C. and Shih, M. J. (2007). Effects of Ca2+ or Na+ on metallothionein expression in tilapia larvae (*Oreochromis mossambicus*) exposed to cadmium or copper. *Arch Environ Con Tox* **52**, 229-234.

Wu, S. M., Jong, K. J. and Kuo, S. Y. (2003). Effects of copper sulfate on ion balance and growth in tilapia larvae (*Oreochromis mossambicus*). *Arch Environ Con Tox* **45**, 357-363.

Zappasodi, F., Salustri, C., Babiloni, C., Cassetta, E., Del, P. C., Ercolani, M., Rossini, P. M. and Squitti, R. (2008). An observational study on the influence of the APOE-epsilon4 allele on the correlation between 'free' copper toxicosis and EEG activity in Alzheimer disease. *Brain Res* **1215**, 183-9.

Zheng, L., Roeder, R. G. and Luo, Y. (2003). S phase activation of the histone H2B promoter by OCA-S, a coactivator complex that contains GAPDH as a key component. *Cell* **114**, 255-66.

Zhou, H. Y., Cheung, R., Chan, K. M. and Wong, M. H. (1998). Metal concentrations in sediments and Tilapia collected from inland waters of Hong Kong. *Water Res* **32**, 3331-3340.

APPENDIX

Appendix 1. Standard curves of primers used for real-time PCR to amplify 31 genes in tilapia. Four folds serially diluted cDNAs were used as templates to perform real time PCR detected by SYBR green. GAPDH gene and 18 S gene were used as control genes respectly.

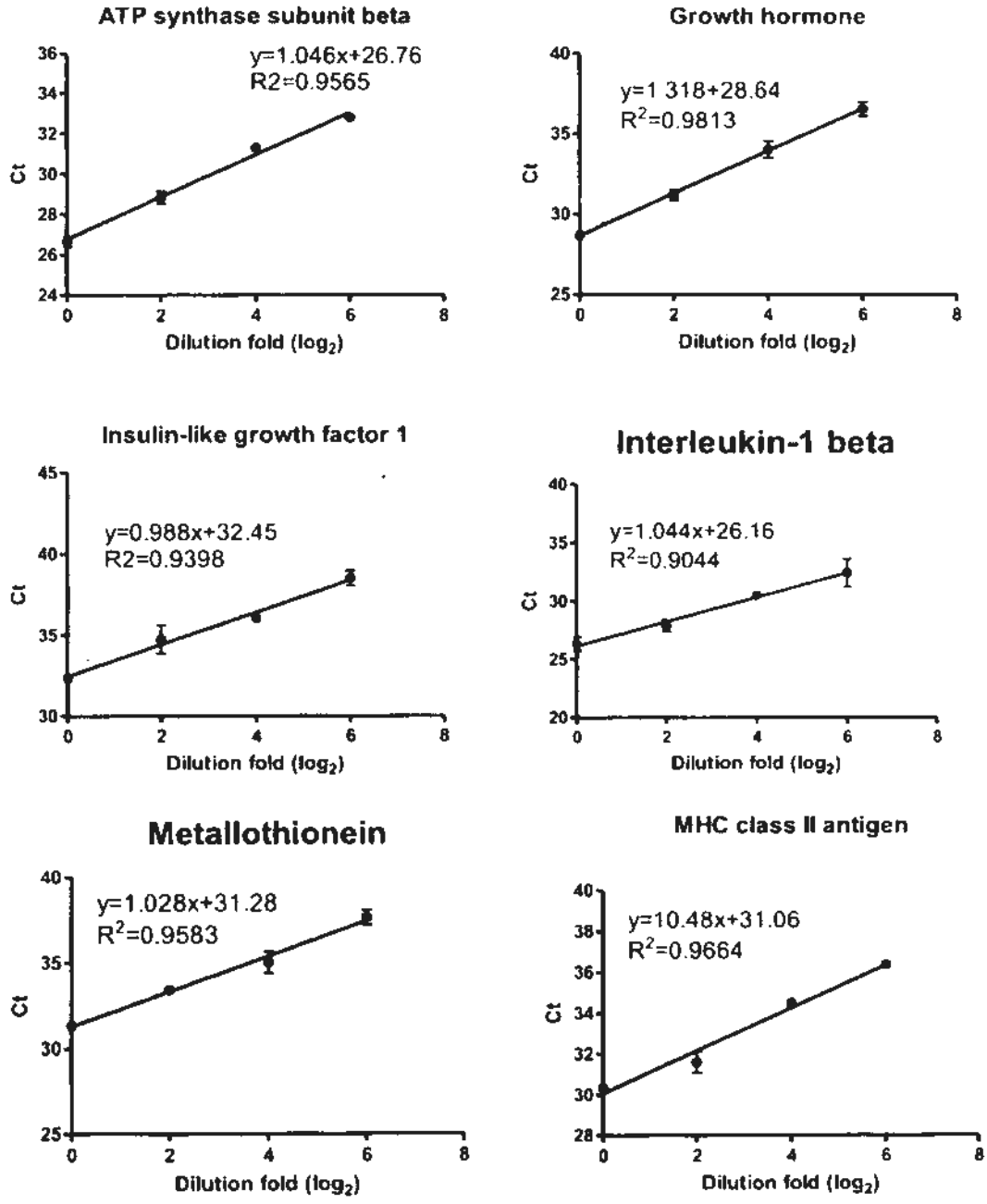

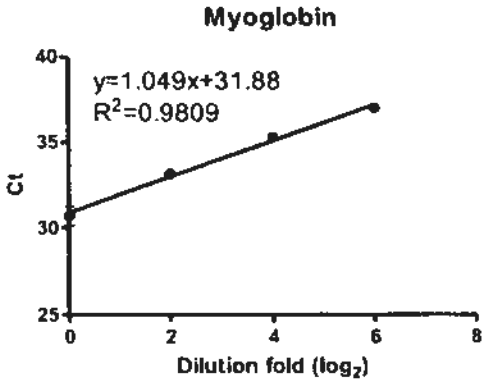
Myoglobin
y=1.049x+31.88
R²=0.9809
Ct
Dilution fold (log₂)

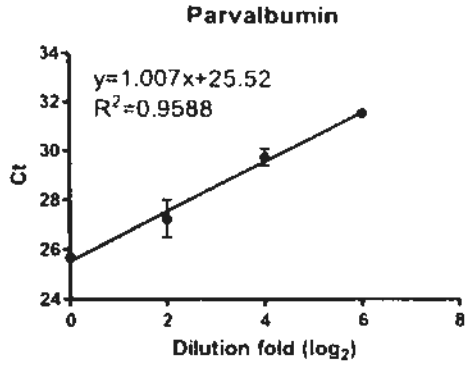
Parvalbumin
y=1.007x+25.52
R²=0.9588
Ct
Dilution fold (log₂)

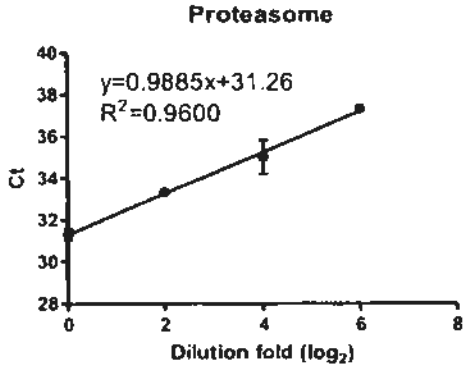
Proteasome
y=0.9885x+31.26
R²=0.9600
Ct
Dilution fold (log₂)

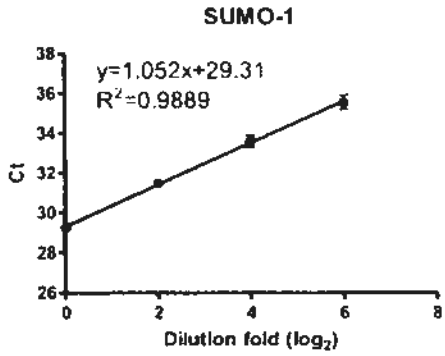
SUMO-1
y=1.052x+29.31
R²=0.9889
Ct
Dilution fold (log₂)

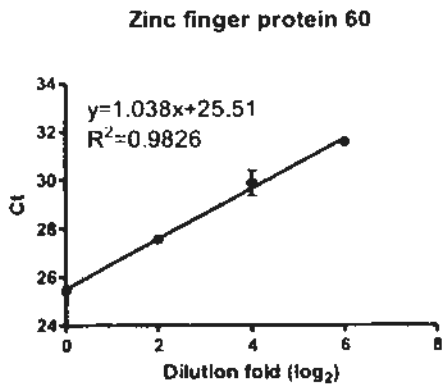
Zinc finger protein 60
y=1.038x+25.51
R²=0.9826
Ct
Dilution fold (log₂)

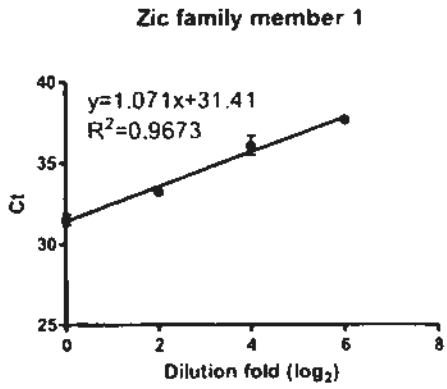
Zic family member 1
y=1.071x+31.41
R²=0.9673
Ct
Dilution fold (log₂)

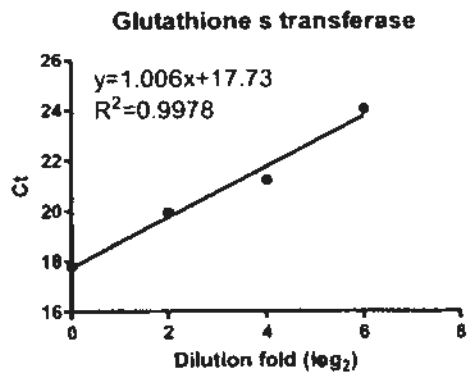
Glutathione s transferase
y=1.006x+17.73
R²=0.9978
Ct
Dilution fold (log₂)

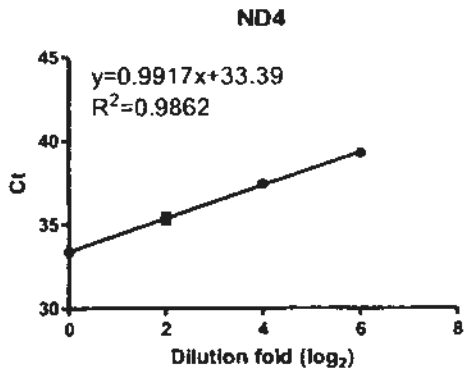
ND4
y=0.9917x+33.39
R²=0.9862
Ct
Dilution fold (log₂)

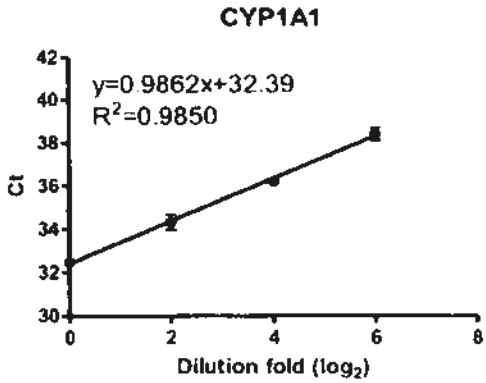
CYP1A1
y=0.9862x+32.39
R²=0.9850
Ct
Dilution fold (log₂)

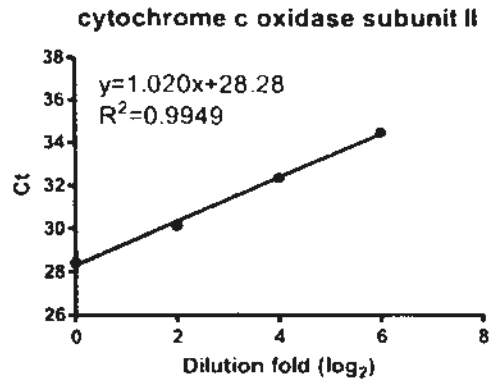
cytochrome c oxidase subunit II
y=1.020x+28.28
R²=0.9949
Ct
Dilution fold (log₂)

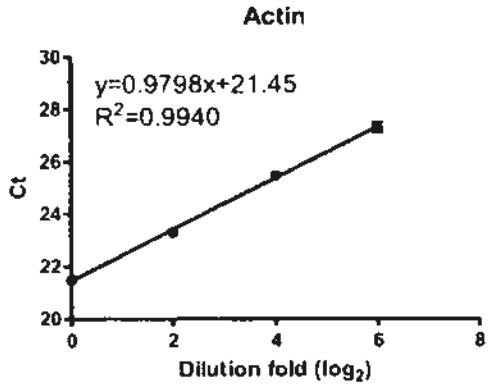
Actin
y=0.9798x+21.45
R²=0.9940
Ct
Dilution fold (log₂)

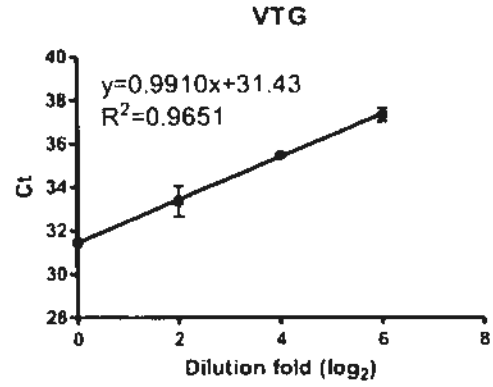
VTG
y=0.9910x+31.43
R²=0.9651
Ct
Dilution fold (log₂)

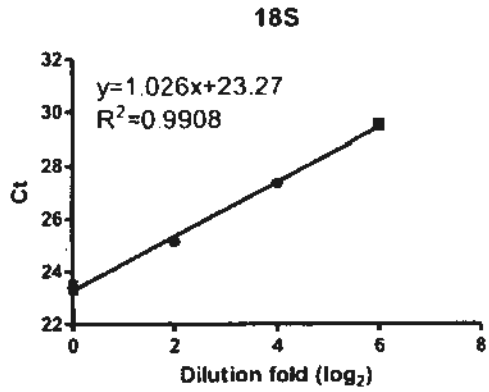
18S
y=1.026x+23.27
R²=0.9908
Ct
Dilution fold (log₂)

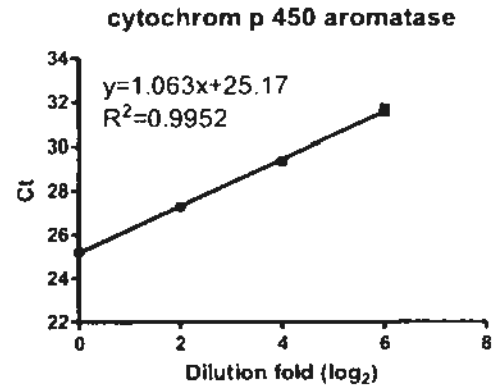
cytochrom p 450 aromatase
y=1.063x+25.17
R²=0.9952
Ct
Dilution fold (log₂)

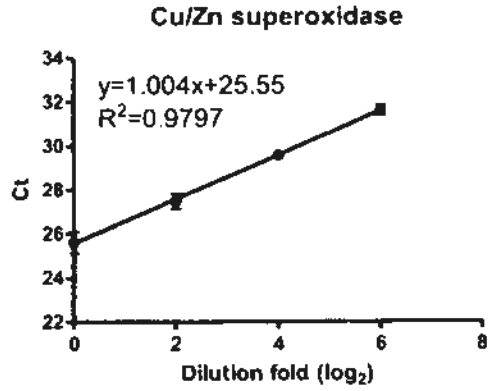
Cu/Zn superoxidase
y=1.004x+25.55
R²=0.9797
Ct
Dilution fold (log₂)

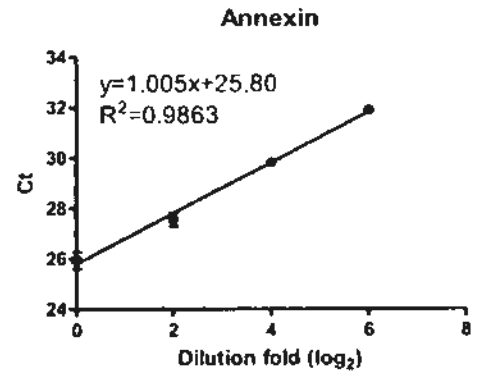
Annexin
y=1.005x+25.80
R²=0.9863
Ct
Dilution fold (log₂)

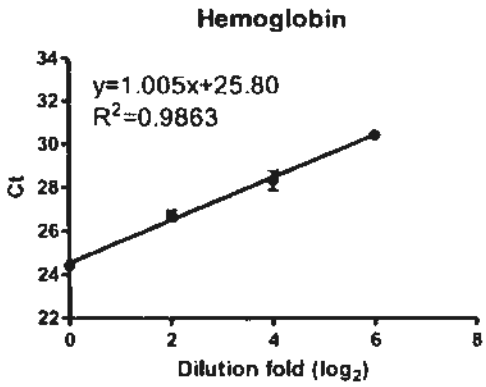
Hemoglobin
y=1.005x+25.80
R²=0.9863
Ct
Dilution fold (log₂)

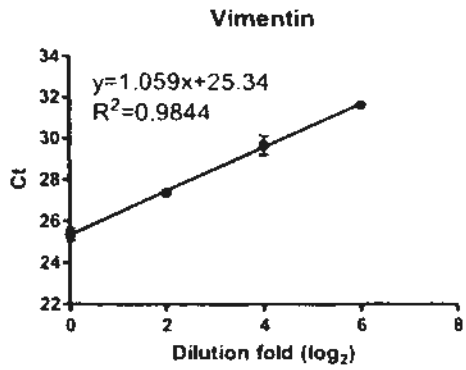
Vimentin
y=1.059x+25.34
R²=0.9844
Ct
Dilution fold (log₂)

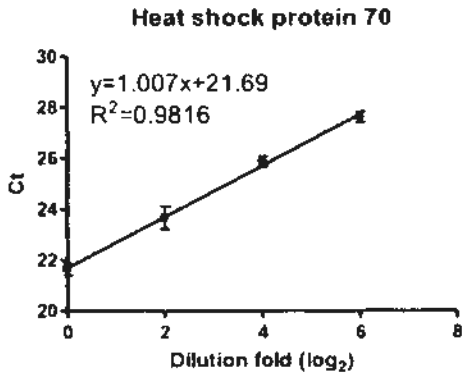
Heat shock protein 70
y=1.007x+21.69
R²=0.9816
Ct
Dilution fold (log₂)

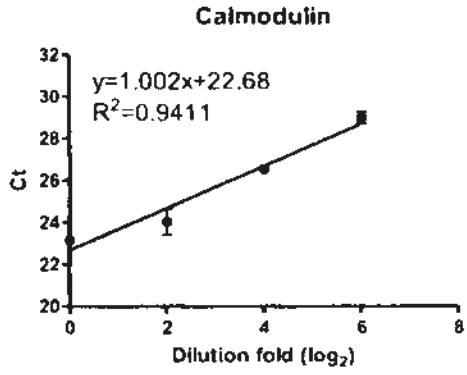
Calmodulin
y=1.002x+22.68
R²=0.9411
Ct
Dilution fold (log₂)

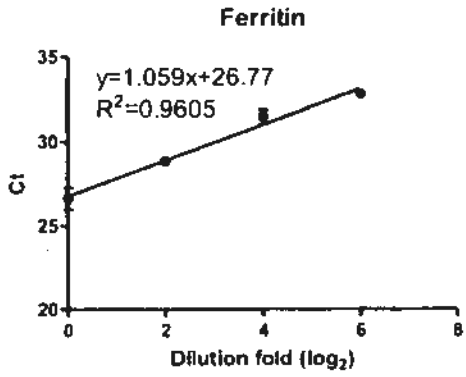
Ferritin
y=1.059x+26.77
R²=0.9605
Ct
Dilution fold (log₂)

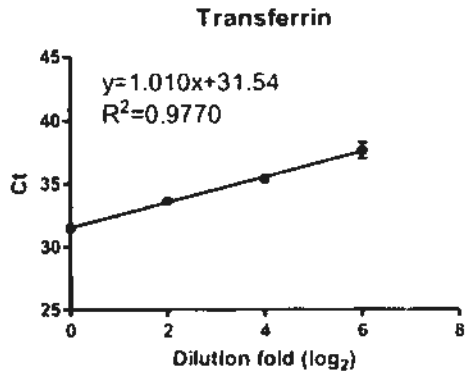
Transferrin
y=1.010x+31.54
R²=0.9770
Ct
Dilution fold (log₂)

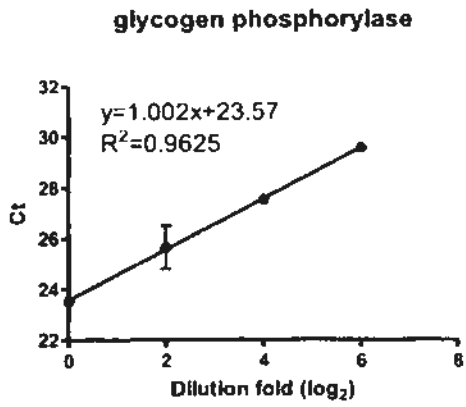
glycogen phosphorylase
y=1.002x+23.57
R²=0.9625
Ct
Dilution fold (log₂)

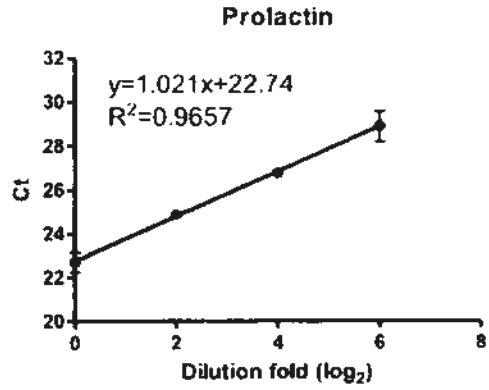
Prolactin
y=1.021x+22.74
R²=0.9657
Ct
Dilution fold (log₂)

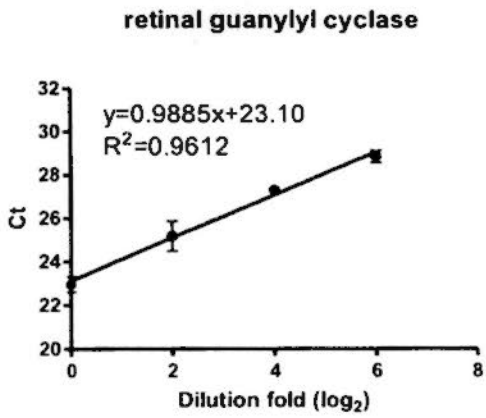
retinal guanylyl cyclase
y=0.9885x+23.10
R²=0.9612
Ct
Dilution fold (log₂)

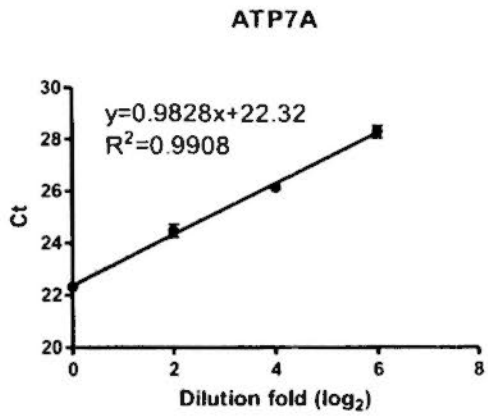
ATP7A
y=0.9828x+22.32
R²=0.9908
Ct
Dilution fold (log₂)

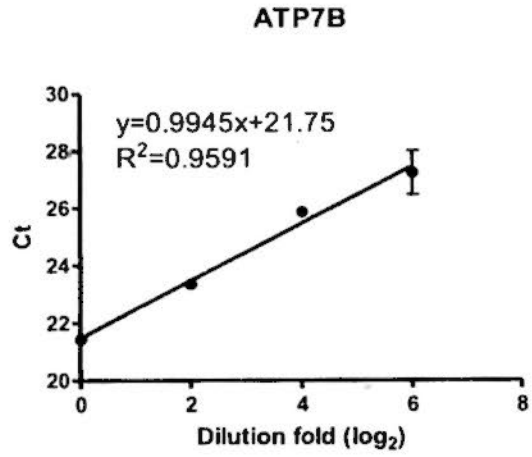
ATP7B
y=0.9945x+21.75
R²=0.9591
Ct
Dilution fold (log₂)

Appendix 2. Relative efficiency plots of primers used for real-time PCR to amplify 31 genes in tilapia. Four folds serially diluted cDNAs were used as templates to perform real time PCR detected by SYBR green. GAPDH gene and 18 S gene were used as control genes respectively.

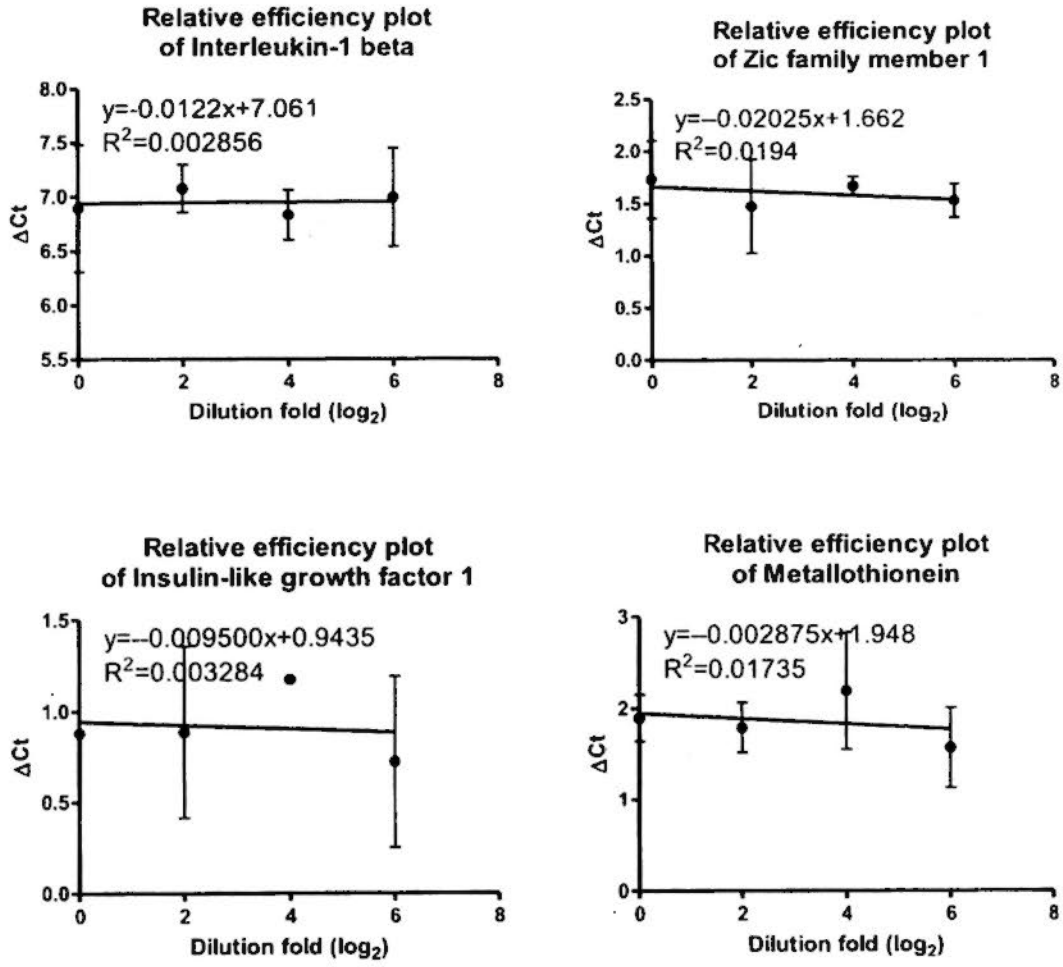

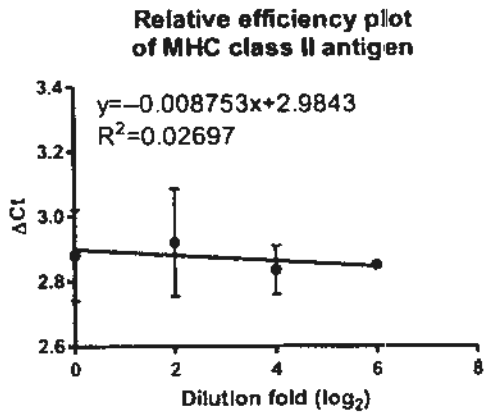
Relative efficiency plot
of MHC class II antigen
y=–0.008753x+2.9843
R2=0.02697
ΔCt
Dilution fold (log2)

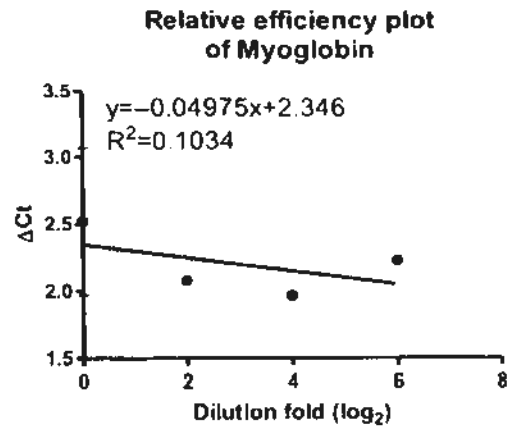
Relative efficiency plot
of Myoglobin
y=–0.04975x+2.346
R2=0.1034
ΔCt
Dilution fold (log2)

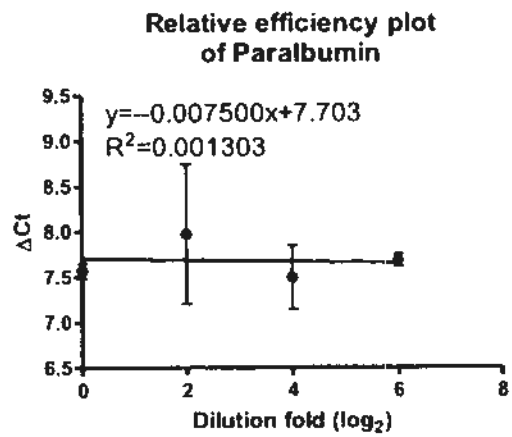
Relative efficiency plot
of Paralbumin
y=–0.007500x+7.703
R2=0.001303
ΔCt
Dilution fold (log2)

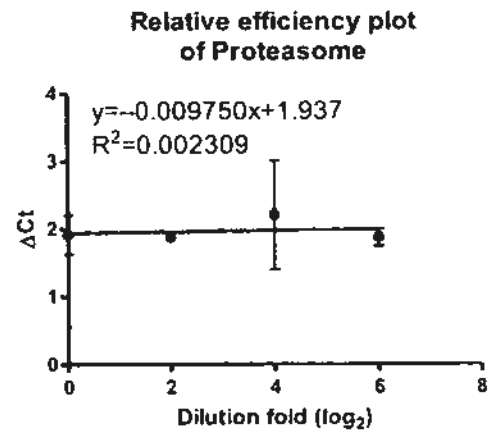
Relative efficiency plot
of Proteasome
y=–0.009750x+1.937
R2=0.002309
ΔCt
Dilution fold (log2)

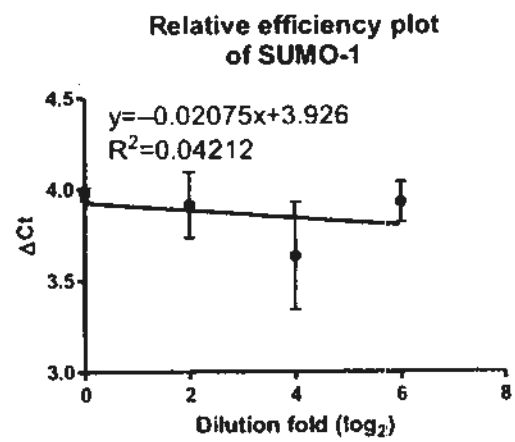
Relative efficiency plot
of SUMO-1
y=–0.02075x+3.926
R2=0.04212
ΔCt
Dilution fold (log2)

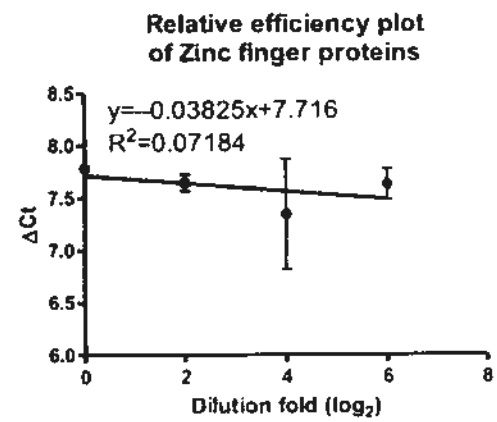
Relative efficiency plot
of Zinc finger proteins
y=–0.03825x+7.716
R2=0.07184
ΔCt
Dilution fold (log2)

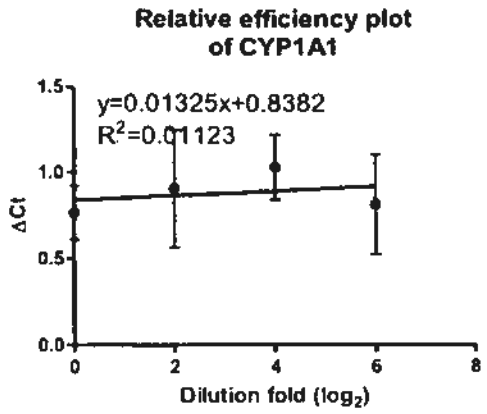
Relative efficiency plot
of CYP1A1
y=0.01325x+0.8382
R²=0.01123
ΔCt
Dilution fold (log₂)

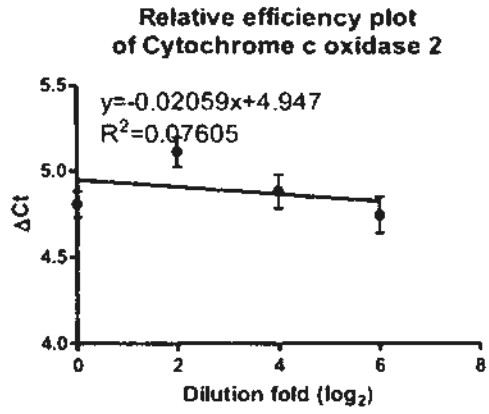
Relative efficiency plot
of Cytochrome c oxidase 2
y=-0.02059x+4.947
R²=0.07605
ΔCt
Dilution fold (log₂)

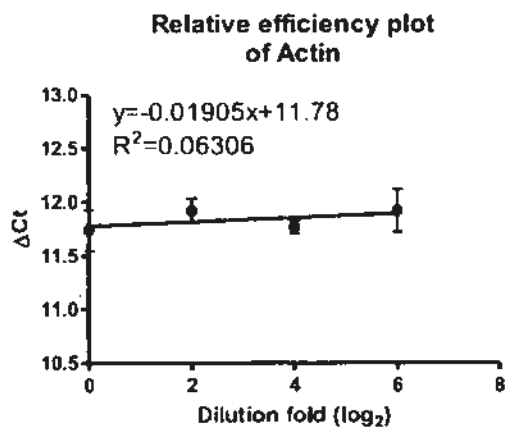
Relative efficiency plot
of Actin
y=-0.01905x+11.78
R²=0.06306
ΔCt
Dilution fold (log₂)

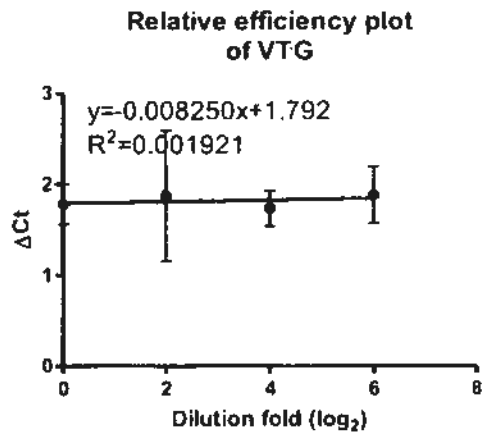
Relative efficiency plot
of VTG
y=-0.008250x+1.792
R²=0.001921
ΔCt
Dilution fold (log₂)

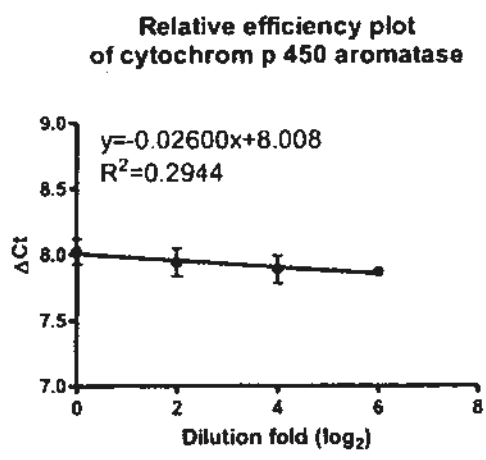
Relative efficiency plot
of cytochrom p 450 aromatase
y=-0.02600x+8.008
R²=0.2944
ΔCt
Dilution fold (log₂)

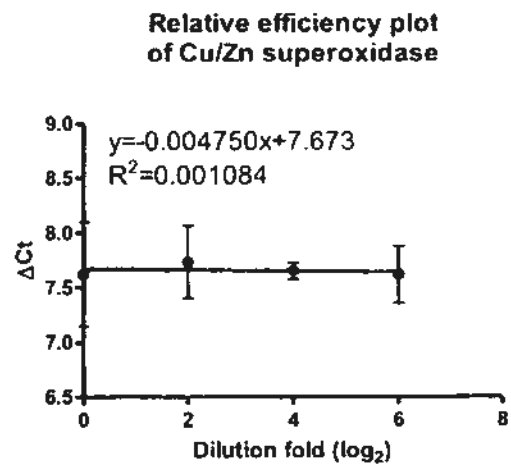
Relative efficiency plot
of Cu/Zn superoxidase
y=-0.004750x+7.673
R²=0.001084
ΔCt
Dilution fold (log₂)

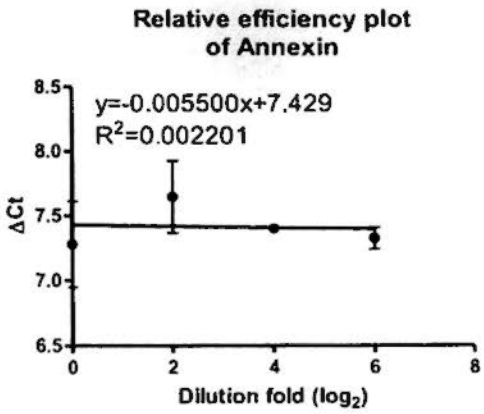
Relative efficiency plot
of Annexin
y=-0.005500x+7.429
R2=0.002201
ΔCt
8.5
8.0
7.5
7.0
6.5
0
2
4
6
8
Dilution fold (log2)

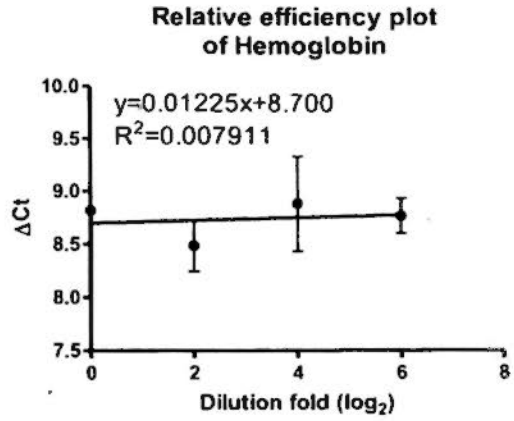
Relative efficiency plot
of Hemoglobin
y=0.01225x+8.700
R2=0.007911
ΔCt
10.0
9.5
9.0
8.5
8.0
7.5
0
2
4
6
8
Dilution fold (log2)

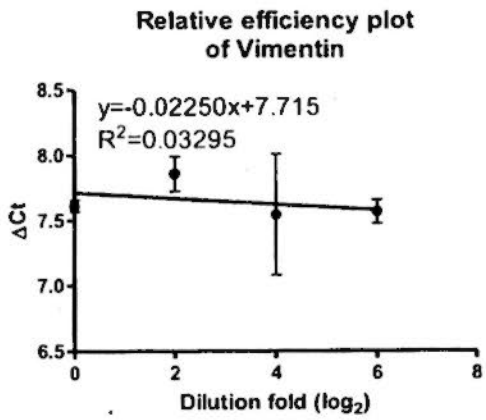
Relative efficiency plot
of Vimentin
y=-0.02250x+7.715
R2=0.03295
ΔCt
8.5
8.0
7.5
7.0
6.5
0
2
4
6
8
Dilution fold (log2)

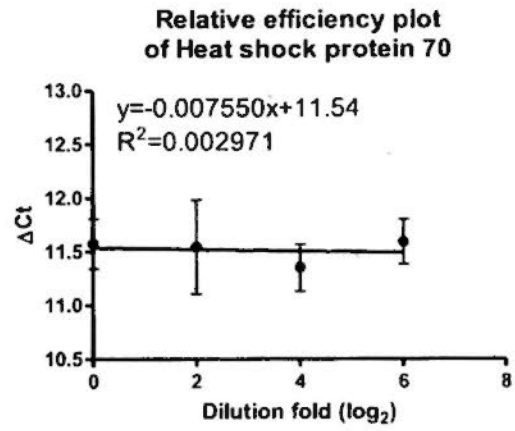
Relative efficiency plot
of Heat shock protein 70
y=-0.007550x+11.54
R2=0.002971
ΔCt
13.0
12.5
12.0
11.5
11.0
10.5
0
2
4
6
8
Dilution fold (log2)

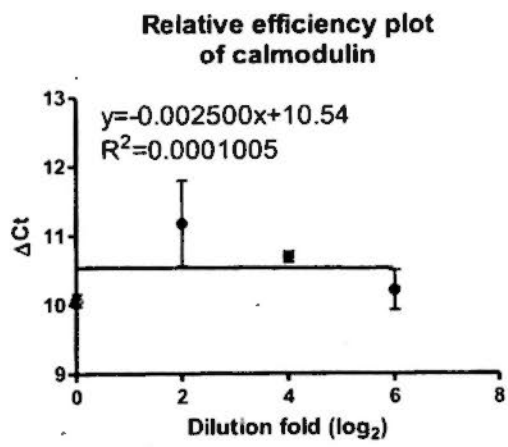
Relative efficiency plot
of calmodulin
y=-0.002500x+10.54
R2=0.0001005
ΔCt
13
12
11
10
9
0
2
4
6
8
Dilution fold (log2)

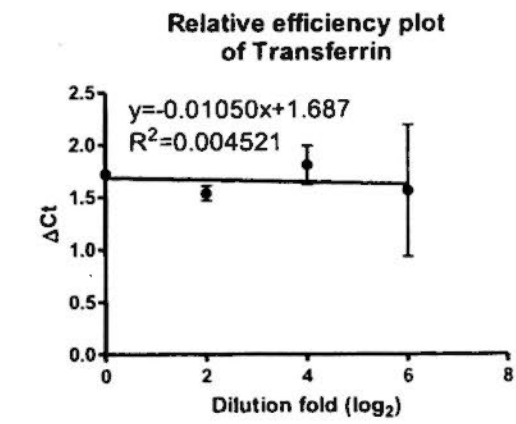
Relative efficiency plot
of Transferrin
y=-0.01050x+1.687
R2=0.004521
ΔCt
2.5
2.0
1.5
1.0
0.5
0.0
0
2
4
6
8
Dilution fold (log2)

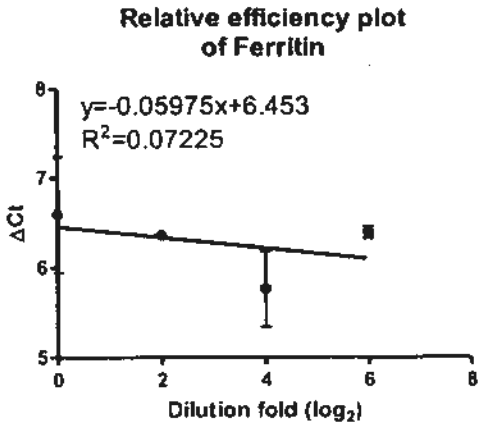
Relative efficiency plot
of Ferritin
y=-0.05975x+6.453
R²=0.07225
ΔCt
Dilution fold (log₂)

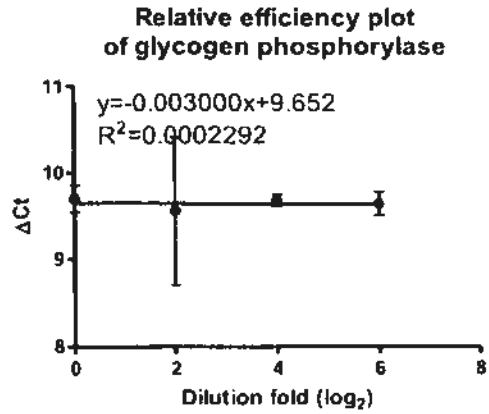
Relative efficiency plot
of glycogen phosphorylase
y=-0.003000x+9.652
R²=0.0002292
ΔCt
Dilution fold (log₂)

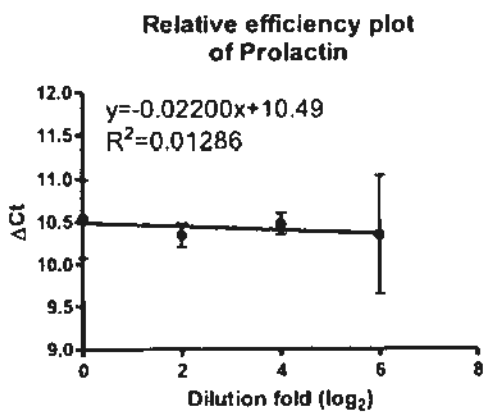
Relative efficiency plot
of Prolactin
y=-0.02200x+10.49
R²=0.01286
ΔCt
Dilution fold (log₂)

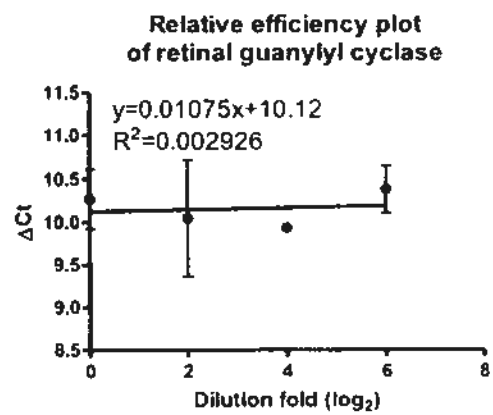
Relative efficiency plot
of retinal guanylyl cyclase
y=0.01075x+10.12
R²=0.002926
ΔCt
Dilution fold (log₂)

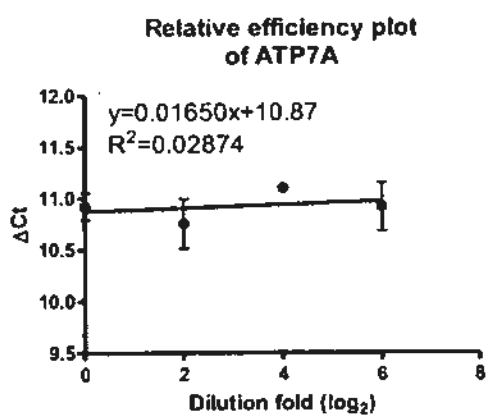
Relative efficiency plot
of ATP7A
y=0.01650x+10.87
R²=0.02874
ΔCt
Dilution fold (log₂)

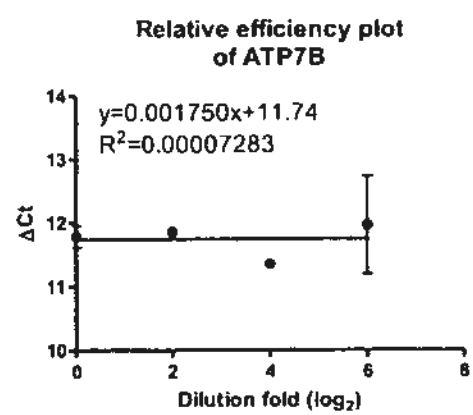
Relative efficiency plot
of ATP7B
y=0.001750x+11.74
R²=0.00007283
ΔCt
Dilution fold (log₂)

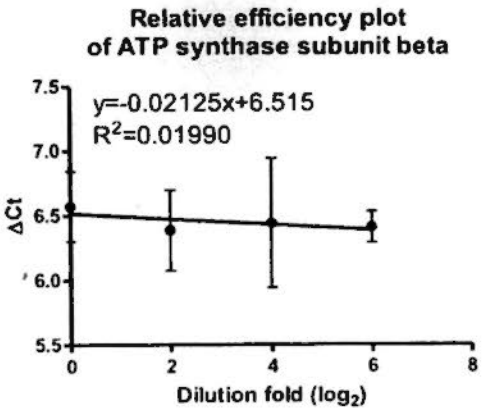
Relative efficiency plot
of ATP synthase subunit beta
y=-0.02125x+6.515
R2=0.01990
ΔCt
7.5
7.0
6.5
6.0
5.5
0
2
4
6
8
Dilution fold (log2)

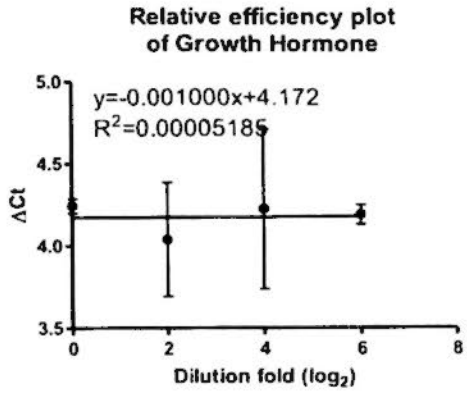
Relative efficiency plot
of Growth Hormone
y=-0.001000x+4.172
R2=0.00005185
ΔCt
5.0
4.5
4.0
3.5
0
2
4
6
8
Dilution fold (log2)

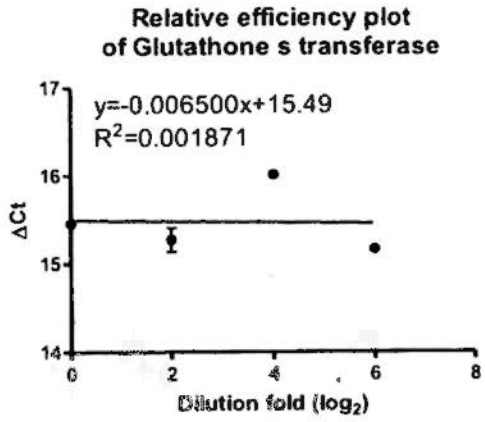
Relative efficiency plot
of Glutathone s transferase
y=-0.006500x+15.49
R2=0.001871
ΔCt
17
16
15
14
0
2
4
6
8
Dilution fold (log2)

Appendix 3. Standard curves of primers used for real-time PCR to amplify 31 genes in Zebrafish. Four folds serially diluted cDNAs were used as templates to perform real time PCR detected by SYBR green. GAPDH gene was used as a control gene.

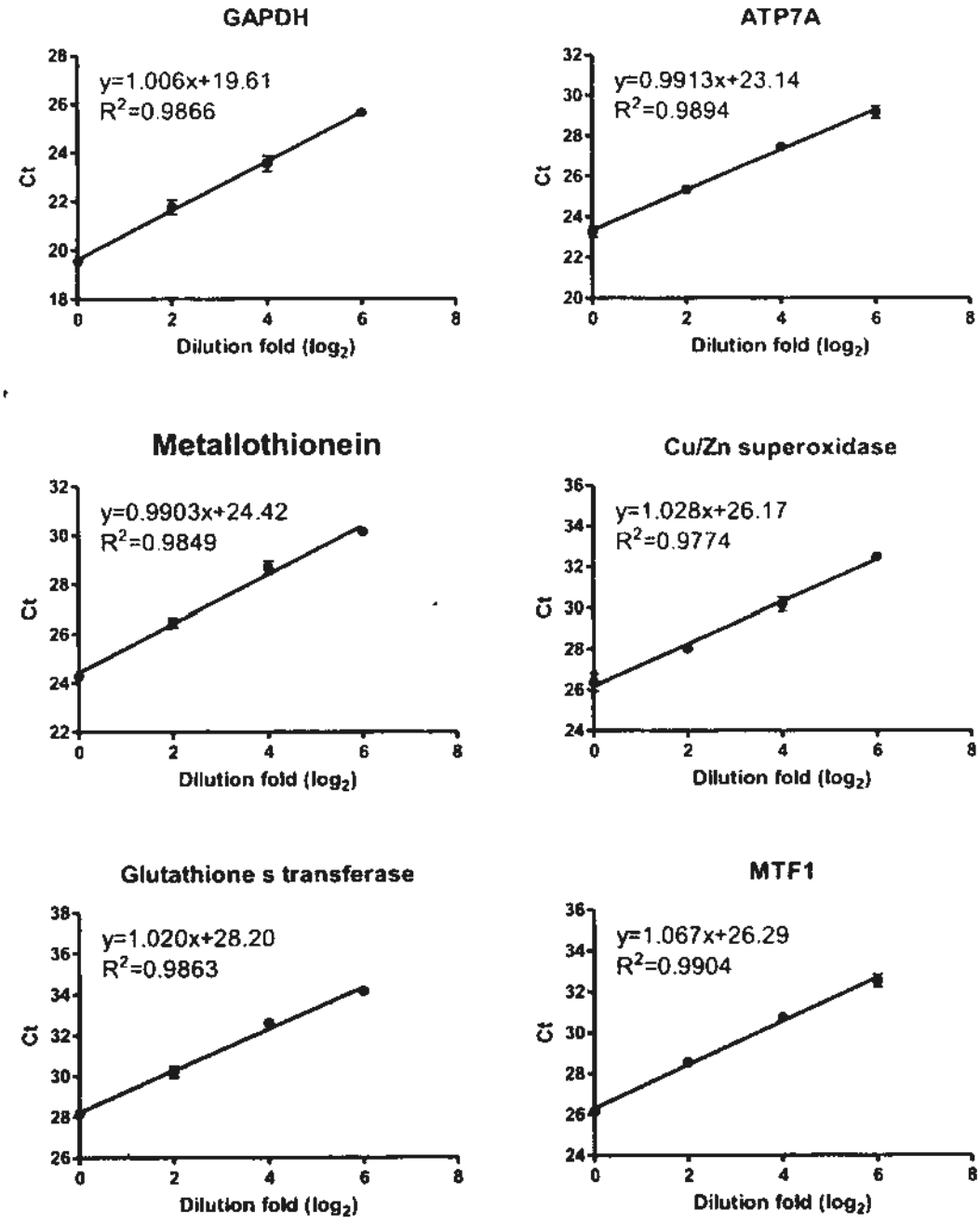

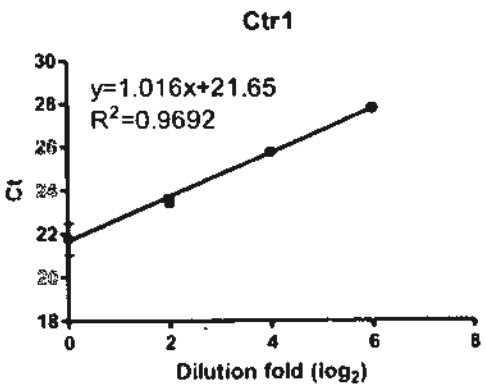
Ctr1
y=1.016x+21.65
R²=0.9692
Ct
30
28
26
24
22
20
18
0
2
4
6
8
Dilution fold (log2)

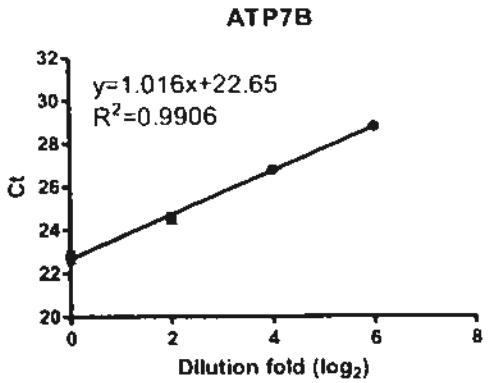
ATP7B
y=1.016x+22.65
R²=0.9906
Ct
32
30
28
26
24
22
20
0
2
4
6
8
Dilution fold (log2)

Appendix 4. Relative efficiency plots of primers used for real-time PCR to amplify 31 genes in tilapia. Four folds serially diluted cDNAs were used as templates to perform real time PCR detected by SYBR green. GAPDH gene was used as a control gene.

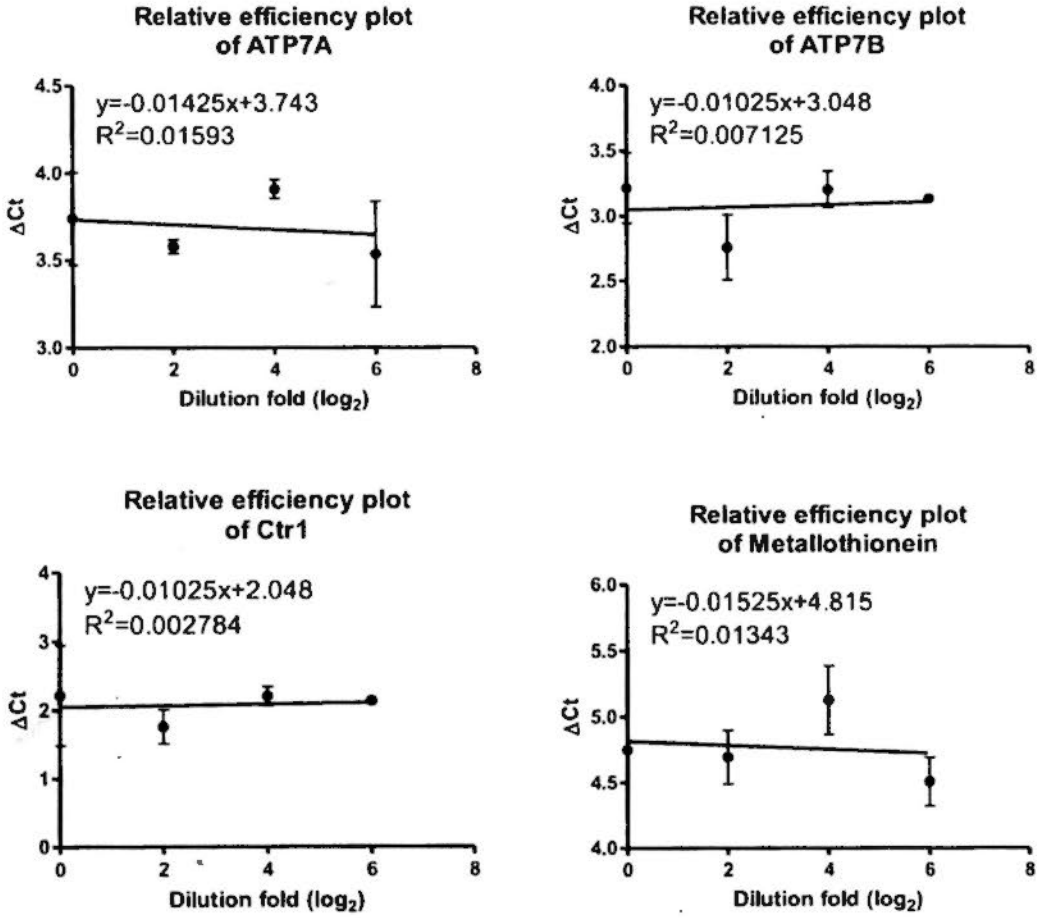

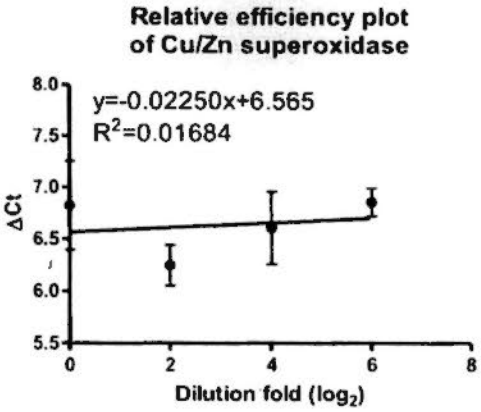
Relative efficiency plot
of Cu/Zn superoxidase
y=-0.02250x+6.565
R2=0.01684
ΔCt
8.0
7.5
7.0
6.5
6.0
5.5
0
2
4
6
8
Dilution fold (log2)

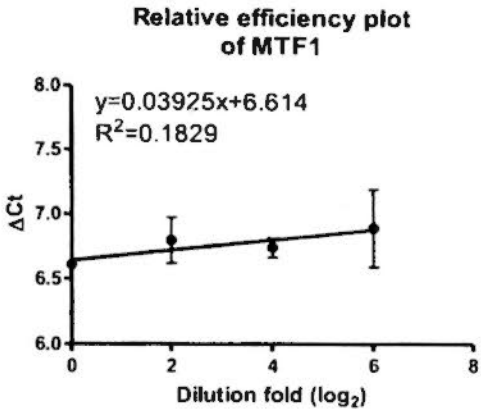
Relative efficiency plot
of MTF1
y=0.03925x+6.614
R2=0.1829
ΔCt
8.0
7.5
7.0
6.5
6.0
0
2
4
6
8
Dilution fold (log2)

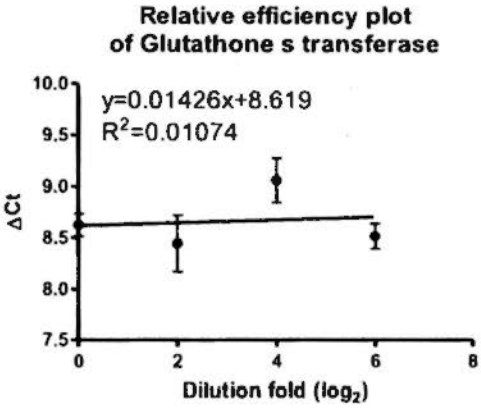
Relative efficiency plot
of Glutathone s transferase
y=0.01426x+8.619
R2=0.01074
ΔCt
10.0
9.5
9.0
8.5
8.0
7.5
0
2
4
6
8
Dilution fold (log2)

Appendix 5. Whole cDNA sequence of tilapia's ATP7A including deduced protein sequence. The primers used in this experiment were showed with arrows.

```
1                                                GAAAAGCATGAGGGGACACAACAAAATT

30    GGTCCACATAGCAGAGTTCTGTGATGACAGAGGAAGAAAACCCTCAATCCAGCACTAGCG

90    ATTATTTCTAGCAGTCCTTGCGATGCAGCGACGTGTCCGCTTTGTTGACTGTAACGTAGG

150   ATGAAGAGTAGATACCTGCTAGTTAGCTTGCTAGCTAAACTTAGCCAAGTCTGACAGTCG

210   GGGTACTAGCCTGTGGCTAACAGTTTGCTTCACGCTGTGAACTGAGACGGAAACGCAGTC
                                                T-7A 3' F1
270   ATGACACAGAAACGCAGCCTGTGTTCAGTTTCTCTTGGAGTGGAGGGTATGACCTGCGGC
1     METThrGlnLysArgSerLeuCysSerValSerLeuGlyValGluGlyMETThrCysGly

330   TCTTGTGTCCAGTCTATAGAGCAGCGCATTGGGTCTCTTCCTGGAGTGATGTATATAAAG
21    SerCysValGlnSerIleGluGlnArgIleGlySerLeuProGlyValMETTyrIleLys

390   GTGTCTTTAGAGGGCAAGAATGCAACTGTCCTATTTGACCCCAGCCATCAGAGCCCAGAG
41    ValSerLeuGluGlyLysAsnAlaThrValLeuPheAspProSerHisGlnSerProGlu

450   TCTCTGTCAGAGGCCATTGAGGACATGGGCTTTGAATCAAGTCTGCCAGCTTCCAGCAAA
61    SerLeuSerGluAlaIleGluAspMETGlyPheGluSerSerLeuProAlaSerSerLys
                                                T-7A 3' F2
510   GCCACACCAGTCCCTACTGATACCCAGGTGGTCTCCACCTCAGGCATGACACCCACAGCC
81    AlaThrProValProThrAspThrGlnValValSerThrSerGlyMETThrProThrAla

570   CAACAGGAAGCATTGAAGAAACTATCACAAATTCAGGGAGTGCTGGATGTCAGAGAGAAC
101   GlnGlnGluAlaLeuLysLysLeuSerGlnIleGlnGlyValLeuAspValArgGluAsn

630   CTGCCACAGACAGGCCTCACCGTCACCTTTGTCCCCTCCCTAACGTCCACGCAGCAGCTT
121   LeuProGlnThrGlyLeuThrValThrPheValProSerLeuThrSerThrGlnGlnLeu
                                    T-7A 5' R2
690   AGTGAGGCGGTGGCCAGCGTAACACCGCCGGAGATCCCCACACCGAGCAGCCCTTTGCAA
141   SerGluAlaValAlaSerValThrProProGluIleProThrProSerSerProLeuGln

750   AAAGACCCCACCTCCTCTCCATCTCAGACCACACGAGGCGGAGCGGCCATCCTTAAGCTG
161   LysAspProThrSerSerProSerGlnThrThrArgGlyGlyAlaAlaIleLeuLysLeu

810   CGCATTGAAGGAATGACCTGTCACTCCTGTACTACCACTATTGAAGGAAAGATTAGTAAA
181   ArgIleGluGlyMETThrCysHisSerCysThrThrThrIleGluGlyLysIleSerLys
                                                T-7A 5' R1
870   CTGAAAGGGATTGAAAAGATCAAAGTTGTTTTAGAGTCTCAGGAAGCTACACTCGTCTAC
201   LeuLysGlyIleGluLysIleLysValValLeuGluSerGlnGluAlaThrLeuValTyr

930   CTGCCTTACCTCCTCACTGTCCAAACCATCATTGATCAAATTGCTGTGGTTGGATTCAAG
221   LeuProTyrLeuLeuThrValGlnThrIleIleAspGlnIleAlaValValGlyPheLys

990   GCCTTTGTGAAGTCTAAGCCCCGCCCCCTGCAGCTGTCCCCCAGTGAAATAGAGCGCTTT
241   AlaPheValLysSerLysProArgProLeuGlnLeuSerProSerGluIleGluArgPhe
                T-7A 3' F3
1050  GTTGATTCTCAAAAACAAACCGTTTCGTCGCCATCTGAGACTTCAGAGGAGACTGAAATC
261   ValAspSerGlnLysGlnThrValSerSerProSerGluThrSerGluGluThrGluIle
```

1110 TTCATAGACACCACACTCATCGCGCTTAGGGTCAAAGGCACGCACTGCCGTTCCTGTGTG
281 PheIleAspThrThrLeuIleAlaLeuArgValLysGlyThrHisCysArgSerCysVal

1170 GTCAACATTCAGGACAATATCTCAGTGCTGCCTGGTGTGTCTTCTGTGGAGGTGTCTTTG
301 ValAsnIleGlnAspAsnIleSerValLeuProGlyValSerSerValGluValSerLeu

1230 GAGAACGAGAAGGCCTCCATCTGTTATGACCCCCAAAAGGTCACAGTGACTCAGCTGCAG
321 GluAsnGluLysAlaSerIleCysTyrAspProGlnLysValThrValThrGlnLeuGln

1290 CAGGCAATTGAAGCACTGCCTCCAGGAAACTTTAAGACTCAACCGTGGGACGACTCGGGT
341 GlnAlaIleGluAlaLeuProProGlyAsnPheLysThrGlnProTrpAspAspSerGly

1350 GCCCTCAGTCCTGTGTCCACATCATCATCATCATGGCCTAGAGGAGCAAACCAGGCCAAA
361 AlaLeuSerProValSerThrSerSerSerSerTrpProArgGlyAlaAsnGlnAlaLys

1410 CCTGCTGTCTTGCAGCCTTGTTTTAATCAGCCACTGGGATCTGTAGTGAATATCCACATT
381 ProAlaValLeuGlnProCysPheAsnGlnProLeuGlySerValValAsnIleHisIle

1470 GAGGGAATGACATGCAACTCCTGTGTTCAGTCCATTGAAGGCATGATCTCCCAAAAGAAA
401 GluGlyMETThrCysAsnSerCysValGlnSerIleGluGlyMETIleSerGlnLysLys

1530 GGAGTCGTGTCAGCCCAGGTGTCTCTGACTGATCACCAGGGGATCTTTGAGTATGACTCT
421 GlyValValSerAlaGlnValSerLeuThrAspHisGlnGlyIlePheGluTyrAspSer

1590 CTGCTGACCACACCAGAGGAGTTGAGGGAGGCCATAGAGGACATGGGCTTCGATGCCTTT
441 LeuLeuThrThrProGluGluLeuArgGluAlaIleGluAspMETGlyPheAspAlaPhe

1650 CTGCCTGAGACCAACTCTCTGCTGCCTTCACCACATCCTCTTTCATCAAAGTCTTCAGGT
461 LeuProGluThrAsnSerLeuLeuProSerProHisProLeuSerSerLysSerSerGly

1710 ATAGCGCCTGTCAAAGGTAAGGAGGTGGACAGTGACCACCATAAAGAAACCCCCCAGGGA
481 IleAlaProValLysGlyLysGluValAspSerAspHisHisLysGluThrProGlnGly

1770 CGGAGTGGAGACACAAACTCTAAATGCTACATCCAGATCGGCGGGATGACCTGTGCTTCC
501 ArgSerGlyAspThrAsnSerLysCysTyrIleGlnIleGlyGlyMETThrCysAlaSer

1830 TGTGTGTCAAACATCGAGCGAAATCTCAAGAATGAACCTGGTATCTACTCTGTTCTGGTG
521 CysValSerAsnIleGluArgAsnLeuLysAsnGluProGlyIleTyrSerValLeuVal

1890 GCGCTAATGGCGAGTAAAGCAGAGGTCCGTTATAACCCTGAAGTCACCGATCCTATGAAG
541 AlaLeuMETAlaSerLysAlaGluValArgTyrAsnProGluValThrAspProMETLys

1950 ATAGCCGAGTGCGTGAAGGAGCTGGGCTTTACCGCCTCTGTTATGGAGAACTATGAAGGT
561 IleAlaGluCysValLysGluLeuGlyPheThrAlaSerValMETGluAsnTyrGluGly

2010 TCAGATGGAACTGTTGAATTAGTGGTCAGGGGAATGACGTGTGCTTCTTGTGTTCACAAA
581 SerAspGlyThrValGluLeuValValArgGlyMETThrCysAlaSerCysValHisLys

2070 ATTGAATCCAACCTCATGAAAGAAAAGGGGATTATCTATGCCTCTGTTGCCTTGGCAACC
601 IleGluSerAsnLeuMETLysGluLysGlyIleIleTyrAlaSerValAlaLeuAlaThr

2130 AACAAAGCACACATTAAATTTGACTCTGAAGTTATTGGACCACGAGACATCATCAAGCTG
621 AsnLysAlaHisIleLysPheAspSerGluValIleGlyProArgAspIleIleLysLeu

2190 ATTGAGAATCTAGGATTTGAAGCATCTTTGGTAAAGAGGGGCCGCACTGCCAGCCACCTG
641 IleGluAsnLeuGlyPheGluAlaSerLeuValLysArgGlyArgThrAlaSerHisLeu

2250 GACCACAGCAAAGAGATACGACAGTGGAGGAAGTCTTTCCTTGTGAGCTTGGTTTTCTGT
661 AspHisSerLysGluIleArgGlnTrpArgLysSerPheLeuValSerLeuValPheCys

2310 GCGCCTGTGATGGGCATGATGACCTACATGATTATTATGGACCACCAGATGACAGTTTCA
681 AlaProValMETGlyMETMETThrTyrMETIleIleMETAspHisGlnMETThrValSer

2370 CATCATCACAACAATACGGCAGAGGACCGCAACCACTACCACTCCACCATGTTTCTGGAG
701 HisHisHisAsnAsnThrAlaGluAspArgAsnHisTyrHisSerThrMETPheLeuGlu

2430 AGACAGCTGCTCCCAGGCCTCTCCATCATGAACCTCCTCTCCTTCCTGTTTTGTGTGCCA
721 ArgGlnLeuLeuProGlyLeuSerIleMETAsnLeuLeuSerPheLeuPheCysValPro

2490 GTACAGTTCATTGGAGGTCCCTACTTCTACATTCAAGCCTGGAAAGCCTTGAAACACAAG
741 ValGlnPheIleGlyGlyArgTyrPheTyrIleGlnAlaTrpLysAlaLeuLysHisLys

2550 TCTGCTAACATGGATGTGCTAATTGTTCTGGCCACTTCCATAGCCTTCACCTACTCATGC
761 SerAlaAsnMETAspValLeuIleValLeuAlaThrSerIleAlaPheThrTyrSerCys

2610 GTCGTCCTAATTGTGGCCATGGCGGAGAAGGCAAAAGTCAATCCCATCACGTTCTTCGAC
781 ValValLeuIleValAlaMETAlaGluLysAlaLysValAsnProIleThrPhePheAsp

2670 ACACCGCCTATGCTCTTTGTCTTCATCTCTCTGGGACGCTGGCTGGAACAGATAGCCAAG
801 ThrProProMETLeuPheValPheIleSerLeuGlyArgTrpLeuGluGlnIleAlaLys

2730 AGCAAGACTTCTGAGGCTTTGTCCAAACTGATGTCTTTACAAGCCACTGAGGCCACAGTT
821 SerLysThrSerGluAlaLeuSerLysLeuMETSerLeuGlnAlaThrGluAlaThrVal

2790 GTCACTCTCGGCAGTGATAATTCAGTTCTCAGTGAGGAGCAGGTGGATGTGGAGCTGGTT
841 ValThrLeuGlySerAspAsnSerValLeuSerGluGluGlnValAspValGluLeuVal

2850 CAGAGGGGTGATATAGTCAAAGTCGTTCCTGGGGGAAAGTTTCCAGTCGATGGGAGGGTC
861 GlnArgGlyAspIleValLysValValProGlyGlyLysPheProValAspGlyArgVal

2910 ATTGAAGGACATTCCATGGCTGATGAGTCCCTCATCACAGGTGAGGCCATGCCAGTGACA
881 IleGluGlyHisSerMETAlaAspGluSerLeuIleThrGlyGluAlaMETProValThr

2970 AAGAAGCCCGGGAGCTCGGTGATTGCAGGCTCCATTAACCAGAACGGCTCTCTGCTCGTC
901 LysLysProGlySerSerValIleAlaGlySerIleAsnGlnAsnGlySerLeuLeuVal

3030 AGTGCTACACATGTTGGCATGGACACCACGCTGTCTCAGATTGTCAAACTAGTGGAGGAG
921 SerAlaThrHisValGlyMETAspThrThrLeuSerGlnIleValLysLeuValGluGlu

T-7A 3' F4
3090 GCTCAGACTTCAAAGGCTCCCATCCAGCAGTATGCAGATAAAATTAGTGGCTACTTTGTA
941 AlaGlnThrSerLysAlaProIleGlnGlnTyrAlaAspLysIleSerGlyTyrPheVal

3150 CCCTTCATTGTTGGCATATCTGTGCTTACCCTGATCGCCTGGATCATCATTGGCTTTTTG
961 ProPheIleValGlyIleSerValLeuThrLeuIleAlaTrpIleIleIleGlyPheLeu

3210 AACTTCTCTCTAGTGGAGATGTACTTTCCTGGTTACGACAAATCCATTTCCAGAACTGAG
981 AsnPheSerLeuValGluMETTyrPheProGlyTyrAspLysSerIleSerArgThrGlu

3270 GCAGTGGTTCGCTTCGCCTTCCAGGCCTCCATAACCGTGTTATGCATCGCCTGTCCCTGT
1001 AlaValValArgPheAlaPheGlnAlaSerIleThrValLeuCysIleAlaCysProCys

3330 TCCCTTGGCTTGGCAACCCCGACAGCTGTCATGGTGGGCACAGGGGTCGGAGCCCAAAAT
1021 SerLeuGlyLeuAlaThrProThrAlaValMETValGlyThrGlyValGlyAlaGlnAsn

3390 GGCATCCTGATAAAGGGGGGAGAGCCACTTGAGATGGCGCATAAGGTTCAGTCTGTGGTG
1041 GlyIleLeuIleLysGlyGlyGluProLeuGluMETAlaHisLysValGlnSerValVal

3450 TTTGACAAGACCGGCACCATTACATACGGGGCCCCAAAGGTTGTTCAAGTAAAGATCGCG
1061 PheAspLysThrGlyThrIleThrTyrGlyAlaProLysValValGlnValLysIleAla

3510 GTGGAGGGGAATAAGATGCCTCGCTCCCGCCTGCTGGCCATTGTAGGCACAGCTGAGAAC
1081 ValGluGlyAsnLysMETProArgSerArgLeuLeuAlaIleValGlyThrAlaGluAsn

3570 AACAGTGAACACCCGCTGGGAGCCGCTATTACCAAATACTGCAAACAGGAGCTTGGCACA
1101 AsnSerGluHisProLeuGlyAlaAlaIleThrLysTyrCysLysGlnGluLeuGlyThr

3630 GAGTCTCTTGGCACGTGCGTGGACTTTCAGGCAGTGCCAGGCTGTGGCATCCGATGTCAG
1121 GluSerLeuGlyThrCysValAspPheGlnAlaValProGlyCysGlyIleArgCysGln

3690 GTGAGCAACACGGAGAATCTGCTGAAGCAGTTGGACAGTGACAGCGAGGACAACAACCAG
1141 ValSerAsnThrGluAsnLeuLeuLysGlnLeuAspSerAspSerGluAspAsnAsnGln

3750 CGCAACAGTGTCCTAGTCCAGATCAGCGACAGCCGGACATGCACCAGCTCCCATCCACTC
1161 ArgAsnSerValLeuValGlnIleSerAspSerArgThrCysThrSerSerHisProLeu

3810 ATCATGGACCCACAGCCGCAAAGCCTGGTTCAGACAGCCACCTATGTAGTCCTGATTGGG
1181 IleMETAspProGlnProGlnSerLeuValGlnThrAlaThrTyrValValLeuIleGly

3870 AACAGGGAGTGGATGAGGAGGAACTGCCTGCAAGTCAAACCTGAAATCGATGAAGCCATG
1201 AsnArgGluTrpMETArgArgAsnCysLeuGlnValLysProGluIleAspGluAlaMET

3930 ATCGAGCACGAGCGCAGAGGACGCACTGCTGTTCTGGTGGCCGTAGACGACCTACTGTGT
1221 IleGluHisGluArgArgGlyArgThrAlaValLeuValAlaValAspAspLeuLeuCys

3990 GCAATGATAGCCATAGCAGACACAGTGAAACCAGAGGCTGAGTTGGCGGTCCACACGCTG
1241 AlaMETIleAlaIleAlaAspThrValLysProGluAlaGluLeuAlaValHisThrLeu

4050 ACCAACATGGGTCTGGAAGTTGTGCTGATGACTGGAGACAACAGCAAGACAGCTCGGGCT
1261 ThrAsnMETGlyLeuGluValValLeuMETThrGlyAspAsnSerLysThrAlaArgAla

4110 ACTGCTGCTCAGGTCGGCATCAGGAAAGTGTTCGCTGAGGTGCTGCCCTCCCACAAGGTG
1281 ThrAlaAlaGlnValGlyIleArgLysValPheAlaGluValLeuProSerHisLysVal

4170 GCCAAAGTGGAACAGCTGCAGCAGGCAGGAAAGAGGGTCGCCATGGTGGGTGACGGCGTC
1301 AlaLysValGluGlnLeuGlnGlnAlaGlyLysArgValAlaMETValGlyAspGlyVal

4230 AACGACTCGCCCGCTCTGGCCATGGCTGACGTGGGCATCGCCATAGGAACCGGGACAGAT
1321 AsnAspSerProAlaLeuAlaMETAlaAspValGlyIleAlaIleGlyThrGlyThrAsp

4290 GTGGCCATAGAGGCCGCAGATGTTGTGCTGATCAGGAATGACCTGCTGGATGTGGTCGGC
1341 ValAlaIleGluAlaAlaAspValValLeuIleArgAsnAspLeuLeuAspValValGly

4350 AGTATTGACCTCTCGAAAAAGACCGTCAAGAGGATCAGGATCAACTTTGTCTTCGCTCTT
1361 SerIleAspLeuSerLysLysThrValLysArgIleArgIleAsnPheValPheAlaLeu

4410 ATCTACAACCTGGTTGGAATTCCTATTGCTGCTGGGGTGTTCCTTCCCATCGGCCTGGTG
1381 IleTyrAsnLeuValGlyIleProIleAlaAlaGlyValPheLeuProIleGlyLeuVal

4470 TTACAGCCGTGGATGGGCTCGGCTGCCATGGCGCTGTCATCCGTCTCTGTGGTTTTGTCC
1401 LeuGlnProTrpMETGlySerAlaAlaMETAlaLeuSerSerValSerValValLeuSer

4530 TCACTTCTACTCAAATGTTACACTAAACCCACTGCAGAGAAGCTGGAGGCCAGACTGGGT
1421 SerLeuLeuLeuLysCysTyrThrLysProThrAlaGluLysLeuGluAlaArgLeuGly

4590 ACCAGCAGGCGGCAGGGCAGCCTGTCTGACGTCAGCGTCCACATCGGCATGGGCGAGATG
1441 ThrSerArgArgGlnGlySerLeuSerAspValSerValHisIleGlyMETGlyGluMET

4650 CGTCGCCCGTCCCCCAAACTCAGTCTGCTAGACCGCATCGTCAACTACAGCCGAGCGTCG
1461 ArgArgProSerProLysLeuSerLeuLeuAspArgIleValAsnTyrSerArgAlaSer

4710 ATCAACTCGCTGCGCTCAGACAAGCATTCGCTCAACAGCTTCGTGCTCAGCGAGCCCGAC
1481 IleAsnSerLeuArgSerAspLysHisSerLeuAsnSerPheValLeuSerGluProAsp

4770 AAACACTCACTACTGGTCGGGGAGGCTGCGAGCCATGAGGATGACTTGTGTTGAATTATT
1501 LysHisSerLeuLeuValGlyGluAlaAlaSerHisGluAspAspLeuCys *

4830 ATCTGAGAAGCTTACAATAGAAAGTGCATTTATTCAAGGCTGGGCCATGCTAAGCCAAAA

4890 GGGTTACATTGAATAATGGCCCTTCCATCTGCTGTAGGTACCCTCAGGGCAGCACTGTTT

4950 ACGTGAAGAAAGCTTGCATGTCCCTTGTTTCCTTTTAGCTCAACCAGCTGATCACATTCT

5010 TCAGACTATGATGAGATGTGTTTTGTTGAGGTTACCGCCCTTGGAGACACTCTTAGAGAA

5070 ACCAATTGACACTACGATCCACAACTCTCCCGTGTCAGCTTCTTCAGAGCCATGAAGCAG

5130 GTGCCACATCCAGGAAGCAGAGCTGTGATCATTGTTGCAACTTTACAATCTTGAACATCT

5190 ATCCAAAGACATTTAAACAGTGGTGCCCTTCCTAAGAGTGGACACAGTAGAGTTTTATTT

5250 TAGTTAATCTTCCTTAAATGGAAAAGTGTTTGTATAATTATATTCCAAACTATTTATACT

5310 TATCTATTTTTTCACTACATCGATGTAAAACATGAAGTTCTTGAATCCAAATGTAAATTA

5370 TGATTTTGACGTTCCCAAAAAAATGTGTGATTGTTCAGAAAGTAATGCATAAAAACTTTA

5430 TAACAAGCTGCAAAAGGGATTAAGCAAAATTAAGGAGTGAGATGTGAATGTCAGTGTTAC

5490 CTAAAGTGCCAGTTGAAGTGCCCCCTGGCAAAGTCCAACCCATTCCAAAGATAGCAGCAT

5550 TCAGAGGTTATTTTGGACTTGATTTTCACAAAGTGTGAGCAGAGGTTTGCTGAAGGTCGA

5610 TTTAAGCTTTAGTTTCAGCATGTGTCAACTCGCTCCAGCTGTAGTCAGTCATCTGTCAAT

5670 GTATGTGAAGATTATTCGCTGTTGCAGTGAAGCAGAAGTTACATGGATTATGATGTTTTT

5730 GGATGTCTTTATGAGTTGTTGCAATTAGACTTGTGTTTTGAAATGGCTGAACTTTAAAAA

5790 AAAAAAAAAAAAAAAAAAAAAAAAAAAAAAAAA

I declare that the assignment here submitted is original except for source material explicitly acknowledged, and that the same or related material has not been previously submitted for another course. I also acknowledge that I am aware of University policy and regulations on honesty in academic work, and of the disciplinary guidelines and procedures applicable to breaches of such policy and regulations, as contained in the website.

CHEN Pengshi	2010 9 . 27
Signature	Date
CHEN Pengshi	2010. 09. 27
Name	Student ID
BCH	Biochemistry
Course code	Course title